MULTIPLE SPAN STRUCTURAL BEHAVIOUR OF INSULATING SANDWICH CLADDINGS FOR BUILDINGS

A thesis submitted to the university of Southampton
for the degree of
Master of Philosophy

by

SAMAR .M. ARNAOUT

Department of Civil Engineering
University of Southampton
United Kingdom

May 1991

IN THE NAME OF GOD, THE ALL MERCIFUL, THE ALL COMPASSIONATE.

" Read: In the name of thy lord who created,
who created man from something which clings,
Read! Thy lord is the most Noble,
who taught by the pen,
who taught man what he did not know."

HOLY KORAN
Surah"Al-alaq" verses (1-5)

TO MY FAMILY AND HUSBAND.....

Thy lord hath decreed
that ye worship none but him,
and that ye be kind
to parents, whether one
or both of them attain
old age in thy life,
say not to them a word
of contempt; nor repel them,
but address them
*in terms of honour**
And, out of kindness
lower to them the wing
of humility, and say:
"My lord! bestow on them
thy mercy even as they
*cherished me in childhood**
Your lord knoweth best
what is in your hearts:
If ye do deeds of righteousness
verily He is most forgiving
to those who turn to Him
*again and again**

HOLY KORAN
Surah"Al-Israa", verses (23-25)

TABLE OF CONTENTS

ABSTRACT

Sandwich panels with thin steel faces and polystyrene core are finding increasing use as the cladding of buildings. Such panels are subject to wind load as well as to large temperature differences between the faces which give rise to significant stresses and deflections.

This work presents a general review of sandwich panels with relatively thin cores, their materials, production technology, failure mode, requirements and their design criteria. The relevant standard tests are also outlined. No general design theory has yet been published for multi - span panels, hence the need for the present study. Thick, highly insulated two - span panels are investigated in more detail by this research.

The aim of this work is to outline a new approach which can be adopted for the design of multi - span panels subjected to simulated wind load and thermal gradient. Wind load is simulated by an equivalent uniformly distributed load. Maintaining a constant thermal gradient over a long period of time is quite impractical in a large scale test. Therefore, the deflections due to thermal gradient are reproduced by the application of a "simulated temperature load".

Analysis is made to study the behaviour of multi - span panels subjected to wind load and either "simulated temperature load" or a thermal gradient between outer and inner steel faces of the panels.

The performance of multi-span sandwich panels in bending is evaluated analytically by means of a computer program and experimentally by testing three different core density panels in bending under simulated wind and temperature loads.

The results of the experiments are shown to conform in general to the theoretical values determined by the computational analysis. It is shown that temperature loading causes significant stresses and deflections in these panels and can not be ignored. It also shows that subjecting the panels to a thermal gradient gives different results to those obtained when the same panels are subjected to a "simulated temperature load".

Some of the material properties of the thicker than normal panels are assessed in this research by adopting modified standard tensile and shear tests.

As a result of this work, suggestions for future work are made to improve further the structural and economical performance in the use of multi-span panels in the building industry.

ACKNOWLEDGEMENTS

The author would like to express her deep sense of gratitude to **Dr. C.K. Jolly**, her supervisor, for the inspiration, guidance and support provided throughout the course of her work.

Sincere thanks are also due to **Mr. K. Yeates and his staff in the Civil Engineering laboratories** for their great assistance in the experimental work.

The author wishes also to thank the **Hariri Foundation** for their financial support without which this work would never have been possible.

Sincere appreciation should also be expressed to **Mr. George Sweet at L. R. Insulations Limited** for supplying all the sandwich panels.

Finally, the author would like to express her gratitude and thanks to **Mohamad Abdul-Ghani, her husband,** for his patience, assistance and love, which helped her all the way through the completion of this work, and to **her family in Lebanon** for their love and support which enabled her to endure all difficulties and problems in order to achieve her aim.

CHAPTER ONE

INTRODUCTION

1.1 Definition of sandwich panels:

The European Committee for Constructional Steelwork[4] defines sandwich panels as "wall or roof units, where both the inner and outer faces are formed of flat or profiled metal and a relatively low strength core material having suitable insulating and stiffening properties." The components of the sandwich must be bonded together in such a manner as to provide a load-bearing composite cladding unit. The bonding may be achieved by a line foaming process, a separate adhesive or a mechanical fastening.

1.2 Origin of sandwich technology:

Fairbairn[1] (1849) is believed to be the first person to have described the principles of sandwich construction. Since then, sandwich technology has been used in aviation and space flight. The second world war "Mosquito" aircraft and the space ship which landed on the moon in 1969, are good examples of incorporating sandwich panel technology in structural design.

Around 1960, sandwich technology found its use in other industries such as buildings, cold storing, automobile and ship building industries. This was the beginning of prefabricated light weight building elements for diverse applications.

1.3 Principal forming of sandwich panels:

In principle, the structure of sandwich panels always follows the same pattern: Two thin, stiff and strong sheets of dense material separated by a thick layer of low density material which may be less stiff and strong. An efficient sandwich is obtained when the weight of the core is roughly equal to the weight of the two steel faces. A great variety of sandwich elements could be obtained by combining different types and shapes of materials. This point will be discussed in chapter two.

1.4 Sandwich properties:

The excellent structural performance of sandwich panels depends on the core and the steel faces acting together as one unit. For instance the bending stiffness of the sandwich is much greater than that of a single solid element made from the same material of the faces and having the same weight.

The core itself has several vital functions, it must be stiff enough in the direction perpendicular to the faces to ensure that they remain the same distance apart. It must be stiff enough in shear to ensure that the faces do not slide over each other when the panel is bent, otherwise the faces would act as two separate beams and the whole sandwich effect would be lost. The core must also be stiff enough to keep the faces flat so that no buckling can occur if the faces are subjected to compressive stress.

The properties of sandwich panels depend on the properties of the face material and of the core acting together. Each material contributes to the overall behaviour of the sandwich element. These properties are:

-a- The high load bearing capacity for low self weight.

-b- The excellent and durable heat insulation.

-c- An absolute water and vapour barrier.

-d- The resistance to weather effects and aggressive atmospheric conditions.

-e- The good sound insulation compared with homogenous wall or roof elements of the same weight.

-f- Easy repair or replacement in case of damage.

-g- The possibility of economic and uniform quality production.

-h- Low cost of erection resulting from prefabrication and ease of handling.

-i- The long life at low maintenance cost.

Naturally, sandwich panels as any engineering product have their own disadvantages, such as:

-a- The behaviour under fire of elements with synthetic polymer cores.

-b- The deformation under unilateral exposure to heat of metal faces.

-c- The creep behaviour under permanent loads which increases deflections and affects the distribution of internal stresses.

-d- The low heat-storing capacity.

Despite the disadvantages mentioned above, sandwich panels have been increasingly used in the building industry. One of their major applications is their use as cladding of buildings due to their strength, stiffness, lightness ,

durability and their high insulating qualities. This represents the optimum use of their properties to form the various components of a complete cladding system.

Because of their relatively recent introduction to the building industry, there have been only few articles written on the behaviour of such panels[34-38]. Most studies has been conducted for single - span panels. Few experiments were conducted on panels for two - span conditions[39]. However, no general design theory has yet been published for multi - span panels.

The aim of the present research is to provide a new approach for the design of multi - span panels subjected to wind loads and thermal gradient.

The present research considers the type of sandwich panels which are suitable for semi-structural building applications with a primarily insulating function. These are panels made from thin sheets of steel or aluminium with polystyrene core. They have been mainly used in abattoirs, food stores, restaurants and meat packaging factories. In such applications, it is necessary to understand and evaluate the structural performance of the sandwich panels in bending under uniform load, in compression and under thermal bowing. It is therefore the purpose of this research to obtain such experimental results and to compare them with theoretical and design values.

A detailed review of the sandwich materials, their production techniques, the available types of panels, their failure modes, their design criteria and the various tests which can be carried out on sandwich panels are outlined in **CHAPTER TWO.**

CHAPTER THREE covers the analytical design of multi-span panels subjected to wind loads and temperature effects. All the necessary equations are derived in order to predict the deflection of the panels under load. This chapter includes

also a computer program which put the equations in a general form in order to use them to predict the panel deflection under any load combination.

CHAPTER FOUR covers the secondary tests adopted in order to assess the material properties of the sandwich. These included bond strength, shear strength and shear modulus. A full discussion and interpretation of the results of the material tests is covered in this chapter as well as the various graphs obtained from these tests.

CHAPTER FIVE deals with the main experimental work carried out on two - span panels to calculate their deflection under simulated wind and temperature loads for comparison with the computational results.

This chapter includes a detailed discussion of the results obtained and an interpretation of those results. Results data and plotted graphs are also included in this chapter.

In **CHAPTER SIX,** conclusions from the completed research and a plan for future work are given.

CHAPTER TWO

DESIGN OF STRUCTURAL SANDWICH PANELS.

2.1 Introduction:

Sandwich panels consists basically of two thin metal skins for the facings and a rigid foam material for the core. Material combinations other than the basic one are possible and they are usually designed for special purposes.
Regardless of the material combination, it is always beneficial to design sandwich panels of high mechanical, physical and productional properties at a reasonably low cost.

2.2 Materials

2.2.1 Facing materials

The facing material of sandwich panels should be thin and of a high strength. It should also meet The following criteria:

-a- The requirements of capability for roll-forming and bending.
-b- The functional requirements of wind, water and vapour tightness.
-c- The security guidelines of having capacity to distribute point loads, acting as pressed or stressed parts of a composite beam.
-d- The resistance to corrosion and fire.

The facings of sandwich panels could be made of various types of materials namely: Steel, aluminium or other materials such as glass-reinforced plastics, asbestos

cement, plywood, glass-reinforced cement, plasterboard, resin-impregnated paper, hardboard and ferro-cement. This review covers only steel or aluminium metal faces which could be either galvanised or plastic coated.

2.2.1.1 Steel sheeting

Hot-dip galvanised material is used as a basic material with additional steel surface for outdoor facings. The thickness of steel faces ranges from 0.5 mm to 1.5 mm.

The choice of the appropriate coating, suitable for corrosion protection, is highly influenced by the following conditions:

-a- The environmental conditions of the building such as rainfall, local pollution and deposition of grime on the surface.
-b- The internal conditions expected inside the building such as the concentration of chemical fumes and condensation.

ECCS (European Committee for Constructional Steelwork) has set up recommendations, for nearly all cases of different environmental conditions, about the expected lifetime of galvanised and coated steel[4] . Some of these recommendations included:

-a- Galvanised steel sheet as facing material is only recommended in a rural atmosphere if a short lifetime is required. A short life stands for about five years before the breakdown of the metallic coating starts as a result of rust staining or rust spots. They are also used for the inside of buildings where no condensation is expected i.e.in a dry atmosphere with temperature ranging from 5 to 25°C

-b- Galvanised and coated steel sheets with 25μm thick

coating based on polyester or acrylic is recommended for use in rural and urban atmosphere for a medium life (about 10 years) and in industrial atmosphere for a short life (about 5 years).

-c- PVC coating systems are recommended for maritime climates with a reservation for their relatively low thermal stability and low colour stability.

-d- PVC and PVDF coating systems are recommended for long life in rural, urban and industrial as well as costal areas.

The coating of the steel sheets protects them against corrosion during fabrication and storing. It also increases the bonding effect between the faces and the core .

Stainless steel facings are provided for sandwich panels used as wall or roof elements for buildings with very hygienic demands e.g. in manufacturing plants for pharmaceutical products, dairies and breweries. Stainless steel sheets should undergo a surface treatment of mechanical and chemical descaling, thermal treatment and pickling in order to give them sufficient bonding to the line-foamed core. Thereafter, no special corrosion protection is necessary for stainless steel sheets.

2.2.1.2 Aluminium sheeting

This type of sheeting is the most popular next to steel facings. It may be used where special requirements for resistance to corrosion or hygienic demands in food production and storage are to be fulfilled. The thickness of aluminium faces ranges from 0.7 mm to 1.2 mm to avoid local deformation in handling. However, 0.5 mm thick sheets may be used if carefully handled. Aluminium facings are normally colour-coated to give them a decorative appearance. Uncoated surfaces will oxidize in a short time. The oxide

layer is then resistant to weather and humidity within a PH range of 5 to 8. Hence, a 25 μm thick coating is essential to protect aluminium skins where aggressive atmospheric conditions are expected.

The aluminium alloys used for the facing sheets are AlMnMg, AlMn and AlMg. The choice of alloys components influences the corrosion resistance e.g. Magnesium increases the resistance to seawater and Manganese increases the overall durability.

The metal faces may be produced in three different forms:

-a- Panels with flat faces (Fig 2.1a).
-b- Panels with lightly profiled faces also known as quasi-flat, lined or micro-profiled faces (Fig 2.1b).
-c- Panels with profiled faces (Fig 2.1c).

2.2.2 Core material

The core of sandwich panels is usually thick and light relative to the faces and with adequate stiffness in the plane perpendicular to the panel. The core of a sandwich panel may be produced in different forms:

-a- Panels with expanded plastic core (Fig 2.2a).
-b- Panels with honeycomb core (Fig 2.2b and Fig 2.4).
-c- Panels with corrugated core (Fig 2.2c and Fig 2.3).

In order to choose a core material best suited for sandwich panels, special properties should be taken into consideration. These are mechanical, physical and manufacturing properties. It is always difficult for one material to satisfy all requirements. Therefore, a compromise will have to be made after deciding on the priority of the demands to be met including the economic point of view.

The mechanical properties include the tensile, compression and shear strengths and moduli. These are essential to enable assessment by design calculation of sandwich panels under long term load and temperature.

The physical properties consist of the high thermal insulation of the core material, its resistance to soaking and fire and its sound insulation.

Finally, the manufacturing properties must suit the production process.

Generally, two types of core material are used for sandwich panels:

-a- Rigid foam material.
-b- Inorganic fibre material.

Other material could also be used for special requirements namely: Foamed glass, lightweight concrete, clay products and expanded plastics.

2.2.2.1 Rigid foam material

Cores made from rigid foam material are of different types. The most frequently used are:

-a- Polyurethane (PUR)
-b- Polyisocyanurate (PIR)
-c- Phenolic Resin (PF)
-d- Polystyrene

Each of these materials has particular properties, but all of them have in common their low density and a closed cellular structure.

The low density of rigid foam material is very important to get the required physical properties at a low raw material cost. In addition, mechanical properties are dependent on

the density of the rigid foam core material.

Figures 2.5 and 2.6 show some typical dependencies for PUR material. An increase of density is associated with to an increase of mechanical values.

The closed cellular structure of rigid foam material is very important. Such a structure does not allow water to penetrate and it has high soaking resistance caused by the same all round compression on the air or gas within the cell.

Particular attention should be given to the core resistance to solvent attack when selecting suitable adhesives. Solvent based adhesives tend to weaken the rigid foam structure.

The application of plastic foams has its weak points. First of all, they are combustible. Their behaviour in fire could be improved by use of selected raw material, special foaming processes or by using retarding agents. Secondly, all plastic foam materials change their dimensions under temperature strain. This is due to the fact that the gas inside the cells would cause them to enlarge under excess pressure through heating. The gas will then diffuse and escape, allowing the foam structure to shrink.

All plastic foams should ensure a thermal stability towards temperature up to at least 80° C. Polystyrene materials just cover this value, whereas PUR retains stability up to 100°C and PF material to more than 130°C.

PUR, PIR and PF are plastic foams where the mixed components of the basic materials foam during a chemical reaction. However, polystyrene is made of a polystyrene granulate containing highly volatile fluids causing the granulate to foam under the influence of temperature.

Polystyrene is one of the best known thermal insulation material. When comparing physical and mechanical values of

polystyrene and PUR foams, it is found that half the weight of polystyrene produces the same values of those of PUR. This is due to the low density of polystyrene (30 - 50 Kg/m^3) and its low water absorption (zero).

The major disadvantage of polystyrene foam material is its low solvent resistance. Thus, when gluing it to the metal faces, it is recommended that solvent free adhesives are used.

2.2.2.2 Inorganic core material

The most common materials are fibre wool slabs of inorganic base, minerals, glass or blast furnace slag. Mineral wool is the most popular.

Compared to rigid foam material, mineral fibres show a high degree of bending elasticity and open cell structure. As a consequence of their structure, mineral fibres have low tensile, shear and compressive strength values for densities ranging from 50 to 300 Kg/m^3. The figures are 0.025-0.08 N/mm^2 for compression strength and 0.002-0.007 N/mm^2 for tensile strength.

Due to the open cell structure of the mineral fibres, the slabs are open to water absorption and vapour diffusion. However, the fibre wool is non-combustible.

2.3 Types of sandwich panels

Different types of sandwich panels are produced according to their constructional function in a structure. The most common types available are:

-a- Wall panels
-b- Roof panels
-c- Panels for cold stores

-d- Panels for aircraft structures
-e- Panels for radomes

2.3.1 Wall panels

The metal faces of this type of panels are very thin (of minimum thickness of about 0.5 mm for steel sheet and 0.7 mm for aluminium sheets). The sheets should be rigid enough for safe handling during fabrication and erection. The width of these sheets ranges from 600 mm to 1200 mm.

The surfaces of metal faces are usually reinforced by small longitudinal stiffeners for many reasons: Firstly, to increase the rigidity of the facings and consequently the bearing capacity of the panels. Secondly, to give the sheets a better surface appearance and finally, to facilitate the provision of special joints between the elements when stiffeners are used in edge zones.

The construction of edge zone should be considered very carefully in order to form tight connections between adjacent elements. This would be achieved by "tongue and groove" connections which ensure that thermal insulation between metal sheets is maintained. It also make the panel adequately water proof and air - tight by using soft sealant on the groove end.

2.3.2 Roof panels

Roof panels tend to have strongly profiled faces as long term loads are taken by these faces. Roof panels are influenced by the tendency of foam material to creep under sustained loads. Flat and lightly profiled faces are not recommended for use as roof panels. They have little bending stiffness and creep is unconstrained.

Sheet thicknesses of roof panels are larger than those of

wall panels. The minimum thickness is 0.75 mm, since roof panels are walked on during construction and maintenance work.

The method of connecting longitudinal joints in roof panels is known as "overlapping". In this method, elements are connected by means of screws or blind rivets in the two overlapping sheets at 0.5 to 1.0 m spacing.

2.3.3 Panels for cold stores

The main requirement for cold stores panels is that they should have adequate insulating material. An example of these panels is the panel[6] shown in Figure 2.7 in which a core of expanded polystyrene, styrofoam, urethane, isocyanurate or other suitable solid insulation is bonded under heat and pressure between two skins of galvanised sheeting with plastisol or approved finishes.

The thickness of such panels is not limited. It ranges from 25 mm to 300 mm. Their standard width is up to 1200 mm with length up to 13.00 m. Due to its structure, these panels are able to withstand stresses and loads not usually associated with insulated panels. The faces may be flat or lightly profiled, the finishes of the galvanised steel skins can be left plain, PVC coated or specially finished using any suitable material. In order to provide rigidity when the panel is used for cold stores, "tongue and groove joints" are built into the edges of the panel together with the application of non hardening mastic which provides an efficient vapour seal and water tight joint.

2.3.4 Panels for aircraft structures

This type of panels consists of metal faces with metal honeycomb or corrugated cores. The honeycomb is formed from strips of thin aluminium alloy or steel foil deformed and

joined together. The corrugated core is a fluted metal sheet attached alternately to the upper and lower faces. Panels for aircraft should be light in weight.

2.3.5 Panels for radomes

This type of panels should be permeable to radar waves. It utilizes glass-reinforced plastics for the faces and either the same material or resin-impregnated paper for the honeycomb core.

2.4 Production technology

The wide range of sandwich elements available for use necessitates a variety of production methods. The production process for sandwich panels with metal faces is defined as :" The manufacture and design of the two structural parts facings and core layer and their durable connection for composite action".[5]

An economical production is dictated by a number of factors namely:

-a- The geometrical design of the panels. This includes the shape of the facing material (flat, lightly profiled or fully profiled), the lengths and widths of the panels and the edge forming (longitudinally or on four sides).

-b- The availability of the basic materials and the type of insulating material that influences the production process.

-c- The quantities and the variations of panels to be produced.

2.4.1 Facing production

Metal facings may be produced in different shapes and design depending on their application. They may be flat, lightly profiled or fully profiled. Small batches of facings of different core sections can economically be shaped means of folding process or deep-drawing. When outstanding quality is required, large quantities of uniformly shaped profiles with different lengths are preferably roll - formed.

The cost of operating the tools should be considered before choosing the production process. Folding is a hand operation and wage intensive process, whereas roll - foaming is a continuous operation with automatic feed but at high costs of investment.

2.4.2 Core material

The core foam is formed either by bonding together the heat insulating slabs or by foaming rigid plastic material into the cavity formed by the facings.

2.4.2.1 Bonding process

The core material, available in form of prefabricated insulating slabs is bonded to the metal faces by means of adhesives. Two different types of adhesives may be used in this process. They could either be adhesives containing solvents or two component types containing epoxy resin or polyurethane. The choice of the adhesives is dominated by their applications.

2.4.2.2 Foaming process

Sandwich panels owe their reputation to their foamed cores. Both the heat insulation and the bonding to the faces

originate from the foaming process. The basic materials used in foaming are polyurethane and polyisocyanurate.

Rigid foam cores are obtained from a chemical reaction between the liquid components and the activator (Fig 2.8)[5]. This reaction will cause the mixture to foam and harden. The proportion between the components and the additions determines the foam density, its rigidity and other technical characteristics as well as the time for the whole foaming process.

Mould foaming, is when foam is applied in closed moulds of dimensions corresponding to the dimensions of the panel required. The moulds may be placed horizontally so that the injected foam falls on the lower face plainly placed onto the bottom of the mould. The injected foam then rises to meet the upper face kept a certain distance apart. This type of mould foaming may result in different degrees of adhesion to the two faces and a non-uniform foam properties. Moreover, there is a danger that the foam may rise unevenly, trapping small air pockets. This would increase the susceptibility to blistering.

The moulds may also be positioned vertically so that the foam rises in contact with the two metal faces at the same time. This method is claimed to avoid some inherent problems of the horizontal foaming.

Mould foaming is probably best adopted when panels with very complicated cross sections are required. This is due to the fact that this method produces panels in small quantities.

2.4.2.3 Continuous production

In this type of production, two metal strips are run-off a coil then pass through a surface and edge forming station. The continuously passing strips are heated up to the required temperature. A two component mixture is applied

then the strips enter a double conveyor. This keeps the faces at a certain distance since they tend to enlarge as the process begins. Small chain belts run laterally to ensure tightness of the rolling mould. As the foamed core reaches the end of the conveyor, which could be up to 30 m long, The foam is hardened. A flying saw then cuts the panel to the required length. The diagram shown in Figure 2.9 summarizes the production process.

Despite the fact that continuous production process is expensive, it has the capacity to produce large quantities of panels of consistent quality and various lengths.

2.5 Requirements for sandwich panels

Sandwich structures profit from the advantage of choosing the right material combination best suited for a planned application. This ensures an optimal conformity with all design requirements. These requirements may vary from one industry to another depending on the type of panels and their application. For instance, in the aviation industry, stability problems are dominant, followed by structural and productional requirements. Considering these problems is necessary to achieve the most favourable proportion of stiffness to weight. In the building industry however, the cost to effectivity relationship is the first priority because of the many competing types of construction.

The design requirements can either be general or special. The general requirement include mechanical, physical, productional and economical requirements. They cover the material combination for the composite panels, the properties of these materials and their effects on the performance of the sandwich elements. General requirements also cover the availability of the material, their cost, and last but not least the economical consideration.

For specific design purposes, special requirements should be

taken into account. These requirements are under the aspect of security, function and durability. The most essential requirements are:

-a- Stability under stresses during fabrication, transport and erection.
-b- The capacity to compensate strain resulting from temperature influences, particularly from unilateral exposure to sunlight.
-c- An adequate capability of resisting fire or at least a minimum risk of fire.
-d- Long term weather resistance.
-e- The capacity to prevent water, snow, air and gas from penetrating the surfaces and joints.
-f- An adequate protection against humidity resulting from water condensation.
-g- Good sound insulation.
-h- A high heat insulating and heat storing capacity.

Furthermore, constructional requirements have to be considered such as:

-a- The construction of cross- sections relevant to materials.
-b- Joints between the elements and connections adapted for fast and easy mounting.
-c- Statically secure and optically neat fasteners.

In addition to all the above requirements, the aspect of erection plays a major role. Handling and finishing of the panels at site should be easy to carry out with the usual tools. Transporting the panels must not also be complicated.

It is a fact that meeting all the requirements at a time is quite impossible. As a general rule, a compromise should be reached combining the desirable properties with the performable possibilities of fabrication.

The choice of sandwich panels for specific design purposes

depends mainly on their role in the structure. The panels tested in this work are used as cladding for cold storage structure. Therefore, the main requirement to consider is the thermal insulation of the panels.

Sandwich elements, used as wall panels, are known for their stability to shield from external influence of weather. In other word, ensuring a uniform atmospheric conditions within the building. The efficiency of the panels depends on their build-up, especially on the materials chosen for the insulating core. The core of the panel is almost entirely responsible for panel heat insulation. Its function is to insulate and prevent the flow of heat, hindering it by means of a heat resistance and by storing heat within the wall. The thickness of the core material and its coefficient of thermal conductivity are decisive for the insulating capability of the panel. Table 2.1[5] summarizes the insulating capability of various core materials for different core thicknesses. The insulating capability of the core material depends also on the quality of the connections to the structure. The joints between adjacent elements should be carefully designed to avoid the formation of thermal bridges.

In order to maintain the insulating function, it is absolutely imperative to provide a rain proof and vapour tight cover which in the case of metal facings is an inherent property.

2.6 Modes of failure

The design of sandwich panels must take into account a number of failure modes. Material safety factors would be considered with respect to each type of failure then used in the design of panels for structural application. The most important modes of failure are :

-a- Yield of metal faces.

-b- Wrinkling of flat or lightly profiled faces.
-c- Shear failure of core.
-d- Shear bond failure between core and faces.
-e- Crushing at a point of support or local load.
-f- Failure of fasteners.
-g- Failure at points of connection to supporting structure.
-h- Blistering.

In this research, attention will be concentrated on some particular failure modes, namely: Wrinkling of the faces; shear failure and shear bond failure, and last but not least crushing at points of support.

2.6.1 Wrinkling of flat or lightly profiled faces

This type of failure is unique to sandwich panels. It occurs when a sandwich panel is subjected to bending action. The face in compression exhibits short wavelength buckles which start to form at a low load then increase in amplitude gradually as loading progresses. The foam core stabilises the buckles. Wrinkling failure takes place when a single buckle, usually at the section of maximum bending becomes unstable and form a fold.

Allen[2] and Plantema[3] studied this phenomenon and in their books give full details of the theory of elastic wrinkling. The equations given in this section are based on their analysis of the theory.

The compressive strength at which elastic buckling takes place is given in the following equation:

$$\sigma_{cr} = K_1 \, [G_c . \, E_c . \, E_f]^{\frac{1}{3}} \quad \ldots\ldots\ldots\ldots\ldots\ldots\ldots\ldots\ldots\ldots\ldots\ldots (2.1)$$

Where:

G_c : Shear modulus of the core

E_c : Elastic modulus of the core. The compression modulus should be considered as the elastic modulus of the core is sometimes smaller in compression than in tension.

E_f : Elastic modulus of the faces

K_1 : Constant which depends on poisson's ratio of the core material ≈ 0.85

Factors such as imperfections, non linear material behaviour and finite core thickness ensure that the stresses from the above equation are not generally achieved in practise. In fact, the failure takes place at a lower stress. Therefore, a reduction factor must be applied and the wrinkling stress of a flat face of a sandwich panel is usually estimated as follows:

$$\sigma_{wr} = 0.6\ [G_c.\ E_c.\ E_f]^{\frac{1}{3}} \quad \text{.....(2.2)}$$

It can be concluded from the above equations that, wrinkling stress is independent of the thickness of the core material or the metal faces. It only depends on the material properties of both the core and the faces.

In the case of panels with lightly profiled faces, the wrinkling stress may be estimated using the following equation:

$$\sigma_{wr} = 0.6\ \alpha\ [G_c.\ E_c.\ E_f]^{\frac{1}{3}} \quad \text{.....(2.3)}$$

Where:

α is a numerical factor which depends on the core thickness. Although no analytical evaluation is available, α is generally taken in the range of 1.0 to 1.4.

2.6.2 Shear failure of the core and shear bond failure

Shear stresses, one of the significant stresses in the foam core of a sandwich panel, are necessary to obtain composite action between the two metal faces. They are nearly uniform over the depth of the core. Provided that the shear strength of the core and its bond strength with the faces are known, shear stresses are easily calculated as well as serviceability and ultimate limit state checks at the section of maximum shear force.

The shear strength of the core is rarely a critical factor in design calculations. Nevertheless, it is sometimes determined by test only to be compared with the theory and design values.

2.6.3 Crushing at a point of support

Points of support give rise to line loads on the panel. For panels with flat faces, this force is mainly resisted by the core, aided to an extent by bending of the metal faces.

A simplified approach to overcome this problem, is to ignore some factors (namely; The bending stiffness of the faces, the dispersion of the load and the interaction of crushing and wrinkling) and simply to check that the compressive strength of the core, taken over the area of the load, is adequate to resist the line load.

Lightly profiled and fully profiled faces could be treated using a different approach. Details of such an approach is described in Allen's book[2].

2.7 Design criteria

In the design of sandwich panels, the basic concept is to space thin facings far enough apart with a thick core. This formation provides a core that is stiff and strong enough to hold the facings flat through the bonding medium such as an adhesive layer. The core must also be thick enough to ensure that it has a sufficient shear resistance.

The advantage of spaced facings is to provide greater stiffness without much increase in the weight of material needed. The structural sandwich is analogous to I - beams, with the facings carrying direct compression and tension loads, as do I - beam flanges, and with the core carrying shear loads, as does the I - beam web.

2.7.1 Sandwich panel types for design purposes:

For design purposes, it is always necessary to distinguish between panels used as wall units and those used as roof units. Wall panels do not usually have any permanent loads in the normal direction. Therefore, long-term creep can be ignored and wall panels can be designed for short-term loading only. In contrast, roof panels carry their self weight and the weight of other permanent parts of the structure as permanent loads. A long-term loading should be taken into account in the design of roof panels. In addition, creep under snow loads should not be ignored. For design purposes, it is adequate to calculate the long-term loading using a reduced value for the shear modulus of the core. This reduced value of G_c should be calculated for a period of 2000 hours for snow loads and 100 000 hours for dead loads.

$$G_c = \frac{G}{1+\phi_t} \quad \text{.....(2.4)}$$

Where:

ϕ_t is the creep coefficient for the foam core material.

Sandwich panels have a very high degree of thermal insulation provided by the foam plastic cores. It is always necessary, in the design of panels, to include the stresses induced by the difference in temperature between the inner and outer faces of the panels. Under summer conditions, a reduced value of the shear modulus, corresponding to elevated temperature, should be used.

The temperature of the inner facing is normally equal to 20°C in winter and 25°C in summer. The temperature of the outer facing varies from -20°C in winter to up to 80°C in summer depending on the colour and brightness of the metal faces[9].

2.7.2 Safety factors and load combinations.

The safety factors for steel faced panels, as recommended in BS 5950 part 6 [10], are appropriate to adopt for sandwich panels.

For walls, where creep has no influence, four load cases can arise individually or in combination:

-a- Positive wind pressure.
-b- Negative wind pressure.
-c- Summer temperature difference.
-d- Winter temperature difference.

For roof panels, creep is significant. Therefore, it is necessary to consider the additional stresses due to creep effects. The loads to be considered are:

-a- Permanent (dead) loads.
-b- Snow loads (quasi-permanent)

-c- Wind loads.

-a- Wind pressure.

-b- Wind suction.

-d- Temperature loads.

-a- Summer case.

-b- Winter case.

-e- Long-term effects.

2.7.3 Design cases.

From the structural point of view, three design cases are considered. They are as follows:

-a- **Simply supported panel with flat or lightly profiled faces**

When subjected to a uniformly distributed load, a simply supported panel deflects under bending and shear action. Under temperature loads, the panel tends to bend into an arc of a circle. For panels with flat or lightly profiled faces, temperature loads cause significant deflection but there are no significant stresses.

-b- **Simply supported panel with profiled faces.**

For panels with profiled faces, temperature loads cause some internal stresses in the core and faces in addition to shear stresses near the ends of the panel.

-c- **Panels which are continuous over two or more spans.**

The tendency of the panel to bend into an arc of a circle is prevented by the presence of internal supports. This will lead to large support forces. Hence, larger bending moments and shear forces occur. In the case of continuous panels, the design may be based on a **pseudo-plastic theory** which assumes plastic hinges of zero bending capacity at the internal supports. This approach however, is not applicable if shear stresses in the core are critical.

Allen[2] covers in his book all design cases for simply supported panels with thin and thick faces, isotropic and orthotropic panels. Only the elementary analysis will be discussed in this section. Full analysis of two - span panels is covered in chapter three.

2.7.3.1 Elementary analysis of single span panels

The design of sandwich panels is not entirely given by the flexural stiffness. It must also include the deflection due to shearing deformations. The deflection of sandwich beam under load may be expressed by the following:

$$\frac{d^2y}{dx^2} = \frac{M_x}{D} + \frac{1}{N}\left[\frac{dV_x}{dx}\right] \quad \text{.....(2.5)}$$

Where:

y : deflection

x : distance along the beam

M_x : bending moment at point x

V_x : shear load at point x

D : flexural stiffness

$$D = E_f\frac{bt_sd^2}{2} + E_f\frac{bt_s^3}{6} \quad \text{.....(2.6)}$$

N : shear stiffness of the sandwich

$$N = D_Q = AG_c = G_c\left[\frac{h+c}{2}\right]b \quad \text{.....(2.7)}$$

Integrating equation (2.5) twice, leads to the following general expression for central deflection of a sandwich panel subjected to a central point load P (for panels with thin faces where the stiffness of the faces is ignored).

$$Y = \frac{PL^3}{48D} + \frac{PL}{4N} \quad \text{.....(2.8)}$$

For panels with thick or corrugated faces, the shear stress distribution becomes more complicated. The applied load is partly supported by the beam as a whole and partly by local bending actions in the faces which are in turn, associated with shear deformations in the core. The general equation for central deflection becomes:

$$Y = \frac{PL^3}{48D} + \frac{PL}{4N}[1-\frac{D_f}{D}]^2 S_1 \quad \text{.....(2.9)}$$

Where D_f is the flexural rigidity of the thin faces

$$D_f = E_f \frac{bt^3}{6} \quad \text{.....(2.10)}$$

$$S_1 = 1 - \frac{\tanh\theta}{\theta} \quad \text{.....(2.11)}$$

$$\theta = \left[\sqrt{\frac{\frac{D_Q}{D_f}}{1-\frac{D_f}{D}}}\right] \frac{L}{2} \quad \text{.....(2.12)}$$

Equation (2.9) covers the extreme cases in design. For any particular design problem, it is required to evaluate

$\frac{D}{D_Q L^2}$, $\frac{D_f}{D}$. The following cases can be distinguished:

- $\frac{D}{D_Q L^2} < 0.01$: Shear deflections are small. Bending

theory is used to calculate the deflections and stresses.

- $0.01 < \frac{D}{D_Q L^2} < 0.1$: Shear deflections are comparable with the bending deflections. Stresses in the faces are predicted by ordinary bending theory ($D_Q = \infty$) except under concentrated load.

- $0.1 < \frac{D}{D_Q L^2} < 10$: Shear deflections are dominant. Stresses in the faces are no longer predicted by bending theory.

- $10 < \frac{D}{D_Q L^2}$: The core ceases to connect the faces together effectively. The faces act virtually as independent beams and the sandwich effect is lost all together.

More details regarding the assumptions considered in the design of sandwich panels and the complete derivation of deflection equations are covered in chapter three which includes the analytical design of the sandwich panels.

2.8 Testing methods for sandwich panels and their components.

Often, in order to prove a design, it is necessary to test complete sandwich panels or small specimens. It may even be necessary to evaluate the core material properties by some material tests. In general, tests on sandwich panels fall into two distinct groups namely:

-a- Material tests
-b- Tests on complete sandwich panels.

Relevant standard test procedures are covered by a number of organisations such as:

- The American Society for Testing Materials (ASTM)[11]
- The German standard (DIN)[17-22,25-27]
- The International Standard Organisation (ISO)[12-16]

In general, there are no relevant British Standard test procedures in relation to sandwich construction.

2.8.1 Material tests

Successful sandwich panel design depends crucially on the knowledge of quality control of the mechanical properties of the foam core. As a general point, it should be noted that it is customary to test the core material with the metal faces still attached to it. This will ensure that, when appropriate, the test would also include a check on the bond between the core and faces as it is the case in tensile and shear tests.

The most common material tests will be reviewed in this section. All these tests involving properties of foam material are likely to be influenced to some extent by the temperature and the humidity conditions under which the tests are conducted. Therefore, most standards recommend that before testing, specimens should be stored for at least 72 hours under the following conditions:

Temperature: 23°C ± 1°C (73°F ± 2°F)

Humidity : 50 ± 2 %

The number of specimens to be tested, is recommended in most standards to be at least three. This is due to the fact that the foam properties can be variable. Thus, it is never possible to rely on one single test result.

Table 2.2 summarizes the specimens dimensions recommended by each different standard for some material tests.

2.8.1.1 Average foam density test (ASTM C 271-61[11], ISO R845[12], DIN 53420[17])

Although the average foam density does not appear in any design calculations, it should always be determined as a general indication of the material characteristics.

The procedure of this test is the same in all standards. It consists of weighing a known volume of the core material. The specimen's size varies from 50 mm cubes to 100 mm square prisms of height equal to the depth of the panel.

2.8.1.2 Tensile test

(ASTM C 287-61[11], DIN 53290[18]), includes bond test with faces.
(BS 5350 part C6[23]), includes bond strength in direct tension.
(ISO R 1926[13], DIN 53430[19]), includes tensile behaviour of foam alone.

The aim of this test is to investigate the tensile bond between the core and the faces and to estimate the bond strength. The test consists of subjecting a sandwich specimen to tensile load normal to the plane of the sandwich. This load would be transmitted through thick loading blocks bonded to the faces. The first three standards, mentioned above, follow the same test procedure on specimens of a rectangular prism shape (Fig 2.10). The last two standards require a rather larger dumbbell shaped specimen. It is then tested in a tensile machine with the aid of clamps.

2.8.1.3 Compression test (ASTM C 365-57[11], ISO R 844[16], DIN 53421[20])

The purpose of this test is to assess the compressive properties of sandwich cores in a direction normal to the

plane of the faces. The test consists of applying a load to the specimen through a spherical loading block, of the self aligning type. The block should distributes the load as uniformly as possible over the entire loading surface of the specimen. The load should be applied at a constant rate. Readings of the applied load and the corresponding displacement should then be plotted in a load/ deformation graph. The compressive modulus of elasticity and the compressive strength are determined from the fitting lines of the graph.

2.8.1.4 Shear test (ASTM C 273-61[11], ISO 1922[14], DIN 53427 & 53294[22]).

This test is used for the determination of shear strength parallel to the plane of the sandwich (Fig 2.11 & 2.12). It is also used to assess the shear modulus associated with strains in a plane normal to the facings. When panels are loaded in bending, the core acts in shear to provide a composite action between the faces. In panels with flat faces, the core carries the entire shear force.

The testing device consists of two force application plates bonded to the faces of the specimen. The dimensions of the testing device shall be selected so that the force axis runs along the diagonal of the specimen.

In this test, the specimen is primarily stressed by a shearing force, acting along the diagonal of the specimen (Fig 2.11a and 2.11b). The resulting relative displacement of the interfaces of the specimen are measured then plotted in a force / shear deformation diagram.

Although shear testing methods differ from one standard to another, no comparison results are available in order to judge the suitability of each method. Basu[24] however, showed that shear stress - strain relationships determined

experimentally could be critically dependant on the test method used. His research adopted four alternative methods for inhomogeneous polyurethane foam core of average density of 50 Kg/m^3. (46 Kg/m^3 at the centre and 65 Kg/m^3 at the faces). A summary of the results is shown in Figure 2.13 and Table 2.3.

The four test methods may be compared as follows:

-a- Single span dynamic:

This methods consists of measuring the frequency of vibration of a simply supported beam. The beam has plane steel faces and a single mass at mid-span. This method gives the greatest value of the shear modulus. This is due to the short period of vibration. The main advantage of this test is that it gives an upper bound reference value. However, it does not provide any information regarding the upper parts of the stress - strain curve or the shear stress at failure.

-b- 4- pinned square:

This method consists of testing a square prism specimen, of side 60 mm to 100 mm, in a square steel linkage. The specimen is glued into four stiff steel plates with hinges at the corner as shown in Figure 2.14. The tensile load is then applied across the diagonals resulting in a state of pure shear in the core.

The shear stress and shear strain are calculated as follows:

$$\tau = \frac{P}{\sqrt{2 \times A}} \quad \ldots\ldots\ldots\ldots\ldots\ldots\ldots\ldots\ldots\ldots\ldots\ldots (2.13)$$

$$\delta = \frac{\sqrt{2}\ x\ U}{L} \quad \ldots\ldots\ldots\ldots\ldots\ldots\ldots\ldots\ldots\ldots\ldots\ldots (2.14)$$

Where:

A = L.H is the area of one side of the specimen.

Basu[24] claims that this method dives the most accurate value of the shear modulus and the shear strength. One of the main advantages of this method is that if the specimen length is taken equal to the depth of the panel, then the upper and lower faces of the specimen are retained and glued to one pair of the plates of the linkage, this test could be used as a test for adhesion failure between the core and the faces. For specimens with small core depths (30 mm), the specimen's length would be relatively small. Hence, deterioration in the test results is inevitable.

-c- Single span static :

This test consists of four point loading of a single beam. The deflection of the beam δ is a combination of bending deflection δ_b and the shear deflection δ_s . Subtracting the theoretical bending deflection , the shear deflection could be evaluated and hence the corresponding shear stress.

Referring to Figure 2.15, for equal loads at the third points, the deflection of the beam can be calculated as follows:

$$\delta_s = \delta - [\frac{PL^3}{28.2\ EI}] \quad \text{.....(2.15)}$$

and the shear modulus:

$$G_c = \frac{PL}{3bh\delta_s} \quad \text{.....(2.16)}$$

Where:

b: specimen width

h: specimen height

The main disadvantage of this method is that failure generally occurs as a combination of wrinkling and shear and sometimes, core crushing at the points of load. Therefore, it is not possible to determine the shear strength of the core in all cases.

-d- **Double shear test:**

This method is considered to be a refinement of the ASTM and ISO methods. The significant factor of this test is that it gives a shear modulus approximately half the value given by the other methods.

The shear stress at failure is similarly reduced. The reason for this is thought to be due to the fact that the applied shear stress is not uniform over the length of the specimen. It varies considerably between the ends and the middle.

The results obtained from the test methods described before, show that it is preferable to use either the square steel linkage or the beam tests for the determination of shear properties.

In chapter five, different shear tests were adopted. That is because if the dimensions recommended by the standards (Table 2.2), were to be considered, the test specimen would have been very large and very heavy to handle due to the weight of loading plates.

In addition to the above described tests for sandwich panels, other tests may be used to determine sandwich properties. Some of these tests are:

-a- Determination of bending strength and modulus for core material only (ISO R1209[15] and DIN 53423[25]).

-b- Test on the adhesion of faces to core (DIN 53292[26]).

-c- Bending test on sandwich construction (DIN 53293[27]).

2.8.2 Tests on complete sandwich panels:

The behaviour of sandwich elements is best defined or verified by testing complete sandwich panels. These tests are necessary in order to assess and treat some structural design problems which panels might encounter under loading. The following tests should therefore, form part of any design programme:

2.8.2.1 Tests on simply supported panels under uniformly distributed load.

This test provides the most reliable value of the core shear modulus for design purposes according to Davies[8].

The calculation of the stresses at failure (wrinkling and local buckling) involves safe approximations, regardless of the nature of the faces under compression(flat, lightly or fully profiled). The stresses at failure calculated from such tests have proved to give an economical and more reliable design.

It is necessary to note that when testing panels under compression, tests should be repeated with the panels inverted, so as to obtain the failure stresses of both faces under compression.

2.8.2.2 Tests on simply supported panels under line loads.

When a continuous panel is subjected to either distributed or temperature loading, the face in compression at an

internal support is subjected to a support force tending to compress the core and thus aggravate wrinkling. The resulting interaction between moment and point of line load is tested by simulating the behaviour of an internal support on the basis of Figure 2.16.

2.8.2.3 Tests to verify connection capacity.

Sandwich panels are fixed to the supporting structure by means of specially designed clips or other fixings. Under wind suction conditions, these fixings carry high loads. Hence, the connection capacity can be very critical. This can only be determined by testing complete panels.

Insulation material	thermal conductivity coefficient λ	Heat transfer coefficient U			
		Material thickness (mm)			
		40.00	60.00	100.00	150.00
polyurethane	0.020	0.46	0.32	0.19	0.13
phenolic resin	0.030	0.67	0.46	0.29	0.19
polystyrene	0.035	0.76	0.53	0.33	0.25
mineral fibre wool	0.040	0.85	0.60	0.37	0.26

Table 2.1 Values of λ and U for special insulating materials

Where: U is the heat transfer coefficient

$$U = \frac{1}{\frac{1}{\alpha_i} + \frac{1}{\nu} + \frac{1}{\alpha_a}}$$

$\frac{1}{\alpha_i}$, $\frac{1}{\alpha_a}$ constitute heat transfer factors between air and outside panel surface, inside panel surface and inside atmosphere respectively.

$\frac{1}{\nu} = \frac{s}{\lambda}$ material dependent factor for heat resistance.

s thickness of heat insulating material.

λ coefficient of thermal conductivity.

Test	Standard	Specimen's dimensions(mm)
Average foam density	ASTM C271-61	76 x 76 x t
	ISO R 845	Any Known volume
	DIN 53420	50 x 50 x 50 or 100 x 100 x t
Tension strength and modulus		square or round specimen
- Bond with faces	ASTM 297-61	25 x 25 minimum or 50 x 50
	DIN 53292	side length= 50
- Bond strength in direct tension	BS 5360 C6	50 x 50 (for t=12 to 25mm)
- Tensile behaviour of foam alone	ISO 1926	b= 10 ± 0.1 mm, L= 25 ± 0.1 mm
	DIN 53430	b= 10 ± 0.1 mm, L= 25 ± 0.1 mm
Shear modulus and shear strength of foam	ASTM 273-61	b > 2 t, L > 12 t
	ISO 1922	L=250 ±5, b=50 ±1,t=20 ±0.5
	DIN 53427	L=250 ±5, b=50±1, t=20 ±0.5
	DIN 53294	for t < 20: b= 50, L= 200
		for 20 <t<40: b= 100, L= 400
		for 40 <t< 60: b= 150, L= 600
		for t > 60: b= 150, L= 800
Compressive modulus and strength of foam	ASTM C365-57	square or circular specimen
		$625\ mm^2 < A_o < 10^6\ mm^2$
	ISO R 844	square or circular specimen
		$2500\ mm^2 < A_o < 23000\ mm^2$
		or prism with sides of 100 ±1
	DIN 53421	t > 12, t < 4(width)
		for t > 50, 50 x 50 x 50
		for t < 50, 50 x 50 x t
Bending test	DIN 53293	b > 2.5 t, L= 24 t
Bending strength and modulus	DIN 53423 and ISO R 1209	b= 25 ±0.25 mm L= 120 ±1.2 mm t= 20 ± 0.2 mm

Table 2.2 Summary of standard tests and specimen's dimension.

Where: t (thickness of the sandwich), A_o (cross sectional area), b (specimen's width), L (specimen's length).

Test method	Dimensions of specimen (mm x mm x mm)	Shear modulus G (N /mm^2)
A (single span dynamic)	35 x 110 x 2000	5.5
B (4-pinned square)	35 x 35 x 20	4.6
C (single span static)	35 x 140 x 1000	4.3
D (pull out test)	35 x 105 x 420	2.4

Table 2.3 Results of the four shear test methods adopted by Basu[24]

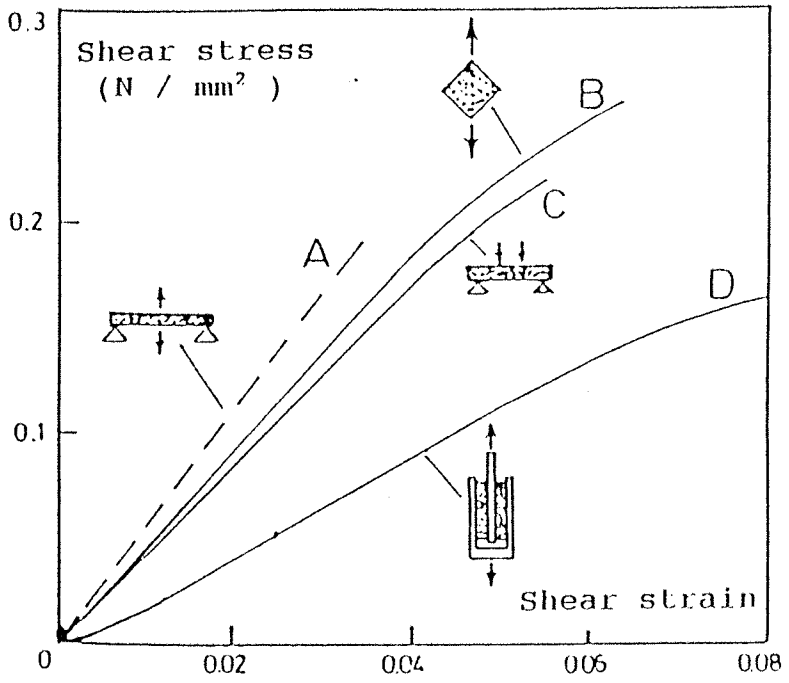

Fig 2.13 Results from alternative tests to determine the shear modulus of the core material.

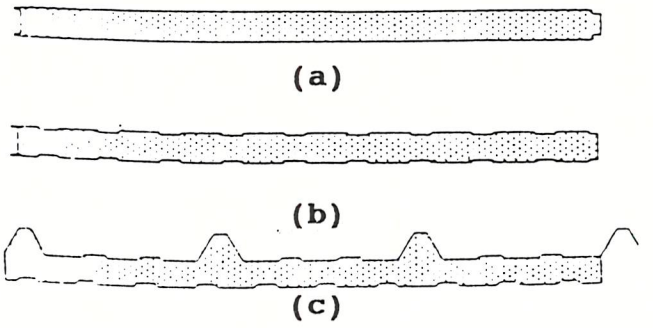

Fig 2.1 Typical cross-sections of sandwich panels.
(a) - Panel with flat faces.
(b) - Panel with lightly profiled faces.
(c) - Panel with profiled faces.

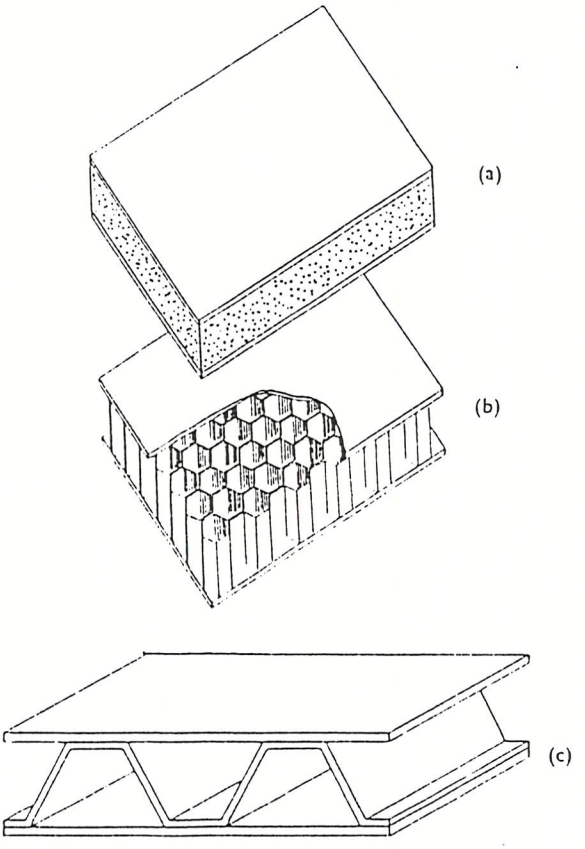

Fig 2.2 Sandwich panels with:
(a) - Expanded plastic core.
(b) - Honeycomb core.
(c) - Corrugated core.

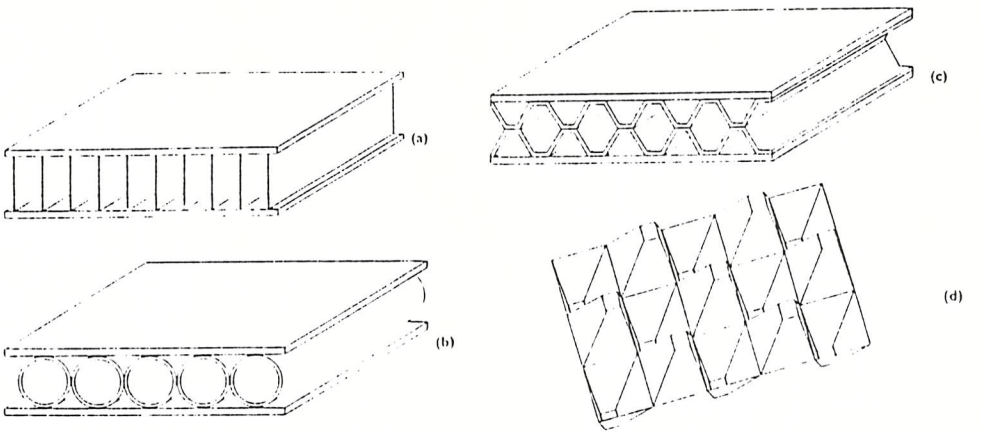

Fig 2.3 Variations of the corrugated core.

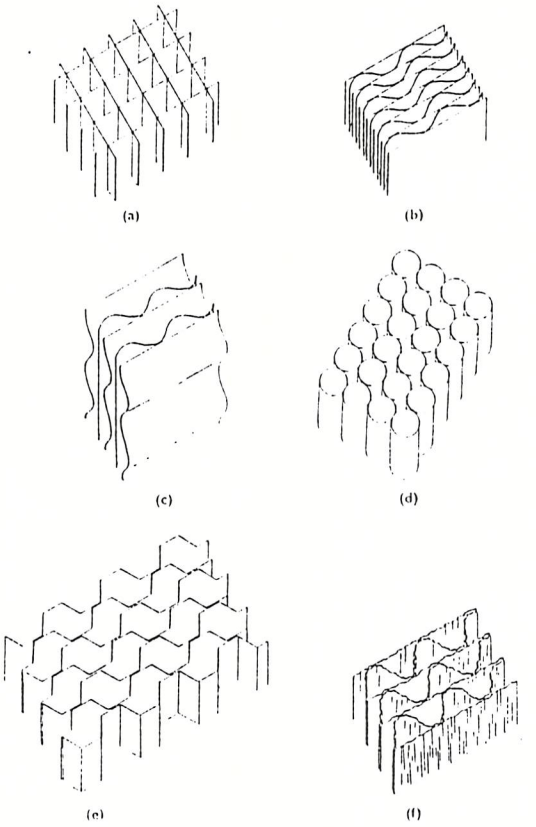

Fig 2.4 Types of honeycomb core.

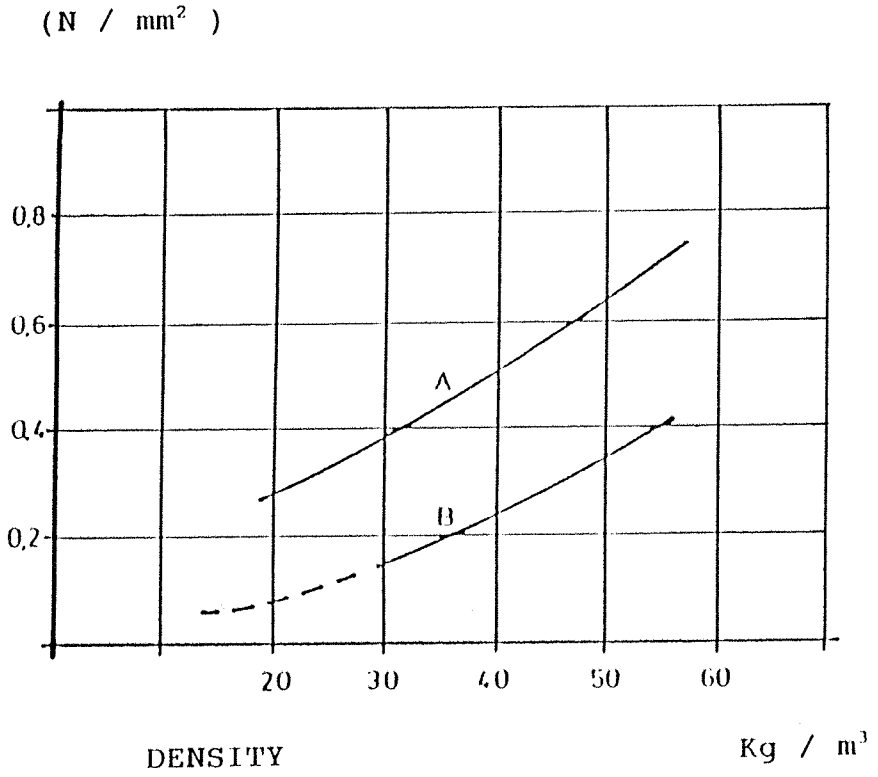

Fig 2.5 Relationship between density, tensile strength and compression strength of PUR rigid foam.
A : Tensile strength.
B : Compression strength.

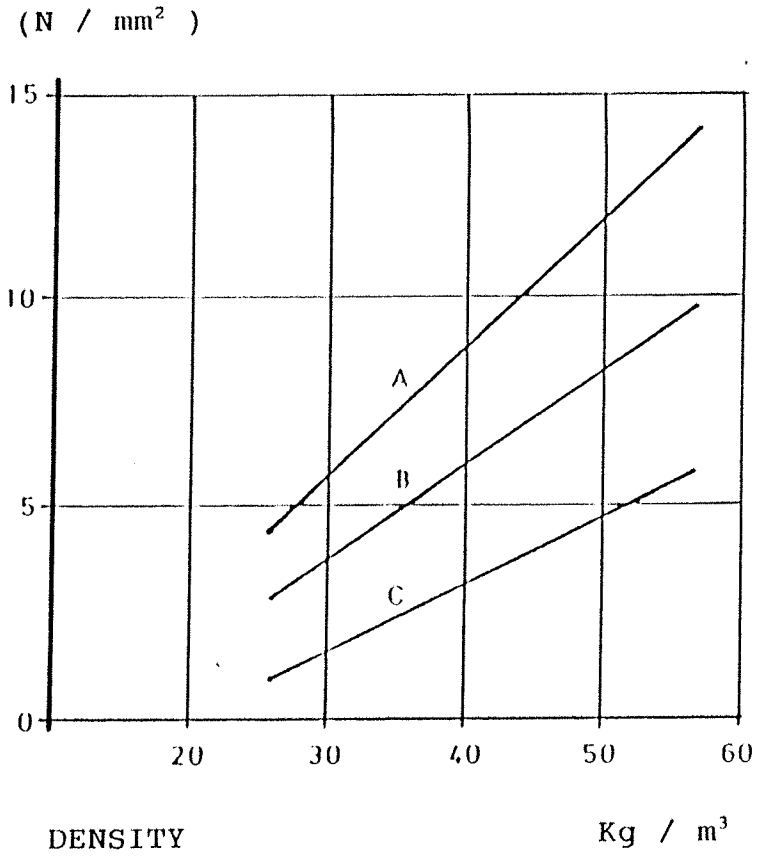

Fig 2.6 Relationship between density and moduli of elasticity of PUR rigid foam.

A : Tensile modulus.

B : Compression modulus.

C : Shear modulus.

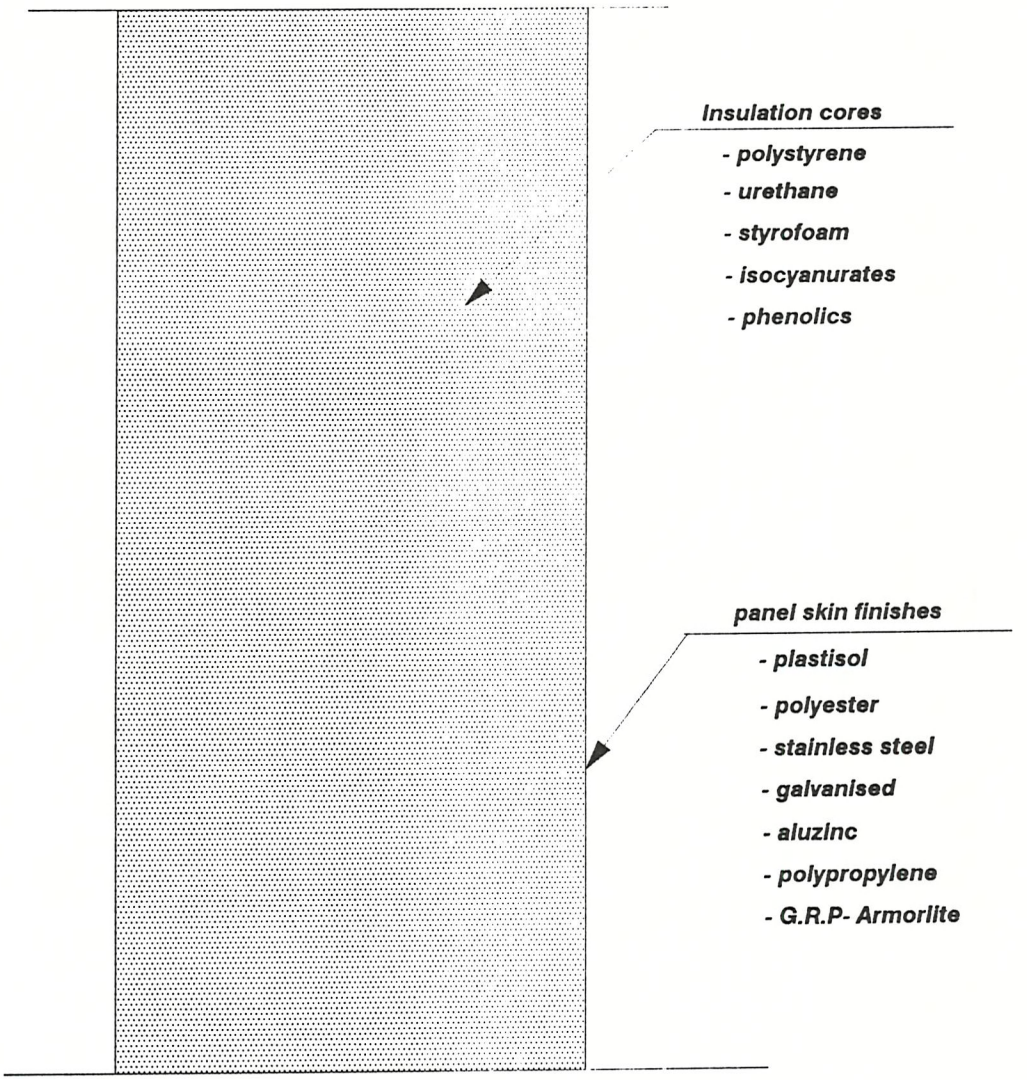

Fig 2.7 Larin panel used for cold stores

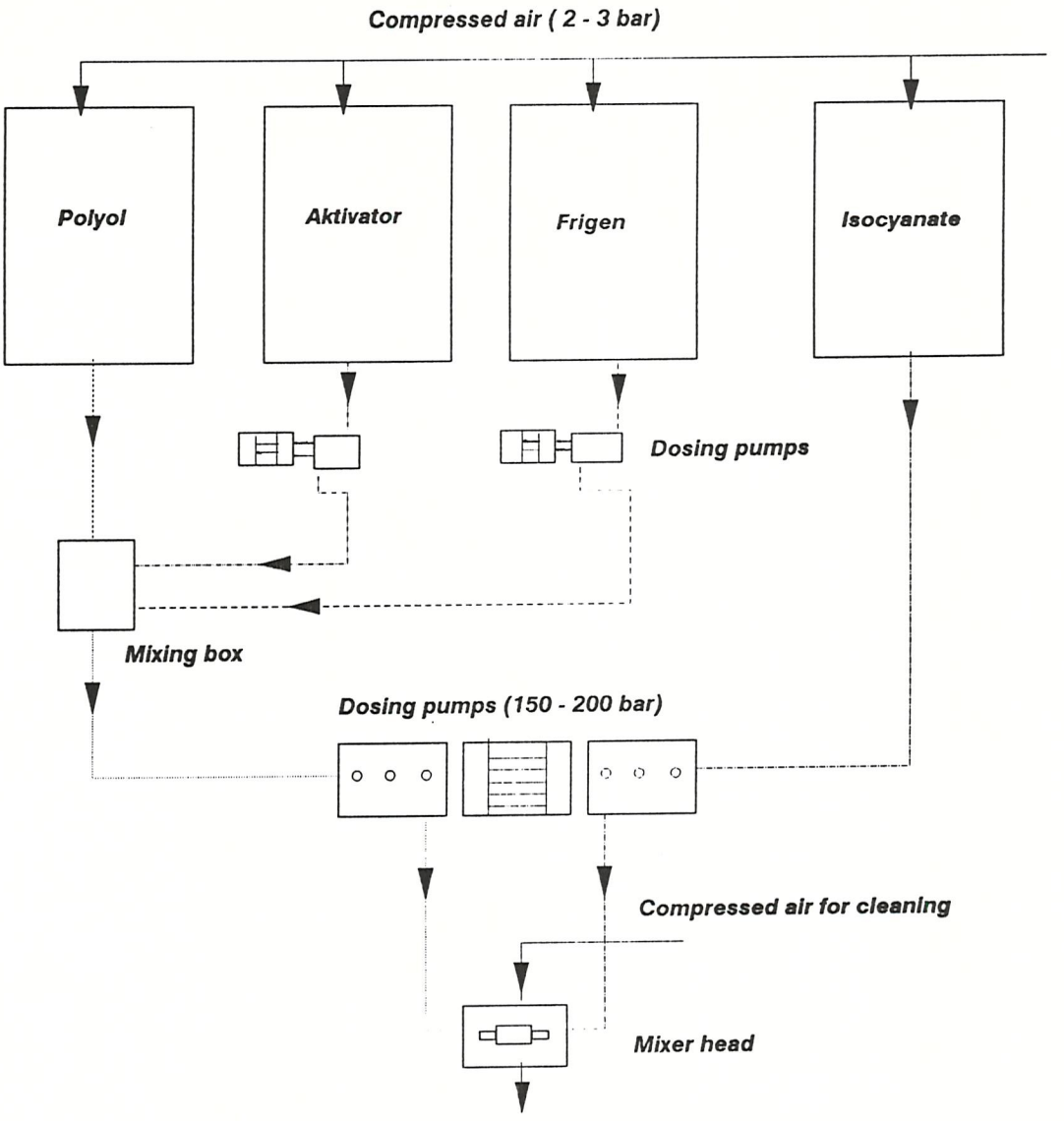

Fig 2.8 Principal foam processing with high pressure foaming equipment.

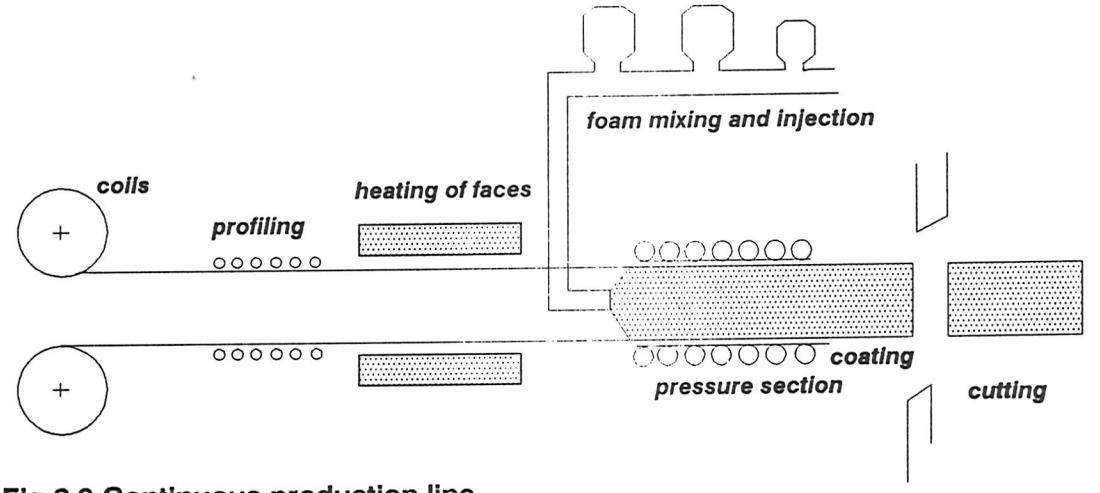

Fig 2.9 Continuous production line.

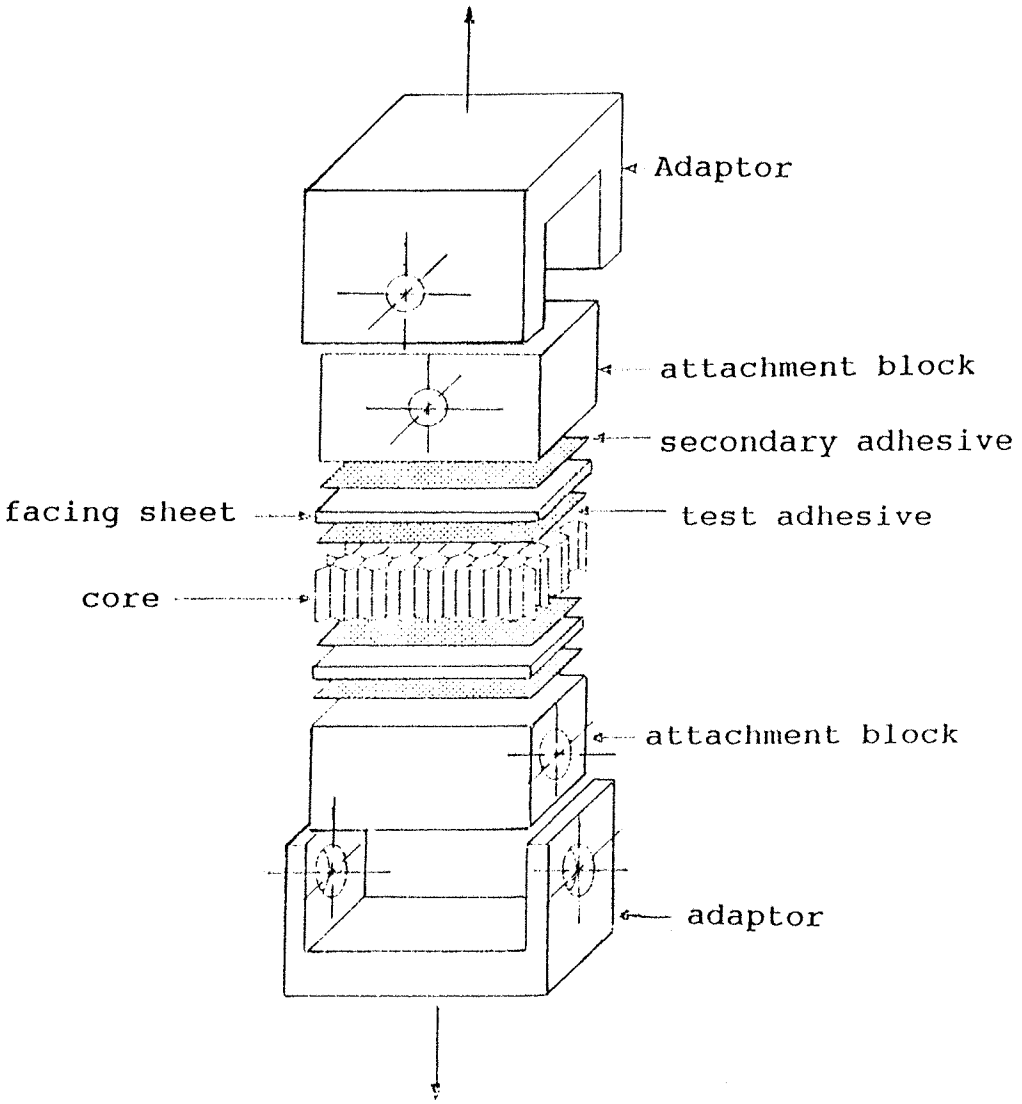

Fig 2.10 Set up of the tensile test (BS 5360 Part C6)

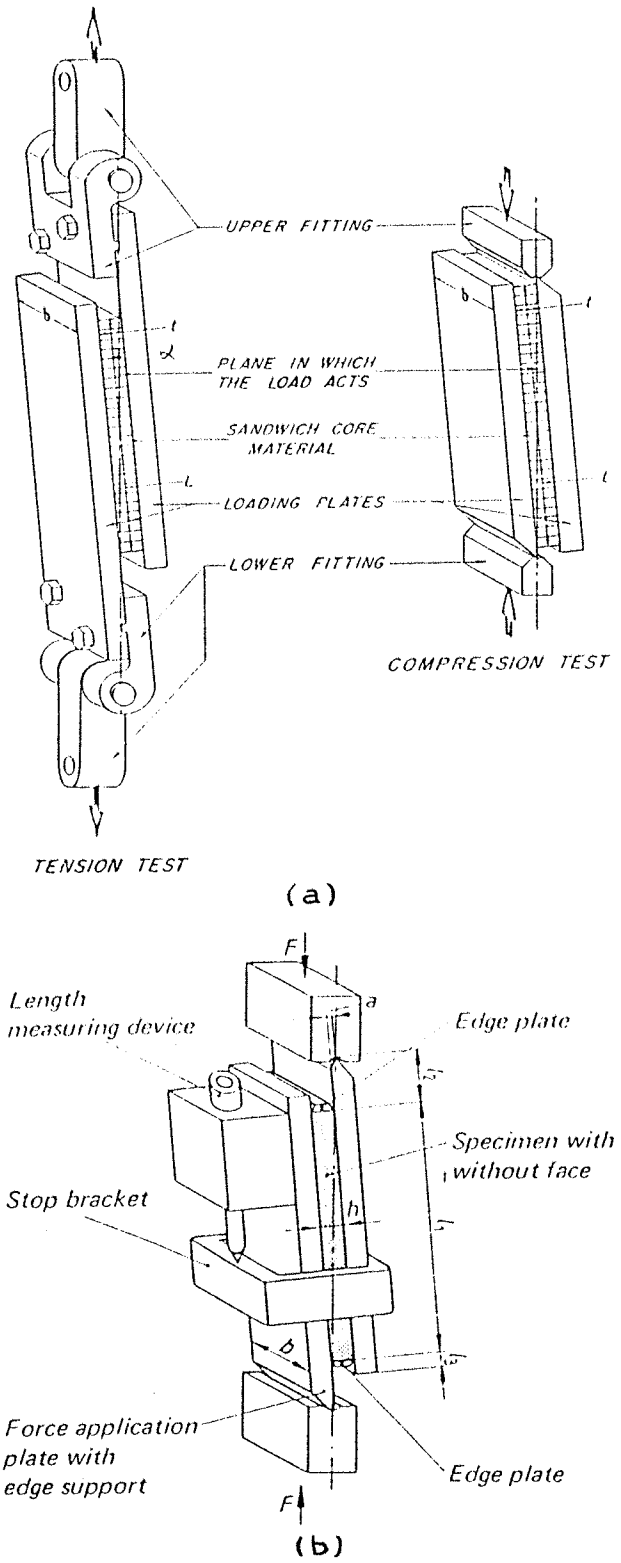

Fig 2.11 Arrangement of apparatus and test specimen for shear test.

(a) - ASTM C 273-61.

(b) - DIN 53294.

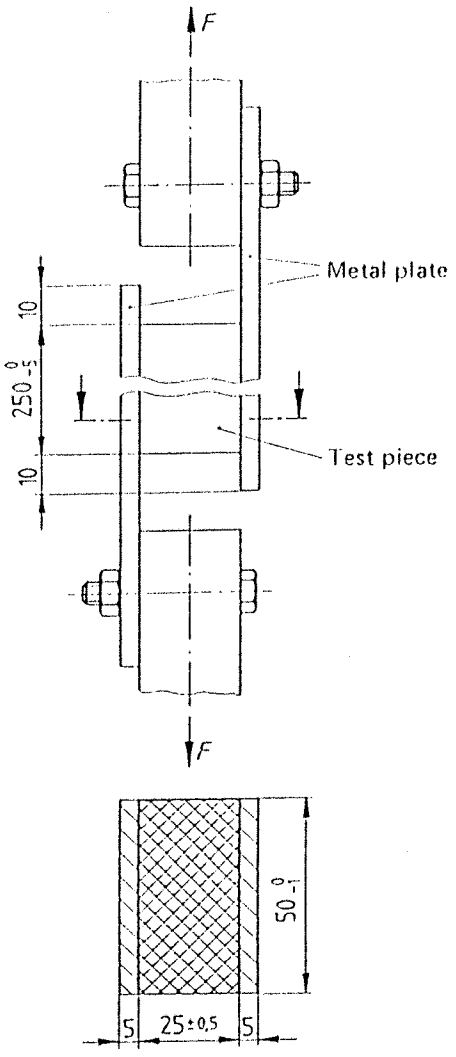

Fig 2.12 Arrangement of apparatus and test specimen for determining shear strength (DIN 53427).

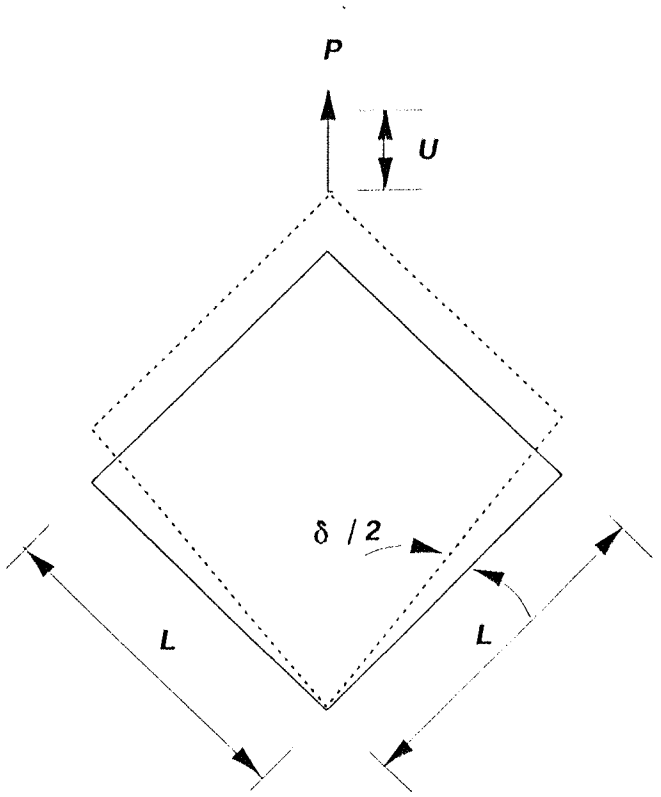

L = 60 to 100 mm

Fig 2.14 Test assembly for the four pinned square shear test

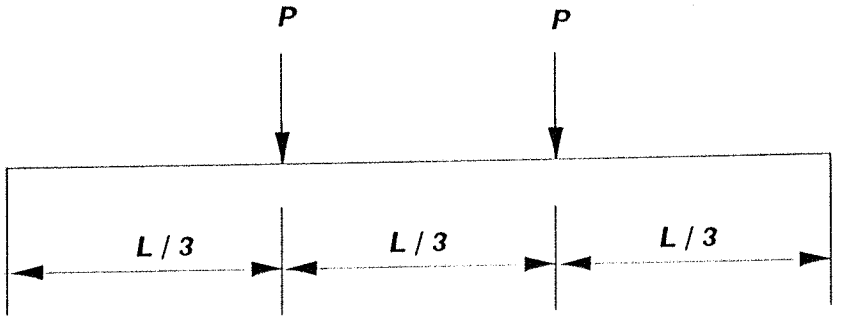

Fig 2.15 Loading of a single beam in a single span static shear test.

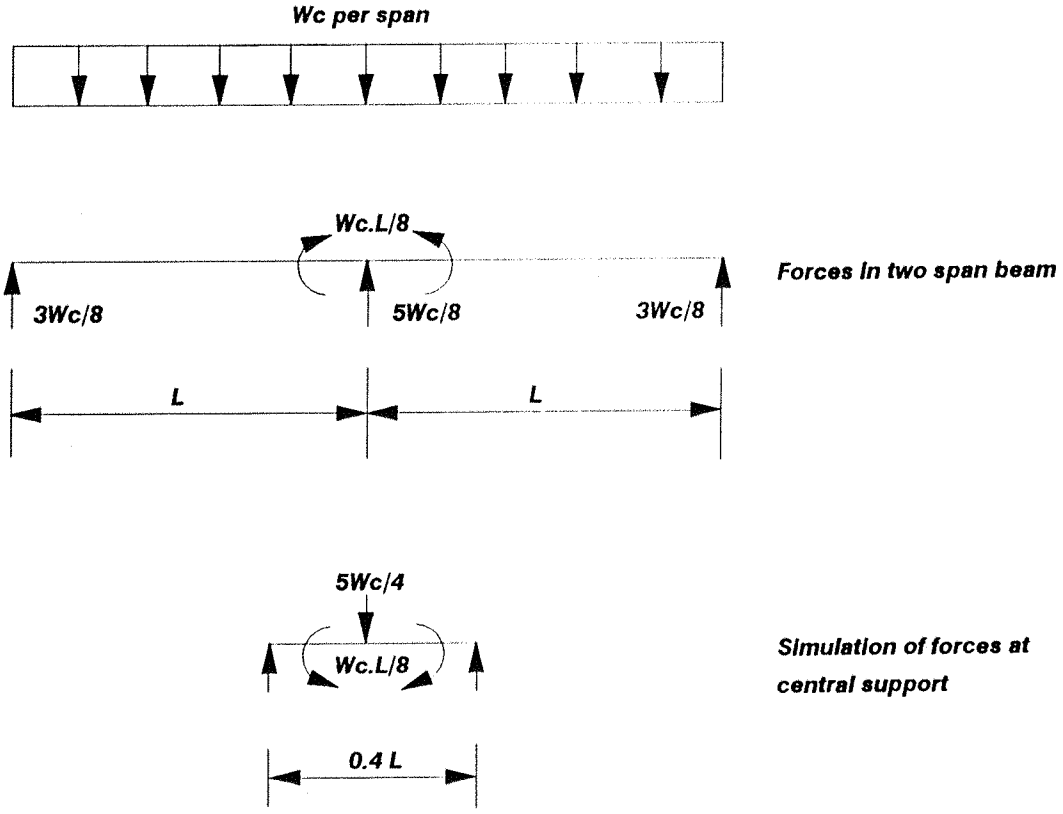

Fig 2.16 Simulated central support test.

CHAPTER THREE

ANALYTICAL DESIGN OF TWO - SPAN SANDWICH PANELS.

3.1 Introduction

The design of simply supported panels is straightforward and covered in details in many publications[2,3,5,34-38]. For panels which are continuous over two or more spans, the design becomes more complicated as it is limited by wrinkling and shear deflection at the internal supports. Few experiments have been conducted on panels for two - span conditions[39]. However, no general design theory has yet been published for multi - span panels.

The aim of this chapter is to outline the approach adopted in this research for the design of multi - span panels subjected to simulated wind load and thermal gradient. Maintaining a constant thermal gradient over a long period of time is quite impractical in a large scale test. Therefore, the deflections due to thermal gradient were reproduced by the application of a "simulated temperature load".

The design theory covered in this chapter is based on using the method of consistent deformation (section 3.4, Fig 3.4). This method assumes that the deflection of a two - span panel under a uniformly distributed load can be considered as the sum of deflections from two design cases. The first is the case a single span panel subjected to a uniformly distributed load. The second case is a single span panel subjected to an upward point load representing the central support reaction.

For each design case, an ordinary fourth order differential

equation is formulated from integrating the basic differential equations (chapter two, section 2.7.3.1).

The internal support is simulated by a sheeting rail. The deflection of the sheeting rail, which is a function of the reaction it provides to the panels, varies according to the position of the panels along the sheeting rail (end, middle, inside panels).

Final deflection equations are derived in their general form. Calculations are then made for the specific panels under consideration. Based on these derived equations, a computer program has been written (Appendix II). The results obtained from this program will be the data of the experimental work covered in Chapter Five.

3.2 Notation

Before analyzing sandwich panels, it is essential to understand the terms used in the calculations to follow.

3.2.1 Dimensions and displacements

Figure 3.1 shows the typical dimensions of a sandwich panel.

L : Span of the panel (4500 mm)
b : Panel width (1200 mm)
t : Total thickness of the panel (150 mm)
t_s : Thickness of the metal face (0.53 mm)
c : Thickness of the core = $t - 2t_s$ (148.94 mm)
d : Distance between the centroid of upper and lower faces. $d = c + t_s = \frac{t+c}{2}$ (149.47 mm)
l : Span of the sheeting rail (6000 mm)
q : Wind load (KN / m^2)
w : Total design uniformly distributed load over the

panel (KN / mm length)

w' : Uniform load simulating the temperature load. (KN / mm length)

F : Internal support reaction (KN)

M_x : Bending moment at any section x along the span

S : Shear stress due to thermal warp

K : Thermal expansion coefficient for steel (1.2 E-05 per°C)

ΔT_1 , ΔT_2 : Temperature changes of inner and outer faces respectively.

Δ : Deflection due to W at any section (mm)

Δ_{max} : Maximum deflection due to W (mm)

d_F : Deflection of the panel due to internal support reaction only (mm)

d_b : Bending deflection of the panel due to internal support reaction only (mm)

d_s : Shear deflection of the panel due to internal support reaction only (mm)

δ : Deflection of the sheeting rail due to internal support reaction (mm)

$\delta_{support} = \delta_s$: Deflection at the support of the sheeting rail (mm)

3.2.2 Material properties

E_f : Elastic modulus of face material (210 KN /mm^2)

E_c : Elastic modulus of polystyrene core material (KN / m^2)

G_c : Shear modulus of the core (N / mm^2)

Table 3.1 shows some typical physical and mechanical properties of the sandwich components.

3.2.3 Derived properties

D : Overall flexural rigidity of the cross section of the sandwich. It is equivalent to EI value of the

section treated as a beam, ignoring any effects attributable to shear deformation of the core.

$$D = E_f . \frac{b t_s^3}{6} + E_f . \frac{b t_s d^2}{2} + E_c . \frac{b c^3}{12}$$

D_f : Sum of the flexural rigidity of the two faces, considered as two separate beams not connected by the core.

$D_Q = A.G_c$: Shear stiffness of the core. It is approximately equal to the shear modulus of the core, multiplied by the cross sectional area of the core.

3.2.4 Derived properties for panels with very thin flat faces.

Metal faces of sandwich panels are considered thin or thick if they satisfy the following conditions:

- $\frac{d}{t_s} > 100$, $A = b.d$ Very thin faces
- $5.77 < \frac{d}{t_s} < 100$, $A = \frac{bd^2}{c}$ Thin faces
- $\frac{d}{t_s} < 5.77$, $A = \frac{bd^2}{c}$ Thick faces

For the sandwich panels used in this research:

$t_s = 0.53mm$, $d = 149.47mm$

$$\therefore \frac{d}{t_s} = \frac{149.47}{0.53} = 282.02 > 100$$

Therefore, the metal faces are considered very thin. The following properties should then be used in the design of the panels:

- $A = bd$: Area of the core.

- $D_Q = A.G_c = bd.G_c$:Shear stiffness of the core.

- The local bending stiffness of the faces about their own axes is small. Therefore, the term $E_f \frac{bt_s^3}{6}$ is neglected.

- The core is antiplane (i.e. $\sigma_x = \sigma_y = \tau_{xy} = 0$). Therefore, $E_c \frac{bc^3}{12}$ is neglected.

- The total flexural rigidity of the sandwich becomes:

$$D = E_f \frac{bt_s d^2}{2} = EI$$

3.2.5 Assumptions

The following assumptions are implicit in the analysis of sandwich panels:

-a- The stresses in the faces and the core in the Z-Z direction are of no importance and may be neglected.

-b- In the X - Y plane, the faces and the core are isotropic.

-c- In the X - Y plane, the core is much less stiff than the faces. Therefore, the contribution of the core to the flexural rigidity of the sandwich may be neglected. The core shear stresses at any position (x,y) are therefore independent of Z and constant throughout the depth of the core. (The core carries the entire shear force in the sandwich)

-d- Because the faces are thin in comparison with the thickness of the core, the local bending stiffness of the faces is negligible (c is considered equivalent to d)

-e- Shear deflection in the faces are neglected. This is due to the fact the faces carry no local bending moments and no local shear forces.

-f- Core strains perpendicular to the faces are neglected.

-g- 100 % efficient adhesive bonding between core and faces

so that no delamination is allowed in the test.

-h- Compression modulus of the core is not considered.

-i- Temperature does not exceed 160°F (71°C) in order to avoid melting of the polystyrene foam.

3.3 Loading

The panels, used as cladding units , are subjected to wind load and to temperature gradient between the outer and inner atmosphere. The assessment of wind load is straightforward. The thermal gradient however is more complicated. These loads are estimated as follows:

3.3.1 Wind load

The assessment of wind load is based on the British standard CP3 chapter five (wind loads)[32]. The following calculation provides a practical example of wind loads as considered in the analytical design of multi - span panels. The wind load applied to the structure is assumed to be constant for the three different core density panels under consideration.

The calculation of wind loads should be made as follows:

-a- The basic wind speed V appropriate to the location of the structure is determined in accordance with section 5.2 (CP3).
$\therefore$ $V = 46\ m/s$ The structure is assumed to be located in Sheffield.

-b- The design wind speed is determined by multiplying the basic wind speed by some factors as follows:

$$V_s = S_1 \cdot S_2 \cdot S_3 \cdot V$$

Where:

S_1 is the topographic factor. It is taken as equal to 1.0 because the average slope of the ground is assumed $\prec$ 0.05 within a kilometre radius of the site (section 5.4. CP3).

S_2 takes account of the ground roughness and the variation of wind speed with height and size of building (section 5.5. CP3)

The structure is in an area with many windbreaks. Therefore it falls in the category of ground roughness 3.
The structure is classified as class A (section 5.5. CP3)

From table 3. (CP3), $S_2 = 0.78$ *for* $H = 10\ m$
where H is the height taken to the top of the structure.

S_3 is a factor based on statistical concepts. It takes into account the degree of security and the period of time in years during which there will be exposure to wind.

Normally wind loads on completed structures and buildings should be calculated at $S_3 = 1.0$ (section 5.6. CP3). This value of S_3 is calculated for an exposure period of 50 years at a probability level of 0.63. For this building the probability that the wind speed would exceed its design value was considered to be greater than it is usual. Therefore, the design wind speed factor $S_3 = 1.13$ was based on a wind return period of 30 years with a probability level of 0.1.

$V_s = 1 \times 0.78 \times 1.13 \times 46 = 40.6\ m / s$

-c- The design wind speed is converted to dynamic pressure using the following relationship:

$$q = K V_s^2 = 0.613 \times (40.6)^2 \simeq 1012\ N / m^2$$

where $K = 0.613$ *(SI units)* (section 6. CP3)

$$\therefore\ q = 1012\ N/m^2$$

-d- The dynamic pressure is then multiplied by a pressure coefficient C_p to give the pressure p exerted at any point on the surface of the building.

$$p = C_p \cdot q$$

The resultant wind load on an element of surface acting in a direction normal to that surface is:

$$F = (C_{pe} - C_p)\, q\, A$$

Where C_{pe} is the coefficient of external pressure
C_p is the coefficient of internal pressure
A is the area of the surface

-a- External pressure coefficient :
Assume that all faces of the structure are of equal permeability except for one major opening on the face parallel to the wind direction. Wind angle for face C = 90°
$\therefore C_{pe} = 0.7$ (appendix E CP3)

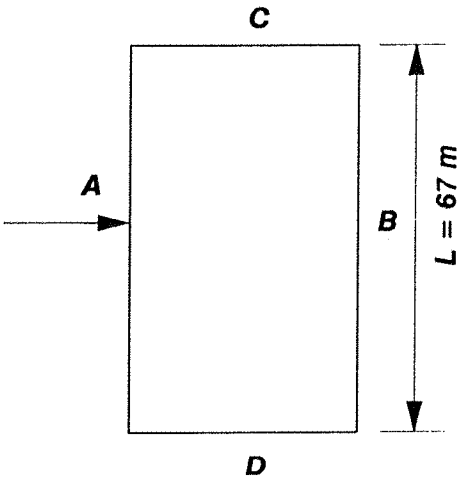

-b- Internal pressure coefficient :

For situations where a dominant opening is likely to occur as in a warehouse, C_p should be taken as 75% of the value of C_{pe} outside the opening.

$\therefore\ C_p = 0.75\ (0.7) = 0.525$

This value should be taken negative as it is acting in the same direction of the external pressure.

For walls: $C_p = -1.0$

and the pressure $p = (-1.0)\,.\,q$

For ceilings: $C_p = 0.75$, $p = 0.75\,.\,q$

The effective distributed load on the ceiling = the pressure p - the self weight of the ceiling.

Therefore, the design wind pressure on the wall panels is:

$p = (-1.0)\,.\,q = -1.012\ KN\ /\ m^2$

and the total design wind load uniformly distributed over the panels is:

$q = -1.012\ x\ 1.2 = -1.2144\ KN\ /\ m\ length$

3.3.2 Thermal warp

3.3.2.1 General theory

Temperature changes between the inner and outer faces of the panels, as well as loads, can cause deflection of panels in a structure. These changes can cause the faces to either expand or contract. If one face expands or contracts more

than the other, the panel will bow, or develop "thermal warp". Differences in thermal expansion and contraction can occur if the faces have different thermal expansion coefficients, or if the temperature change of one face differs from that of the other face. This condition is common for rigid foam filled sandwich panels because of the high insulating value provided by the core.

A complete and detailed analysis on the thermal warp of foam filled single span sandwich panels has been presented by Hartsock [41].

For panels with thin and flat faces, the temperature changes cause the panel to deflect as shown in Figure 3.2.

The following assumptions should be made in the derivation of thermal stresses equation:

-a- Thermal bowing only occurs along the length of the panel.
-b- Shear core modulus is constant and there is no side or end restraint against thermal expansion.
-c- Tensile and compressive stresses are neglected in the foam core.

Figure 3.3 shows the principle of thermal warp of panels with flat and thin faces.

The relative change in length of the faces due to thermal warp δx , over the element of length dx is:

$$\delta x = (K_2.\Delta T_2 - K_1.\Delta T_1).dx \quad \text{.....(3.1)}$$

If the panel is held flat, the core is deformed in shear. However, in sandwich panels, the resistances of the uncombined faces and core to bending are negligible.
The panel will bow until there is no shear deformation. The element of angle dA , formed by the change in length of the faces is:

$$dA = \frac{\delta x}{t} = \frac{K(\Delta T_2 - \Delta T_1) . dx}{t}$$

The angle formed by the bowing of the panel $d\theta$ is equal to dA

$$d\theta = dA = \frac{\delta x}{t}$$

$$= \frac{K(\Delta T_2 - \Delta T_1) . dx}{t}$$

Dividing both sides by dx

$$\frac{d\theta}{dx} = \frac{K(\Delta T_2 - \Delta T_1)}{t}$$

However $\frac{d\theta}{dx} = \frac{d^2y}{dx^2}$

$$\therefore \frac{d^2y}{dx^2} = \frac{K(\Delta T_2 - \Delta T_1)}{t}$$

Integrating the above equation twice gives:

$$y = \frac{K(\Delta T_2 - \Delta T_1)}{t} \left[\frac{x^2}{2}\right] + C_1 x + C_2$$

$$At\ x = \frac{L}{2}\ ,\ \frac{dy}{dx} = 0 \quad \therefore C_1 = 0$$

$$At\ x = 0\ ,\ L = 0\ ,\ y = 0 \quad \therefore C_2 = 0$$

Therefore, the deflection due to thermal warp becomes:

$$y = \frac{K(\Delta T_2 - \Delta T_1)}{t} \left[\frac{x^2}{2} - \frac{xL}{2}\right] \quad \text{.....(3.2)}$$

The deflection is maximum at x = L/2

$$\therefore y = -\frac{K(\Delta T_2 - \Delta T_1)}{t} \left[\frac{L^2}{8}\right] \quad \text{.....(3.3)}$$

It is necessary to note that for panels with thin, flat faces, no stresses are developed in the faces or the core due to thermal warp. This assumes that the thermal warp is only in one direction.

A positive deflection sign means an upward deflection, the outer face has expanded while the inner face has contracted.

3.2.2.2 Application to multiple span test samples.

Due to the fact that it is quite difficult to maintain a constant high temperature difference between the faces during the experiment, the deflection calculated above will be converted into stresses and then into uniformly distributed load acting along the panel.

For simply supported panels with thin, flat faces, Hartsock[41] assumes that no stresses are developed within the faces or core due to thermal warp. However, for multi -span panels, Davies[8] considers that the tendency of the panel to bend under temperature loads is prevented by the internal supports with the result that large support forces occur. These in turn give rise to bending moments and shear forces much larger than those arising in single span panels. It is possible for failure in multi - span panels to arise from thermal effects alone. In general, the stresses arising from temperature loading cannot be ignored and should be considered in conjunction with other relevant load cases.

It is to be noted that according to Hartsock[41] the deflection due to thermal warp does not depend on the core material density (equ 3.2).

Introduction of intermediate supports causes the full length panel which is deflecting under thermal gradient to carry the reaction point loads at the same time. These point reactions lead to significant stresses.

According to Davies[8], stresses due to thermal effects are significant for multi - span panels. This will lead to a large support reaction to negate the initially large unsupported central deflection.

It is necessary to analyze a test for which thermal gradient cannot be easily applied. However, the experimental deflections and stresses should reflect those due to both thermal and transverse loading in practice.

It is not possible to maintain both the deflection distribution and the stress distribution along the panel. Consequently, the deflections due to thermal gradient were reproduced by the application of a "simulated temperature load". Effectively, this means that the analysis is based on a sandwich in which the core is relatively stiff and would therefore introduce face stresses due to thermal gradient.

Based on the above, the simulated temperature load is calculated from the stresses assumed to be induced by the deflection due to thermal effects.

The deformation δx induces a stress of the following value:

$$S = E \cdot \frac{\delta x}{dx} \qquad \text{.....(3.4)}$$

From equation 3.1,

$$\delta x = K(\Delta T_2 - \Delta T_1) \cdot dx$$

$$\therefore S = \frac{E\,K(\Delta T_2 - \Delta T_1) \cdot dx}{dx}$$

$$\therefore S = E\,K(\Delta T_2 - \Delta T_1) \qquad \text{.....(3.5)}$$

The maximum stress in the face is obtained at t/2 from the centroidal axis of the panel. It is equal to:

$$S_f = \frac{M.E_f}{D} \cdot \left(\frac{t}{2}\right) \qquad \text{.....(3.6)}$$

For a single span panel subjected to a U.D.L (W'), the maximum stress in the faces is equal to :

$$S_f = \frac{W' L^2}{8\ t_s.b.t} \quad \text{.....(3.7)}$$

The stress calculated from equation 3.5 is the value of the stress shared between the two faces. For horizontal equilibrium, the stress in each face should be taken as 1/2 the calculated value S

By equating the two equations 3.4 and 3.7, the load which causes strains equivalent to the strains induced by the temperature gradient between the faces of the sandwich panel is then obtained.

The total design load (W) which will be considered in the analysis to follow is taken as the sum of calculated wind load (q) and the simulated temperature load (W').

3.4 Design criteria

The general theory for single span sandwich panels has been analyzed by Hartsock and Chong[38]. To analyze continuous panels, the method of consistent deformation is employed[39]. Figure 3.4 shows a schematic diagram of how this method works.

The method of consistent deformation assumes that the deflection of two - span panel under a uniformly distributed load (case I section 3.5) can be considered as the sum of deflections from two design cases: The first is the case of a single span panel subjected to a uniformly distributed load (case II, section 3.4.1.2). The second case is a single span panel subjected to an upward point load representing the central support reaction (case III, section 3.4.2).

3.4.1 Deflection of a Single span sandwich panel under uniformly distributed load.

3.4.1.1 General form:

This case analyzes the behaviour of a single span sandwich panel subjected to a uniformly distributed load. This load simulates the wind load and the equivalent load induced by the temperature gradient between the two faces of the panel. The stresses and deflections of a single span panel may be found by the use of ordinary theory of bending. The theory is based on the assumption that the cross-sections which are plane and perpendicular to the longitudinal axis of the unloaded panel remain so when bending takes place.

Allen's book[2] covers in details the analysis of single span sandwich panel. From his analysis, it can be concluded that for a single span sandwich panel of a span L subjected to a uniformly distributed load W . The deflection is composed of two contributions: One due to bending and the other to shear.

Bending deflections are due to bending action under load, where the upper face of the sandwich is compressed while the lower face is under tension.

The shear stress and strain in the core lead to another kind of deformation (shear deflection). This deformation is caused by the tilting of the faces and the longitudinal centre line of the sandwich.

The bending deflections are found in the usual way and the shear deflections by using the following general form equation[2]:

$$\Delta_{shear} = \frac{M}{AG} + constant \quad \text{.....(3.8)}$$

Thus the central deflection of the panel may be expressed as follows:

$$\Delta_{max} = \Delta bending + \Delta shear$$

In other word:

$$\Delta_{\frac{L}{2}} = \frac{5WL^4}{384D} + \frac{WL^2}{8AG_c} \quad \text{.....(3.9)}$$

The normal stresses in the faces and core are given by the following equations:

$$\sigma_f = \frac{M.z}{D}.E_f \quad (\frac{c}{2} \le z \le \frac{h}{2} \; ; \; -\frac{h}{2} \le z \le -\frac{c}{2}) \quad \text{.....(3.10)}$$

$$\sigma_c = \frac{M.z}{D}.E_c \quad (-\frac{c}{2} \le z \le \frac{c}{2}) \quad \text{.....(3.11)}$$

The maximum stresses in the faces and the core are obtained at $z = \pm \frac{t}{2}$, $\pm \frac{c}{2}$ respectively.

The shear stress in the core may be obtained from the following equation :

$$\tau = \frac{Q}{b.d} \quad \text{.....(3.12)}$$

Where Q is the shear force at the section under consideration. It is maximum at the supports where it is equal to: $Q = \frac{W.L}{2}$.

The maximum core shear stress becomes:

$$\tau_{max} = \frac{W.L}{2\ b.d} \quad \text{.....(3.13)}$$

and the shear strain which is constant throughout the depth of the core:

$$\gamma = \frac{W.L}{2\ G_c.b.d} \quad \text{.....(3.14)}$$

3.4.1.2 Deflection of single span panel subjected to the simulated wind and temperature loads (Case II).

Applying the general design theory covered in the previous section, the total deflection Δ of a single span panel subjected to a uniformly distributed load equivalent to simulated wind and temperature loads is equal to the sum of bending deflection y_b and shear deflection . y_s

Consider a sandwich panel of a span L subjected to a uniformly distributed load W, bending and shear deflections are calculated as follows:

At any position x from the support A:

$$EI\frac{d^2y}{dx^2} = -M_x = \frac{-WL}{2}x + Wx\frac{x}{2}$$

$$EIy = \int\int EI\frac{d^2y}{dx^2}$$

$$\therefore EIy = -\frac{WL}{12}x^3 + \frac{W}{24}x^4 + Ax + B$$

$$At\ x = 0\ ,\ L \quad y = 0 \quad \therefore B = 0\ ,\ A = \frac{WL^3}{24}$$

$$\therefore\ EIy = -\frac{WL}{12}x^3 + \frac{Wx^4}{24} + \frac{WL^3}{24}x \qquad \text{.....(3.15)}$$

The deflection due to shear is calculated as follows:

At any section x from support A:

$$M_x = \frac{WLx}{2} - \frac{Wx^2}{2}$$

$$y_s = \frac{M}{AG} = \left[\frac{\frac{WLx}{2} - \frac{Wx^2}{2}}{AG}\right]$$

$$\therefore\ y_s = \frac{WLx - Wx^2}{2AG} \qquad \text{.....(3.16)}$$

The combined bending and shear deflection becomes:

$$\Delta = y_b + y_s$$

$$\Delta = \frac{-WLx^3}{12EI} + \frac{Wx^4}{24EI} + \frac{WL^3x}{24EI} + \left[\frac{WLx - Wx^2}{2AG}\right] \qquad \text{.....(3.17)}$$

The deflection is maximum at mid span. It can be expressed in the following general form:

$$\Delta_{max} = \Delta_{\frac{L}{2}} = \frac{5WL^4}{384D} + \frac{WL^2}{8AG_c} \qquad \text{.....(3.18)}$$

3.4.2 Deflection distribution of a single span sandwich panel subjected to a central upward point load F (case III):

For two - span panel, the shear deflection at the internal support is difficult to predict. Therefore, this following analysis considers the case of a single span panel subjected to an upward point load representing the internal support reaction (case III of the method of consistent deformation (Fig 3.4)).

The total deflection of the sandwich panel due to an upward point load F representing the internal reaction from the sheeting rail d_F is equal to:

$$d_F = d_{bending} + d_{shear}$$

At any section x from support A:

$$EI\frac{d^2y}{dx^2} = -M_x = \frac{F}{2}x - F(x - \frac{L}{2})$$

$$EIy = \int\int EI\frac{d^2y}{dx^2} = \frac{Fx^3}{12} - \frac{F}{6}(x - \frac{L}{2})^3 + Ax + B$$

$$At\ x = 0\ ,\ y = 0 \quad \therefore \quad B = 0$$

$$At\ x = \frac{L}{2}\ ,\ y = 0 \quad \therefore \quad A = -\frac{FL^2}{16}$$

$$\therefore EId_b = \left[\frac{Fx^3}{12} - \frac{F}{6}(x - \frac{L}{2})^3 - \frac{FL^2x}{16}\right] \quad FOR\ (\frac{L}{2} \le x \le L)$$

$$EId_b = \left[\frac{Fx^3}{12} - \frac{FL^2x}{16}\right] \quad FOR\ (x \le \frac{L}{2})$$

Similarly, the shear deflection is equal to :

$$d_{shear} = d_s = \frac{M_x}{AG}$$

$$d_s = \frac{-Fx}{2AG} \qquad FOR \quad (0 \le x \le \frac{L}{2})$$

$$d_s = \left[\frac{\frac{-Fx}{2} + F(x - \frac{L}{2})}{AG} \right]$$

$$= \frac{F(x - L)}{2AG} \qquad FOR \quad (\frac{L}{2} \le x \le L)$$

The total deflection due to the point load F may be expressed in the following general form:

$$d_F = d_b + d_s$$

FOR $(\frac{L}{2} \le x \le L)$:

$$d_F = \left[\frac{Fx^3}{12EI} - \frac{F}{6EI}(x - \frac{L}{2})^3 - \frac{FL^2x}{16EI} + \frac{F(x - L)}{2AG} \right] \quad .....(3.19)$$

FOR $(o \le x \le \frac{L}{2})$:

$$d_F = \left[\frac{Fx^3}{12EI} - \frac{FL^2x}{16EI} + (\frac{-Fx}{2AG}) \right] \quad .....(3.20)$$

The deflection due to a central point load is maximum at x = L / 2 . It is equal to:

$$d_F = \frac{FL^3}{48D} + \frac{FL}{4AG} \quad .....(3.21)$$

3.4.3 Determination of load and deflection distribution on the sheeting rail.

The internal support is simulated by a sheeting rail of 6.0 m span . The reaction of this internal support is the load on the sheeting rail corresponding to each panel along the span of the rail. The sandwich panels considered in this research are 1.2 m wide, therefore five panels run across the span of the sheeting rail.

The deflection of the sheeting rail, which is a function of the reaction it provides to the panels according to the position of the panels along the sheeting rail (end, inside and middle panels). Therefore, the load on the sheeting rail should be distributed in a way so that the deflection δ at points a, b, c, d, e (Fig 3.5), is equivalent to the total central deflection on the panel (i.e deflection due to total design load W and deflection due to the internal support reaction from the sheeting rail $\Delta_{max} - d_F$). In order to achieve the above condition the load distribution should be considered as shown in Figure 3.6

Before analyzing the load distribution on the sheeting rail, it is necessary to study the behaviour of the sheeting rail under various loading cases and to derive the corresponding deflection equations.

3.4.3.1 Deflection distribution of the sheeting rail in case of the load acting only on the middle panel (panel 3).

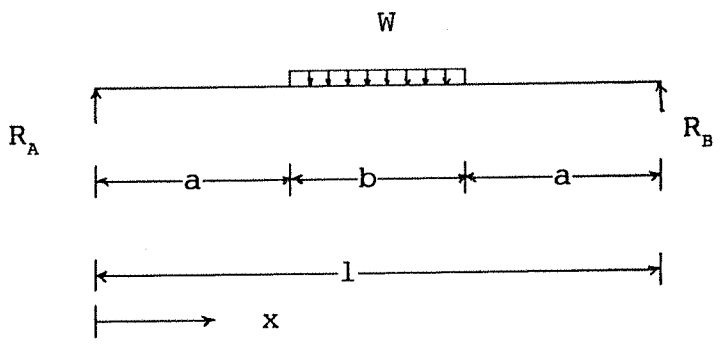

For a uniformly distributed load acting on the middle panel as shown in the figure above, the support reactions are

equal to: $R_A = R_B = \frac{W.b}{2}$

For $x \leq a$:

$$M_x = R_A.x = -EI\frac{d^2y}{dx^2}$$

$$EI\frac{d^2y}{dx^2} = -M_x = \frac{-W.b}{2}.x$$

$$EI\frac{dy}{dx} = \frac{-W.b}{2}.\frac{x^2}{2} + A$$

$$EIy = \frac{-W.b}{12}.x^3 + A.x + B$$

$$at \quad x = 0, \qquad y = 0 \qquad \therefore B = 0$$

For $a \leq x \leq (a+b)$

$$M_x = -EI\frac{d^2y}{dx^2} = -R_A.x + W(x-a)\left(\frac{x-a}{2}\right)$$

$$EI\frac{d^2y}{dx^2} = \frac{-W.b}{2}.x + W\frac{(x-a)^2}{2}$$

$$EI\frac{dy}{dx} = \frac{-W.b}{4}.x^2 + \frac{W(x-a)^3}{6} + D$$

$$EIy = \frac{-W.b}{12}.x^3 + \frac{W(x-a)^4}{24} + Dx + E$$

At mid span $x = \frac{l}{2}$, $\frac{dy}{dx} = 0$

$$\therefore EI\frac{dy}{dx} = \frac{-W.b}{4}.x^2 + \frac{W(x-a)^3}{6} + D = 0$$

$$\therefore 0 = \frac{-W.b}{4}.\left(\frac{l}{2}\right)^2 + \frac{W}{6}\left(\frac{l}{2} - a\right)^3 + D$$

$$but \quad \frac{l}{2} - a = \frac{b}{2}$$

$$\therefore 0 = \frac{-W.b.l^2}{16} + \frac{W}{6}\left(\frac{b}{2}\right)^3 + D$$

$$\therefore D = \frac{Wbl^2}{16} - \frac{Wb^3}{48}$$

$$\therefore D = \frac{Wb}{48}(3l^2 - b^2)$$

<u>*At x = a*</u>

$$\left.\frac{dy}{dx}\right|_{x \le a} = \left.\frac{dy}{dx}\right|_{x \ge a}$$

$$\therefore \left[\frac{-Wbx^2}{4} + A\right]_{x \le a} = \left[\frac{-Wbx^2}{4} + \frac{W(x-a)^3}{6} + D\right]_{x \ge a}$$

$$\therefore \frac{-Wba^2}{4} + A = \frac{-Wba^2}{4} + \frac{W(a-a)^3}{6} + \frac{Wb}{48}(3l^2 - b^2)$$

$$\therefore A = \frac{Wb}{48}(3l^2 - b^2)$$

<u>*At x = a :*</u>

$$\left.y\right|_{x \le a} = \left.y\right|_{x \ge a}$$

$$\left[\frac{-Wbx^3}{12} + A.x\right]_{x \le a} = \left[\frac{-Wbx^3}{12} + \frac{W(x-a)^4}{24} + D.x + E\right]_{x \ge a}$$

$$\frac{-Wba^3}{12} + \frac{Wb(3l^2 - b^2)a}{48} = \frac{-Wba^3}{12} + \frac{W(a-a)^4}{24} + \frac{Wb(3l^2 - b^2)a}{48} + E$$

$\therefore E = 0$

The deflection equations for $x \le a$, $(a+b) \le x \le l$ may be expressed as follows:

$$EI.y = \frac{-Wbx^3}{12} + \frac{wb(3l^2 - b^2)}{48}x$$

FOR ($x \le a$)

$$EI.y = \frac{Wb}{48}[-4x^3 + x(3l^2 - b^2)]$$

FOR ($a + b \le x \le l$)

$$EI.y = \frac{Wb}{48}[-4(l - x)^3 + (l - x)(3l^2 - b^2)]$$

The deflection equation for $a \le x \le (a+b)$ is expressed in the following:

$$EI.y = \left[\frac{-Wbx^3}{12} + \frac{W(x - a)^4}{24} + \frac{Wb(3l^2 - b^2)}{48}x\right]$$

FOR ($a \le x \le a + b$)

$$EI.y = \frac{W}{48}[-4bx^3 + 2(x - a)^4 + b(3l^2 - b^2)x]$$

$$\underline{At\ x = \frac{l}{2}}$$

$$EIy_{max} = \frac{W}{48}\left[\frac{-4bl^3}{8} + 2\left(\frac{l}{2} - a\right)^4 + \frac{bl(3l^2 - b^2)}{2}\right]$$

$$but\ \ \frac{l}{2} - a = \frac{b}{2}$$

$$EIy_{max} = \frac{W}{48}\left[\frac{-bl^3}{2} + \frac{2b^4}{16} + \frac{3bl^3}{2} + \frac{b^3 l}{2}\right]$$

$$EIy_{max} = \frac{Wb}{384}\left[8l^3 + b^3 - 4b^2 l\right] \qquad .....(3.22)$$

The deflection equation may be expressed in the following general form:

$$EI.y = \left[\frac{-Wbx^3}{12} + \frac{Wb(3l^2 - b^2)}{48}x\right]_0^a$$

$$+ \left[\frac{-Wbx^3}{12} + \frac{W(x - a)^4}{24} + \frac{Wb(3l^2 - b^2)}{48}x\right]_a^{(a+b)}$$

$$+ \left[\frac{-Wb(l - x)^3}{12} + \frac{Wb(3l^2 - b^2)}{48}(l - x)\right]_{(a+b)}^{l} \qquad .....(3.23)$$

3.4.2.2 Deflection distribution of the sheeting rail in case of the load acting on one of the end panels (panel 1 or 5).

-a- Case of the load acting on panel 1:

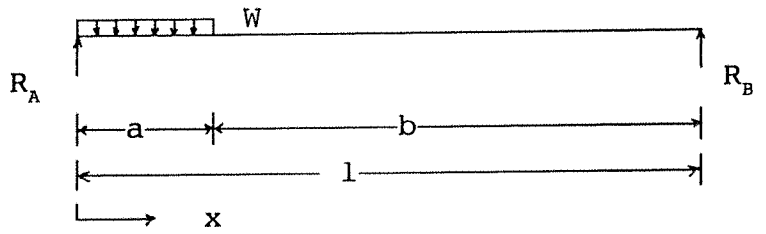

a is the loaded span

$$R_A = \frac{Wa}{2l}(2l - a)$$

$$R_B = \frac{Wa^2}{2l}$$

$$x_0 = \frac{R_A}{W} = \frac{a(2l - a)}{2l} \quad \textit{Point of max moment}$$

<u>*At $x \le a$*</u>

$$M_x = -EI\frac{d^2y}{dx^2} = \frac{-Wa(2l - a)}{2l}x + \frac{Wx^2}{2}$$

$$EI\frac{dy}{dx} = \frac{-Wa(2l - a)}{2l}\frac{x^2}{2} + \frac{Wx^3}{6} + A$$

$$EIy = \frac{-Wa(2l - a)}{2l}\frac{x^3}{6} + \frac{Wx^4}{24} + Ax + B$$

$$at \quad x = 0, \quad y = 0 \quad \therefore B = 0$$

<u>*At $x \ge a$*</u>

$$M_x = -EI\frac{d^2y}{dx^2} = -R_B(l - x) = -\frac{Wa^2(l - x)}{2l}$$

$$EI\frac{dy}{dx} = \frac{-Wa^2}{2}x + \frac{Wa^2}{2l}\frac{x^2}{2} + D$$

$$EIy = \frac{-Wa^2}{4}x^2 + \frac{Wa^2}{12l}x^3 + Dx + E$$

$$AT\ x = l\ ,\ y = 0$$

$$\therefore\ 0 = \frac{-Wa^2l^2}{4} + \frac{Wa^2l^2}{12l} + Dl + E$$

$$\therefore\ E = \frac{Wa^2l^2}{6} - Dl$$

<u>*At x = a*</u>

$$EI\frac{dy}{dx}|x \leq a = EI\frac{dy}{dx}|x \geq a$$

$$\frac{-Wa(2l - a)}{2l}\frac{a^2}{2} + \frac{Wa^3}{6} + A = \frac{-Wa^2}{2}a + \frac{Wa^2}{4l}a^2 + D$$

$$\frac{-Wa^3}{2} + \frac{Wa^4}{4l} + \frac{Wa^3}{6} + A = \frac{-Wa^3}{2} + \frac{Wa^4}{4l} + D$$

$$\therefore\ A = D - \frac{Wa^3}{6}$$

$$E = \frac{Wa^2l^2}{6} - Dl$$

$$\therefore\ E = \frac{Wa^2l^2}{6} - \frac{Wa^2}{24l}(4l^2 + a^2)l$$

$$\therefore\ E = -\frac{Wa^4}{24}$$

$$A = D - \frac{Wa^3}{6}$$

$$\therefore\ A = \frac{Wa^2}{24l}(4l^2 + a^2) - \frac{Wa^3}{6}$$

$$\therefore\ A = \frac{Wa^2}{24l}[2l - a]^2$$

Therefore, the deflection at any section $x \leq a$ can be calculated from the following equation:

$$EIy = \frac{-Wa(2l - a)}{2l}\frac{x^3}{6} + \frac{Wx^4}{24} + \frac{Wa^2(2l - a)^2}{24l}x$$

$$EIy = \frac{-Wa(2l - a)}{12l}x^3 + \frac{Wx^4}{24} + \frac{Wa^2(2l - a)^2}{24l}x$$

$$EIy = \frac{W}{24l}[-2a(2l - a)x^3 + x^4l + a^2(2l - a)^2x]$$

$$EIy = \frac{Wx}{24l}[-2a(2l - a)x^2 + x^3l + a^2(2l - a)^2]$$

At any section where $x \geq a$, the deflection may be calculated using the equation below:

$$EIy = \frac{-Wa^2x^2}{4} + \frac{Wa^2x^3}{12l} + \frac{Wa^2(4l^2 + a^2)x}{24l} - \frac{Wa^4}{24}$$

$$EIy = \frac{Wa^2}{24l}[-6lx^2 + 2x^3 + x(4l^2 + a^2) - a^2l]$$

$$EIy = \frac{Wa^2(l-x)}{24l}[4xl - 2x^2 - a^2]$$

At mid span point where $x = \frac{l}{2}$ the deflection can be expressed as follows:

$$EIy = \frac{Wa^2}{24l}(l - \frac{l}{2})[4.\frac{l}{2}.l - 2\frac{l^2}{4} - a^2]$$

$$EIy = \frac{Wa^2}{24l}(\frac{l}{2})[2l^2 - \frac{l^2}{2} - a^2]$$

$$EIy = \frac{Wa^2}{96}[3l^2 - 2a^2] \qquad \text{.....(3.24)}$$

The above equations may be summarized in a general equation of the form:

$$EIy = \left[\frac{Wx}{24l}\left[-2a(2l - a)x^2 + x^3 l + a^2(2l - a)^2\right]\right]_0^a$$

$$+ \left[\frac{Wa^2}{24l}(l - x)(4xl - 2x^2 - a^2)\right]_a^l \qquad \text{.....(3.25)}$$

-b- Case of the load acting on panel 5:

If the load is acting at the other end B of the span (on panel 5), the support reactions becomes:

$$R_A = \frac{Wa^2}{2l} \ , \ R_B = \frac{Wa}{2l}(2l - a)$$

and the deflection equation becomes:

$$EIy = \left[\frac{W(l - x)}{24l}\left[-2a(2l - a)(l - x)^2 + (l - x)^3 l + a^2(2l - a)^2\right]\right]_b^l$$

$$+ \left[\frac{Wa^2 x}{24l}\left[4(l - x)l - 2(l - x)^2 - a^2\right]\right]_0^b$$

3.4.3.3 Deflection distribution of the sheeting rail in case of the load acting on panels 2 or 4.

-a- Case of the load acting on panel 2:

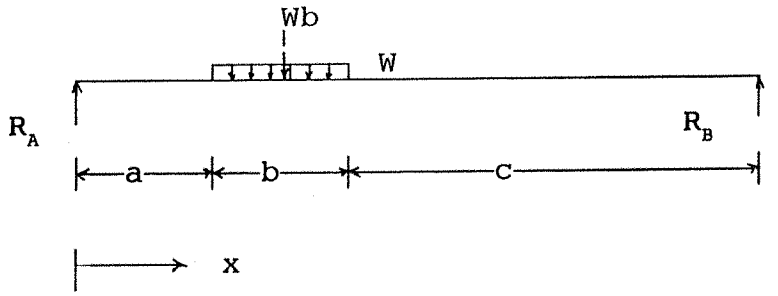

$$R_A = \frac{Wb}{l}\left(c + \frac{b}{2}\right) \quad , \quad R_B = \frac{Wb}{l}\left(a + \frac{b}{2}\right)$$

$$\text{Where} \quad c + \frac{b}{2} = n \quad , \quad a + \frac{b}{2} = m$$

The load W acting over span b may be considered as equal to the sum of the two cases as shown in the figure below:

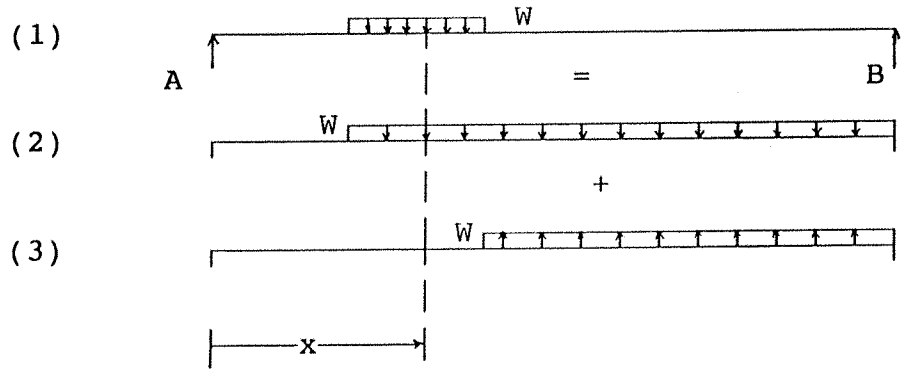

$$\text{For } x \le a : \quad M_x = R_A . x$$

$$\text{For } a \le x \le (a+b) : \quad M_x = R_A . x - \frac{W(x-a)^2}{2}$$

$$\text{For } x \ge (a+b) : \quad M_x : R_A . x - \frac{W(x-a)^2}{2} + \frac{W(x-a-b)^2}{2}$$

$$EI\frac{d^2y}{dx^2} = -M_x = -R_A . x + \left[\frac{W(x-a)^2}{2}\right] - \left[\frac{W(x-a-b)^2}{2}\right]$$

$$EI\frac{dy}{dx} = -R_A\frac{x^2}{2} + \left[\frac{W(x-a)^3}{6}\right] - \left[\frac{W(x-a-b)^3}{6}\right] + A$$

The terms in both brackets are omitted when $x \le a$ while only the second bracket is omitted when $a \le x \le (a+b)$.

Integrating once more:

$$EIy = -R_A\frac{x^3}{6} + \left[\frac{W(x-a)^4}{24}\right] - \left[\frac{W(x-a-b)^4}{24}\right] + A.x + B$$

For $x = 0$, $y = 0$, $\therefore \quad B = 0$

For $x = l$, $y = 0$

$$\therefore \quad 0 = -R_A\frac{l^3}{6} + \left[\frac{W(l-a)^4}{24}\right] - \left[\frac{W(l-a-b)^4}{24}\right] + Al$$

BUT $R_A = \frac{Wbn}{l}$, $(l-a) = b + c$, $(l-a-b) = c$

$$\therefore \quad 0 = \frac{-Wbn}{l}\left(\frac{l^3}{6}\right) + \frac{W(b+c)^4}{24} - \frac{Wc^4}{24} + Al$$

$$0 = \frac{-Wbnl^2}{6} + \frac{Wb^3}{24}(b + 4c) + \frac{Wc^2b}{24}(4c + 6b) + Al$$

BUT $\frac{b}{2} + c = n$, $\quad \therefore \quad b + 2c = 2n$

$$0 = \frac{Wb}{24l}\left[-4nl^2 + b^2(2n + 2c) + c^2(4n + 4b)\right] + A$$

$$\therefore \quad A = \frac{-Wb}{24l}\left[-4nl^2 + b^2(2n + 2c) + c^2(4n + 4b)\right]$$

Rearranging the above equation:

$$A = \frac{-Wbn}{24l}\left[-4l^2 + 2b^2 + 4c^2 + 4bc\right]$$

BUT $l = a + b + c$

$$\therefore A = \frac{-Wbn}{24l}\left[-4(a + b)^2 - 8c(a + \frac{b}{2}) + 2b^2\right]$$

Rearranging again for $(a + \frac{b}{2}) = m$, the above equation becomes:

$$A = \frac{Wbn}{24l}\left[4m(n + l) - b^2\right]$$

To summarize the above equations, the deflection at any section x from A can be calculated from the general equation of the following form:

$$EIy = \frac{-Wbn}{6l}(x^3) + \left[\frac{W}{24}(x - a)^4\right] - \left[\frac{W}{24}(x - a - b)^4\right]$$

$$+ \frac{Wbn}{24l}\left[4m(n + l) - b^2\right] x \qquad .....(3.26)$$

-b- Case of the load acting on panel 4:

If the load is acting on panel 4, using the same procedure as for panel 2, the deflection equation may be expressed in the following general form:

$$EIy = \frac{-R_A(l - x)^3}{6} + \left[\frac{W(l - x - a)^4}{24}\right] - \left[\frac{W(l - x - a - b)^4}{24}\right]$$

$$- \frac{Wbn}{24l}\left[4m(n + l) - b^2\right](l - x)$$

The terms in the second and third brackets are omitted when $x \geq (b + c)$, $(l - x) \leq a$.

Only the term in the third bracket is omitted when

$c \leq x \leq (c + b)$, $a \leq (l - x) \leq (a + b)$.

Where $R_A = \frac{Wbn}{l}$ is the reaction of the support nearest to

the load as shown in the figure below:

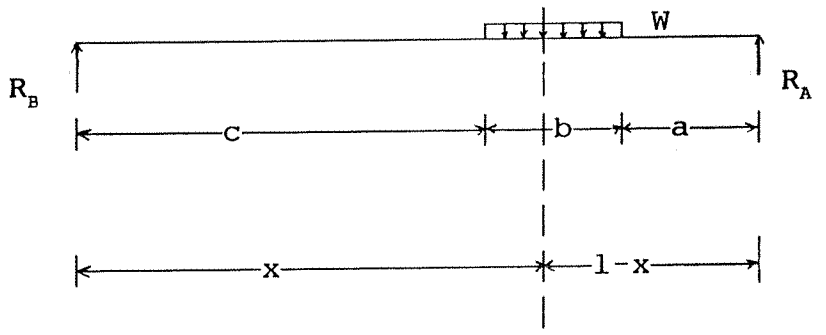

All the equations derived in section 3.4 are in their general form. These equations will be the base for the written computer program (Appendix II). The deflections along the span of the sandwich panels are calculated for cases II and III using the equations derived in sections 3.4.1.2 and 3.4.2 respectively.

The deflection of a two - span sandwich panel (case I) is then determined by adding the deflection values obtained from cases II and III. The deflection results obtained from these calculations will be plotted into graphs along the span of the sandwich panel. These graphs will be the design data for the experimental work adopted in Chapter Five.

Three different core density sandwich panels (16 oz/ft^3, 18 oz/ft^3, 20 oz/ft^3) are to be designed and tested in this work. Therefore, all calculations will be made for each of these panels and all graphs will be plotted accordingly.

3.5 Calculations (case I):

3.5.1 Evaluation of simulated temperature load:

Based on the equations derived in section 3.3.2.2, the simulated temperature load is assessed.

Using equation 3.1, the relative change in length of the

faces due to thermal warp is calculated as follows:

$$\delta x = K(\Delta T_2 - \Delta T_1).dx$$

$$\delta x = 1.2\ E\text{-}05\ (-28-65.5).dx$$

Where

$K_1 = K_2 = K = 1.2\ E\text{-}05$ are the coefficient of thermal expansion of the outer and inner steel faces.

ΔT_1 , ΔT_2 are the respective changes in temperature.

$\Delta T_1 = 65.5°C$, $\Delta T_2 = -28°C$

The central deflection due to thermal warp calculated from equation 3.3 becomes:

$$y = \frac{-1.2\ E\text{-}05(-28 - 65.5)}{8\ (150)}.(4500)^2$$

$$\therefore y = 18.93\ mm$$

The positive sign is due to an upward deflection, the outer face has expanded while the inner face has contracted.

If stresses in the faces and core are considered insignificant due to thermal effects, the simulated temperature load is calculated from equation 3.9 (section 3.4.1.2) as the load which gives the same central deflection as that estimated above from equation 3.3.

Using equation 3.9, the uniformly distributed load for each of the three different core density panels is equal to:

For the first panel: $W' = 2.645\ E\text{-}03\ KN / mm\ length$

For the second panel: $W' = 2.632\ E\text{-}03\ KN / mm\ length$

For the third panel: $W' = 1.912\ E\text{-}03\ KN / mm\ length$

It is clear from the above calculated loads that they depend on the core material density. These loads do not really simulate the thermal effects, as they contradict the theory that deflection due to thermal effects doe not depend on the core material density. Therefore, a "simulated temperature load" is assessed based on the assumption made in section 3.3.2.2 in which the core is considered stiff and would introduce face stresses due to thermal gradient.

The stress in the face S_f is considered as equal to 1/2 the value calculated S from equation 3.5 for horizontal equilibrium. Hence:

$$S = E\,K(\Delta T_2 - \Delta T_1)$$

$$\therefore S = -0.2352 \quad KN / mm^2$$

$$\text{Therefore, } S_f = \frac{(-0.2352)}{2} = -0.11765 \; KN / mm^2$$

Substituting the above calculated value in equation 3.8, the simulated temperature load is assessed as follows:

$$-0.11765 = \frac{W' L^2}{8\; t_s.b.t}$$

$$\therefore W' = \frac{8\; t_s.b.t}{L^2}.(-0.11765)$$

$$\therefore W' = \frac{8(0.53)(1200)(150)(-0.11765)}{(4500)^2}$$

$$\therefore W' = -4.434\; E\text{-}03 \; KN / mm\; length$$

The total design load is then considered as the sum of wind load (section 3.3.1) and the above calculated "simulated temperature load".

Therefore, the total design load becomes:

$W = q + W'$

$W = -1.2144\ E\text{-}03 + -4.434\ E\text{-}03$

$\therefore W = -5.6484\ E\text{-}03\ KN\ /\ mm\ length$

3.5.2 Evaluation of the deflection for design case II:

Based on the equations derived in section 3.4.1.2, the central deflection of single span sandwich panels under consideration, is assessed. The deflection values and the core shear stiffness are summarised in Table 3.2 for the three different core density panels.

For the three panels under consideration in this research, and based on the data outlined in section 3.2 of this chapter the central deflection of the panels subjected to a uniformly distributed load (case I) is calculated as follows:

$W = -5.648\ E\text{-}03\ \ KN\ /mm\ length$

$$D = E_f . \frac{b . t_s . d^2}{2} = (210) . \frac{1200\ x\ 0.53\ x\ 148.94^2}{2}$$

$D = 1.48\ E\text{+}09\ KN\ /mm^2$

$$\Delta_{max} = \frac{5WL^4}{384\ D} + \frac{WL^2}{8AG_c}$$

3.5.3 Assessment of the sheeting rail deflection :

The general form equations derived in section 3.4.3 are used to evaluate the deflection of the sheeting rail simulating the internal support. These equations are reproduced for

the specific data of section 3.2.

Appendix I summarizes the final form of equations used to derive the deflection values of the sheeting rail y1, y2, y3, y4 and y5 at points a, b, c, d, and e respectively (Fig 3.5). Deflection at these points are calculated as a function of the load F and the moment of inertia of the sheeting rail I_s . Table 3.3 summarizes the results of the above deflections.

The deflection of the sheeting rail is calculated for the case when all panels are loaded (mid, inside and end panels). In other word:

$\delta_i = \sum y_i$ When all panels are loaded.

The loads F_1 , F_2 , F_3 acting on the sheeting rail simulate the internal support reaction of the sandwich panel.

3.5.4 Evaluation of internal support reactions to satisfy the design criterion for limiting deflection:

Span/240 is the limiting deflection which will be used as a design criterion in the following calculations for the sandwich panels subjected to a uniformly distributed load and simulated temperature load.

$$\delta_{max} \leq \frac{4500}{240} \quad \therefore \delta_{max} \leq 18.75\ mm$$

The design calculations to follow in this section are made on the middle panel (panel 3) which has the largest and critical deflection.

The internal support is rigid compared to the end supports, therefore, some deflection is expected at this support.

Hence:

The deflection at mid span of the sheeting rail = total deflection at mid span of sandwich panel due to the simulated wind and temperature loads W (case II) and to the upward central point load F (case III).
In other word:

$$\delta_3 = \Delta_{\frac{L}{2}} - d_{F_3}$$

From Table 3.2, the deflection of middle panel is equal to:

$$\delta_3 = \sum y_3$$

$$\delta_3 = \frac{1}{I_s}(12514285.72\ F_1 + 33428571.42\ F_2 + 21047619.05\ F_3)$$

.....(3.27)

The mid span deflection of the middle panel due to F is:

$$d_3 = \frac{F_3 L^3}{48D} + \frac{F_3 L}{4AG}$$

$$d_3 = F_3\left(\frac{L^3}{48D} + \frac{L}{4AG}\right)$$

$$d_3 = F_3\left(1.2827 + \frac{1125}{AG}\right)$$

$$\therefore \delta_3 = \Delta_{\frac{L}{2}} - F_3\left(1.2827 + \frac{1125}{AG}\right)$$

$$\therefore F_3 = \frac{\Delta_{\frac{L}{2}} - \delta_3}{1.2827 + \frac{1125}{AG}}$$

Let us assume that $\delta_3 = \delta_{max} = 18.75\ mm$.

For end panels, the deflection at the supports is equal to zero.
Therefore, $\delta_{support} = \Delta_{\frac{L}{2}} - d_{support} = 0$.

The support load is calculated from the following equation:

$$F_{support} = F_s$$

$$0 = \Delta_{\frac{L}{2}} - F_s\left(1.2827 + \frac{1125}{AG}\right)$$

$$\therefore F_s = \frac{\Delta_{\frac{L}{2}}}{1.2827 + \frac{1125}{AG}}$$

The load distribution on the sheeting rail is assumed to be a second degree polynomial of the form shown in Figure 3.5 in order to satisfy the condition outlined in section 3.4.3.

$$F_x = F_{x1} + F_{x2}$$

$$BUT\ F_{x2} = -\frac{4Fx(l - x)}{l^2}$$

$$\therefore F_x = F_{x1} - \frac{4F(xl - x^2)}{l^2}$$

$$Where\ F_{x1} = F_s \quad , \quad F = F_s - F_3$$

Using the above assumptions and the corresponding equations, the primary values of F_1 , F_2 , F_3 , F_s are calculated and summarizes in Table 3.4 for the three different panels. Considering these initial calculated values of the loads, the moment of inertia of the required sheeting rail can be obtained.

Rearranging equation 3.27, with $\delta_3 = \delta_{max} = 18.75\ mm$ and the values of F_1 , F_2 , F_3 as shown in Table 3.4 for the sandwich panel of core density 16 oz/ft^3. The required sheeting rail has a moment of inertia equal to (35818407.82 mm^4). A channel of dimensions 229 x 89 mm is chosen, its moment of inertia is $I_s = 33900000\ mm^4$

After determining the actual moment of inertia of the sheeting rail I_s , the loads on the sheeting rail corresponding to each panel should be calculated precisely

(F_1 for end panels, F_2 for second and fourth panels and F_3 for middle panel). The loads on the sheeting rail, for which the central deflection on the sheeting rail is equivalent to the total central deflection on the sandwich panels, are equivalent to the internal support reaction on the panel.

The value of F_1 , F_2 , F_3 are initial values used to obtain the exact internal reactions which will satisfy the design condition:

$$\delta_{\frac{l}{2}} = \Delta_{\frac{L}{2}} - d_F$$

For end panels (1 & 5):

$$\delta_1 = \Delta_{\frac{L}{2}} - d_1 \qquad \text{.....(3.28)}$$

For panels 2 & 4:

$$\delta_2 = \Delta_{\frac{L}{2}} - d_2 \qquad \text{.....(3.29)}$$

For the middle panel:

$$\delta_3 = \Delta_{\frac{L}{2}} - d_3 \qquad \text{.....(3.30)}$$

Three simultaneous equations are obtained by substituting the following values in the above equations (3.28, 3.29 and 3.30).

δ_1 , δ_2 , δ_3 shown in table (3.3),

F_1 , F_2 , F_3 from table (3.4)

I_s

$\Delta_{\frac{L}{2}}$, AG from table (3.4)

The three equations can be expressed as follows:

$$\frac{1}{I_s}[4307142.857\ F_1 + 10457142.86\ F_2 + 6257142.858\ F_3]$$

$$= \Delta_{\frac{L}{2}} - F_1(1.2827 + \frac{1125}{AG})$$

$$\frac{1}{I_s}[10457142.86\ F_1 + 27278571.43\ F_2 + 16714285.71\ F_3]$$

$$= \Delta_{\frac{L}{2}} - F_2(1.2827 + \frac{1125}{AG})$$

$$\frac{1}{I_s}[12514285.72\ F_1 + 33428571.42\ F_2 + 21047619.05\ F_3]$$

$$= \Delta_{\frac{L}{2}} - F_3(1.2827 + \frac{1125}{AG})$$

Where the value of $\Delta_{\frac{L}{2}}$, AG varies from one panel to another according to the panel's core density as shown in Table 3.4.

Solving the above simultaneous equations for each panel, the exact value of the loads F_1 , F_2 , F_3 are obtained as shown in Table 3.5. Figures 3.7 to 3.9 show the load distribution on the sheeting rail corresponding to each of the three panels.

The calculated values of internal support reaction and the simulated wind and temperature loads become the data in the computer program shown in Appendix II. The results of this computer program includes the deflection of the sandwich panels under each of the design cases (case I, II and III). The results are plotted in graphs (Fig 3.10 to 3.20). These figures show the bending, shear and combined bending and shear deflections for each of the three different density

panels for load cases I, II and III.

These results will form the design data for an experimental work. The three different density panels will be tested under the design load simulated in this chapter.
Chapter Five of this research covers the experimental work adopted to test the three panels. These panels will be subjected to the simulated wind and temperature loads. Their behaviour under the load will be evaluated and the deflection along the span of the panels will be assessed.

The computational results obtained from the calculations in this chapter should later be compared with the experimental results. Comparison of both results is necessary to check whether or not the adopted design theory can be considered satisfactory for the design of multi - span sandwich panels.

3.6 Analysis of multi - span sandwich panels subjected to a uniformly distributed wind load and thermal gradient (Second analysis)

3.6.1 General form.

The calculations made in section 3.5 were based on the assumption made in section 3.3.2.2. The deflections due to thermal gradient were reproduced by the application of a "simulated temperature load". This meant that the analysis was based on the assumption that face stresses due to thermal gradient were introduced for a relatively stiff core.

Section 3.3.2.1 however, assumes that for sandwich panels with thin, flat faces, no stresses are developed in the faces or the core due to thermal gradient. Based on this assumption, the design and calculations covered in the next section will evaluate the behaviour of two - span sandwich panels subjected to :

- a - Wind load acting as a uniformly distributed load over the span of the panel.

- b - Thermal gradient between outer and inner faces of the panel.

The design theory adopted in section 3.4 (method of consistent deformation) will in this analysis consist of the following:

- Case II (a): This is the case of a single span panel subjected to a uniformly distributed load simulating the applied wind load.

- Case II (b): This is the case of a single span panel subjected to a thermal gradient between outer and inner faces of the panel.

- Case III: This is the case of a single span panel subjected to an upward central point load simulating the internal support reaction.

- Case I: This is the case of a two - span panel subjected to wind load, thermal gradient and an upward central point load. It is the sum of the three above cases.

3.6.2 Application:

The design cases outlined in the previous section are considered in details as follows:

3.6.2.1 Case of single span panel subjected to wind load (case II a).

Due to wind load (assessed in section 3.3.1), the deflection along the span of a single span panel and the maximum central deflection are calculated using equation

3.17 and 3.18 derived in section 3.4.1.2 respectively.

3.6.2.2 Case of a single span panel subjected to thermal gradient (case II b).

Due to thermal gradient, the deflection of a single span panel satisfies equation 3.2 as derived in section 3.3.2.1. The maximum central deflection is calculated from equation 3.3.

3.6.2.3 Case of a single span panel subjected to an upward central point load equivalent to the internal support reaction (case III).

For a single span panel subjected to a central point load, the deflection along the span and the mid - span deflection are calculated using equation 3.19, 3.20 and 3.21 respectively (section 3.4.2)

3.6.2.4 Case of a two - span panel subjected to wind load, thermal gradient and an upward central point load (case I).

The deflection of a two - span panel subjected to wind load, thermal gradient and central point load is calculated as the sum of the cases outlined in sections 3.6.2.1, 3.6.2.2 and 3.6.2.3.

In general form, the deflection due to cases II (a) and II (b) can be expressed by the following equation:

$$\Delta_{\frac{L}{2}} + y_{\frac{L}{2}} = \left[\frac{-qLx^3}{12EI} + \frac{qx^4}{24EI} + \frac{qL^3x}{24EI} + \frac{qLx - qx^2}{2AG}\right]$$

$$+ \left[\frac{K(\Delta T_2 - \Delta T_1)}{t}\left(\frac{x^2}{2} - \frac{xL}{2}\right)\right]$$

The mid span deflection for case III satisfies equation 3.21 (section 3.4.2).

Therefore, the total mid span deflection due to wind load, thermal gradient and internal support reaction becomes:

$$\delta = \Delta_{\frac{L}{2}} + y_{\frac{L}{2}} - d_F$$

3.6.3 Evaluation of the deflection for all design cases.

For the three different core density panels, the central deflection is calculated using equation 3.18 for the data of section 3.2.1. The results are summarized in Table 3.6.

Similarly, the mid span deflection due to thermal warp is calculated from equation 3.3. This deflection is the same for the three panels regardless of their core density. This deflection is equal to 18.93 mm.

The deflection along the span of the sheeting rail is the same as that shown in Table 3.3.

Following the same calculations of section 3.5.4, the loads on the sheeting rail are obtained for the three panels. The initial values of these loads are summarized in Table 3.6 Rearranging equation 3.27 with the limiting mid span deflection and the values of F_1 , F_2 , F_3 shown in Table 3.6, the required sheeting rail is chosen as a channel section 178 x 89 of mass 26.81 Kg/m. Its moment of inertia is equal to 17500000 mm^4.

Using equations 3.28 to 3.30 with the values of $\Delta_{\frac{L}{2}}$ taken as the sum of mid span deflections due to wind load and thermal gradient (Table 3.6), three simultaneous equations are obtained for each of the three different core density panels. The loads on the sheeting rail are calculated from these equations. The magnitude of these loads which

satisfies the design criterion for the limiting deflection are shown in Table 3.7.

3.7 Conclusion

The equations derived in section 3.5 for the first analysis have been enumerated for the panels to be tested in Chapter Five. The calculations made in section 3.6 for the second analysis however, are only considered for comparison with those of the first analysis.

Comparing the theoretical results of both first and second analyses shows that the applied loads corresponding to the first analysis are much larger than those evaluated from the second analysis. Consequently, first analysis's deflection of the panels and internal support reactions are greater than the second analysis's values.

Further calculations for shear and compressive stresses will be made in Chapter Five. These stresses will then be compared with the stresses calculated from the analysis of section 3.5 and those obtained from the experimental work of Chapter Five. Comparison of the stresses and the ratio of maximum stresses in the lower face to maximum stresses in the upper face of the panel is crucial. This comparison will assess whether or not the simulation of temperature effects can be considered satisfactory in the design of multi - span panels. It will also show the effects of the assumptions made in section 3.3.2 on the behaviour of panels subjected to either simulated temperature load or temperature gradient.

Material Properties	Steel faces	Polystyrene core		
		Panel 3	Panel 2	Panel 1
Thickness	0.53 mm	150 mm	150 mm	150 mm
Density		16 oz / ft^3	18 oz / ft^3	20 oz / ft^3
Elastic modulus	210 KN /mm^2	1500 KN / m^2	2635 KN /m^2	2665 KN / m^2
Thermal expansion	1.2 E-05 per°C	–	–	–
Shear modulus	–	2.25 N / mm^2	3.95 N / mm^2	3.99 N / mm^2
Temperature range	-28°C to 65.5°C	–	–	–

Table 3.1 Some typical material properties of the core and faces of the sandwich panels.

Panel No.	1	2	3
Core density	20 oz / ft^3	18 oz /ft^3	16 oz / ft^3
D (KN/mm^2)	1.48 E+09	1.48 E+09	1.48 E+09
G_c (KN/mm^2)	3.99 E-03	3.95 E-03	2.25 E-03
$A.G_c$ (KN)	713.125	705.976	402.138
$\Delta_{bending}$	-20.37 mm	-20.37 mm	-20.37 mm
Δ_{shear}	-20.05 mm	-20.25 mm	-35.55 mm
Δ_{max}	-40.42 mm	-40.62 mm	-55.92 mm

Table 3.2 Deflection and shear stiffness values for the three panels of various core density.

Distance x from support A along the span in mm.	Deflection δ of the sheeting rail at corresponding x in mm
Zero or 6000	$\delta_{support} = \delta_s = 0$
600 or 5400	$\delta_1 = \delta_5 = 4307142.857(F_1/I_s) + 10457142.86(F_2/I_s) + 6257142.858(F_3/I_s)$
1800 or 4200	$\delta_2 = \delta_4 = 10457142.86(F_1/I_s) + 27278571.43(F_2/I_s) + 16714285.71(F_3/I_s)$
3000	$\delta_3 = 12514285.72(F_1/I_s) + 33428571.42(F_2/I_s) + 21047619.05(F_3/I_s)$

Table 3.3 Deflection of the sheeting rail as a function of I_s and the central load of each panel.

panel	20 oz/ft^3	18 oz/ft^3	16 oz/ft^3
AG	713.125	705.976	402.138
$\Delta_{\frac{L}{2}}$	40.42 mm	40.62 mm	55.92 mm
d_3	2.860 F_3	2.883 F_3	4.080 F_3
F_s	14.13 KN	14.09 KN	13.70 KN
F_1	11.77 KN	11.75 KN	12.05 KN
F_2	8.62 KN	8.63 KN	9.84 KN
F_3	7.57 KN	7.58 KN	9.11 KN

Table 3.4 Primary values of internal support reaction corresponding to each of the three panels for the first analysis.

panel	20 oz/ft^3	18 oz/ft^3	16 oz/ft^3
F_s	14.13 KN	14.09 KN	13.70 KN
F_1	12.13 KN	12.10 KN	12.18 KN
F_2	8.97 KN	8.96 KN	9.78 KN
F_3	7.78 KN	7.80 KN	8.89 KN

Table 3.5 Final load on the sheeting rail corresponding to each sandwich panel for the first analysis.

panel	20 oz/ft^3	18 oz/ft^3	16 oz/ft^3
AG	713.125	705.976	402.138
$\Delta_{\frac{L}{2}}$	8.692 mm	8.735 mm	12.025 mm
$y_{\frac{L}{2}}$	18.93 mm	18.93 mm	18.93 mm
total $\Delta_{\frac{L}{2}}$	27.622 mm	27.665 mm	30.955 mm
d_3	2.860 F_3	2.883 F_3	4.080 F_3
F_s	9.657 KN	9.618 KN	7.586 KN
F_1	7.297 KN	7.271 KN	5.931 KN
F_2	4.151 KN	4.142 KN	3.725 KN
F_3	3.102 KN	3.099 KN	2.990 KN

Table 3.6 Primary values of internal support reaction corresponding to each of the three panels for the second analysis.

panel	20 oz/ft^3	18 oz/ft^3	16 oz/ft^3
F_s	9.657 KN	9.618 KN	7.586 KN
F_1	7.734 KN	7.618 KN	6.283 KN
F_2	4.486 KN	4.492 KN	4.235 KN
F_3	3.328 KN	3.344 KN	3.478 KN

Table 3.7 Final load on the sheeting rail corresponding to each sandwich panel for the second analysis.

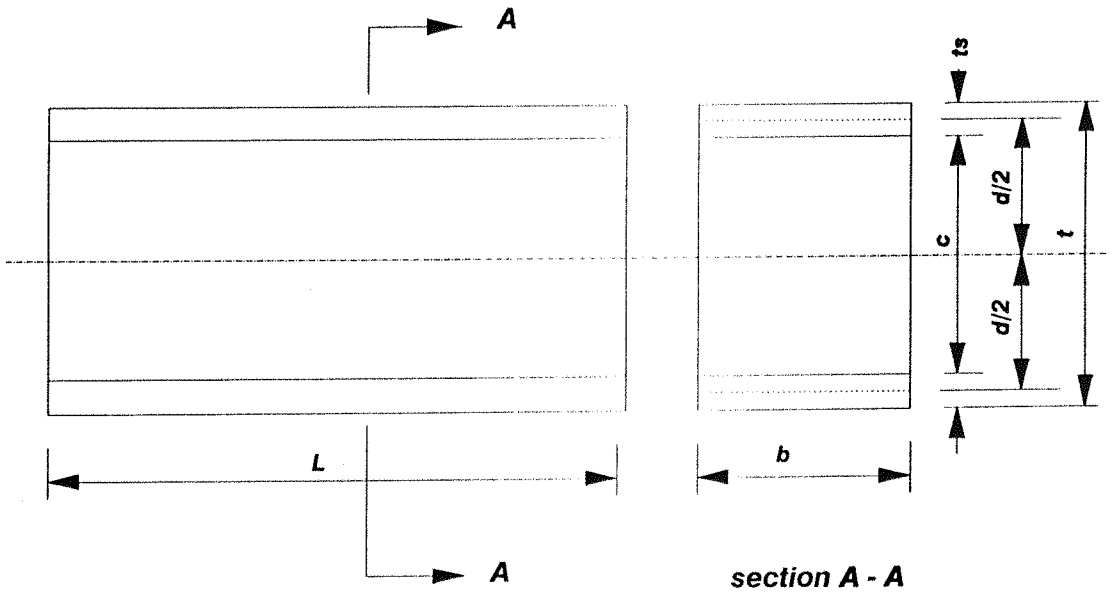

Fig 3.1 Dimensions of a sandwich panel.

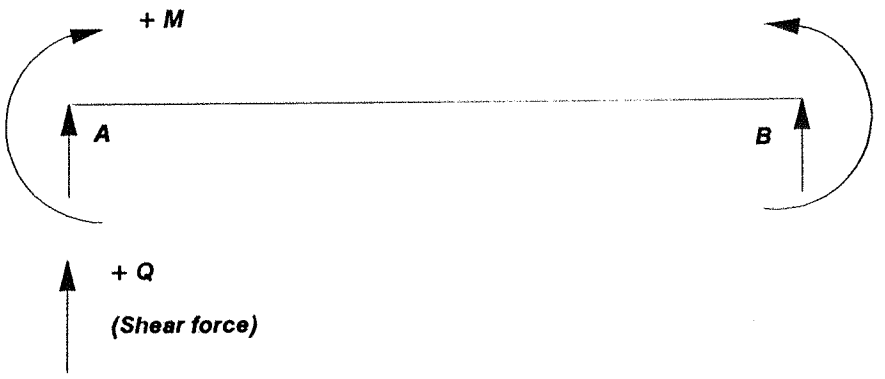

$$\text{Moment : } M = -EI\,\frac{d^2y}{dx^2}$$

$$\text{Curvature : } \frac{d^2y}{dx^2}$$

$$\text{Slope : } \frac{dy}{dx}$$

Deflection : y

Sign convention

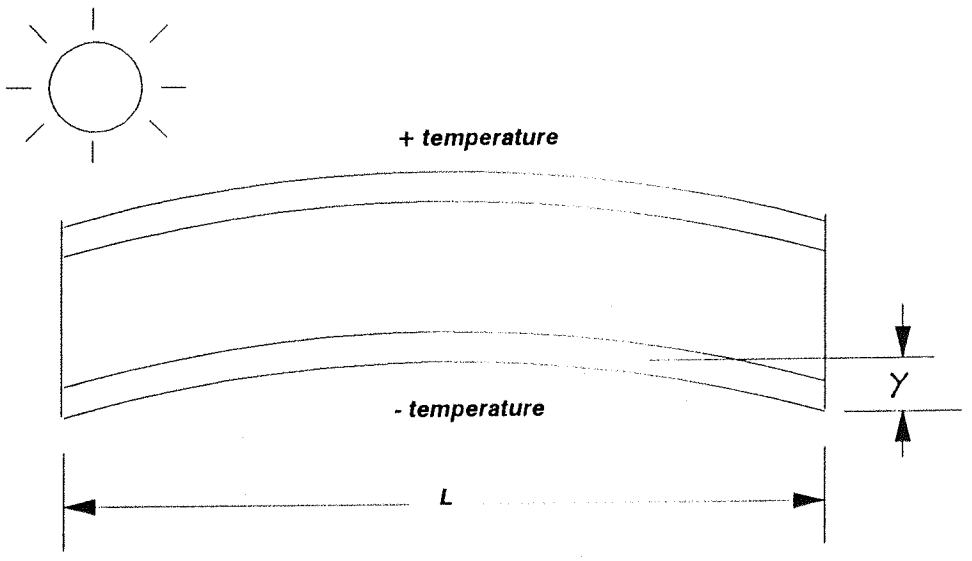

Fig 3.2 Deflection under thermal bowing.

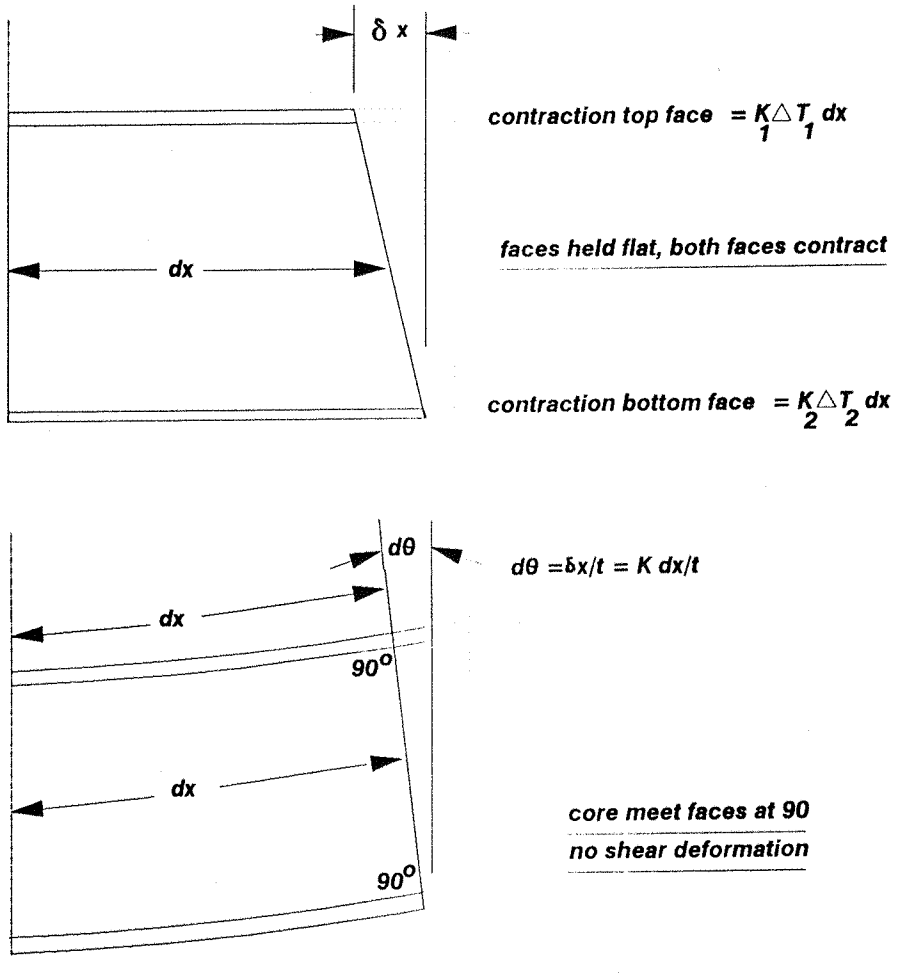

Fig 3.3 Thermal warp of a sandwich panel with thin flat faces

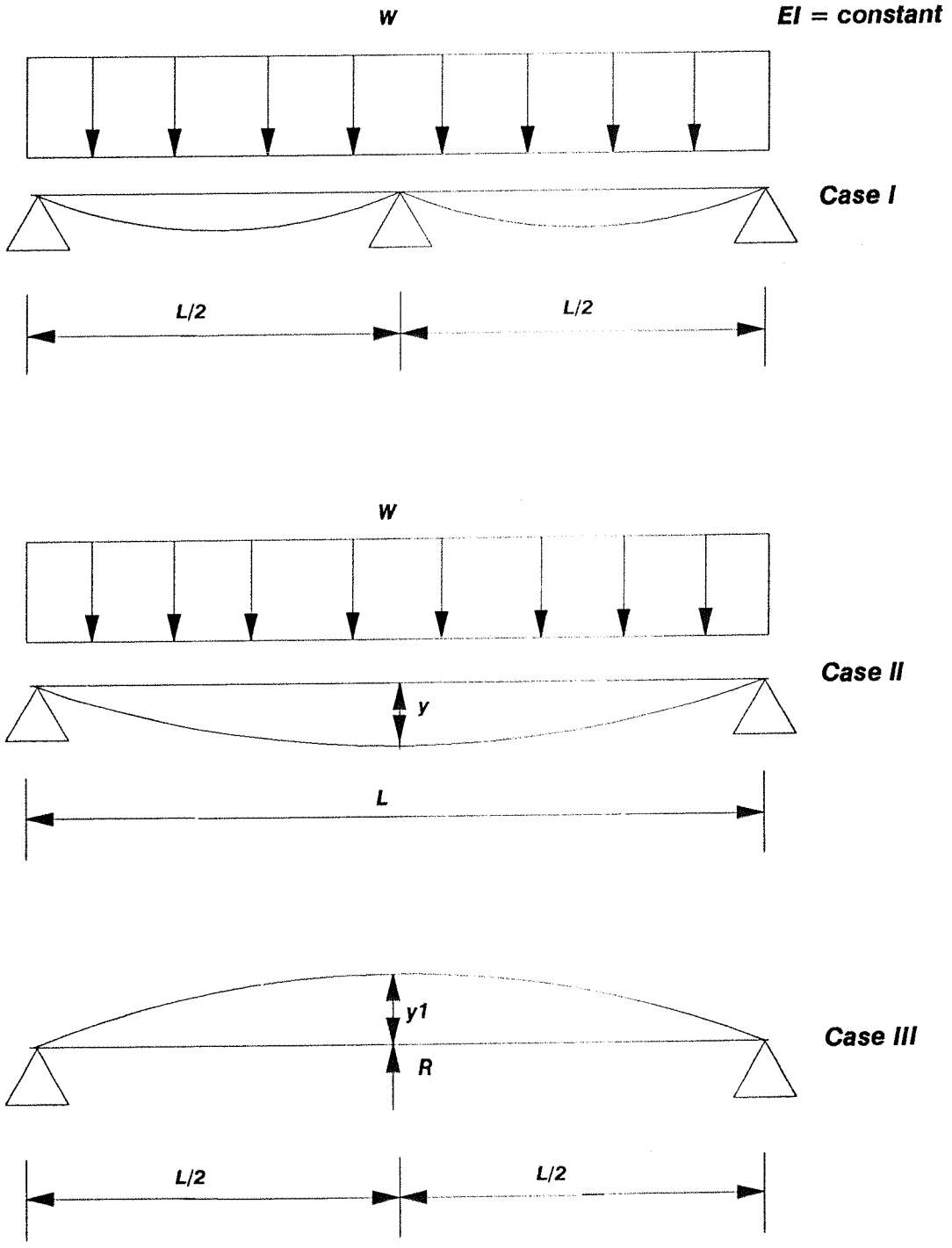

Fig 3.4 Concept for the method of consistent deformation

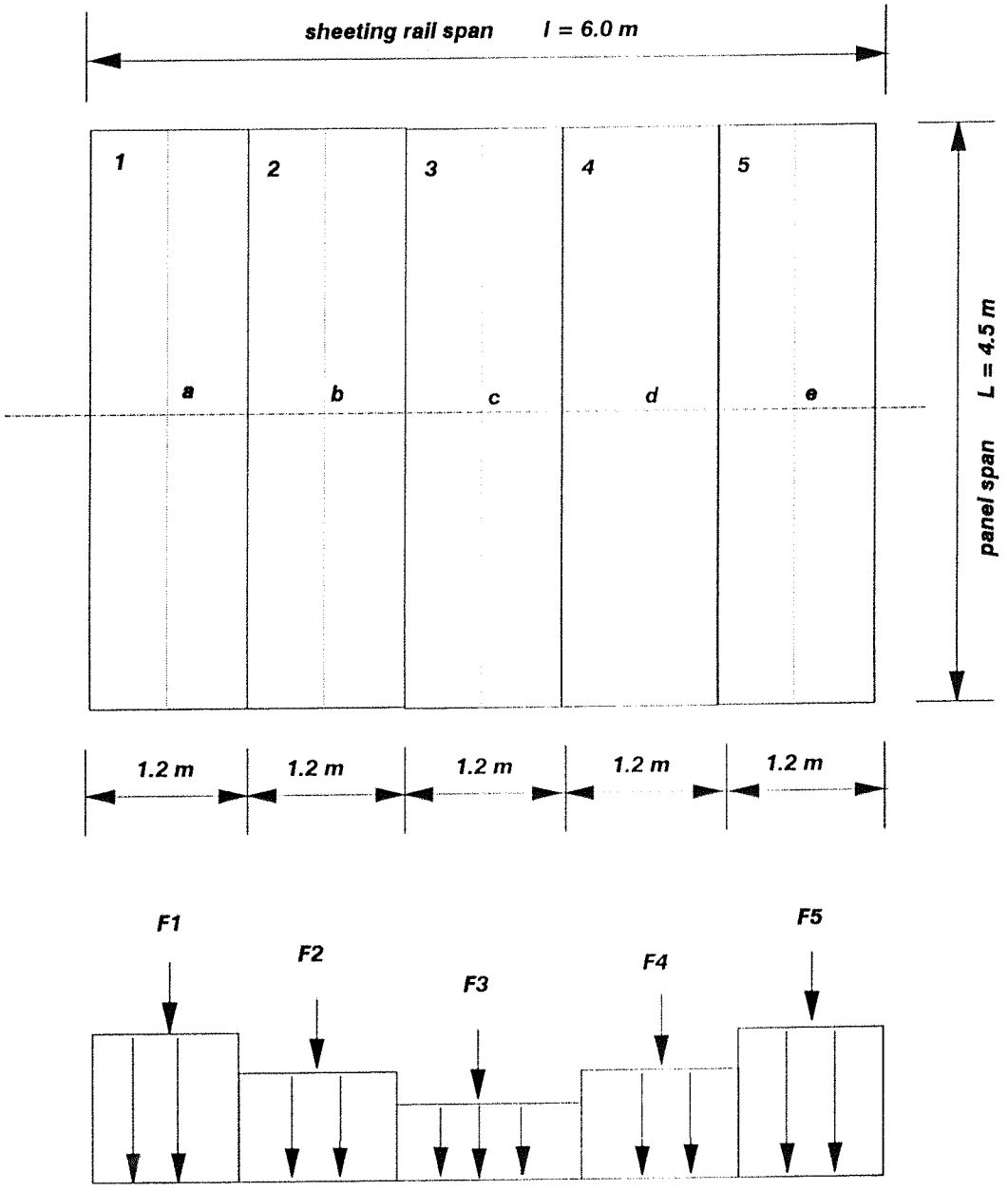

Fig 3.5 Load distribution on the sheeting rail.

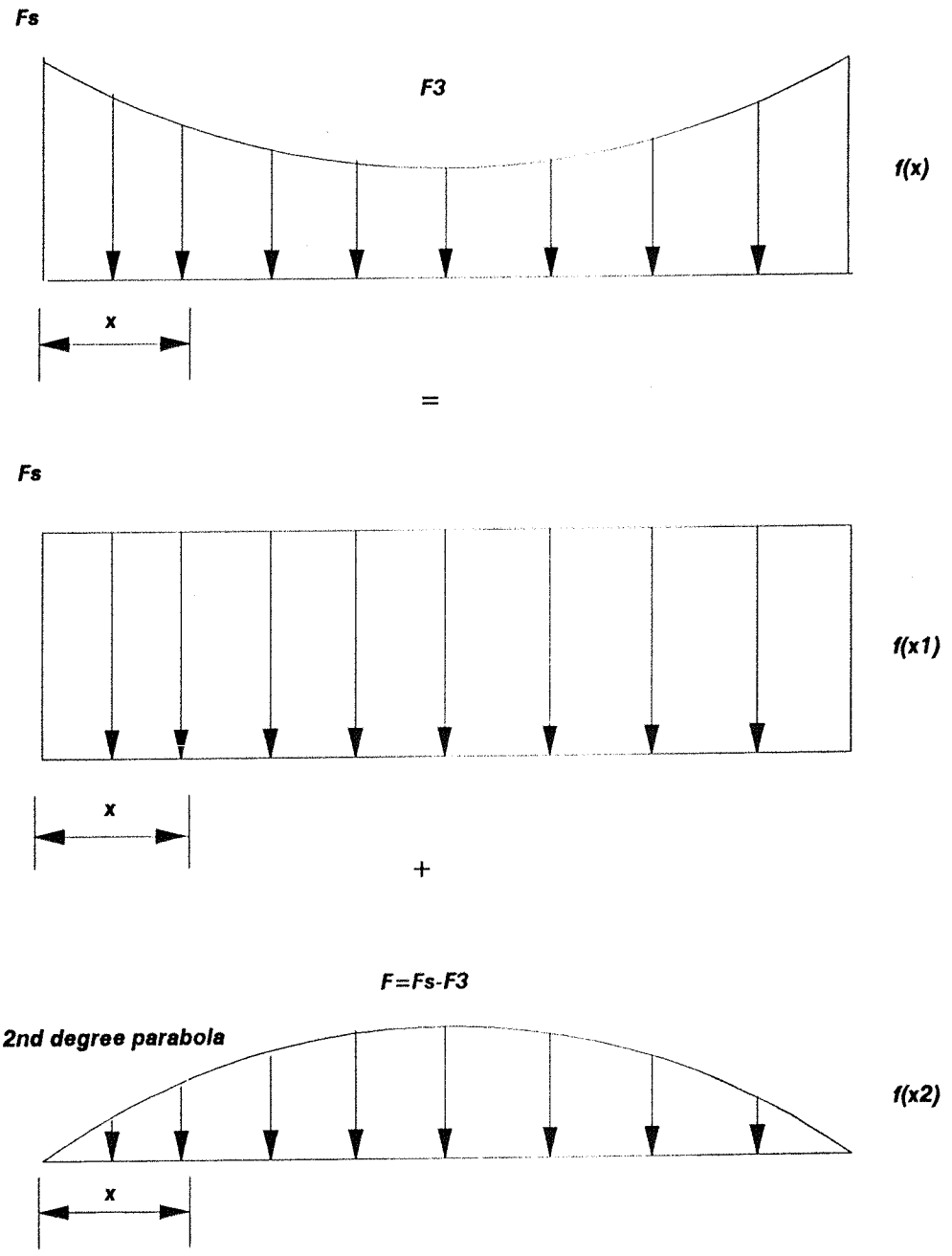

Fig 3.6 Load distribution on the sheeting rail.

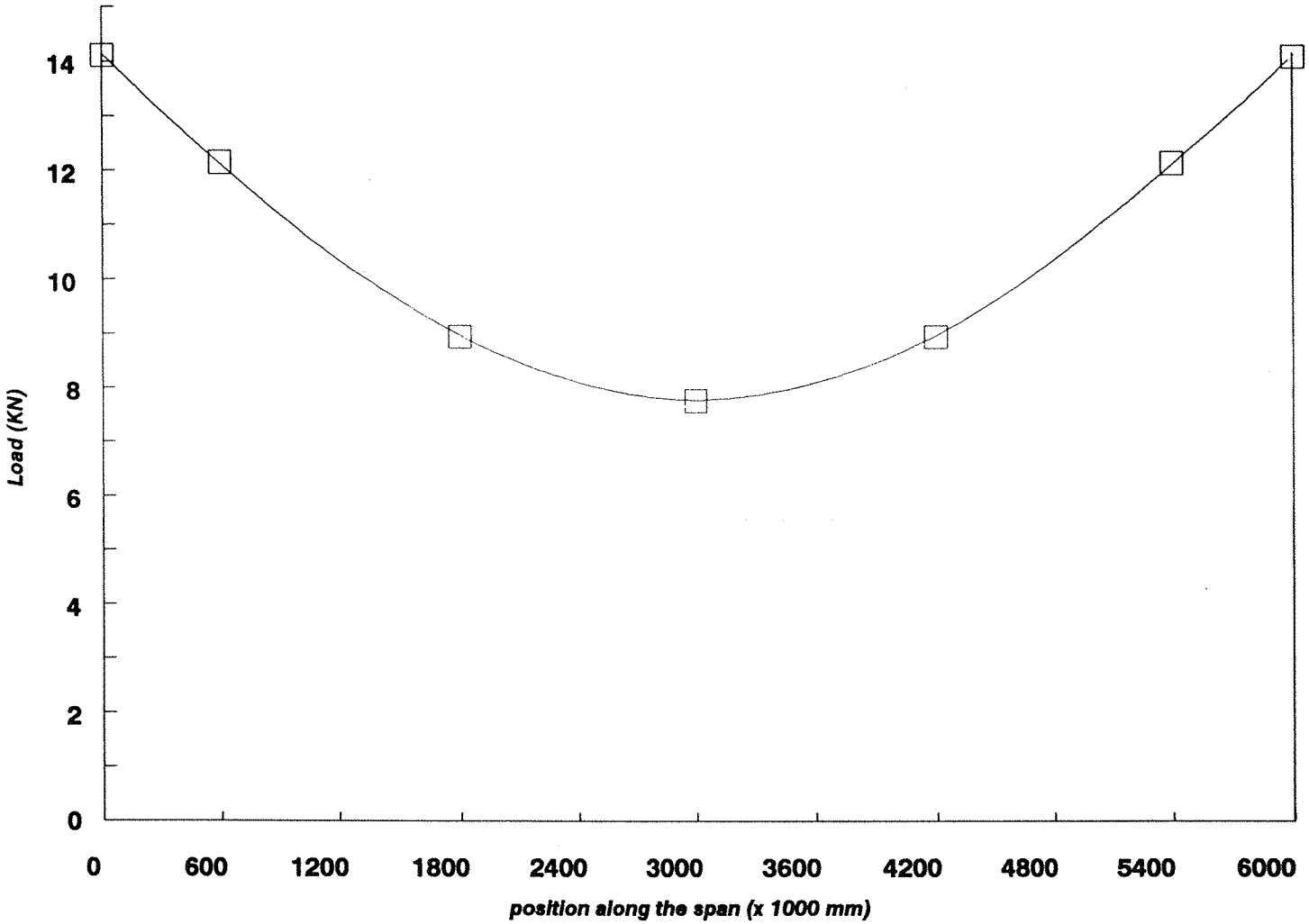

Fig 3.7 Load distribution on the sheeting rail corresponding to the first panel

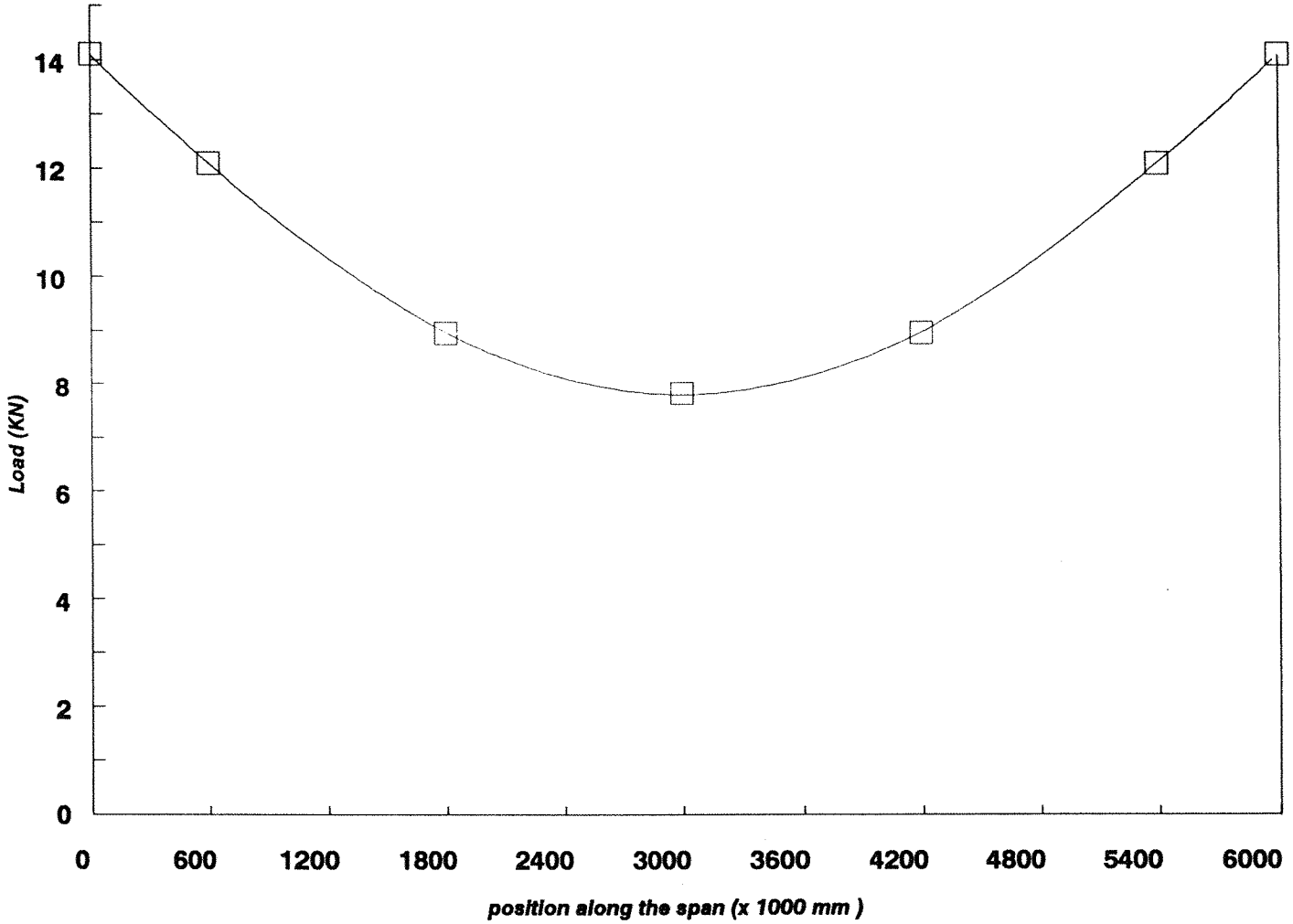

Fig 3.8 Load distribution on the sheeting rail corresponding to the second panel

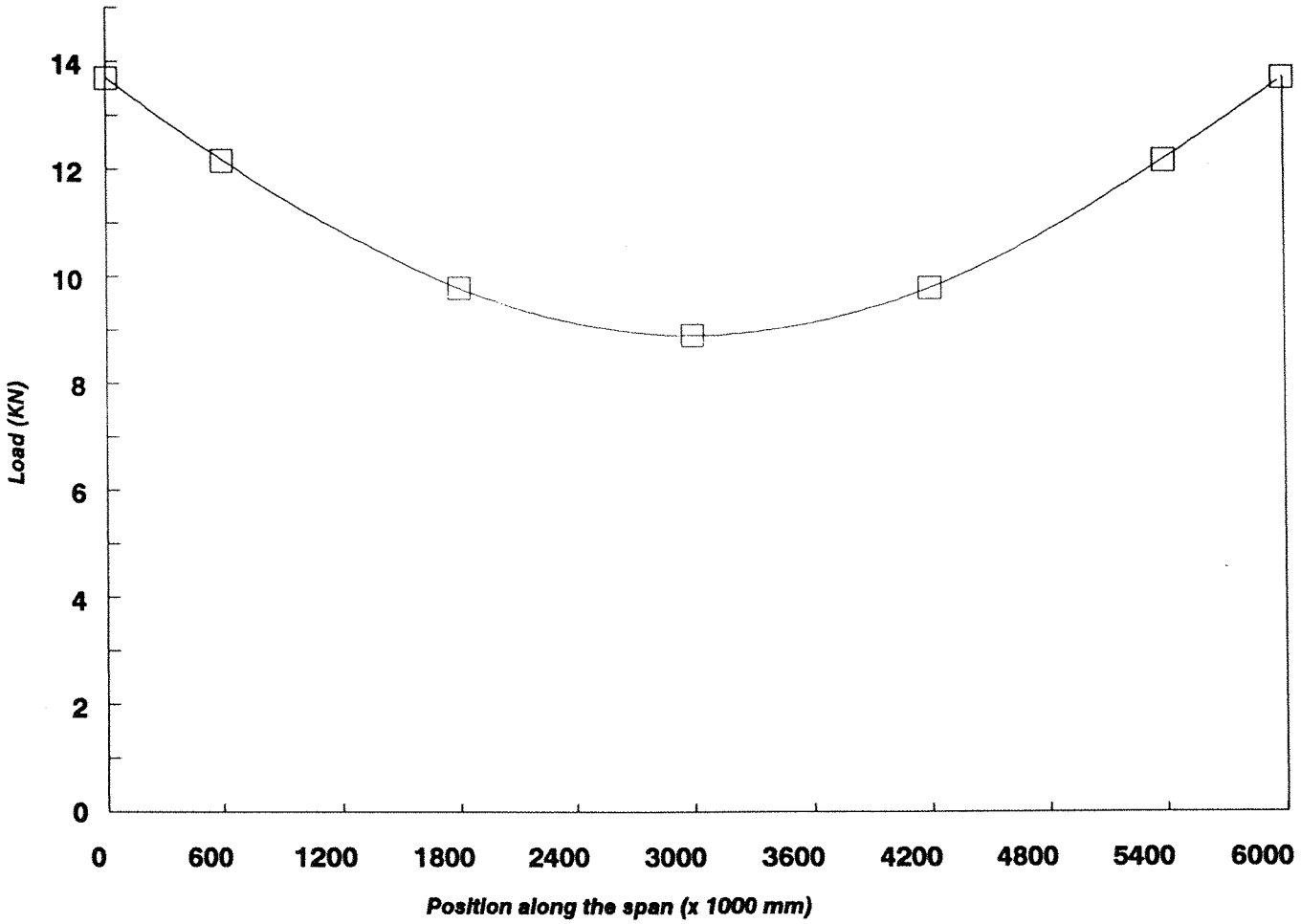

Fig 3.9 Load distribution on the sheeting rail corresponding to the third panel

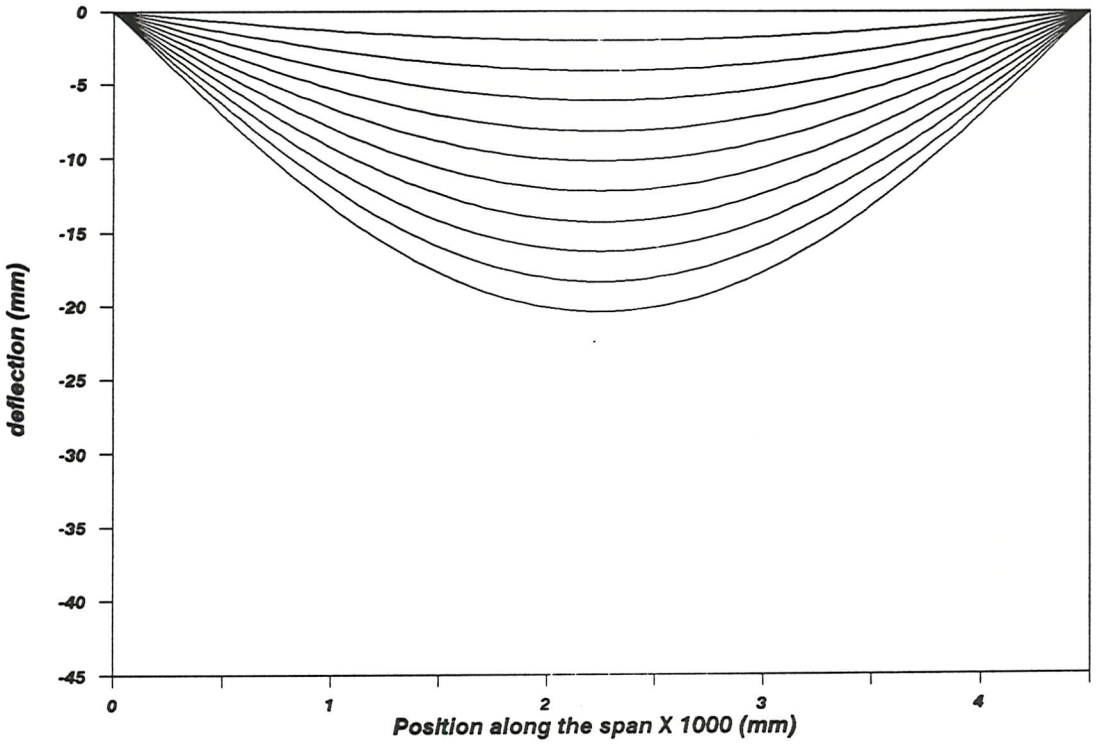

Fig 3.10 Bending deflection due to wind and temperature load (W) from 10 % to 100 % of the ultimate load W

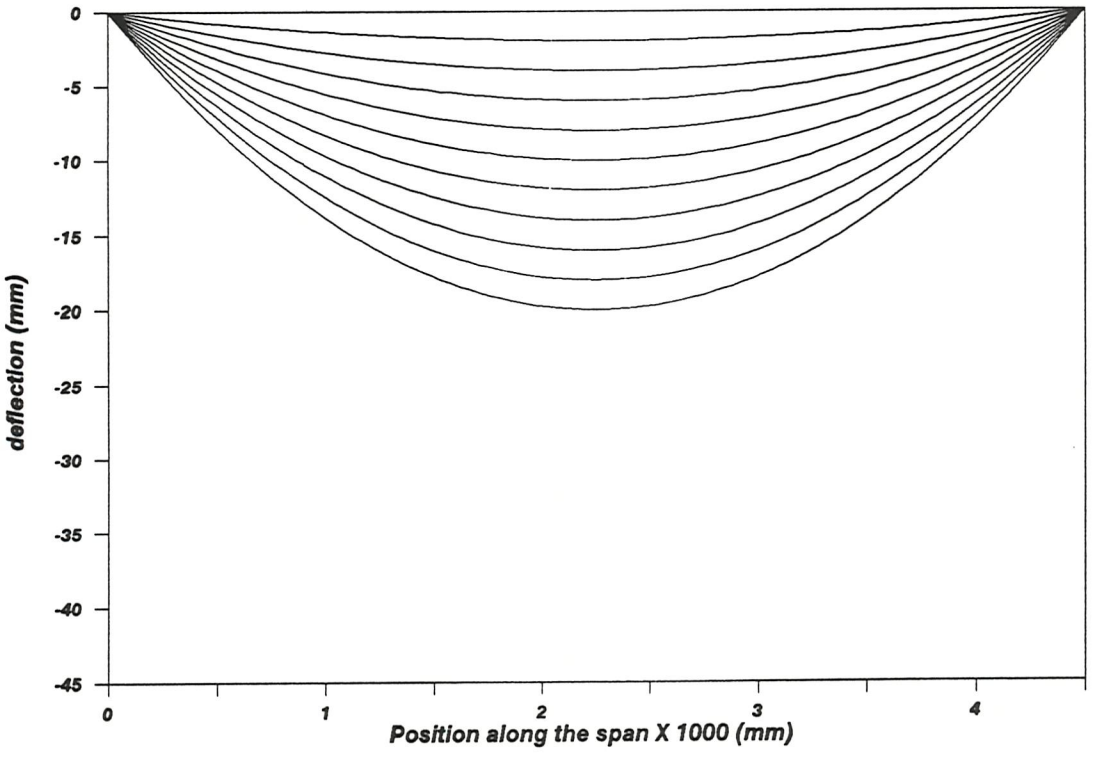

Fig 3.11 Shear deflection due to wind and temperature load (W) from 10 % to 100 % of the ultimate load W

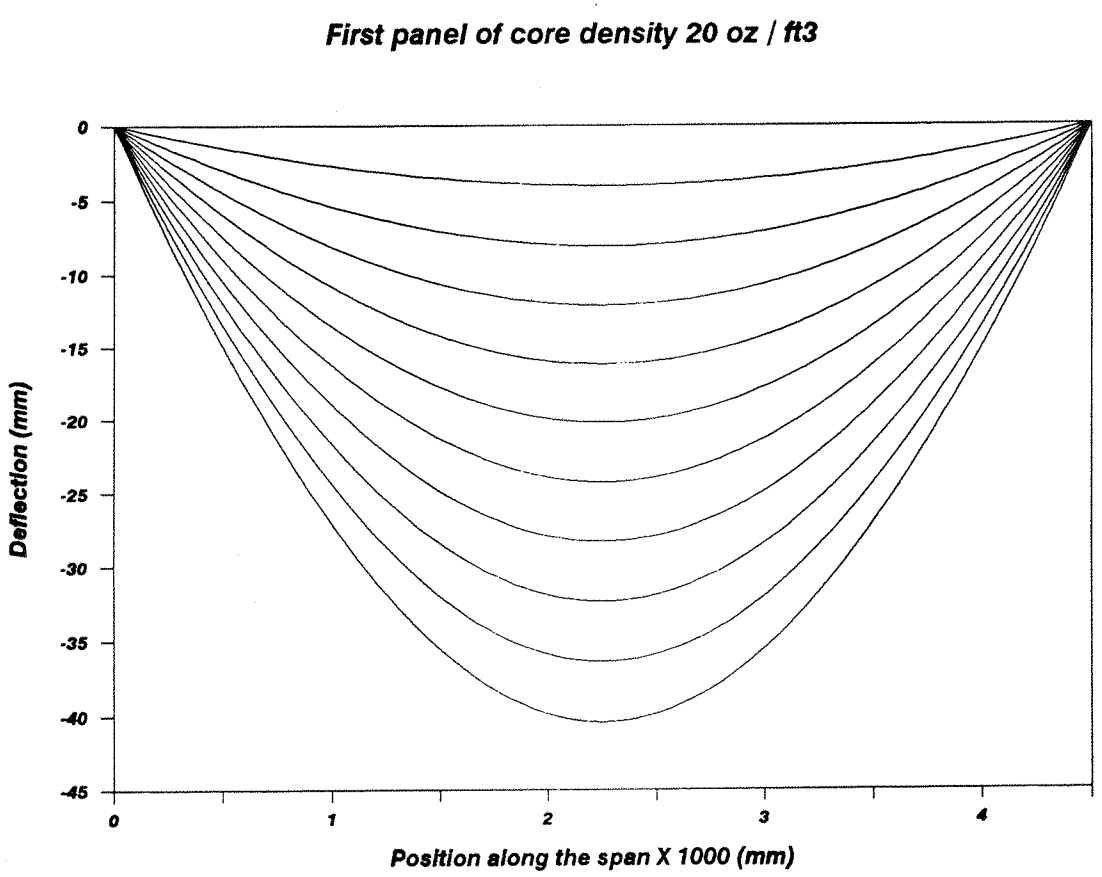

Fig 3.12 Combined bending and shear deflections due to the uniformly distributed load (W) from 10 % to 100 % of the ultimate load W

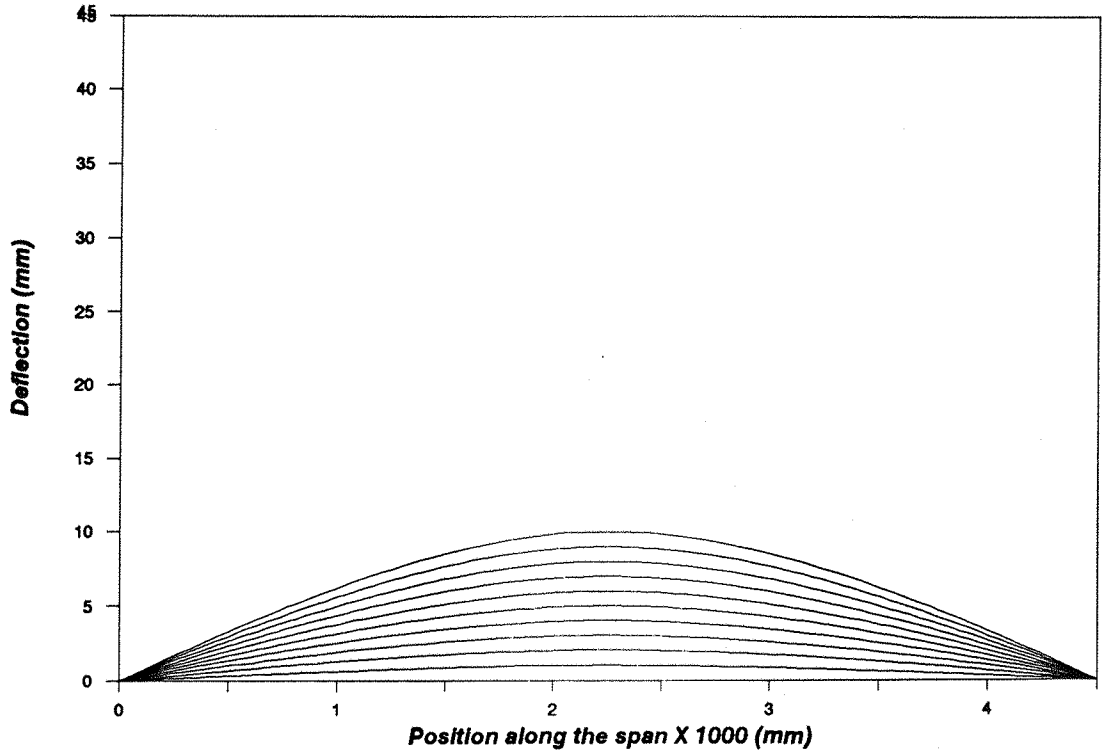

Fig 3.13 Bending deflection due to internal support reaction (F) from 10 % to 100 % of the ultimate load F

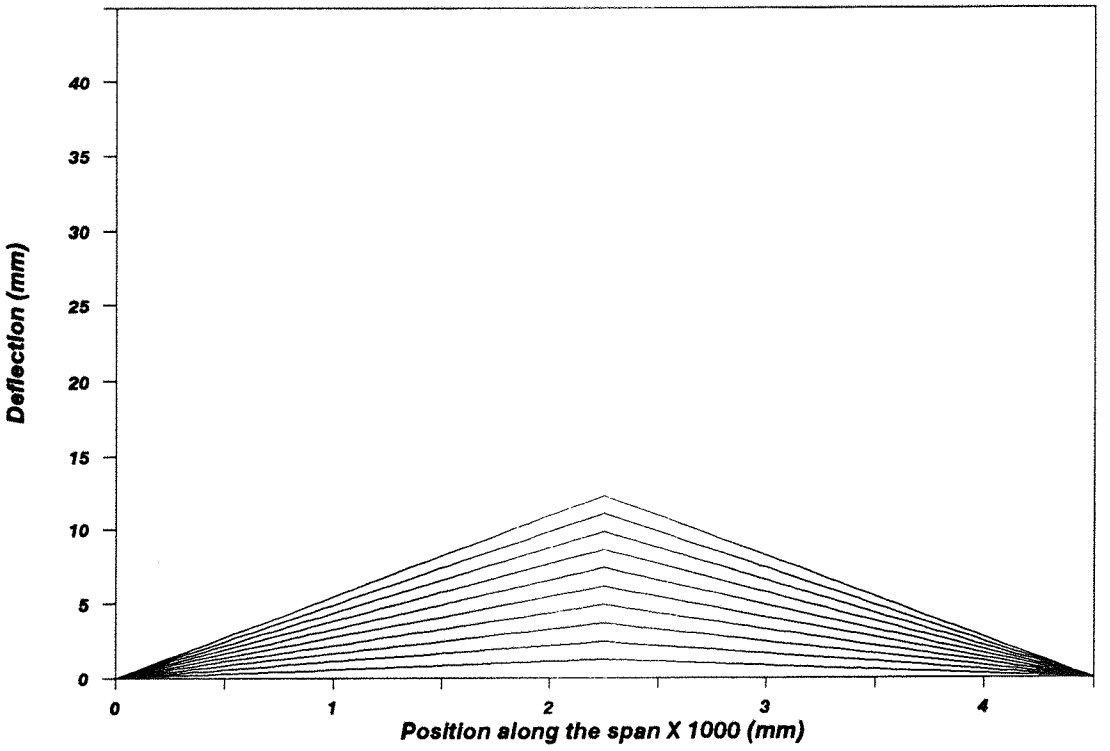

Fig 3.14 Shear deflection due to internal support reaction (F) from 10 % to 100 % of the ultimate load F

First panel of core density 20 oz / ft3

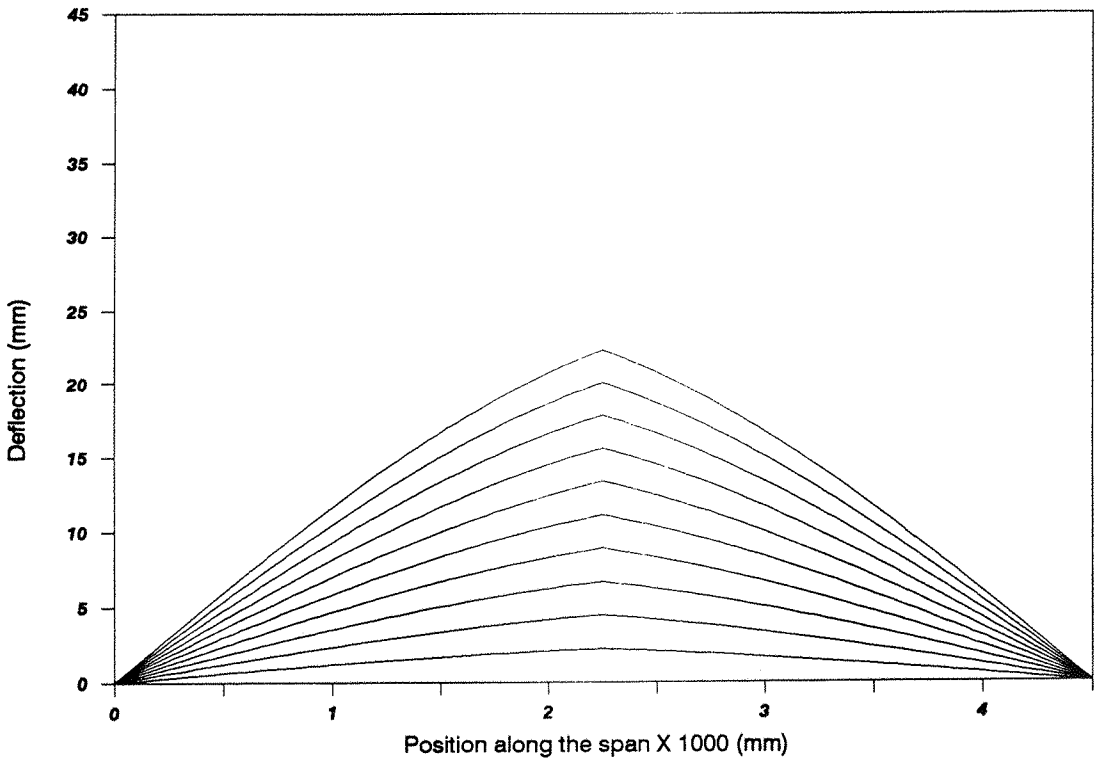

Fig 3.15 Combined bending and shear deflections due to internal support reaction (F) from 10 % to 100 % of the ultimate load F

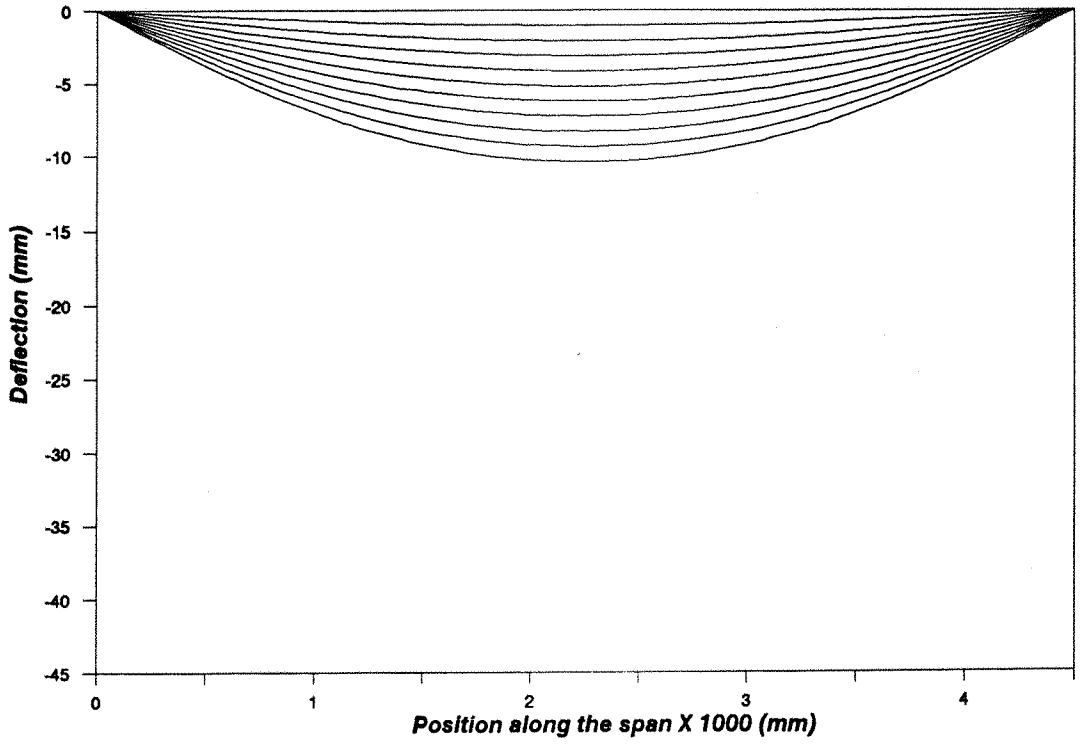

Fig 3.16 Bending deflection due to (W) and (F) from 10 % to 100 % of the ultimate loads W and F

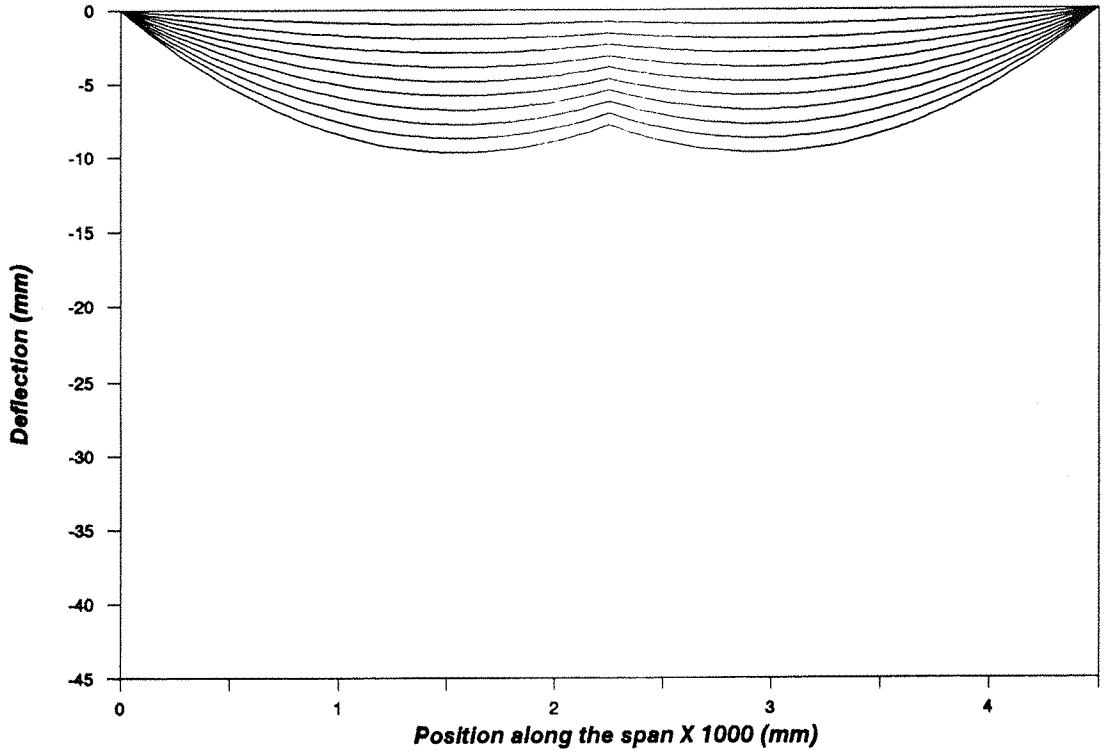

Fig 3.17 Shear deflection due to (W) and (F) from 10 % to 100 % of the ultimate loads W and F

First panel of core density 20 oz / ft3

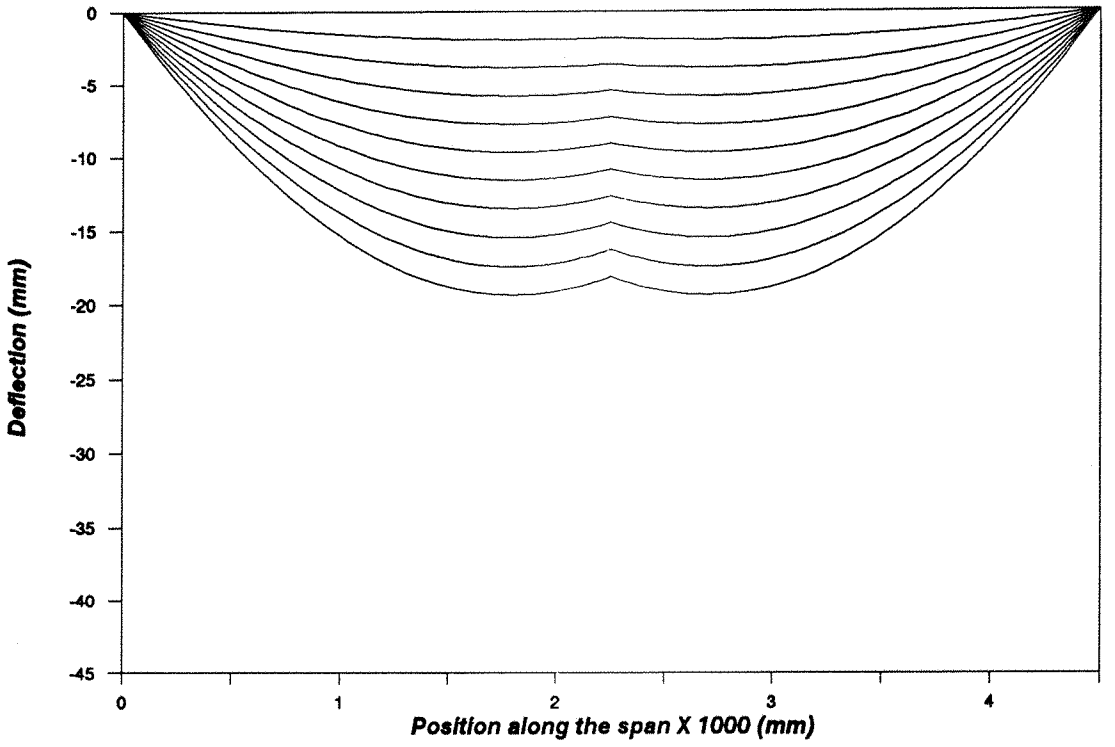

Fig 3.18 Combined bending and shear deflections due to (W) and (F) from 10 % to 100 % of the ultimate loads W and F

Second panel of core density 18 oz / ft3

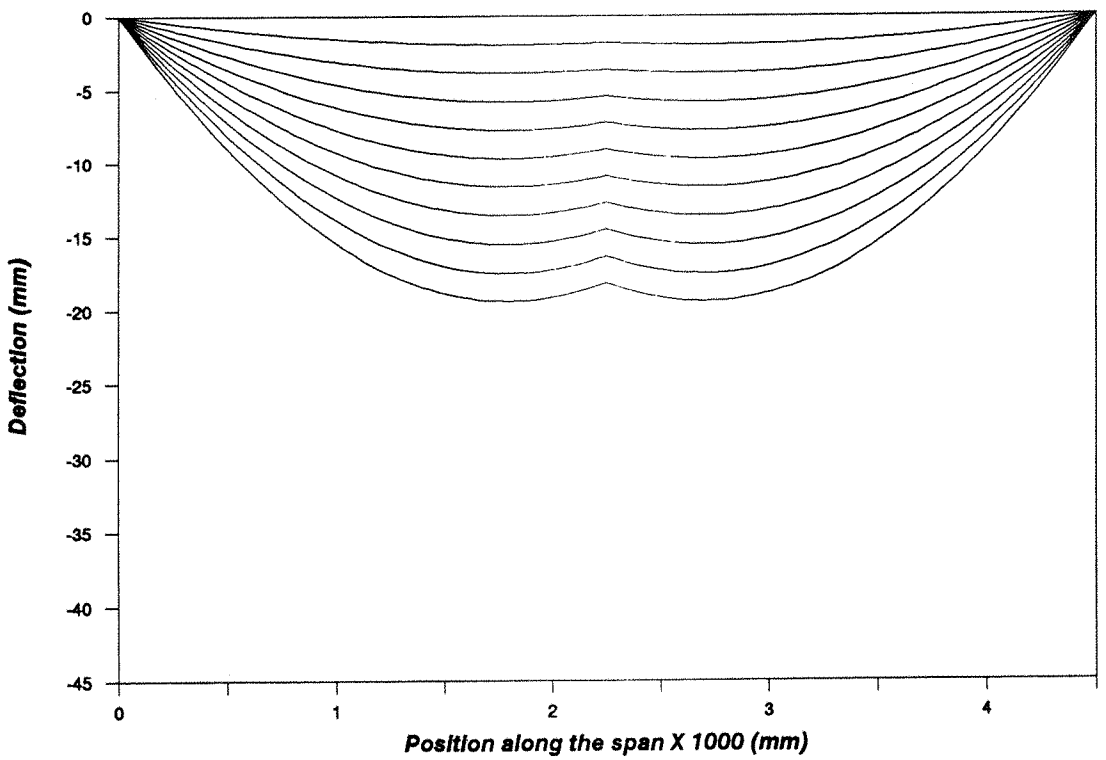

Fig 3.19 Combined bending and shear deflections due to (W) and (F) from 10 % to 100 % of the ultimate loads W and F

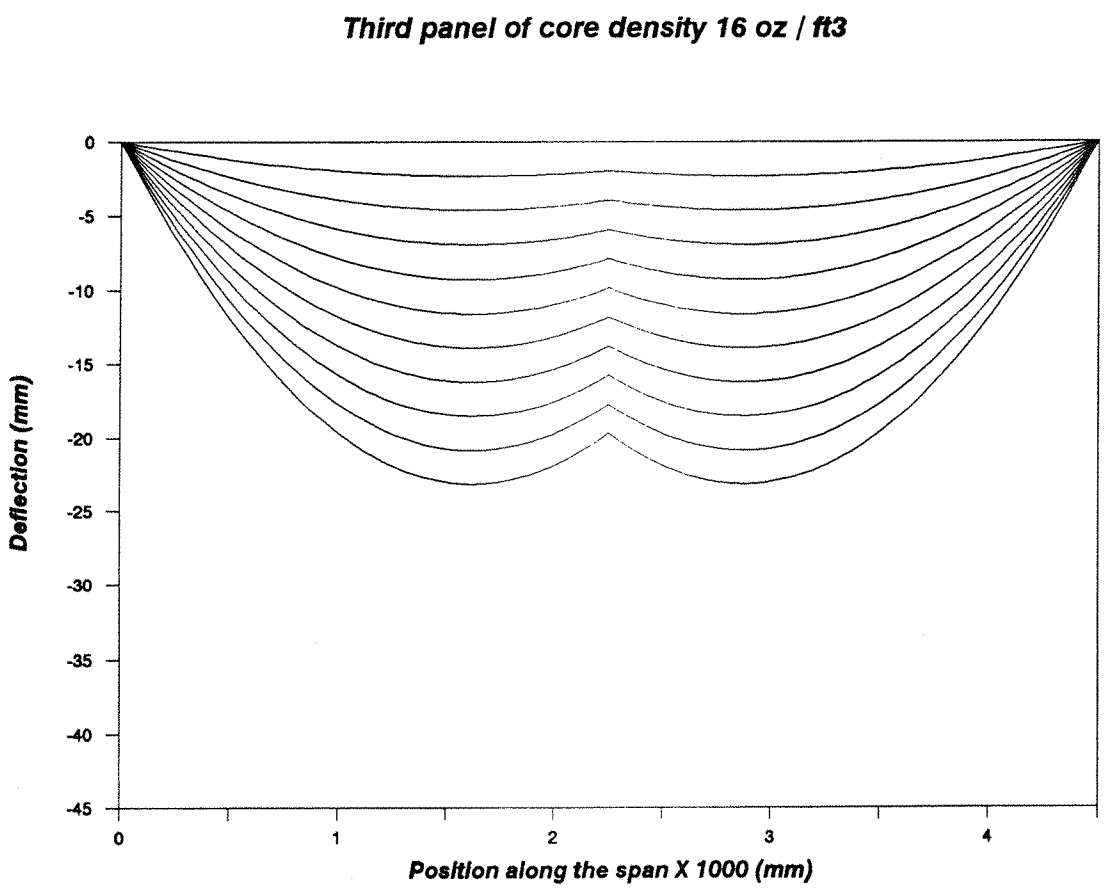

Fig 3.20 Combined bending and shear deflections due to (W) and (F) from 10 % to 100 % of the ultimate loads W and F

CHAPTER FOUR

MATERIAL TESTS.

4.1 Introduction.

In addition to the main test carried out on complete sandwich panels, material tests were necessary to be carried out to evaluate the core properties of the sandwich elements. Among many material tests published by the American Society for Testing Materials (ASTM), the German standard (DIN) and the British standard (BS), only two are adopted in this research. These tests are:

-a- Bond strength in direct tension (based on BS 5350 part C and DIN 53 292)

-b- Shear test (based on DIN 53 294 and ASTM C-273)

4.2 Determination of bond strength in direct tension in sandwich panels.(Based on BS 5350 part C6 & DIN 53292)

4.2.1 Field of application and purpose:

This test method is intended for estimating the bond strength between the core and the facing sheets of a sandwich panel, it can also be used for assessing the strength and deformation behaviour of sandwiches under tensile stress perpendicular to the faces.

This test can be applied to any type of adhesive and can be used over a wide range of test temperature. The adhesive bond strength may be greater than the cohesive strength of

either the core material or the facing, but the test may still provide useful information if the type of failure is taken into account.

This method can also be used to test the bond to the core material alone. In this case, the core is bonded to the attachment blocks by the test adhesives.

4.2.2 Apparatus:

-a- A standard tensile testing machine.

-b- A section of a universal column 305 x 305 of mass 97 Kg/m length cut, as shown in Figure 4.1, has been used as rigid attachment blocks bonded to the test piece. The use of this heavy section is to ensure even transfer of the stress to the specimen.

-c- Secondary adhesive which should be strong enough to ensure that the tensile force should cause failure within the adhesive under test or within the materials of the test piece. Two types of adhesives were used in this test:

-a- 24 hour Araldite epoxy resin 2001 for the first and second specimen.
-b- Bostik epoxy adhesive for the third specimen.

4.2.3 Specimens:

All specimens were cut from sandwich panels of the different core densities 16 oz/ft^3, 18 oz/ft^3, 20 oz/ft^3 respectively. The specimens were of square cross-section, with a side length of 300 mm, the specimen height corresponded to the sandwich thickness, 150 mm.

4.2.4 Preparation of the test specimen:

The metal faces of the specimens and the attachment blocks were cleaned of paint using Emery papers, then degreased (using Trichloroethylene) to ensure that surfaces were clean from any dust or grease before applying the adhesive. The adhesive was then applied to both metal faces of the specimen and the attachment blocks. In order to secure the test pieces against any displacement while bonding, the specimen and the attachment blocks were held together using clamps. The test piece was then left to set for 24 hours under the heat of a lamp.

The same attachment blocks were used for all the specimens, after being cleaned of any residue of the previous adhesive.

4.2.5 Procedure of the test:

The test piece assembly was located in the calibrated tensile testing machine. The test piece was subjected to a force which was increased at a constant rate of strain (the crosshead speed = 1 mm / minute), the displacement of the machine and the corresponding applied force were plotted on a chart which moved at a speed of 50 mm / minute. The force at rupture and the mode of failure were recorded for all the test pieces.

4.2.6 Evaluation:

-a- Tensile strength :

$$\sigma_B = \frac{F_{max}}{A_0} \quad N/mm^2 \qquad \text{.....(4.1)}$$

-b- **Tensile stress at rupture :**

$$\sigma_R = \frac{F_R}{A_0} \quad N/mm^2 \qquad \text{.....(4.2)}$$

Where :

F_{max} is the maximum force in Newton.

F_R is the force at rupture of the sandwich in Newton.

-c- **Tensile modulus E_t :**

From the slope of the tensile stress / strain diagram (Fig 4.2), the tensile modulus is calculated as follows:

$$E_t = \frac{\Delta\sigma}{\Delta\gamma} = \frac{\Delta F}{l.b} \cdot \frac{t}{\Delta X} \qquad \text{.....(4.3)}$$

Where:

ΔF is the tensile force increment in Newton between two measurements.

ΔX is the deformation increment in mm between two measurements.

A_0 is the original cross - sectional area of the specimen in mm^2 (300 x 300).

4.2.7 Test results:

The results obtained from this test are plotted on a tensile stress / strain diagram for each specimen as shown in Figure

4.2.

The tensile stress at rupture for each of the three tested specimens and the tensile modulus are then calculated by applying equations (4.2 and 4.3) shown in section 4.2.6. These results are summarized in Table 4.1.

4.2.8 Modes of failure:

Specimen No.1:

The tensile force applied by the testing machine caused a failure mainly within the polystyrene core material as shown in Figure 4.3. The bond between the metal faces and the core was virtually unaffected i.e. the effect of the tensile force on the adhesives was practically negligible.

Specimen No.2:

Failure in this test occurred mainly in the core material, but with a noticeable bond failure between the facings and the polystyrene core (Fig 4.4). The area peeled off due to bond failure was nearly 25 % of the total original cross - sectional area of the test piece.

Specimen No.3:

For this specimen, a major failure in the bond between the core and the faces occurred, 67 % of the total core cross - sectional area of the specimen was peeled from the face (Fig 4.5).

4.3 Shear test

4.3.1 Purpose of the test:

The shear test is intended to assess the strength and deformation properties of sandwich panels under shear stress. The test is suitable for sandwiches of any structure

and for various core and facing materials.
The shear test could be used for determining:

-a- The shear strength of the sandwich.
-b- The shear stress in the sandwich at a defined shearing strain.
-c- The shear modulus of the core.

Referring to chapter two, section (2.8.1.4), most standard tests are for sandwich panels with relatively thin cores. Therefore, the dimensions of the specimens to be tested were reasonably small to fit into the testing machines. The dimensions should always be proportional to the thickness of the panel. The panels to be tested were all 150 mm thick. This lead to very large specimens and made it quite impractical to carry out the standard tests. Hence, two different shear tests were adopted:

-a- Using a relatively small specimen.
-b- and on a larger specimen.

4.3.2 First shear test:

4.3.2.1 Apparatus:

This shear test was conducted in a shear box usually used for soil testing. Its dimensions are 300 mm x 300 mm with a depth of 200 mm. The apparatus is meant to be operated hydraulically or electrically . However, in this test, manual operation was adopted.

The shear box is attached to a 500 Kg capacity proving ring (Wykeham - Farrance no. 8675) from which applied load can be read (each division in the proving ring is equivalent to 1000/28 Newton). The load is applied by moving the bottom half of the shear box towards the proving ring. Shear through the sample brings with it the top half of the shear box, which bears against the proving ring. Compression in the proving ring gives a measure of the applied load. The

horizontal displacement of the shear box is measured by a length measuring device attached to the outside of the shear box (a dial micrometer which has 0.01 mm graduations mounted to the shear box).

4.3.2.2 Specimens:

The specimen was taken from a sandwich panel with a core density of 16 oz/ft^3 . Its dimensions were 200 mm x 150 mm and its depth was equal to the 150 mm thickness of the panel.

4.3.2.3 Preparation of the specimen:

The specimen was cleaned and degreased before it was glued to steel plates of dimensions 260 mm x 150 mm x 12.7 mm using a 24 hour Araldite epoxy resin adhesive as shown in Figure 4.6.

4.3.2.4 Test procedure:

The specimen was placed in the shear box with wood packing underneath the specimen to prevent any tilting of the test piece during testing. The load was applied gradually and readings were taken for every 0.5 mm horizontal displacement, the load was read from the proving ring until the end of the travel of the shear box.

4.3.2.5 Evaluation:

-a- Shear strength:

$$\tau_b = \frac{F_b}{A_o} = \frac{F_b}{l_1 . b} \quad N/mm^2 \qquad \text{.....(4.4)}$$

-b- Shear modulus G_k :

From the fitting lines of the force / shear deformation diagram, the shear modulus of the core is calculated as:

$$G_k = \frac{\Delta\tau}{\Delta\gamma} = \frac{t}{l_1.b} \cdot \frac{\Delta F}{\Delta v} \quad N/mm^2 \qquad \text{.....(4.5)}$$

Where;

A_o original cross - sectional area of the specimen in mm^2

F_b force in Newton at failure

l_1 specimen length in mm

b specimen width in mm

t specimen height in mm

ΔF force increment in Newton between two measurements.

Δv shear deformation increment in mm between two points measurements.

4.3.2.6 Test results

The specimen started cracking and the metal faces peeled off the polystyrene core. The bond between the test piece and the steel plates failed at the bottom of the sample.

The results obtained for displacement and load were plotted in a force / shear deformation diagram (Fig 4.7) from which the shear modulus and the shear strength of the core material were then calculated using equations (4.4 and 4.5) shown in section 4.3.2.5.

From the test results, the shear strength is calculated as:

$$\tau_b = \frac{896.55}{200\times150} = 0.029885\ N/mm^2$$

and the shear modulus is calculated as:

$G_k = 0.69\ N/mm^2$

During this test, it was clear that the test piece was tilting to one side inside the shear box. The dimensions of the specimen were not proportional to the thickness of the panel. This might have effected the shear action leading to a very low shear modulus. Another test which achieved a better shearing action was required.

4.3.3 Second shear test:

4.3.3.1 Apparatus:

A calibrated hydraulic actuator of 100 KN maximum capacity was used in a frame as a testing machine.

4.3.3.2 Sampling:

The specimens were all cut from complete sandwich panels of core densities of 16 oz/ft^3, 18 oz/ft^3 and 20 oz/ft^3 respectively.

4.3.3.3 Specimens:

-a- Dimensions: The dimensions of the specimens depend on the height of the sandwich. According to DIN 53 294 recommendations for a sandwich panel of height 60 mm and above, the specimen length should be 800 mm, its width 150 mm and the excess face at the ends 25 mm and 10 mm for top and bottom ends respectively. The thickness of the specimen in this test is 300 mm which is equivalent to the height of two test pieces.

-b- Number: Two specimens from each panel were

tested.

4.3.3.4 Procedure:

-a- **Setting up of the test:** The test pieces were first cut from panels to a length of 1100 mm. Then the core material was peeled off the two metal faces to leave a length of 800 mm. Excess ends at the top and bottom of length 76.2 mm and 150 mm respectively remained.

An identical specimen was prepared as above, then the two pieces were joined together as shown in Figure 4.8. The two steel faces at the bottom end of the specimen were fixed to two 6 mm thick steel plates by means of three 6 mm diameter bolts. These plates had a 40 mm diameter hole where a rod pivoted the test piece against a beam fixed to the floor to ensure that no movement would occur during the test.

The metal faces at the top end of the specimen were each fixed to a 6 mm thick plate across the width of the specimen (150 mm) by means of three 6 mm bolts. These plates were welded to a (101.6 mm x 50.8 mm) channel so that it was held horizontally over the top of the specimen. Two holes were drilled in the channel where two dial gauges were inserted to measure the displacement of the core during the experiment.
Two 6 mm thick plates of dimensions (228.6 mm x 50.8 mm) were welded to the outside of the flanges of the channel as shown in Figure 4.8. A rod of 25.4 mm diameter passed through the two plates to hold the specimen to the bottom plate of the actuator.

-b- **Procedure:** The test piece was fitted under the actuator as shown in Figure 4.9. The specimen was stressed by the load applied from the actuator. As the specimen was held in position at the bottom end, the actuator fixed to the outer metal faces of the specimen

moved upwards relative to the inner steel faces. Thus a double shear action was applied to the test specimen.

4.3.3.5 Evaluation:

-a- **Shear strength:**

This was calculated using the same equation (4.4) as in the first shear test, dividing by two as this was a double shear test.

-b- **Shear modulus:**

This was calculated as in the first test from the slope of the shear stress / strain diagrams of each specimen taking the average value of results obtained for each panel.

4.3.3.6 Test results

During the test, the force applied by the actuator and the corresponding shear deformation at each loading were recorded, as well as the readings from the gauges mounted on top of the polystyrene core. The type of failure was also recorded for each specimen. From the results, shear stress/ shear strain diagrams were plotted for each tested specimen (Fig 4.10 to 4.15).

Table 4.2 gives a summary of the results and the calculated values of shear strength and shear modulus for each specimen tested.

It is to be noted that the shear modulus obtained in this test is that of a combination between face plates and the core acting as one unit. The theoretical relationship of this modulus G_k to the modulus of the facings G_f and that of the core G_c is expressed as follows:

$$G_k = \frac{G_c . t}{\left[c + (t-c) . \frac{G_c}{G_f}\right]} \quad \ldots\ldots\ldots\ldots\ldots\ldots\ldots\ldots\ldots\ldots\ldots\ldots\ldots\ldots\ldots\ldots\ldots\ldots\ldots\ldots\ldots\ldots\ldots\ldots\ldots\ldots\ldots\ldots\ldots\ldots\ldots\ldots\ldots\ldots\ldots (4.6)$$

Where t is the total thickness of the sandwich and c is the core thickness. In most sandwich panels G_f is so large compared with G_c and t and c differ so little that G_k is essentially the same as G_c. Therefore, the value of the shear modulus calculated from the test results is that of the polystyrene core material.

In Table 4.2 two sets of values are shown for the shear modulus, one obtained from the readings of the gauges and the other from the actuator's readings. It is necessary to show them both as they differ noticeably, the reason for such differences will be discussed later in the chapter.

4.3.3.7 Mode of failure:

Examining the specimens after testing,it could be concluded that the dominating mode of failure was the bond failure between the metal faces of the sandwich and the polystyrene core. At an average load of 4 KN, the bond started to fail between the inner metal faces and the core at the bottom end of all the test pieces (Fig 4.16). Specimens 1B, 2B and 3A revealed a bond failure between the outer metal faces and the core along the length of the specimens (Fig 4.17). Only specimen 2B showed a clear shear failure in the polystyrene core itself at an angle of approximately 50 degrees to the horizontal (Fig 4.18).

4.4 <u>Analysis of the results:</u>

Analyzing the shear test results, it could be concluded that the first shear test did not provide the expected results for shear strength and modulus. This was due to following

factors:

-a- First of all, the dimensions of the test specimen were not in proportion with the thickness of the core. Maintaining this proportion is necessary in order to ensure a shearing action along the length of the specimen, as recommended by standard tests (Chapter 2, Table 2.3).

-b- Secondly, the test piece inside the shear box kept tilting to one side during the test despite the use of wood packing which was placed underneath the specimen to prevent such movement. This continuous movement of the specimen may have prevented the efficient application of the force along the length of the specimen.

-c- Finally, the allowable travel of the shear box was small with respect to the thickness of the core. This limited travel, in addition to the previous factors, may have helped to prevent any shear failure in the polystyrene core itself. Instead, the applied force acted only on the bond between the steel faces of the specimen and the metal plates where failure occurred.

It is not certain whether additional travel of the shear box would lead to a core shear failure. However, it might be worthwhile to adopt the first shear test allowing further travel of the shear box to check whether or not the failure mode will be affected.

Comparing the value of shear modulus obtained from the first shear test (0.69 N / mm^2) with its design value of (2.25 N/ mm^2), it seems that the experimental shear modulus is low compared with the design value. Hence the conclusion that the first shear test could not be considered adequate. Moreover, the experimental shear modulus is considered unreliable.

Taking all the above factors into account, the need to adopt a second shear test was clear.

The second shear test (double shear test) takes into consideration the dimensions of the specimen in proportion with its thickness.

Examining the test pieces, the bond failure between the steel faces and the polystyrene core started at the lower inner ends of the specimens and at an average load of 4 KN. Furthermore, most specimens showed that failure started first in one of the two test pieces. This was due to a slight misalignment of the actuator which applied the load or an imperfect symmetry in the two pieces of the sample.

A bond failure between the outer steel faces of some specimens and the polystyrene was also recorded.

Table 4.2 illustrates two sets of results corresponding to the actuator's readings and the gauges readings respectively. The noticeable difference between the two sets is due to the fact that the gauges which were mounted on top of the central part of the polystyrene core , did not interpret the exact movement of the core during the test. The core movement was not uniform across the width of the test pieces. In fact, the inner half of the core was sinking in towards the centre of the test piece while the outer half hardly moved. The gauges recorded only the central movement of the polystyrene. Therefore, their readings could be considered unreliable when compared to those recorded by the actuator. The actuator readings gave averaged values of load and displacement.

In the double shear test, the applied stress is not uniform over the length of the specimen, but it varies considerably between the ends and the middle. It is also possible that there may be a significant bending component of load in addition to the desired shear load.

The core shear moduli evaluated from the actuator's readings of the second shear test (Table 4.2) are found to be in close agreement with their design values given by the manufacturer (Fig 4.20).

The shear and bond tests results are plotted in Figures 4.19 to 4.21. These figures show that the material properties of sandwich panels are dependent on the density of the core material. As the density increases, the shear and tensile strengths and moduli increase too. However, core materials are chemically complex and additives such as expanding agents or fire retardants could modify the cell structure and the physical properties of the sandwich unit. The density of the core material is not usually constant over the cross-sectional area of the sandwich panel.

Furthermore, the properties of the core material are not necessarily the same in all directions. This is due to the fact that they are dependent on the particular machinery used in the foaming process and the operating conditions.

Moreover, the mechanical properties of the rigid foam cores are temperature and humidity dependent. The tests adopted in this research were conducted at an ambient temperature (23 + 1°C). If similar tests are to be carried out at different temperatures, the properties of the core material might prove to be significantly different.

specimen	dimension (mm)	type of adhesive	force at rupture (KN)	tensile stress (N/mm^2)	tensile modulus (N/mm^2)
20 oz/ft^3 No.1	300x300x 150	araldite	12.6	0.140	7.01
18 oz/ft^3 No.2	300x300x 150	araldite	7.6	0.084	5.28
16 oz/ft^3 No.3	300x300x 150	bostik	3.6	0.040	2.39

Table 4.1 Bond test results.

specimen	1A	1B	2A	2B	3A	3B
	20 oz /ft^3		18 oz /ft^3		16 oz /ft^3	
shear strength (N/mm^2)	.0542	.0671	.0550	.0500	.0501	.0536
average shear strength	.0606		.0525		.0518	
shear modulus G_k (N/mm^2) (gauges)	7.300	7.460	7.885	5.047	5.810	4.668
average G_k (gauges)	7.380		6.466		5.239	
G_k (actuator)	2.590	3.005	2.770	2.594	2.335	1.923
average G_k (actuator)	2.797		2.682		2.129	

Table 4.2 Second shear test results.

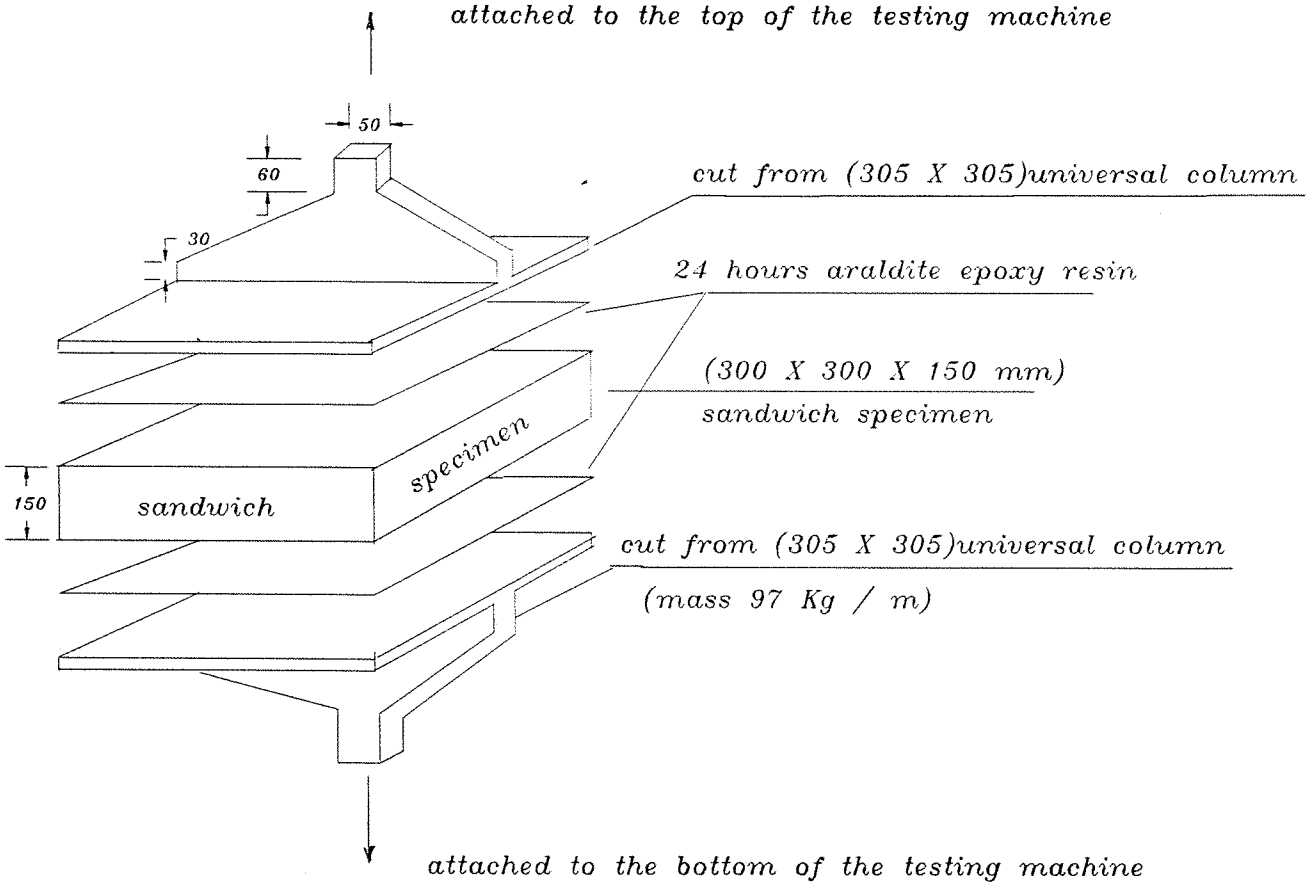

Fig 4.1 Test assembly of the tensile test.

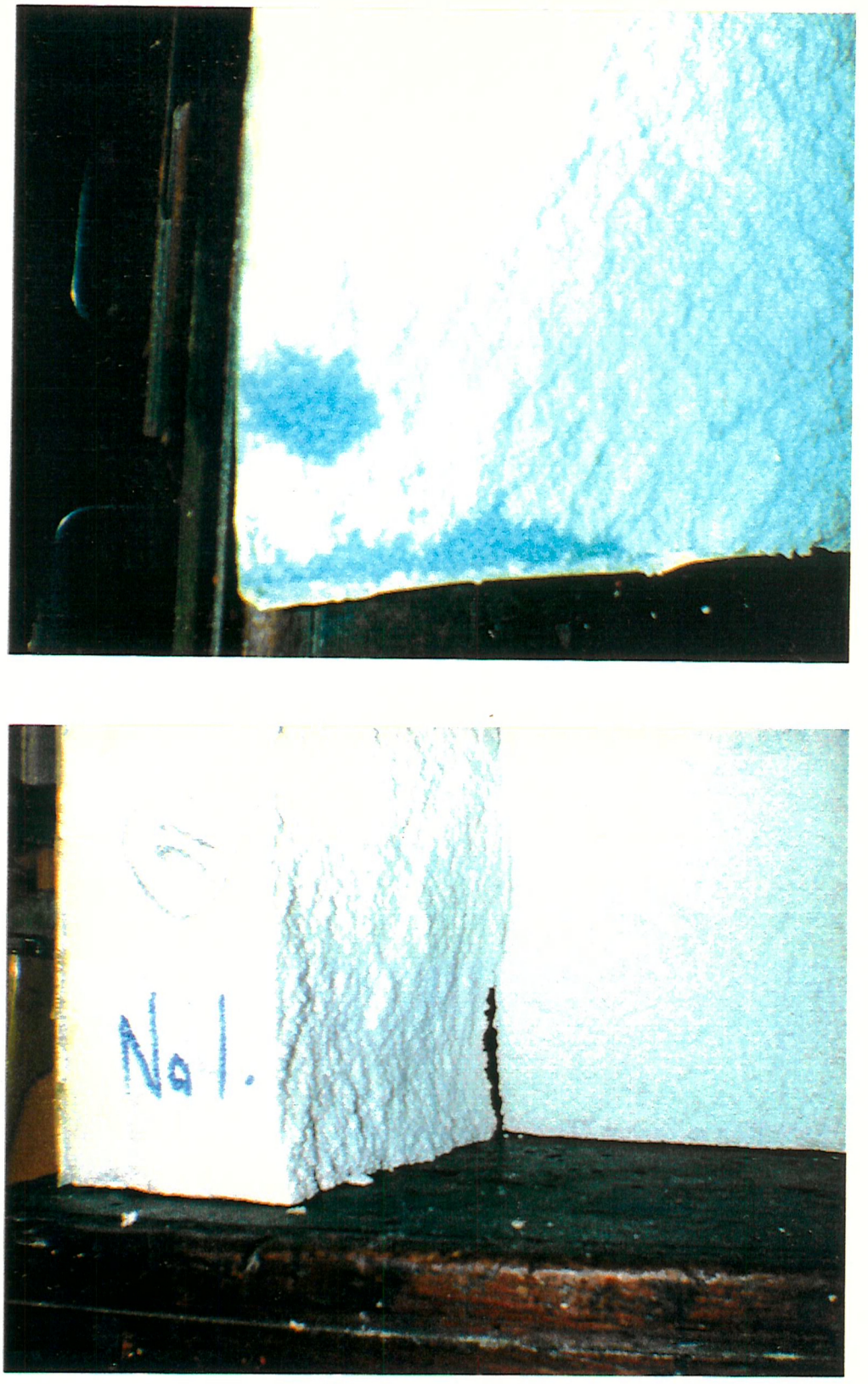

Fig 4.3 Bond failure of the polystyrene core for the first specimen (Tensile test).

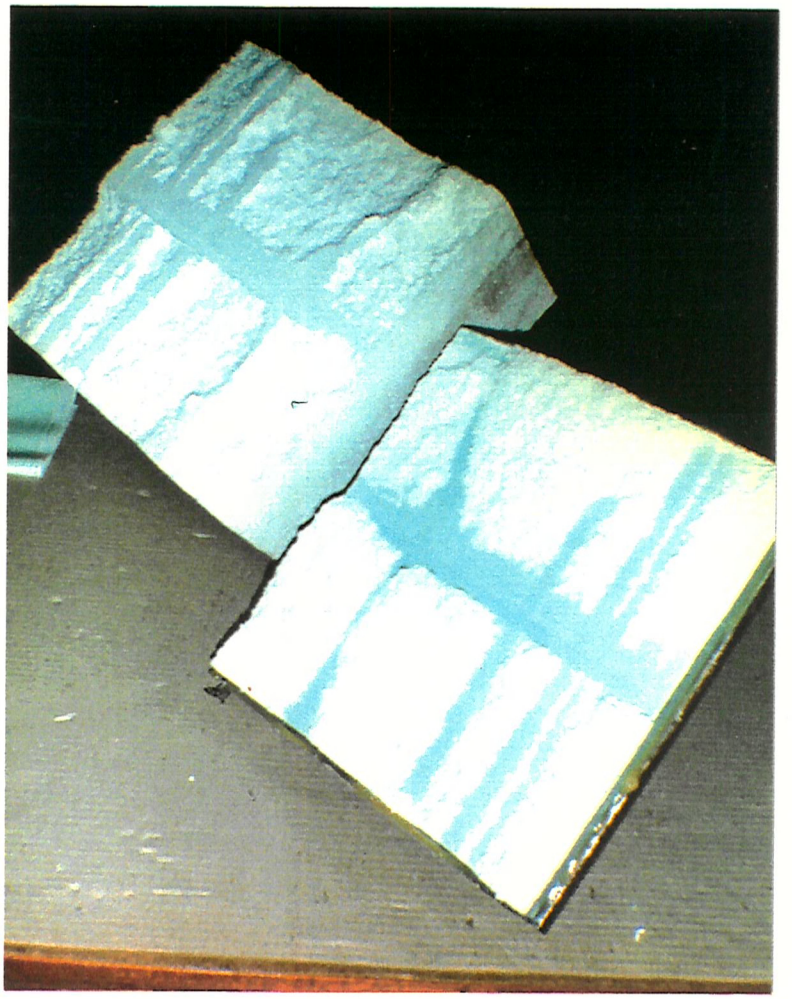

Fig 4.4 Bond failure between steel faces and polystyrene core for the second specimen (Tensile test).

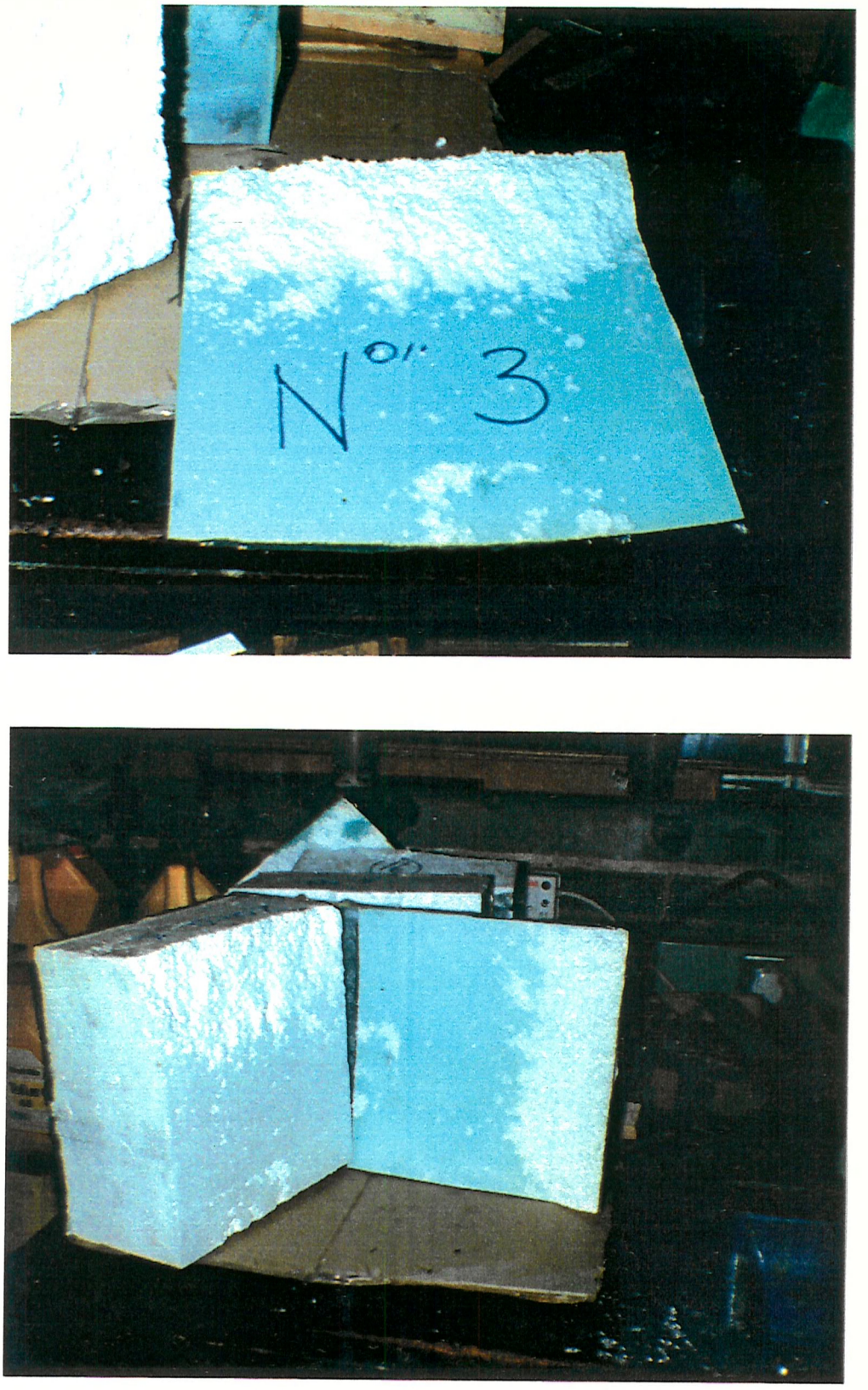

Fig 4.5 Bond failure between steel faces and polystyrene core for the third specimen (Tensile test).

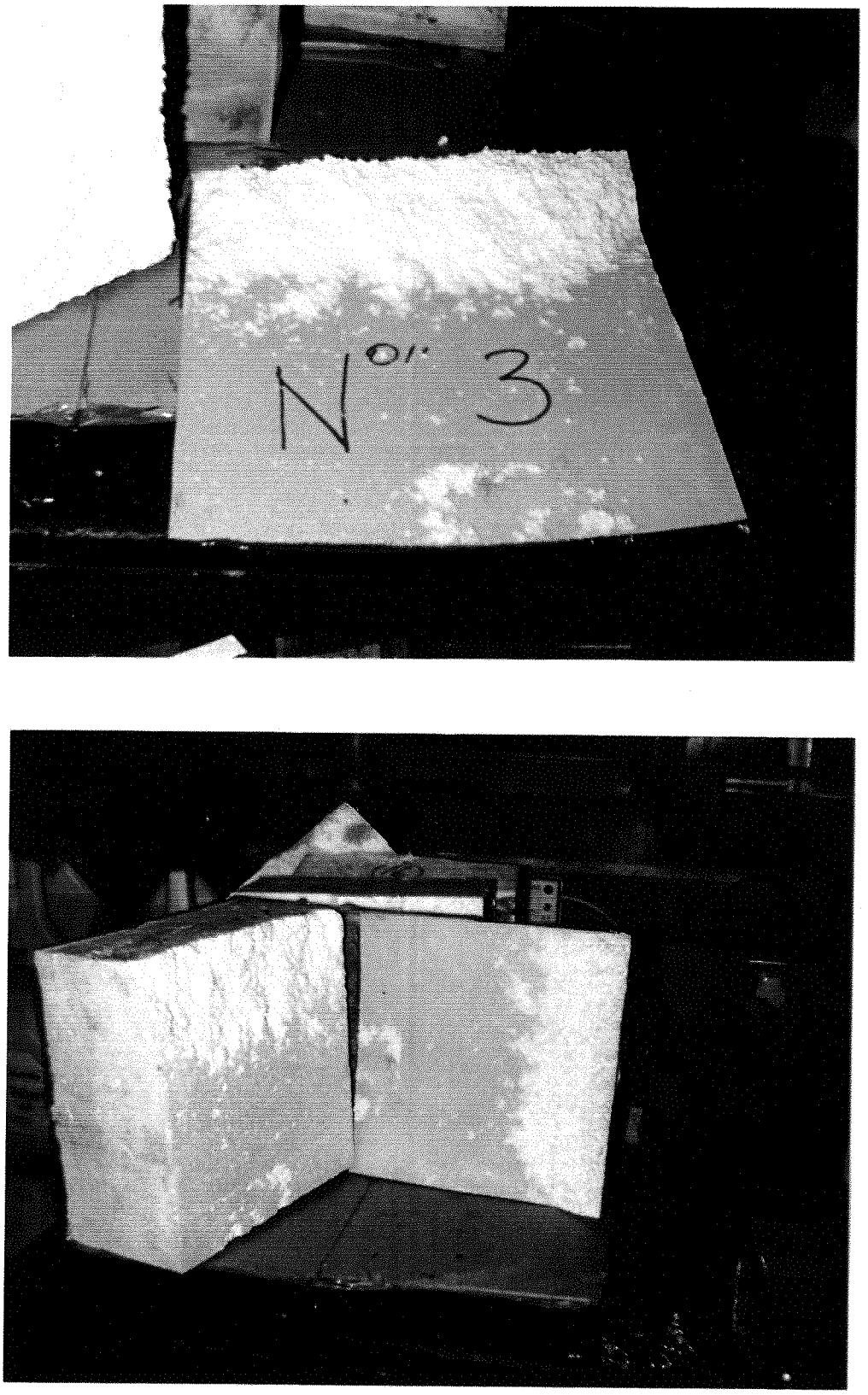

Fig 4.5 Bond failure between steel faces and polystyrene core for the third specimen (Tensile test).

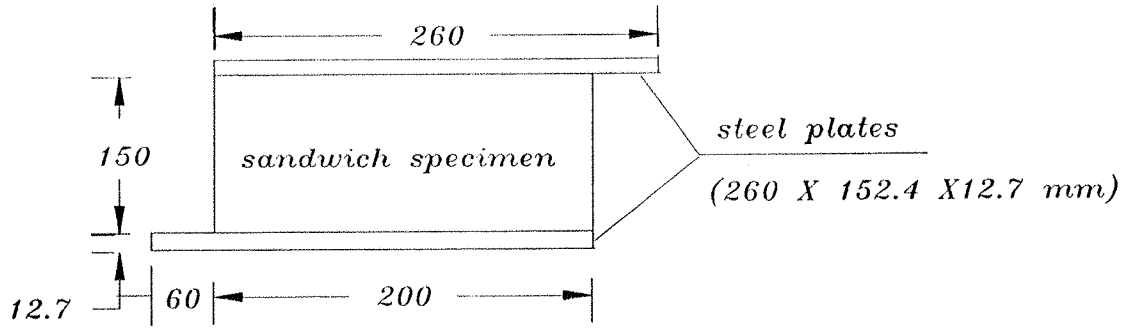

Fig 4.6 Test assembly of the first shear test.

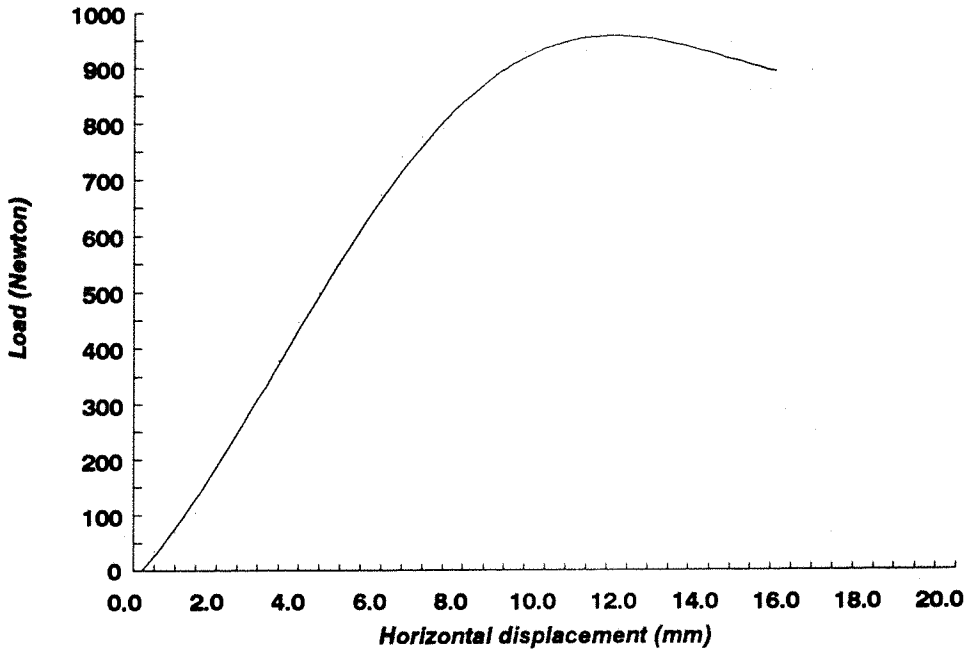

Horizontal movement (mm)	Load (Newton)
0.00	0.00
0.50	34.48
1.00	68.96
1.50	103.45
2.00	172.41
2.50	241.38
3.00	310.35
3.50	379.31
4.00	448.27
4.50	500.00
5.00	551.72
5.50	603.45
6.00	672.41
6.50	741.38
7.00	775.86
7.50	793.10
8.00	827.58
8.50	862.07
9.00	896.55
9.50	931.03
10.00	931.03
10.50	931.03
11.00	931.03
11.50	948.27
12.00	948.27
12.50	965.52
13.00	965.52
13.50	965.52
14.00	965.52
14.50	948.27
15.00	962.07
15.50	962.07
16.00	896.55
16.50	896.55

Fig 4.7 Load / displacement graph of the first shear test

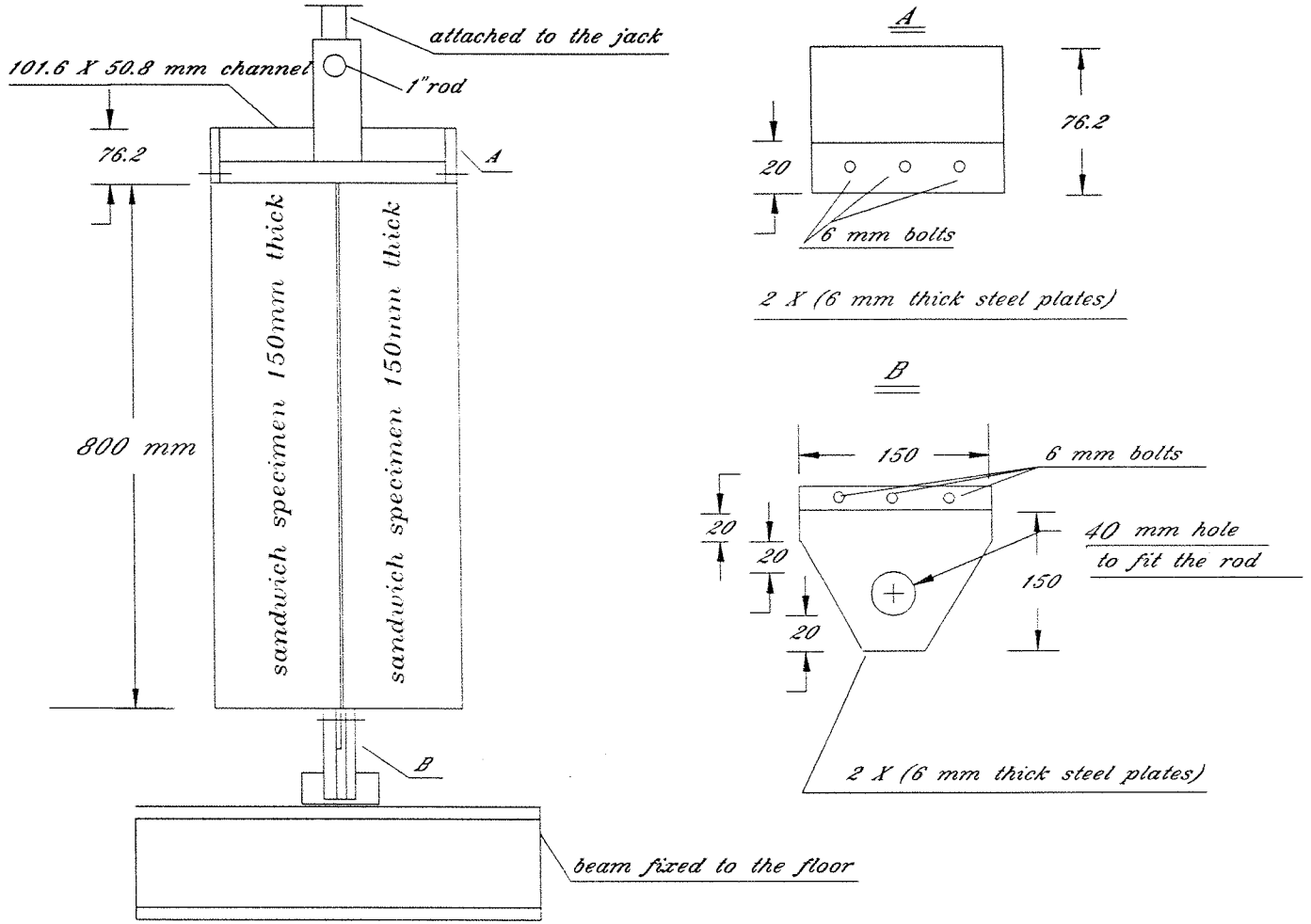

Fig 4.8 Test assembly of the second shear test.

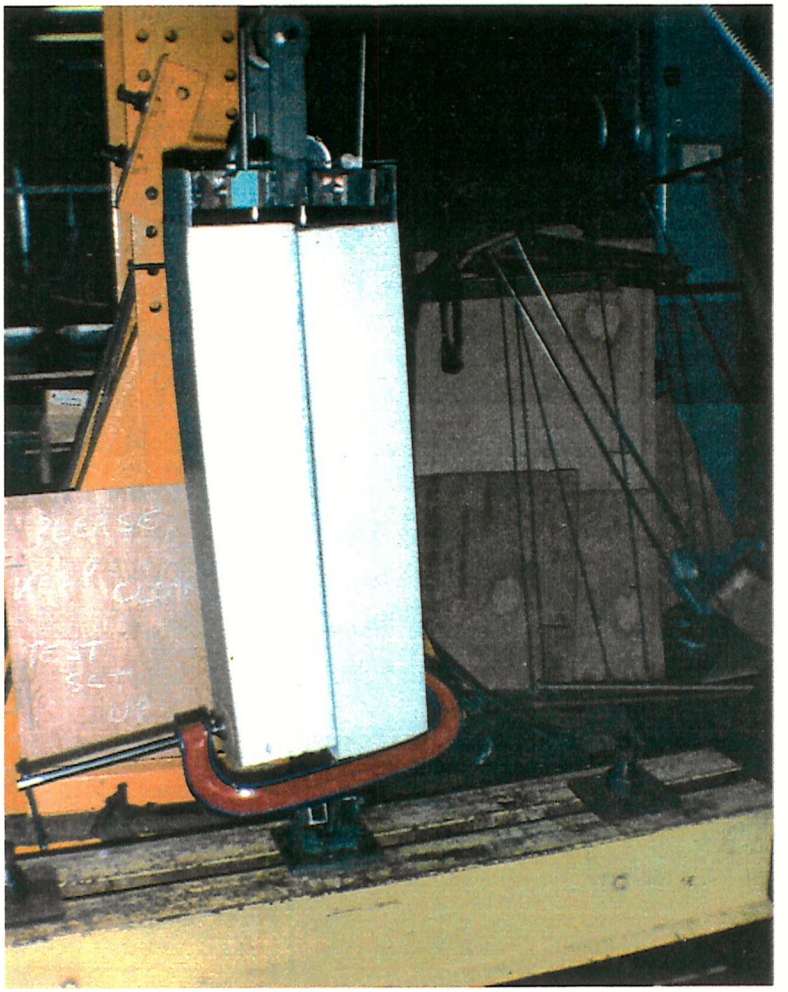

Fig 4.9 General view of a specimen fitted under the actuator during Second shear test.

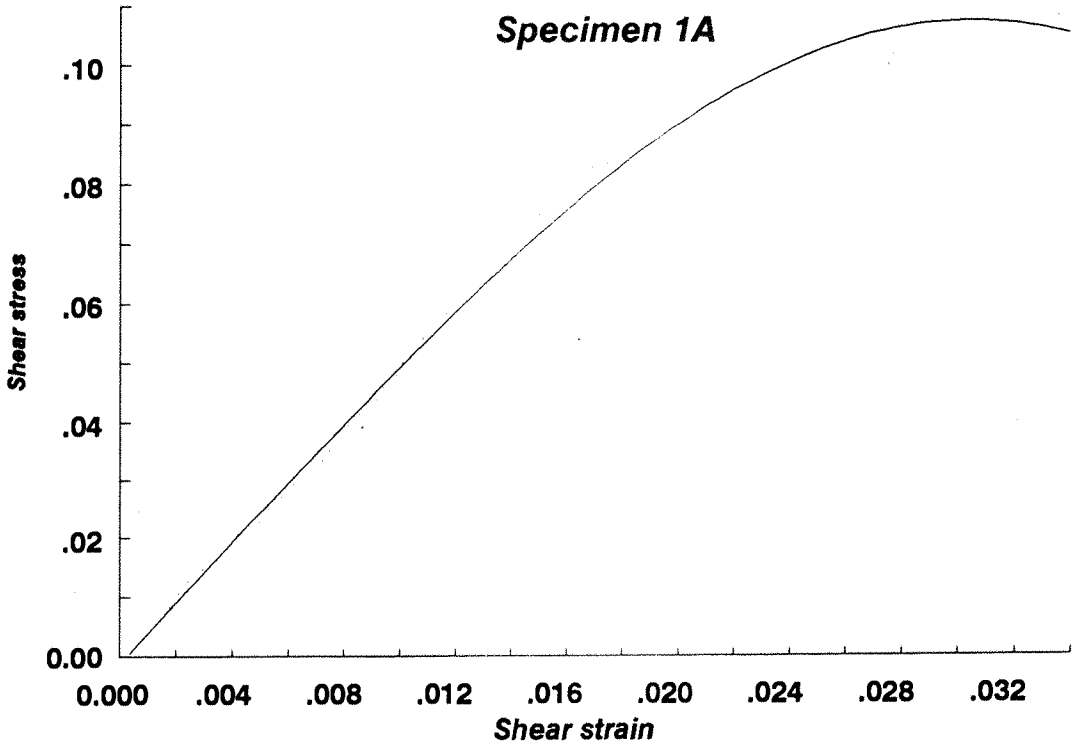

Shear strain	Shear stress (N/mm2)
0.0000	0.0000
0.0018	0.0083
0.0033	0.0167
0.0053	0.0250
0.0072	0.0334
0.0092	0.0439
0.0100	0.0500
0.0117	0.0583
0.0132	0.0667
0.0150	0.0750
0.0175	0.0833
0.0207	0.0917
0.0275	0.1000
0.0336	0.1083

Fig 4.10 Shear stress / strain diagram for the second shear test

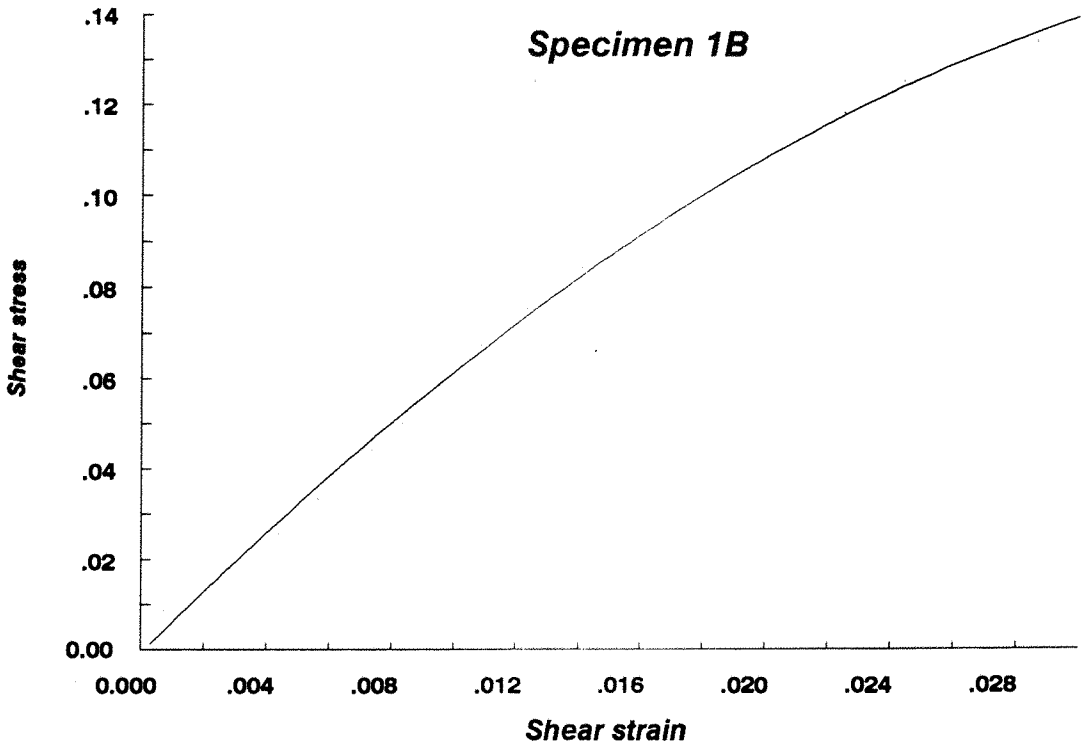

Shear strain	Shear stress (N/mm2)
0.0000	0.0000
0.0028	0.0179
0.0044	0.0256
0.0056	0.0334
0.0073	0.0442
0.0083	0.0503
0.0095	0.0585
0.0109	0.0675
0.0123	0.0753
0.0141	0.0841
0.0161	0.0923
0.0182	0.1018
0.0200	0.1084
0.0225	0.1182
0.0224	0.1252
0.0286	0.1342

Fig 4.11 Shear stress / strain diagram for the second shear test

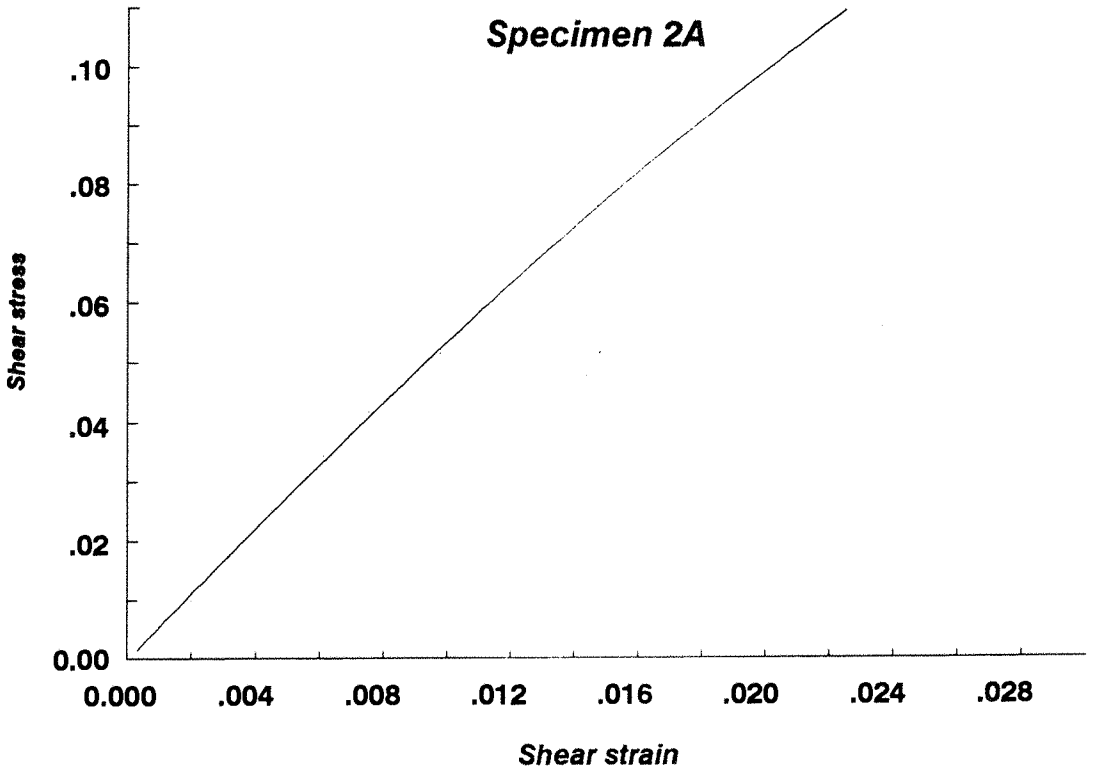

Shear strain	Shear stress (N/mm2)
0.0000	0.0000
0.0020	0.0100
0.0032	0.0174
0.0045	0.0255
0.0061	0.0345
0.0075	0.0418
0.0098	0.0516
0.0116	0.0602
0.0129	0.0672
0.0147	0.0763
0.0162	0.0835
0.0185	0.0934
0.0202	0.1002

Fig 4.12 Shear stress / strain diagram for the second shear test

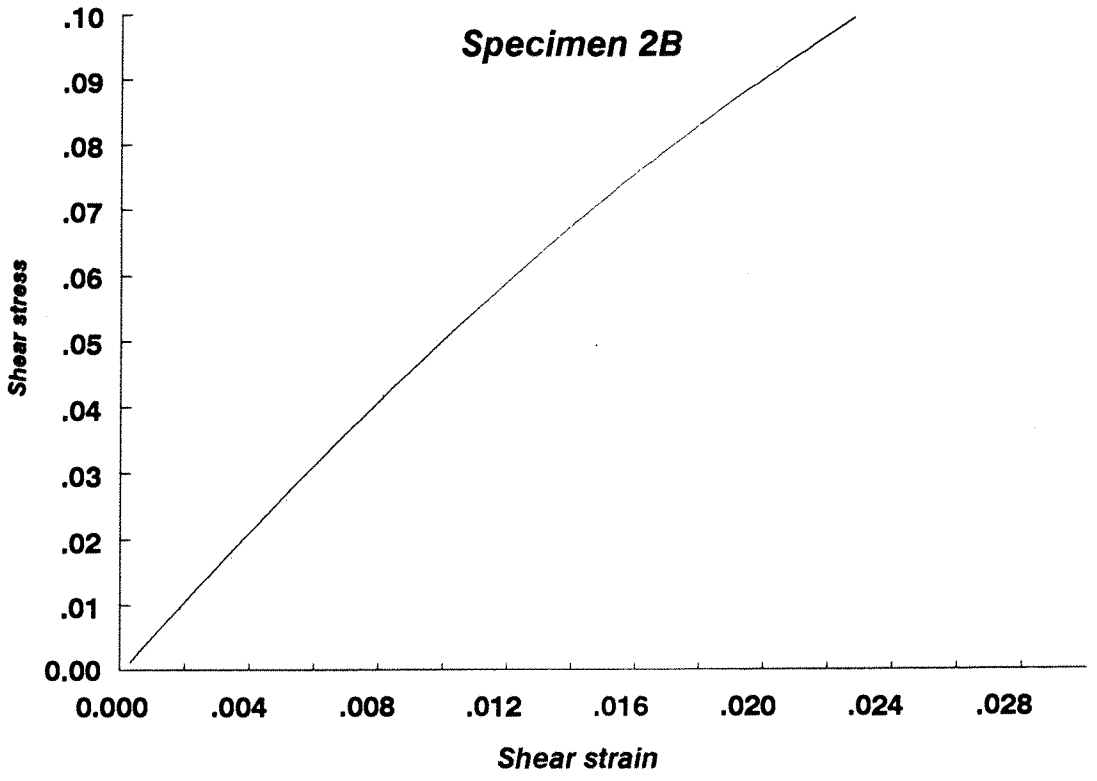

Shear strain	Shear stress (N/mm2)
0.0000	0.0000
0.0018	0.0093
0.0035	0.0173
0.0052	0.0259
0.0065	0.0339
0.0081	0.0418
0.0098	0.0501
0.0118	0.0588
0.0139	0.0674
0.0163	0.0761
0.0182	0.0836
0.0204	0.0922

Fig 4.13 Shear stress / strain diagram for the second shear test

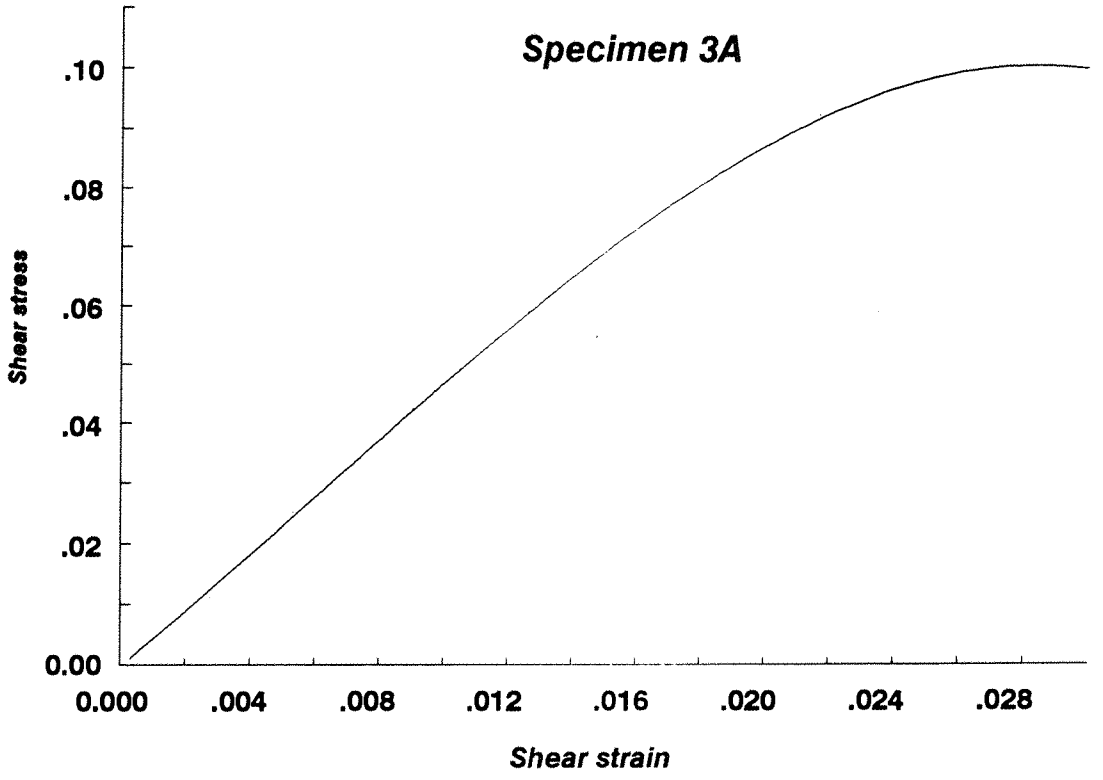

Shear strain	Shear stress (N/mm2)
0.0000	0.0000
0.0028	0.0111
0.0041	0.0188
0.0053	0.0252
0.0072	0.0337
0.0090	0.0425
0.0108	0.0504
0.0126	0.0591
0.0146	0.0669
0.0166	0.0752
0.0190	0.0835
0.0217	0.0923
0.0271	0.1002

Fig 4.14 Shear stress / strain diagram for the second shear test

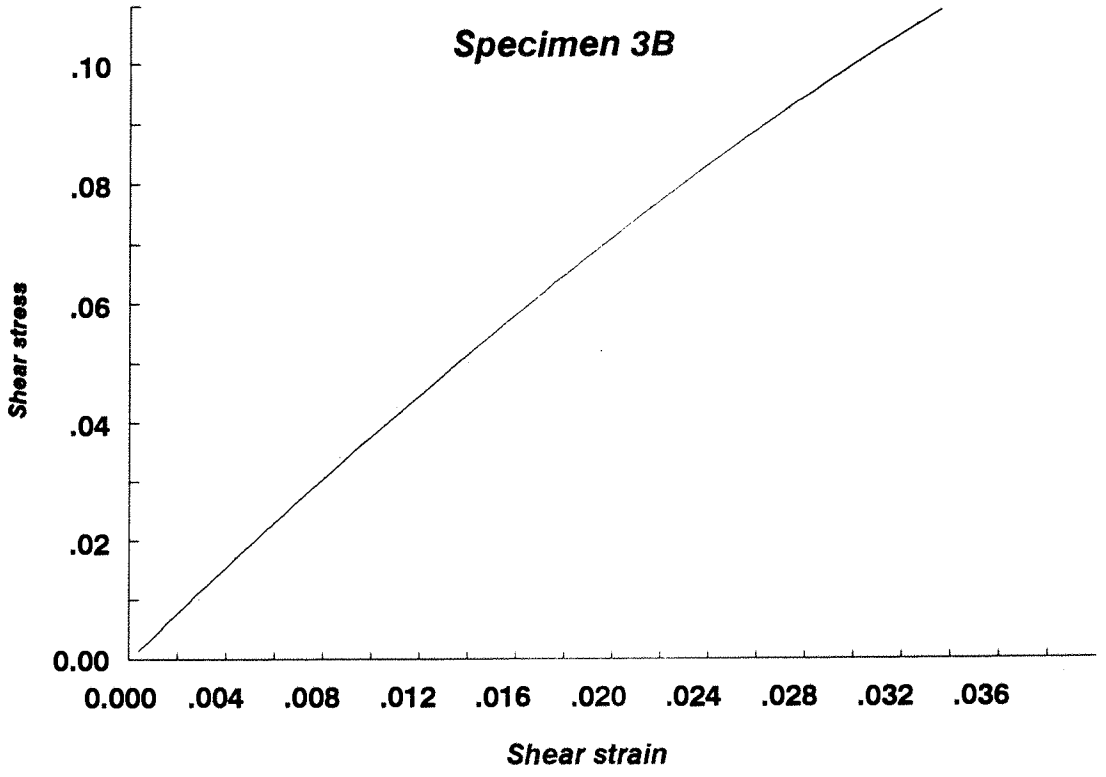

Shear strain	Shear stress (N/mm2)
0.0000	0.0000
0.0029	0.0101
0.0044	0.0172
0.0066	0.0252
0.0087	0.0341
0.0110	0.0425
0.0139	0.0502
0.0168	0.0597
0.0191	0.0683
0.0215	0.0761
0.0239	0.0839
0.0273	0.0925
0.0303	0.1002
0.0326	0.1072

Fig 4.15 Shear stress / strain diagram for the second shear test

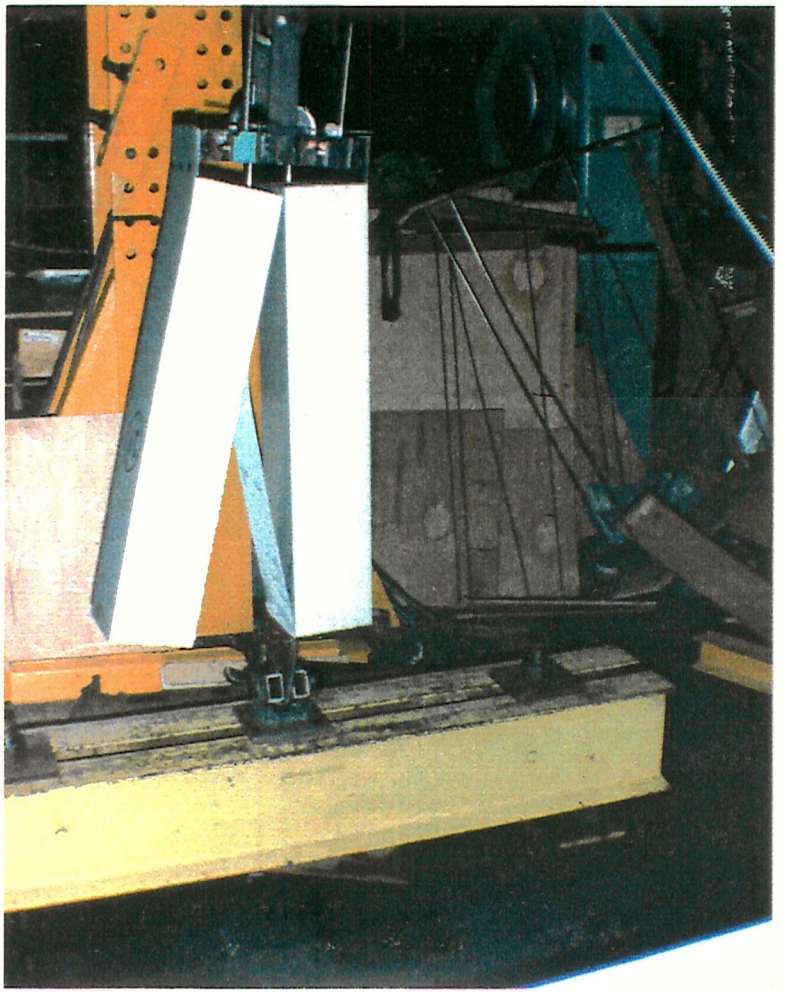

Fig 4.16 Typical bond failure between inner steel faces and polystyrene core (Second shear test)

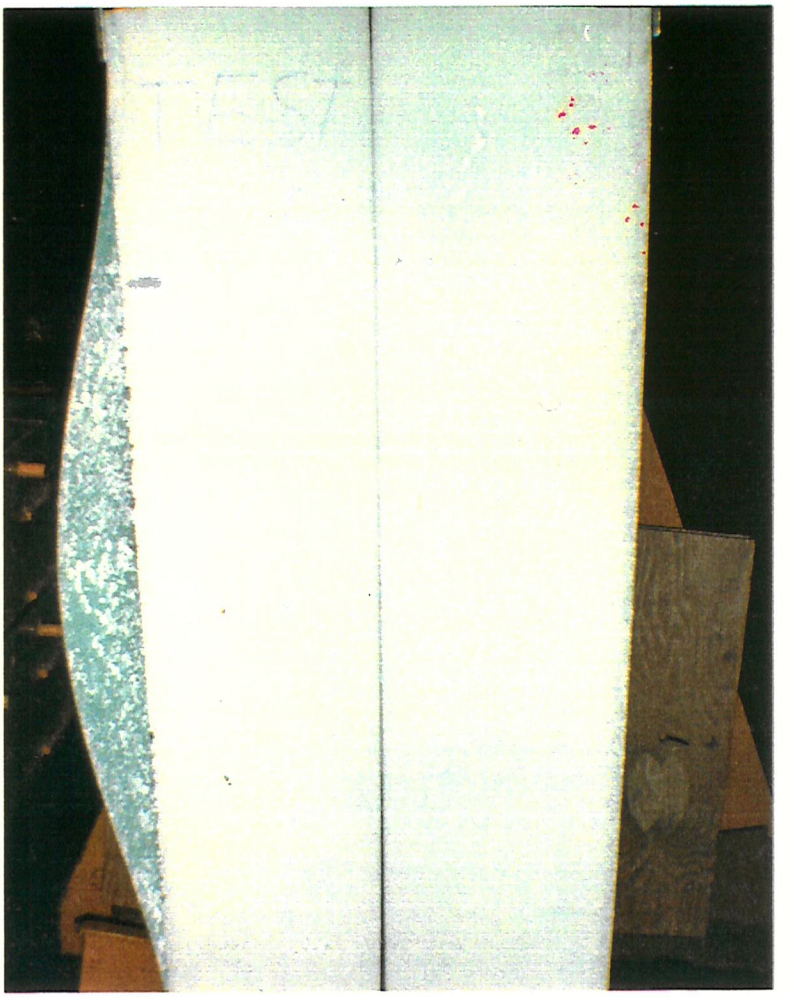

Fig 4.17 Typical bond failure between outer steel faces and polystyrene core (Second shear test)

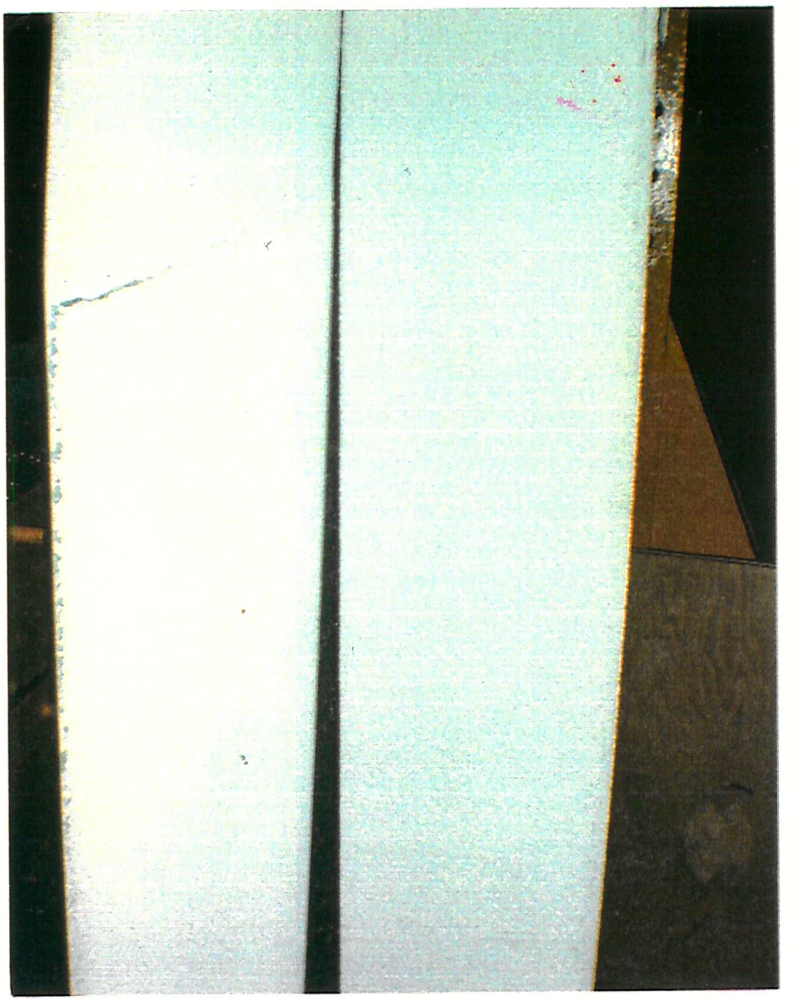

Fig 4.18 Core shear failure for specimen 2B (Second shear test)

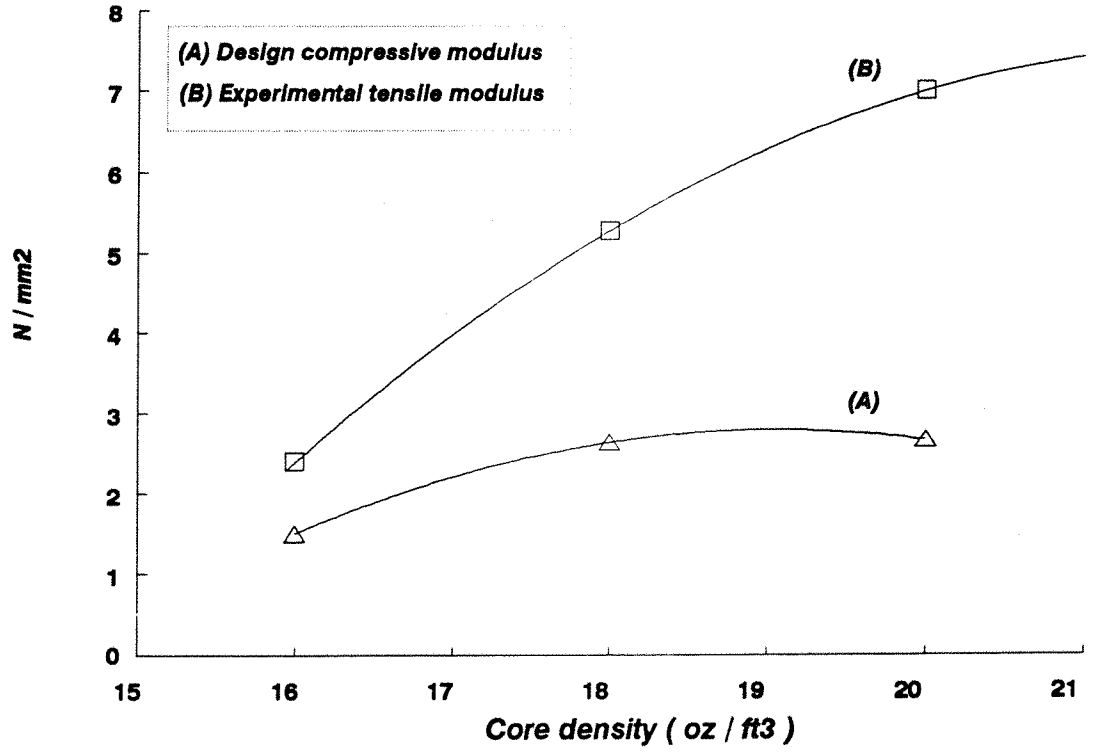

Fig 4.19 Relationship between density and moduli of elasticity of polystyrene.

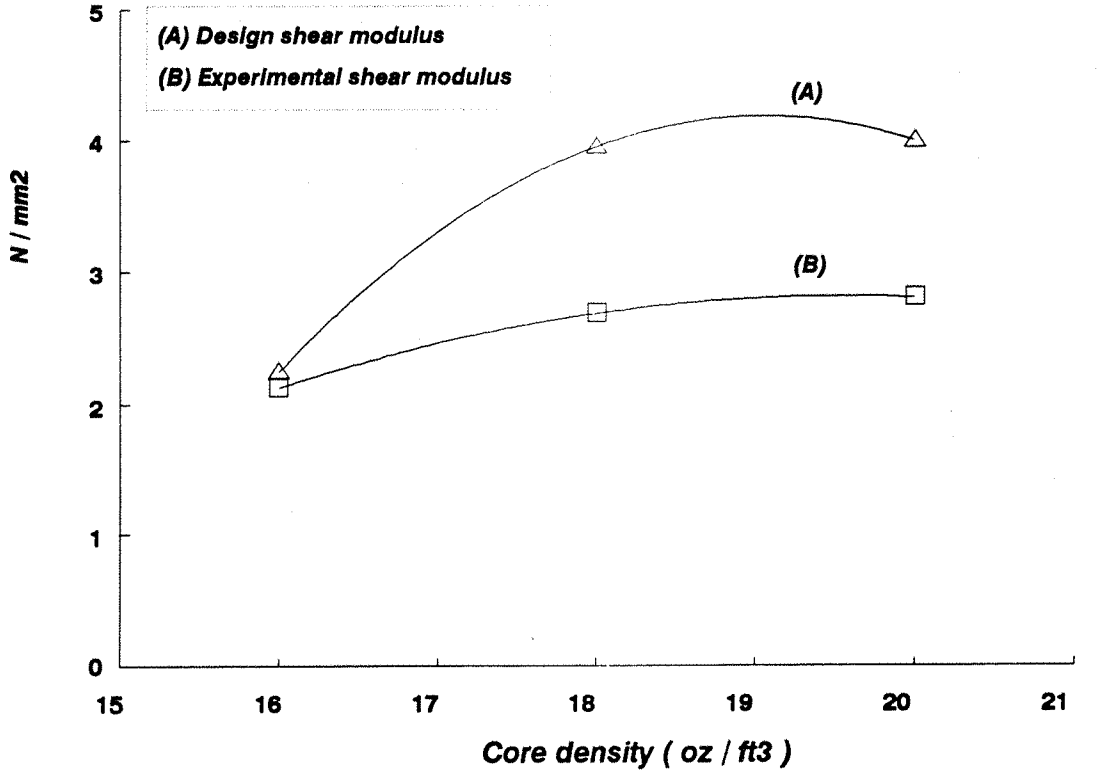

Fig 4.20 Relationship between density and shear modulus of polystyrene core.

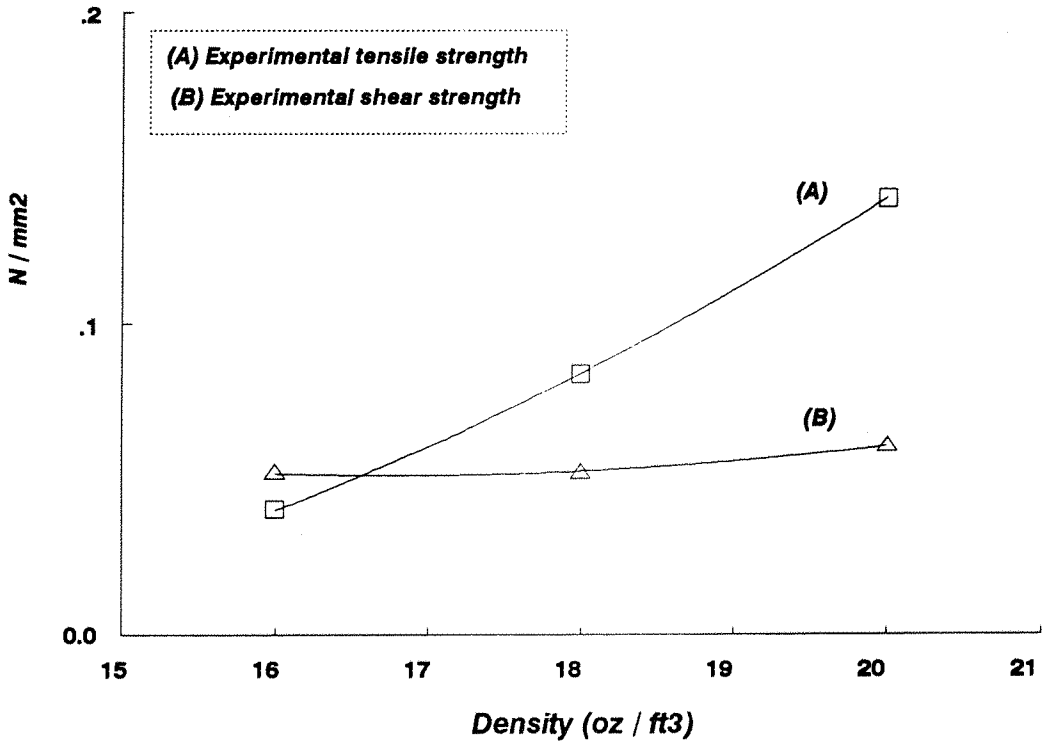

Fig 4.21 Relationship between density, tensile strength and shear strength of ploystyrene core.

CHAPTER FIVE

MAIN TEST ON TWO-SPAN SANDWICH PANELS UNDER SIMULATED LOADS

5.1 Introduction.

This chapter covers the main experimental work and describes the tests carried out on complete sandwich panels of various core densities. The aim of these tests is to study the behaviour of multi-span panels with wind loads and with a temperature gradient between the outer and inner faces of the sandwich. The results obtained from the experiments will then be compared with those predicted from the computational analysis detailed in chapter three.

5.2 Dimensions:

Three panels with densities of 16 , 18 and 20 oz / ft^3 were tested. All three panels were of the same dimensions:

- Panel thickness: 150 mm
- Panel width: 1200 mm
- Panel length: 4600 mm with a span of 4500 mm.

All panels were weighed before test, the densities of the three panels were determined by weighing known volume specimens, the results are shown in Table 5.1.

5.3 Loading:

The panels were tested under dead load which represented both wind load and the equivalent load due to stresses

induced by the temperature difference between the two metal faces of the sandwich. These loads were acting as a uniformly distributed load on the panel of maximum intensity of (5.648E-03 KN/mm). This load is equivalent to 2.5416 tonnes per span. It was applied in ten loading increments of intensity 0.25416 tonnes each.

The reaction from the internal support was simulated by the load applied from a hydraulic actuator. The value of this reaction varied for each of the three panels because of the different core density for each panel.

5.4 Preparation of the specimens and procedure:

Each panel was lifted into position by means of a crane and two strops which held the panel symmetrically. It was then placed in its position over the two end supports, one end support was a roller and the other was supported on a rocker fixed at the span of 4500 mm. The supports were well packed to ensure that no movement would occur during the test.

For the middle support, a 229 X 89 channel of mass 32.76 Kg/m was used. Two 16 mm diameter high tensile bolts held the channel to the bottom plate of the actuator which would apply a load equivalent to the calculated internal support reaction. This load and the corresponding central deflection were easily read from the monitor of the actuator.

The uniformly distributed load was simulated by evenly applied ball bearings over the span of 4500 mm. In order to contain these balls, plywood panels (150 mm wide and 12 mm thick) with different lengths were placed symmetrically around the edges of the panel and held in place using tie bars (Fig 5.1).

The tie bars resting on top of the panel divided the span

into seven sections of different lengths. These sections were loaded proportionally to ensure an even spread of the load over the panel. The length of each section, the corresponding loading and the number of trays used to carry the load are shown in Table 5.2.

The ball bearings were used to simulate the uniformly distributed load on the panel, up to the sixth loading increment, which represented 60 % of the ultimate load. For the seventh, eighth, ninth and tenth loadings, large bins of 50 Kg weight each were used as well as metal trays with the remaining balls. Figure 5.2 shows a typical loading of the panel under test.

The deflections along the span were measured on the underside of the panels by means of dial gauges. These were set at positions span/8, span/4, span/2, and at the points where maximum deflection was expected, 3span/4, 7span/8. In total 14 gauges were used, seven on each side of the panel along its span. All gauges were set to zero before the start of the test. The actuator was allowed to apply a load equivalent to the self weight of half the panel and the corresponding central deflection was recorded to adjust the later deflection readings. Figures (5.3 to 5.5) show in detail the arrangement of the test.

Each loading increment corresponded to :

- 10 percent of the maximum predicted UDL load (0.25416 tonnes).

- A central deflection which was expected to occur at a 10 percent increment of the internal support load.

The readings from the gauges were taken nearly ten minutes after applying the load in order to allow the panel to deflect under load.

During the tests, careful observation were made of critical

areas for deflections, core shear, face wrinkling and eventual fracture mode.

5.5 First panel of core density 20 oz /ft ^{3}:

Ten loading increments were completed and the corresponding deflections were recorded. After applying the full maximum uniform load and the maximum expected central deflection, no failure had occurred. Nonetheless, the panel showed clear deflection along the span. The maximum expected central load 7.785 KN was then applied with the full UDL on the panel, at this stage the panel failed. Table 5.5 summarizes the experimental results at each loading increment as well as the computational deflections along the span.

5.5.1 Mode of failure:

Examining the panel after removing the load, it was quite clear that the dominating failure was a localised wrinkling of the top metal face of the panel at a distance of 1536 mm from the roller support (Fig 5.6).

The bottom face of the panel showed a clear sign of metal face distortion and core crushing at the points of support across the width of the panel (Fig 5.7 & 5.8). This resulted in some deflection of the supports, which was neither taken into account in the analytical design nor measured during the test. The cause of the type of failure recorded in this test will be discussed in details later in this chapter.

5.6 Second panel of core density 18 oz / ft^3:

The same procedure was applied to this panel as for the first one. Two additional gauges were mounted at the supports to measure the deflection there during the test.

No failure occurred after applying the full uniform load and the maximum central deflection. The maximum expected central load 7.8 KN was then applied but still there was no sign of a failure. The central load was gradually increased until it reached 8.3 KN. At this point, the panel failed. the central deflection corresponding to the new applied central load was recorded. Table 5.6 shows the experimental and computational deflection along the span at each loading increment.

5.6.1 Mode of failure:

As in the first panel, the failure mode was mainly wrinkling of the top metal face of the sandwich panel shown at a distance of 1572 mm from the roller support across the width of the panel.

The gauges placed at the supports show some upward deflection caused by the distortion of the bottom metal face and the crushing of the core across the width of the panel (Fig 5.9). The value of these deflections are shown in Table 5.3.

5.7 Third panel of core density 16 oz / ft^3:

The test was conducted in a similar way to the first two panels, but with one significant difference. Deflection at the supports in this test, shown in Table 5.4, were added to the central deflection. Readings of the deflection along the span of the panel were taken with and without considering the support deflections (Table 5.7 & 5.8).

The uniform load was applied as before in increments of 10 percent of the maximum load right up to the ninth loading when the panel failed.

5.7.1 Mode of failure:

This panel showed a different type of failure to the earlier samples. It failed at a load of (4.5184E-03 KN/mm) by core shear failure at the fixed support end as shown in Fig 5.10. This was followed by delamination of the steel / polystyrene interface at the two ends of the panel. The end showed slip of the metal faces beyond the polystyrene core by 6.35 mm at the roller support and by 12.70 mm at the fixed support (Fig 5.11).

5.8 Test results compared with the first analysis.

5.8.1 Adjustment of third panel results:

With reference to section 5.7, the deflection of the supports was taken into account during testing the third panel. The average deflection of the supports was added to the applied central deflection. This added deflection lead to a reduced central support reaction. As a result of the increased deflection, it was necessary to adjust the computational results of the third panel in order to make a more realistic comparison between experimental and analytical results.

Applying a central deflection larger than that predicted from computational analysis represented a less stiff sheeting rail being used as a central support.

For the sheeting rail, the central deflection of the middle panel δ_3 subjected to a load W_3 is proportional to :

$$\Sigma \frac{W_i . l^4}{E I_s}$$

in which E for steel is constant.

W_i are the intensity of load acting on the sheeting rail
l the span of the sheeting rail is constant.

Hence, in order to obtain larger deflection I must vary in a way that it satisfies the following :

$$I_\alpha = I_c \frac{\Delta_c}{\Delta_\alpha}$$

where I_c is the moment of inertia of the sheeting rail as used in the first and second panels. $I_c = 33900000\ mm^4$

I_α is the moment of inertia of the sheeting rail which should have been used to obtain the larger deflection.

Δ_c is the central deflection which should have been applied.

Δ_α is the actual applied central deflection.

From the calculated values of $\frac{\Delta_c}{\Delta_\alpha}$ as shown in Table 5.9 it is clear that this ratio is not constant for all load increments. It varies within a range of 18.5 %. Therefore, it is not possible to consider the mean value of the ratio $\frac{\Delta_c}{\Delta_\alpha}$ in order to obtain a single adjusted value of I_α which will provide the required deflection. As a result, the value of I_α should be calculated from each load increment's value of Δ_c and Δ_α . The corresponding central load prediction may then be calculated accordingly.

The central support load is evaluated using the following procedure:

At the first load increment (10 % of the ultimate load): Using equation 3.27 (Chapter 3), the middle deflection of the sheeting rail is :

$$\delta_3 = \frac{1}{I_s} \left(21047619.05\ F_3 + 12514285.72\ F_1 + 33428571.42\ F_2 \right)$$

substitute the value of I_s by $I_s = I_\alpha = 33855258.8\ mm^4$
For the middle panel on the sheeting rail:

$$\delta_{3(1/2)} = \Delta_{L/2} - d_3$$

From equation 3.13, the middle deflection on the sandwich panel due to the uniform load W is calculated as follows:

$$\Delta_{L/2} = \frac{5WL^4}{384\ D} + \frac{WL^2}{8\ AG}$$

W is equal to 10 % of the ultimate U.D.L = 5.6484E-04 KN/mm length.

$$\therefore\ \Delta_{L/2} = 5.5927\ mm$$

The central deflection of the sandwich panel due to a central support reaction F_3 is calculated using equation 3. as following:

$$d_3 = \frac{F_3 L^3}{48\ D} + \frac{F_3 L}{4\ AG}$$

$$d_3 = F_3 \left[\frac{L^3}{48\ D} + \frac{L}{4\ AG}\right]$$

$$\therefore\ d_3 = 4.08\ F_3$$

Therefore, the central sheeting rail deflection is equal to:

$$\delta_3 = \Delta_{L/2} - d_3$$

$$\delta_3 = 5.5927 - 4.08\ F_3$$

The same procedure is followed to obtain the sheeting rail deflections at the mid span of first, second and end panels.

For first panel:

$$\delta_1 = \frac{1}{I_s}\,[6257142.858\,F_3 + 4307142.857\,F_1 + 10457142.86\,F_2]$$

$$= 5.5927 - 4.08\,F_1$$

For second panel:

$$\delta_2 = \frac{1}{I_s}\,[16714285.71\,F_3 + 10457142.86\,F_1 + 27278571.43\,F_2]$$

$$= 5.5927 - 4.08\,F_2$$

For end panels:

$$\delta_{support} = \Delta_{L/2} - d_{support} = 0$$

$$d_{support} = \Delta_{L/2}$$

$$d_{support} = 5.5927\ mm$$

$$d_{support} = F_{support}\left[\frac{L^3}{48\,D} + \frac{L}{4\,AG}\right]$$

$$\therefore F_{support} = 1.371\ KN$$

Rearranging the above equations as function of F_1 , F_2 , F_3 , the following simultaneous equations are obtained:

$$0.36964082\,F_1 + 0.987396715\,F_2 + 4.701694228\,F_3 = 5.5927$$

$$4.207222269\,F_1 + 0.308877947\,F_2 + 0.18482041\,F_3 = 5.5927$$

$$0.308877947\,F_1 + 4.885741037\,F_2 + 0.493727895\,F_3 = 5.5927$$

Solving the three above equations:

F_1 = 1.218 *KN*

F_2 = 0.978 *KN*

F_3 = 0.888 *KN*

$F_{support}$ = 1.371 *KN*

Using the same method, the load intensity is calculated for other load increments. The results of these calculations are summarized in Table 5.10 .

5.8.2 Analysis of the results and discussion:

Figures 5.6 to 5.10 show the typical failure mode of the three tested panels. It is clear that the dominating failure is the wrinkling of the steel faces under compression (Fig 5.6) as well as the crushing of the lower steel faces at the points of supports (Fig 5.7 & 5.8). A core shear failure of the third panel tested is clearly shown in Figure 5.10.

5.8.2.1 Calculation of the predicted internal support reaction and the uniformly distributed load.

-a- Predicted internal support reaction:

Figures 5.26 To 5.28 show the experimental results of the central support reaction plotted against the central deflection for the three tested panels respectively.
The theoretical line according to equation 3.13 with a limiting central deflection of $\Delta_{L/2} = L/240$ is also shown in the Figures for comparison. (L is the total span = 4500 mm).

The deflection at the central support is calculated using the following equation.

$$\Delta_{L/2} = \left[\frac{5WL^4}{384\ D} + \frac{WL^2}{8\ AG}\right] - \left[\frac{FL^3}{48\ D} + \frac{FL}{4\ AG}\right] \quad \text{.....(5.1)}$$

The deflection value obtained from the above equation is considered equal to the limiting central deflection (18.75 mm).

For the total span L = 4500 mm, the predicted central support reaction is calculated for the limiting deflection value of 18.75 mm and for the total design uniformly distributed load of intensity 5.6484E-03 KN/mm length.
For the third panel of core density 16 oz / ft^3, only 80 % of the ultimate U.D.L was applied. Therefore, the predicted central support reaction is calculated accordingly.

Table 5.11 summarizes the value of the predicted central support reaction (F) and its corresponding applied value for each tested panel.

The three panels tested did satisfy the limiting deflection requirement since at $\Delta_{L/2}$ = 18.75 mm, the applied central support reaction is larger than its predicted value shown in Table 5.11. For the third panel (Fig 5.28) the experimental central load / central deflection results appears to fall below the limiting deflection line after the third loading. This is probably due to the additional deflection caused by shearing of the polystyrene core causing discontinuity at one end of the panel and the subsequent delamination of the steel / polystyrene interface.

-b- <u>Predicted uniformly distributed load.</u>

To calculate the predicted uniformly distributed load, the limiting deflection is considered for half the span at x = 1125mm. The limiting deflection is equal to:

Limiting $\delta_x = \frac{2250}{240} = 9.375\ mm$.

At any section x from the support, the deflection due to the uniformly distributed load is calculated from the following equation:

$$\Delta = \frac{-WLx^3}{12EI} + \frac{Wx^4}{24EI} + \frac{WL^3x}{24EI} + \frac{WLx - Wx^2}{2AG} \quad \text{.....(5.2)}$$

and at any section x from the support, the deflection due to an internal support reaction is calculated from the following equation:

$$d = \frac{Fx^3}{12EI} - \frac{FL^2x}{16EI} - \frac{Fx}{2AG} \quad \text{.....(5.3)}$$

The total deflection at a section x from the support is equal to $[\Delta - d]$ *at* x .

The limiting deflection at x is equal to (the total deflection at x) - ((x/L) the mid span deflection at the internal support).

At x = 1125 mm, the ratio x/L is equal to 1/2.

Mid - span deflection at the internal support is equal to :

$\Delta_{L/2} = 18.159\ mm$ *1st panel*

$= 18.195\ mm$ *2nd panel*

$= 18.852\ mm$ *3rd panel*

Consider the internal support reaction F as calculated from the computational analysis:

$F = 7.78\ KN$ *1st panel*

$= 7.80\ KN$ *2nd panel*

$= 6.346\ KN$ *3rd panel*

The predicted uniformly distributed load is then calculated from the following equation:

At x = 1125 mm :
The limiting deflection = Total deflection at x - 1/2 mid-span deflection.

In other word:

$$limiting\ \delta_x = \left[\frac{-WLx^3}{12EI} + \frac{Wx^4}{24EI} + \frac{WL^3x}{24EI} + \frac{WLx-Wx^2}{2AG}\right] - \left[\frac{Fx^3}{12EI} - \frac{FL^2x}{16EI} - \frac{Fx}{2AG}\right] \qquad \text{.....(5.4)}$$

The predicted uniformly distributed load is calculated for x = 1125 mm for the three panels. The results are summarized below:

$predicted\ W = 9.835\ E\text{-}04\ KN/mm\ length$ (1st panel)

$= 9.648\ E\text{-}04\ KN/mm\ length$ (2nd panel)

$= 5.689\ E\text{-}04\ KN/mm\ length$ (3rd panel)

5.8.2.2 Wrinkling of the upper steel faces.

When a sandwich panel is subjected to bending action, the steel faces under compression exhibit a buckle which starts at a low load and gradually increase with the load.

Wrinkling of the faces under compression occurs when a single buckle becomes unstable and forms a fold. This wrinkling usually occurs at the section of maximum bending moment (zero shear section).

The theoretical wrinkling stresses are calculated using equation (2.2) (Chapter 2, section 2.6.1).

$$\sigma_{wr} = 0.6\ [E_c . E_f . G_c]^{1/3} \qquad \text{.....(5.5)}$$

Table 5.12 summarizes the theoretical value of the wrinkling stresses for the three tested panels.

The wrinkling stresses may also be derived from simple strength of materials theories where:

$$\sigma_E = \frac{M . z}{D} . E_f \qquad \text{.....(5.6)}$$

where:

M is the maximum bending moment at the section under consideration. This moment is equal to the sum of moments due to the uniformly distributed load and the internal support reaction.

$z = \pm \frac{t}{2}$ is the distance from the neutral axis of the panel to the upper or lower steel face.

In order to calculate the maximum bending moment, it is necessary first to find the position along the span where bending moment is maximum. From the shear force diagram, the position of zero shear (maximum bending moment) is found.

For the three panels, the position x of maximum moment is calculated and given as:

For the first panel:

$W = 5.6484\ E\text{-}03\ KN/mm\ length$

$F = 7.78\ KN$

$\therefore x = 1561.3\ mm$

For the second panel:

$W = 5.6484\ E\text{-}03\ KN/mm\ length$

$F = 7.80\ KN$

$\therefore x = 1559.54\ mm$

For the third panel:

$W = 4.51872\ E\text{-}03\ KN/mm\ length$

$F = 6.346\ KN$

$\therefore x = 1547.81\ mm$

The theoretical wrinkling load is calculated as follows:

At any section x from the support, the moment due to the uniformly distributed load and the internal support reaction is equal to :

$$M_x = \left[\frac{WLx}{2} - \frac{Wx^2}{2}\right] - \left[\frac{Fx}{2}\right] \quad \text{.....(5.7)}$$

Substituting the moment calculated from the above equation, at the corresponding x for each panel, in equation 5.6, the theoretical wrinkling load is obtained. The calculated load is shown in Table 5.13 for each of the three panels.

From the experimental results, the first and second panels showed some wrinkling of the upper steel faces at a distance 1536 mm and 1572 mm from the roller support respectively. Figures 5.29 & 5.30 show the deflection at position x plotted against the uniformly distributed load. Wrinkling of the upper steel faces appears to occur at the point where the load / deflection graphs (Fig 5.29 & 5.30) begin to depart from a straight line. In the experiment, wrinkling occurred at a load intensity of 2.8242 E-03 KN/mm length and 3.955 E-03 KN/mm length for the first and second panels respectively. The corresponding wrinkling stresses calculated from equation 5.6 are 0.0608 KN/mm^2 and 0.0619 KN/mm^2 for first and second panel respectively (Table 5.13). These values should be contrasted with the corresponding theoretical values given in Table 5.12.

5.8.2.3 Crushing of the lower steel faces at the internal support.

At the central support, crushing of the lower steel faces of the three tested panels was recorded. The analysis of this mode of failure may be considered as a wrinkling failure since the lower steel faces crushed under excessive compression during the test.

The crushing of the lower steel faces of the panels appears to occur at points where the central load / central deflection curves (Fig 5.26 to 5.28) begin to depart from a straight line.

For the first panel, crushing of the lower steel face occurred at a load of 4.70 KN and eventual collapse at 9.31 KN, the predicted collapse load is calculated as equal to 7.576 KN.

The second panel showed lower steel face crushing at a load of 5.017 KN. Eventual collapse occurred at a central load of intensity equal to 9.137 KN. The predicted collapse load

is equal to 7.604 KN.

The lower steel face of the third panel started crushing at a load of 5.130 KN. Final collapse occurred at a load of 8.38 KN whereas the predicted collapse load is equal to 6.37 KN.

The compressive stresses at the internal support may be calculated using the simple strength of materials theory (Equation 5.6)

Where M is the maximum moment at the central support and it is equal to the sum of moments due to the uniformly distributed load W and the central support reaction F.

Maximum stresses in the faces occur at $z = \pm\frac{t}{2}$

The maximum bending moment at mid span of the panel due to W and F is equal to:

$$M_{max} = \frac{WL^2}{8} - \frac{FL}{4} \quad \text{.....(5.8)}$$

Where the span is equal to 4500 mm.

The values of the maximum bending moment at mid span of the panel obtained from the above equations are used in equation 5.6 to calculate the maximum stresses in the steel faces at mid span. The results of these calculations are summarized in Table 5.14. This Table also illustrates the theoretical values of the compressive stresses in the steel faces.

5.8.2.4 Crushing of the lower steel face at the end supports.

Crushing of the lower steel face at the end supports was due to some upwards deflection at these supports during the

experiment (Table 5.3 & 5.4). Support deflection should be contrasted with the assumption made in section 3.2.5.e (Chapter three). It was assumed that the steel faces of the panels carry no local bending moments or shear forces. The results obtained and the recorded support deflection proved that the above assumption was not fulfilled during the experiment. Therefore, in future design of multi -span panels, shear deflection in the faces should not be neglected and they should be included in the design calculations.

5.8.2.5 Comparison between theoretical and experimental core shear stresses.

When analyzing the failure mode of the tested panels, it is clear that the third panel of density 16 oz / ft^3 failed by a core shear failure followed by interfacial delamination of the steel / polystyrene at the fixed support end of the panel. At the roller support end, there was a failure by interfacial delamination of the steel / polystyrene due to a polystyrene core discontinuity. In contrast with the assumption made in Chapter three (section 3.2.5.g), there was a poor gluing and adhesion at the discontinuity was sheared and then followed by interfacial delamination.

Before analyzing the core shear failure of the third panel. It is necessary to evaluate the experimental values of core shear stresses and shear forces at the supports and to compare them with their theoretical values and the shear stresses obtained from material tests adopted in Chapter four.

The theoretical maximum core shear stresses may be obtained using the following equation:

$$\tau_{max} = \frac{Q_{max}}{bd} \quad \text{.....(5.9)}$$

Where :

Q_{max} is the maximum shear force which occurs at the supports. It is equal to the sum of shear force due to the uniformly distributed load and the central support reaction.

$$Q_{max} = \frac{WL}{2} - \frac{F}{2} \quad \text{.....(5.10)}$$

Table 5.15 illustrates the values of the shear force and the corresponding shear stresses for the three tested panels respectively. Moreover, Table 5.15 shows the value of core shear stresses as obtained from the shear tests adopted in Chapter four (section 4.3.3.5) for comparison.

During the experiments, the central deflection was applied by the actuator and the corresponding central support reaction was higher than its predicted value . This lead to a reduced maximum shear force at the supports and thus smaller shear stresses in particular, for the first and the second panels. The results of the applied central support reaction and the shear forces at the supports in addition to the experimental values of the shear stresses for the three tested panels are summarized in Table 5.16.

The results of the first and second panels show that the maximum shear stresses at the supports (0.04506 and 0.04555 N/mm^2 respectively) are smaller than their theoretical values shown in Table 5.15 (0.04934 and 0.04928 N/mm^2 respectively). Hence, no core shear failure occurred in these panels.

For the third panel, however, the central deflection was increased by the average of the supports deflection. This increased central deflection lead to a reduced central support reaction up to the fifth loading increment (Fig 5.28). It also lead to an increased shear force at the supports when a core shear failure started at the

roller support end. The last three loadings showed larger central support reaction and lower shear force at the supports. This may be due to some losses in the shear force magnitude whilst core shear failure was occurring.

The shear force and shear stresses at the internal support are also calculated. Theoretical and experimental values are summarized in Table 5.17.

5.8.2.6 Bending under the uniformly distributed load and the internal support reaction.

Figures 5.12 to 5.25 show the experimental deflection values plotted with the computational ones for comparison. The graphs show deflections along the span for each panel and at each load increment. It is clear that the three tested panels perform according to the conditions they were designed for.

The results of the test show that no premature failure has occurred in the first and second panels. The third panel however, failed prematurely by a core shear failure hence the graphs for this panel are only plotted up to the eighth loading increment at which failure occurred.

The experimental deflection values obtained for the three tested panels are slightly larger than those predicted in the analytical analysis. This difference between experimental and computational deflections does not cause any major problems and it does not indicate any crucial disagreement between design and experimental results.

The experimental results show that the adhesion between the metal skin and the polystyrene core and the deflection of the supports are crucial to the integral function of sandwich panels.

5.8.2.7 Ratio between maximum compressive stresses in the lower and upper steel faces .

Referring to section 5.8.2.3, the maximum compressive stresses in the lower faces at the central support are calculated theoretically and experimentally (Table 5.14).

The maximum theoretical compressive stresses in the upper steel faces are calculated at points of maximum bending moment (section 5.8.2.2). Table 5.18 summarizes these stresses.

Similarly, the experimental values of the maximum compressive stresses in the upper faces are found at position of maximum bending moment for the three tested panels.

The position of maximum bending moment for the three panels is summarized as follows:

For the first panel:

$W = 5.6484\ E\text{-}03\ KN/mm\ length$

$F = 9.31\ KN$

$\therefore x = 1425.87\ mm$

For the second panel:

$W = 5.6484\ E\text{-}03\ KN/mm\ length$

$F = 9.137\ KN$

$\therefore x = 1441.18\ mm$

For the third panel:

W = 4.51872 E-03 KN/mm $length$

F = 8.38 KN

$\therefore x$ = 1322.75 mm

The maximum bending moment for the three panels is calculated using equation 5.7 , then the maximum compressive stresses are calculated according to equation 5.6. These values are summarized in Table 5.18.

The ratio between maximum compressive stresses in the lower and upper steel faces is calculated for the three tested panels as shown in Table 5.18. This ratio is calculated for both theoretical and experimental results . Both results showed that compressive stresses in the lower steel faces at the internal support are smaller than the stresses in the upper faces.

In addition to the design theory adopted for the experimental work covered in this chapter, theoretical results are obtained for the second theory outlined in section 3.3.2.1 (Chapter Three). Results for both theories will be compared later in this chapter.

5.9 Test results compared with the second analysis.

This section evaluates the shear and compressive stresses for two - span panels subjected to a uniformly distributed wind load, a thermal gradient and an upward central point load.

Referring to section 3.6 in Chapter Three, internal support reactions were calculated assuming that the panels are subjected to :

- a - A uniformly distributed wind load of intensity 1.2144E-03 KN/mm length.

- b - A thermal gradient causing a central deflection of 18.83 mm.

- c - And an upward central point load simulating the internal support reaction.

The following calculations will assess the theoretical maximum core shear stresses and compressive stresses in the upper and lower steel faces in this case. The results are compared later with those obtained for the design case in which the deflection due to thermal gradient was reproduced by the application of a "simulated temperature load" (section 5.8.2.4 and 5.8.2.6 respectively).

5.9.1 Evaluation of maximum core shear force and stresses at the internal support of the panels.

The maximum shear force at the internal support is calculated from the following:

$$Q_{max} = \pm \frac{F}{2} \quad \text{.....(5.11)}$$

The maximum shear stresses in the core are calculated using equation 5.9. The theoretical values of the maximum shear force and stresses in the core are summarized in Table 5.19.

5.9.2 Evaluation of maximum stresses in the upper and lower steel faces of the panels.

Maximum stresses in the upper steel faces occur at the position of maximum bending moment. It is necessary first to find the position along the span where bending moment is maximum. From the shear force diagram, the position of zero shear (maximum bending moment) is found.

For the three panels, the position x of maximum moment is calculated and given as:

For the first panel:

$q = 1.2144\ E\text{-}03\ KN/mm\ length$

$F = 3.328\ KN$

$\therefore x = 879.45\ mm$

For the second panel:

$q = 1.2144\ E\text{-}03\ KN/mm\ length$

$F = 3.343\ KN$

$\therefore x = 873.394\ mm$

For the third panel:

$q = 1.2144\ E\text{-}03\ KN/mm\ length$

$F = 3.478\ KN$

$\therefore x = 818.02\ mm$

The maximum bending moment at position x for each of the three different density panels can be calculated using equation 5.7 with the value of the uniformly distributed load taken equal to the wind load only.

The maximum compressive stresses in the upper steel faces of the three panels are calculated from equation 5.6 at $z = \pm\frac{t}{2}$. These stresses are developed in the faces by the uniformly distributed wind load only. No stresses are assumed to be induced by the thermal gradient. Table 5.20 summarizes the results obtained for each of the three panels.

Similarly, the maximum stresses in the lower steel faces are calculated at the internal support position. Using equation 5.8 the maximum bending moment at the internal support is calculated for the value of the uniform load taken equal to the wind load intensity. Substituting the values of maximum moment in equation 5.6, the maximum stresses in the lower steel face are obtained for each of the three different density panels. Table 5.20 summarizes the results.

The ratio between maximum compressive stresses in the lower and upper steel faces is calculated for the three tested panels as shown in Table 5.20. This ratio proves that when the temperature effects are applied as a thermal gradient between outer and inner steel faces, the stresses in the lower face are expected to be larger than those in the upper face.

5.10 Conclusion

Three sandwich panels of different core density were tested under dead load representing both wind load and "simulated temperature load". The first and second panels failed by wrinkling of the upper steel faces, whereas the third panel failed by core shear followed by interfacial delamination of the steel / polystyrene at the fixed support end. A core discontinuity due to poor gluing caused interfacial delamination at the roller support end. Crushing of the lower steel faces at the supports was also recorded.

Comparing both theoretical and experimental results of deflection, shear stresses and compressive stresses proves that both results are in reasonable agreement for the design theory adopted in the first analysis (section 3.3.2.2) and the experiment. Hence, the following can be concluded:

-1- Under applied loads, the three panels behaved as predicted. The deflection recorded in the test was slightly higher than its predicted value. However, it

did not cause any premature failure.

-2- The simulation of temperature effects as a uniformly distributed load can be considered satisfactory for the assumptions made in section 3.3.2.2 regarding the stiffness of the core material.

-3- Shear stresses in the core were not crucial with the exception of the third panel.

-4- Adhesion between the metal skin and the polystyrene core and the deflection of the support are critical to the integral function of sandwich panels.

When the experimental results are compared with the second analysis (section 3.3.2.1) as well as the first analysis, the following conclusions can also be drawn:

-1- The ratio of the maximum stresses are shown in Tables 5.20 and 5.18. Comparing these stresses at the two critical sections of mid span and central support proves that : If the deflection due to thermal gradient is reproduced by the application of "simulated temperature load", the maximum stresses in the lower face are smaller than those in the upper steel face (Table 5.18). However, if the temperature effects were applied as a thermal gradient between outer and inner steel faces, the stresses in the lower face are larger than those in the upper face (Table 5.20).

-2- Experimental work was not repeated for the case of temperature effects being applied as thermal gradient. The initial calculations and results for the second analysis show that load simulation of thermal gradient cannot be adopted without introducing the potential for major change in the behaviour of the panels.

-3- It is preferable to adopt the design theory based on

the assumptions of section 3.3.2.1 (no stresses are developed in the faces due to thermal gradient). An experiment should be carried out accordingly on similar panels to those tested in this research. The results should then be compared with the theoretical results outlined in Table 5.20. Such an experiment is expected to be very costly and difficult to carry out. This difficulty will arise from the impracticality of maintaining a large constant temperature difference between outer and inner steel faces for the whole duration of the test.

Until such an experiment is carried out, the results obtained from the experimental work covered in this chapter can be considered applicable for two - span sandwich panels only providing the same assumptions made in this work are satisfied.

This approach will overestimate mid-span stresses and hence be conservative for mid-span and end support conditions. The approach lead to an underestimate of the central support stresses, but these could be checked separately by an analysis of the panel under three point load bending (Fig 2.16, Chapter Two).

panel No.	panel weight (Kg)	specimen volume (m^3)	specimen weight $x10^{-3}$ (Kg)	panel density (Kg/m^3) (oz/ft^3)
1	61.00	5.890e-03	122.24	20.725 20.692
2	60.00	12.226e-03	232.60	19.025 18.995
3	56.75	6.110e-03	93.38	15.281 15.256

Table 5.1 Sandwich panels weights and densities.

Section no	Section length (mm)	Load (Kg)	No.of trays x weight(Kg)
1	532.00	30.05	2 x 10.00 1 x 10.05
2	545.00	30.78	2 x 10.00 1 x 10.78
3	585.00	33.04	2 x 10.00 1 x 13.04
4	1100.00	62.13	5 x 10.00 1 x 12.13
5	654.00	36.94	3 x 10.00 1 x 6.94
6	554.00	31.29	2 x 10.00 1 x 11.29
7	530.00	29.94	2 x 10.00 1 x 9.94

Table 5.2 Loading sections and corresponding weights as used in the experiments.

% of load	10 %	20 %	30 %	40 %	50 %	60 %	70 %	80 %	90 %	100%
roller support	N.A	N.A	0.25	0.57	0.92	1.56	2.97	4.13	5.65	6.41
fixed support	N.A	N.A	N.A	0.25	0.59	1.19	1.59	2.74	4.10	5.59

Table 5.3 Supports deflections as read from the gauges after each loading increment for the second panel.

% of load	10 %	20 %	30 %	40 %	50 %	60 %	70 %	80 %
roller support	0.11	0.84	1.11	1.86	2.54	3.41	4.28	5.46
fixed support	0.22	0.51	1.94	1.55	2.40	2.89	2.35	5.46

Table 5.4 Supports deflection as read from the gauges after each loading increment for the third panel.

X / Y	roller support	562.5	1125	1800	2250	2700	3375	3937.5	4500
10%(C)	0	- 0.995	- 1.655	- 1.940	- 1.816	- 1.940	- 1.655	- 0.995	0
10%(E)	N.A	- 1.330	- 2.135	- 2.512	- 1.800	- 2.307	- 2.127	- 1.245	N.A
20%(C)	0	- 1.989	- 3.310	- 3.880	- 3.632	- 3.880	- 3.310	- 1.989	0
20%(E)	N.A	- 2.540	- 3.975	- 4.362	- 3.630	- 4.272	- 3.842	- 2.582	N.A
30%(C)	0	- 2.984	- 4.965	- 5.820	- 5.448	- 5.820	- 4.965	- 2.984	0
30%(E)	N.A	- 3.685	- 5.577	- 6.950	- 5.450	- 6.870	- 5.125	- 3.685	N.A
40%(C)	0	- 3.979	- 6.619	- 7.761	- 7.264	- 7.761	- 6.619	- 3.979	0
40%(E)	N.A	- 5.625	- 7.635	- 8.725	- 7.260	- 8.740	- 7.635	- 5.682	N.A
50%(C)	0	- 4.973	- 8.274	- 9.699	- 9.078	- 9.699	- 8.274	- 4.973	0
50%(E)	N.A	- 6.227	- 9.787	-11.017	- 9.080	-11.007	- 9.752	- 6.532	N.A
60%(C)	0	- 5.968	- 9.929	-11.640	-10.895	-11.640	- 9.929	- 5.968	0
60%(E)	N.A	N.A	N.A	N.A	N.A	N.A	N.A	N.A	N.A
70%(C)	0	- 6.960	-11.580	-13.574	-12.705	-13.574	-11.580	- 6.960	0
70%(E)	N.A	- 8.890	-13.365	-15.725	-12.710	-15.235	-13.367	- 9.290	N.A
80%(C)	0	- 7.957	-13.239	-15.520	-14.527	-15.520	-13.239	- 7.957	0
80%(E)	N.A	-11.760	-16.127	-18.025	-14.530	-17.015	-16.157	-12.125	N.A
90%(C)	0	- 8.952	-14.894	-17.461	-16.343	-17.461	-14.894	- 8.952	0
90%(E)	N.A	-14.245	-18.810	-20.565	-16.340	-19.620	-17.945	-13.947	N.A
100%(C)	0	- 9.946	-16.549	-19.401	-18.159	-19.401	-16.549	- 9.946	0
100%(E)	N.A	-14.900	-20.765	-22.417	-18.160	-22.067	-20.915	-15.135	N.A

Table 5.5 Experimental and computational results of the first panel (20 oz/ft^3).
(C) : Computational results.
(E) : Experimental results.
X : Positions of gauges along the span.
Y : Percentage of the ultimate loads.

X / Y	roller support	562.5	1125	1800	2250	2700	3375	3937.5	4500
10% (C)	0	- 0.999	- 1.662	- 1.946	- 1.819	- 1.946	- 1.662	- 0.999	0
10% (E)	0	- 1.635	- 2.400	- 2.970	- 1.830	- 2.720	- 2.440	- 1.555	0
20% (C)	0	- 1.998	- 3.323	- 3.892	- 3.639	- 3.892	- 3.323	- 1.998	0
20% (E)	0	- 3.395	- 4.295	- 5.100	- 3.650	- 4.780	- 4.295	- 3.295	0
30% (C)	0	- 2.997	- 4.984	- 5.838	- 5.458	- 5.838	- 4.984	- 2.997	0
30% (E)	0	- 4.630	- 6.145	- 7.145	- 5.460	- 6.770	- 6.120	- 4.535	0
40% (C)	0	- 3.996	- 6.646	- 7.784	- 7.278	- 7.784	- 6.646	- 3.996	0
40% (E)	0	- 5.885	- 8.035	- 9.245	- 7.290	- 8.875	- 8.035	- 5.870	0
50% (C)	0	- 4.995	- 8.306	- 9.728	- 9.096	- 9.278	- 8.306	- 4.995	0
50% (E)	0	- 6.340	-10.050	-11.935	- 9.100	-10.990	-10.010	- 6.735	0
60% (C)	0	- 5.995	- 9.968	-11.675	-10.916	-11.675	- 9.968	- 5.995	0
60% (E)	0	- 8.645	-12.110	-14.175	-10.930	-13.235	-12.120	- 8.290	0
70% (C)	0	- 6.991	-11.626	-13.615	-12.730	-13.615	-11.626	- 6.991	0
70% (E)	0	- 9.300	-14.330	-16.055	-12.740	-15.600	-14.260	- 9.885	0
80% (C)	0	- 7.993	-13.292	-15.567	-14.556	-15.567	-13.292	- 7.993	0
80% (E)	0	-11.785	-16.775	-18.995	-14.560	-18.075	-16.795	-12.010	0
90% (C)	0	- 8.992	-14.953	-17.513	-16.375	-17.513	-14.953	- 8.992	0
90% (E)	0	-14.400	-19.305	-21.020	-16.380	-20.585	-18.770	-14.150	0
100%(C)	0	- 9.991	-16.615	-19.459	-18.195	-19.459	-16.615	- 9.991	0
100%(E)	0	-15.335	-21.660	-23.130	-18.200	-23.110	-21.600	-16.085	0

Table 5.6 Experimental and computational results of the second panel (18 oz/ft^3).
(C) : Computational results.
(E) : Experimental results.
X : Positions of gauges along the span.
Y : Percentage of the ultimate loads.

X / Y	roller support	562.5	1125	1620	2250	2880	3375	3937.5	4500
10% (C)	0	- 1.307	- 2.092	- 2.317	- 1.967	- 2.317	- 2.092	- 1.307	0
10% (E)	0.11	- 1.635	- 1.975	- 2.410	- 1.970	- 2.440	- 2.105	- 1.620	0.22
20% (C)	0	- 2.613	- 4.184	- 4.634	- 3.935	- 4.634	- 4.184	- 2.613	0
20% (E)	0.84	- 3.395	- 4.275	- 4.705	- 4.470	- 4.680	- 4.550	- 2.765	0.51
30% (C)	0	- 3.920	- 6.275	- 6.951	- 5.902	- 6.951	- 6.275	- 3.920	0
30% (E)	1.11	- 4.730	- 6.900	- 7.560	- 6.850	- 7.505	- 7.110	- 4.540	1.94
40% (C)	0	- 5.227	- 8.367	- 9.268	- 7.869	- 9.268	- 8.367	- 5.227	0
40% (E)	1.86	- 6.970	- 9.720	-11.150	- 9.320	-11.060	- 9.885	- 6.480	1.55
50% (C)	0	- 6.533	-10.458	-11.583	- 9.835	-11.583	-10.458	- 6.533	0
50% (E)	2.54	- 9.180	-12.855	-14.515	-11.880	-13.870	-12.925	- 8.745	2.40
60% (C)	0	- 7.840	-12.551	-13.902	-11.804	-13.902	-12.551	- 7.840	0
60% (E)	3.41	-12.405	-16.140	-17.920	-14.970	-18.135	-17.395	-12.850	2.89
70% (C)	0	- 9.143	-14.636	-16.213	-13.763	-16.213	-14.636	- 9.143	0
70% (E)	4.28	-15.840	-18.750	-21.805	-17.420	-22.360	-20.500	-17.265	2.35
80% (C)	0	-10.454	-16.735	-18.536	-15.739	-18.536	-16.735	-10.454	0
80% (E)	5.46	-19.650	-23.885	-25.850	-20.390	-27.780	-27.125	-21.935	5.46

Table 5.7 Experimental and computational results of the third panel (16 oz/ft^3) before adjustment.
(C) : Computational results.
(E) : Experimental results.
X : Position of gauges along the span.
Y : Percentage of the ultimate load.

X / Y	roller support	562.5	1125	1620	2250	2880	3375	3937.5	4500
10% (C)	0	- 1.307	- 2.093	- 2.319	- 1.969	- 2.319	- 2.093	- 1.307	0
10% (E)	0	- 1.635	- 1.975	- 2.410	- 1.970	- 2.440	- 2.105	- 1.620	0
20% (C)	0	- 2.720	- 4.392	- 4.923	- 4.307	- 4.923	- 4.392	- 2.720	0
20% (E)	0	- 3.395	- 4.275	- 4.705	- 4.470	- 4.680	- 4.550	- 2.765	0
30% (C)	0	- 4.108	- 6.642	- 7.459	- 6.558	- 7.459	- 6.642	- 4.108	0
30% (E)	0	- 4.730	- 6.900	- 7.560	- 6.850	- 7.505	- 7.110	- 4.540	0
40% (C)	0	- 5.513	- 8.925	-10.042	- 8.868	-10.042	- 8.925	- 5.513	0
40% (E)	0	- 6.970	- 9.720	-11.150	- 9.320	-11.060	- 9.885	- 6.480	0
50% (C)	0	- 6.934	-11.239	-12.667	-11.234	-12.667	-11.239	- 6.934	0
50% (E)	0	- 9.180	-12.855	-14.515	-11.880	-13.870	-12.925	- 8.745	0
60% (C)	0	- 8.452	-13.744	-15.554	-13.938	-15.554	-13.744	- 8.452	0
60% (E)	0	-12.405	-16.140	-17.920	-14.970	-18.135	-17.395	-12.850	0
70% (C)	0	- 9.851	-16.015	-18.122	-16.230	-18.122	-16.015	- 9.851	0
70% (E)	0	-15.840	-18.750	-21.805	-17.420	-22.360	-20.500	-17.265	0
80% (C)	0	-11.346	-18.474	-20.947	-18.852	-20.947	-18.474	-11.346	0
80% (E)	0	-19.650	-23.885	-25.850	-20.390	-27.780	-27.125	-21.935	0

Table 5.8 Experimental and computational results of the third panel (16 oz/ft^3) after adjustment.
(C) : Computational results.
(E) : Experimental results.
X : Position of gauges along the span.
Y : Percentage of the ultimate load.

% of load	Δ_c	Δ_α	$\frac{\Delta_c}{\Delta_\alpha}$	I_α mm^4
10	1.967	1.970	0.99868	33855258.8
20	3.935	4.470	0.88027	29841153.0
30	5.902	6.850	0.86164	29209426.5
40	7.869	9.320	0.84438	28624482.0
50	9.835	11.880	0.82786	28064454.0
60	11.804	14.970	0.78851	26730489.0
70	13.763	17.420	0.79007	26783372.0
80	15.739	20.390	0.77189	26167071.0
90	17.707	23.680	0.74770	25347030.0

Table 5.9 Adjusted moment of inertia of the sheeting rail.

% of load	F_1 (KN)	F_2 (KN)	F_3 (KN)	$F_{support}$ (KN)	δ_3 (mm)
10	1.218	0.978	0.888	1.371	1.968
20	2.408	1.882	1.686	2.742	4.307
30	3.605	2.803	2.505	4.112	6.557
40	4.796	3.712	3.310	5.483	8.866
50	5.984	4.611	4.100	6.854	11.235
60	7.145	5.441	4.809	8.225	13.936
70	8.337	6.353	5.616	9.595	16.238
80	9.505	7.201	6.346	10.966	18.850

Table 5.10 Adjusted sheeting rail loads and central deflection.

panel number	predicted central support reaction F (KN)	Applied central reaction F (KN)
1	7.576 for 100 % W	9.310
2	7.604 for 100 % W	9.137
3	6.370 for 80 % W	8.380

Table 5.11 Predicted and applied values of central support reaction for the limiting central deflection.

Panel	E_f (KN/mm^2)	E_c (KN/mm^2) ($x10^{-3}$)	G_c (KN/mm^2) ($x10^{-3}$)	*theoretical* σ_{wr} (KN/mm^2)
1	210	2.665	3.99	0.07842
2	210	2.635	3.95	0.07816
3	210	1.500	2.25	0.05349

Table 5.12 Theoretical wrinkling stresses and load for the three tested panels.

Panel	Theoretical wrinkling load x 10^{-3} KN/mm length	Experimental wrinkling load x 10^{-3} KN/mm length	Experimental wrinkling stresses KN/mm^2
1	2.647	2.824	0.0608
2	3.826	3.954	0.0619
3	4.349	N.A	N.A

Table 5.13 Experimental wrinkling load and stresses of the upper steel faces.

panel No.	applied F (KN)	σ_E (KN/mm^2) Experimental.	theoretical F (KN)	σ_E (KN/mm^2) Theoretical
1	9.310	0.04065	7.780	0.05901
2	9.137	0.04272	7.800	0.05877
3	8.380	0.02137	6.346	0.04575

Table 5.14 Experimental and theoretical values of compressive stresses in the steel faces at the central support.

panel No.	U.D.L (xE-03) (KN/mm)	F (KN)	Q_{max}	theoretical τ_{max} (N/mm^2)	τ_{max} from shear test
1	5.6484	7.780	8.819	0.04934	0.0606
2	5.6484	7.800	8.809	0.04928	0.0525
3	4.5184	6.346	6.993	0.03913	0.0518

Table 5.15 Theoretical shear force and shear stresses at the supports for the three panels and shear stresses from material test.

panel No	U.D.L (XE-03) (KN/mm length)	applied F (KN)	Experimental Q_{max} (KN)	Experimental τ_{max} (N/mm^2)
1	5.6484	9.310	8.054	0.04506
2	5.6484	9.137	8.141	0.04555
3	4.5184	8.380	5.976	0.03344

Table 5.16 Experimental values of maximum core shear force and shear stresses at the supports of the three tested panels.

panel No	Theoretical Q_{max} (KN)	Theoretical τ_{max} (N/mm^2)	Experimental Q_{max} (KN)	Experimental τ_{max} (N/mm^2)
1	3.89	0.0217	4.655	0.0260
2	3.90	0.0218	4.569	0.0256
3	3.17	0.0176	4.190	0.0234

Table 5.17 Experimental values of maximum core shear force and shear stresses at the central support of the three tested panels.

Panel	Theoretical max σ_E lower face (KN / mm^2)	Theoretical max σ_E upper face (KN / mm^2)	Theoretical ratio $\frac{\max \sigma_E(low)}{\max \sigma_E(upp)}$	Experimental max σ_E lower face (KN / mm^2)	Experimental max σ_E upper face (KN / mm^2)	Experimental ratio $\frac{\max \sigma_E(low)}{\max \sigma_E(upp)}$
1	0.0590	0.0733	0.805	0.0407	0.0611	0.666
2	0.0587	0.0731	0.804	0.0428	0.0624	0.686
3	0.0457	0.0576	0.794	0.0214	0.0431	0.496

Table 5.18 **Experimental and theoretical ratios between maximum compressive stresses in the upper and lower steel faces.**

panel No.	U.D.L q (Xe-03) (KN/mm)	F (KN)	Q_{max}	theoretical τ_{max} (N/mm^2)
1	1.2144	3.328	1.664	0.00931
2	1.2144	3.343	1.672	0.00935
3	1.2144	3.478	1.739	0.00973

Table 5.19 Theoretical shear force and shear stresses at the central support for the three panels corresponding to the second analysis.

Panel	Theoretical max σ_E lower face (KN / mm^2)	Theoretical max σ_E upper face (KN / mm^2)	Theoretical ratio $\frac{\max \sigma_E(lower)}{\max \sigma_E(upper)}$
1	-0.00713	0.00500	1.426
2	-0.00732	0.00493	1.494
3	-0.00893	0.00432	2.070

Table 5.20 Theoretical ratios between maximum compressive stresses in the upper and lower steel faces corresponding to the second analysis.

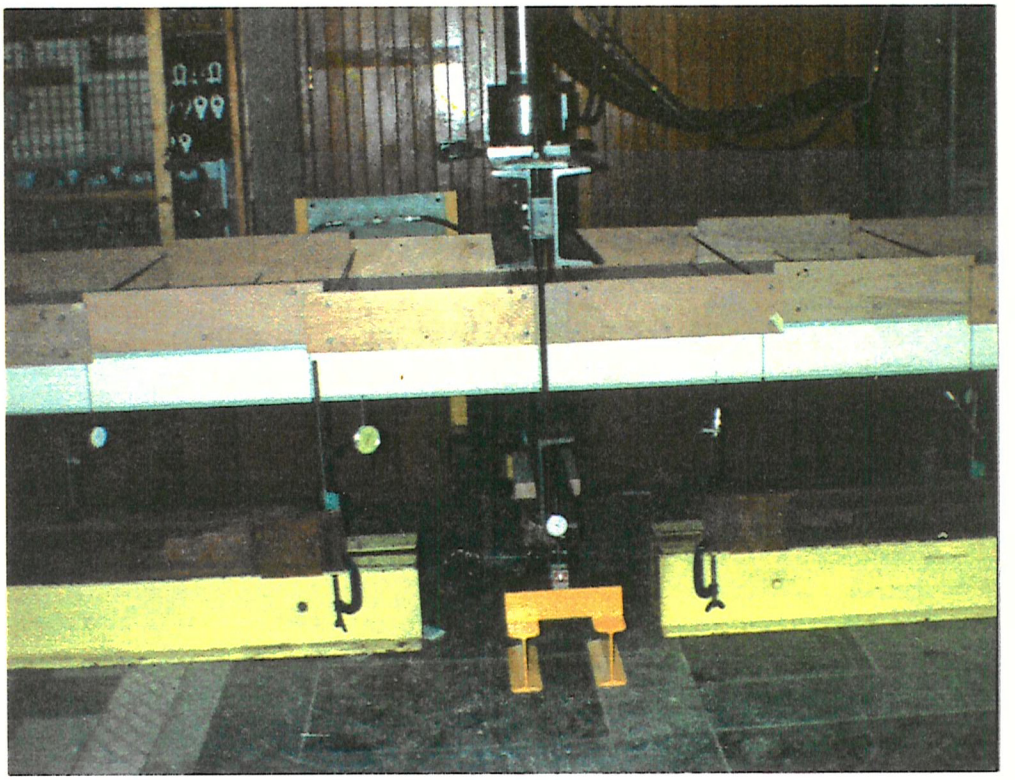

Fig 5.1 Setting up of the main experiment showing the plywood panels and tie bars.

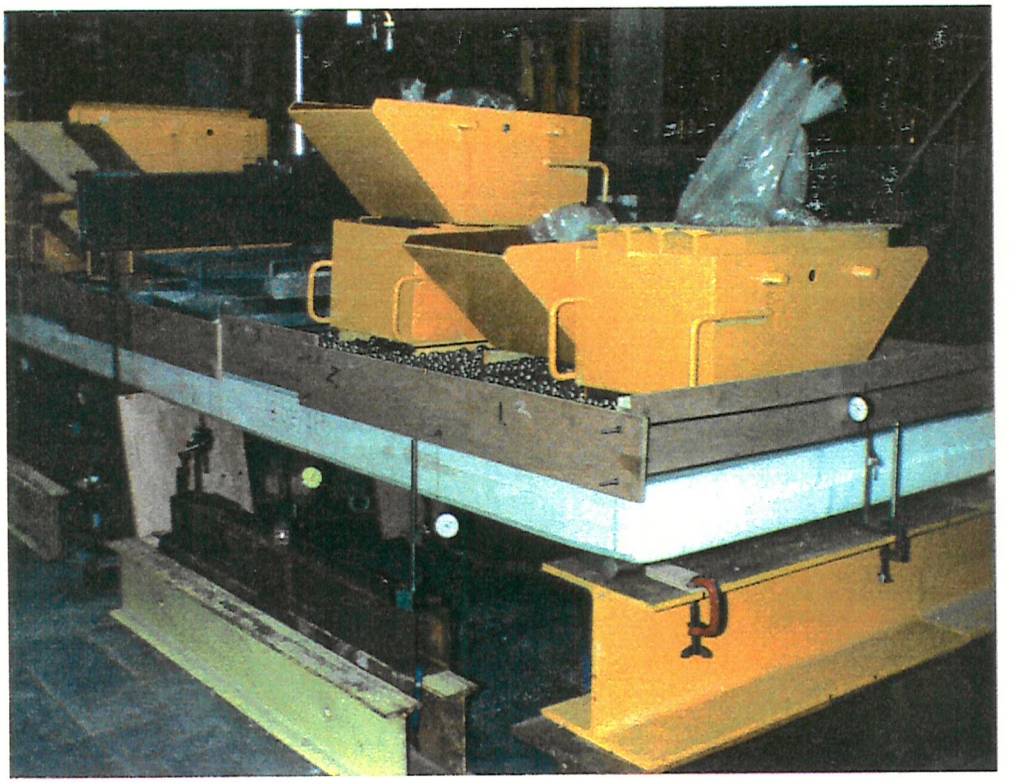

Fig 5.2 Typical loading of a tested panel.

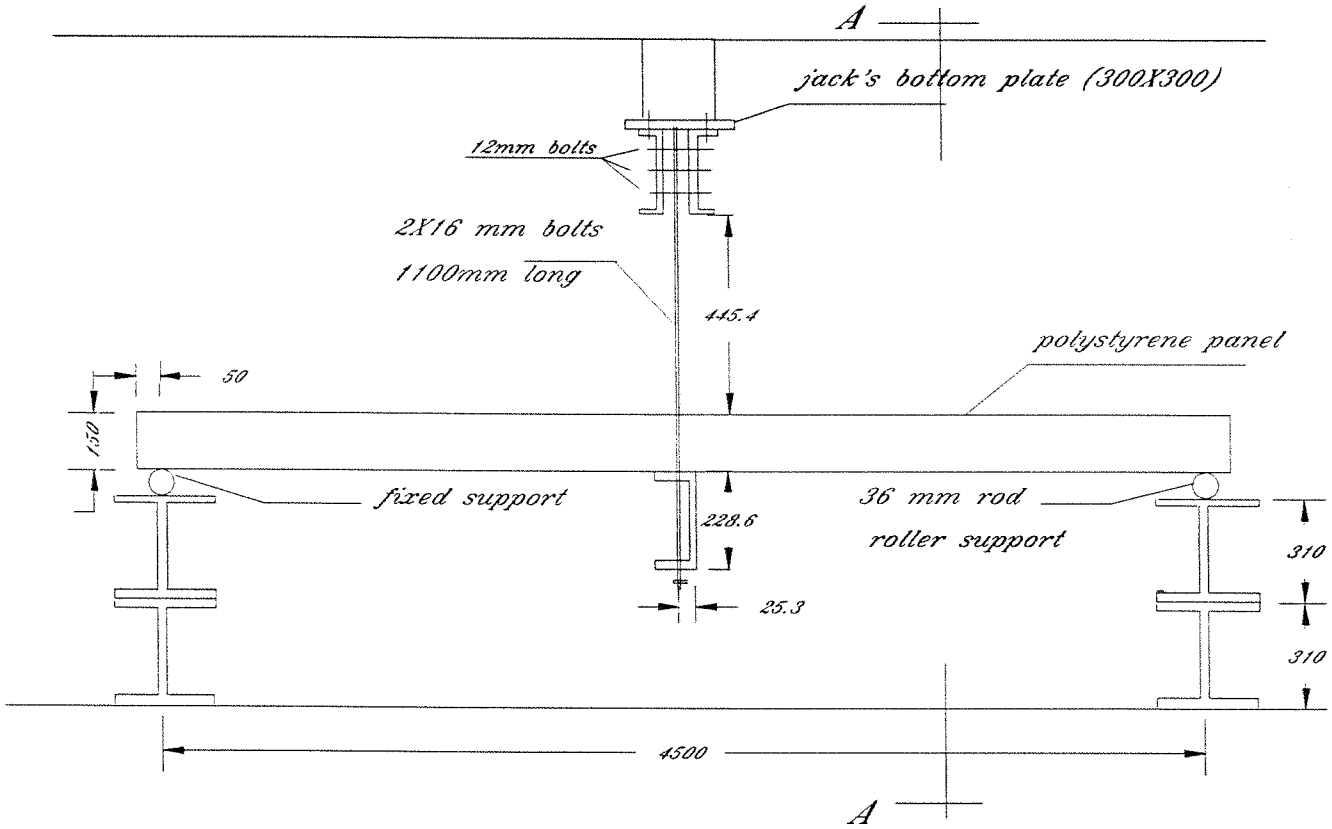

Fig 5.3 Setting up of the main experiment.

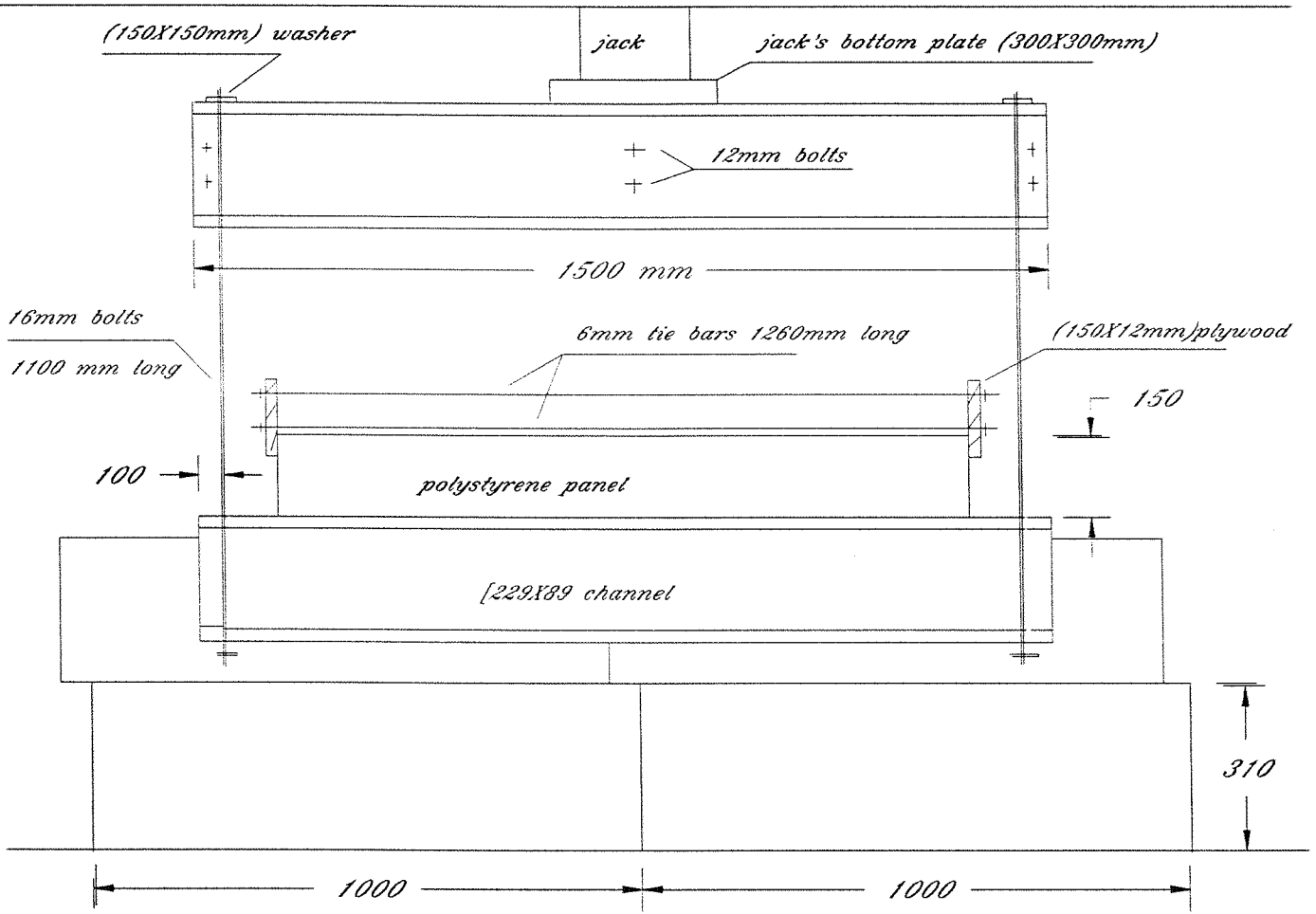

Fig 5.4 Set up of the main experiment. Section A – A

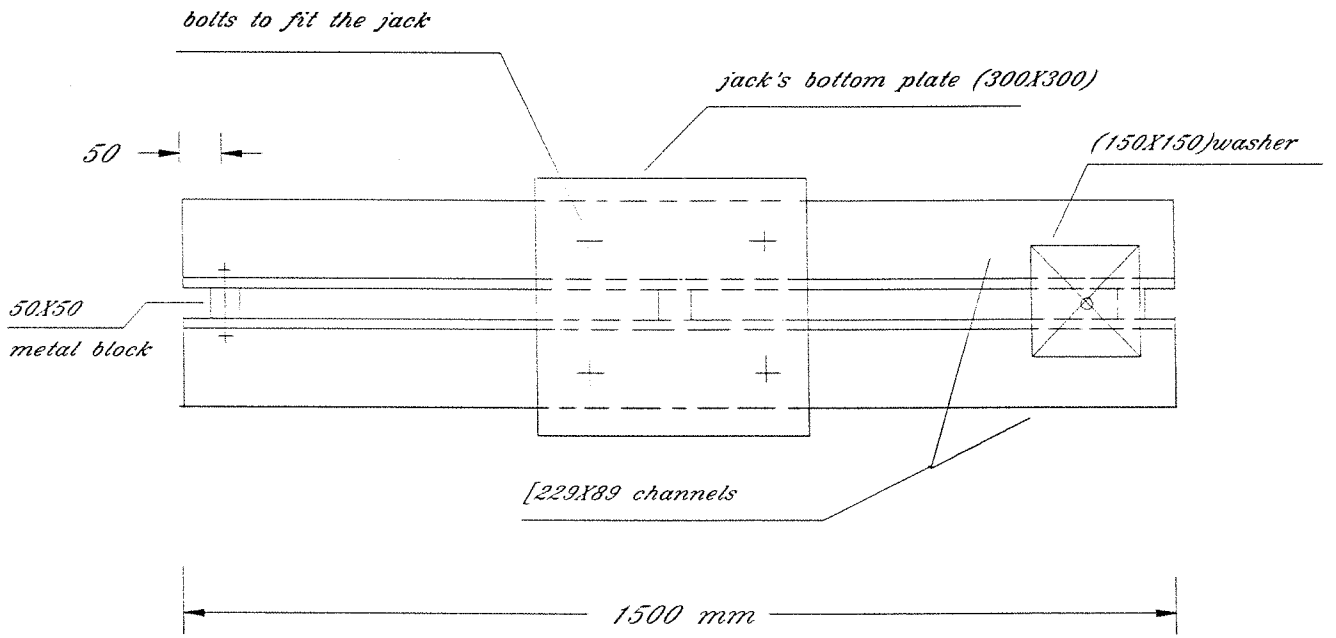

Fig 5.5 Details of the top channels section.

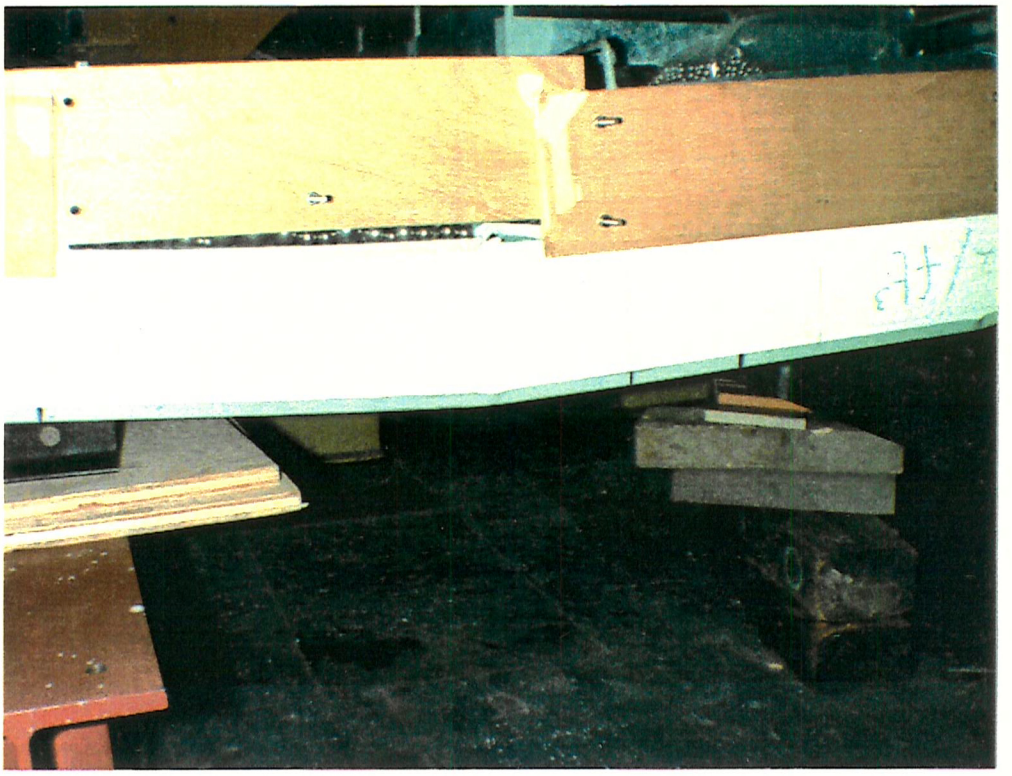

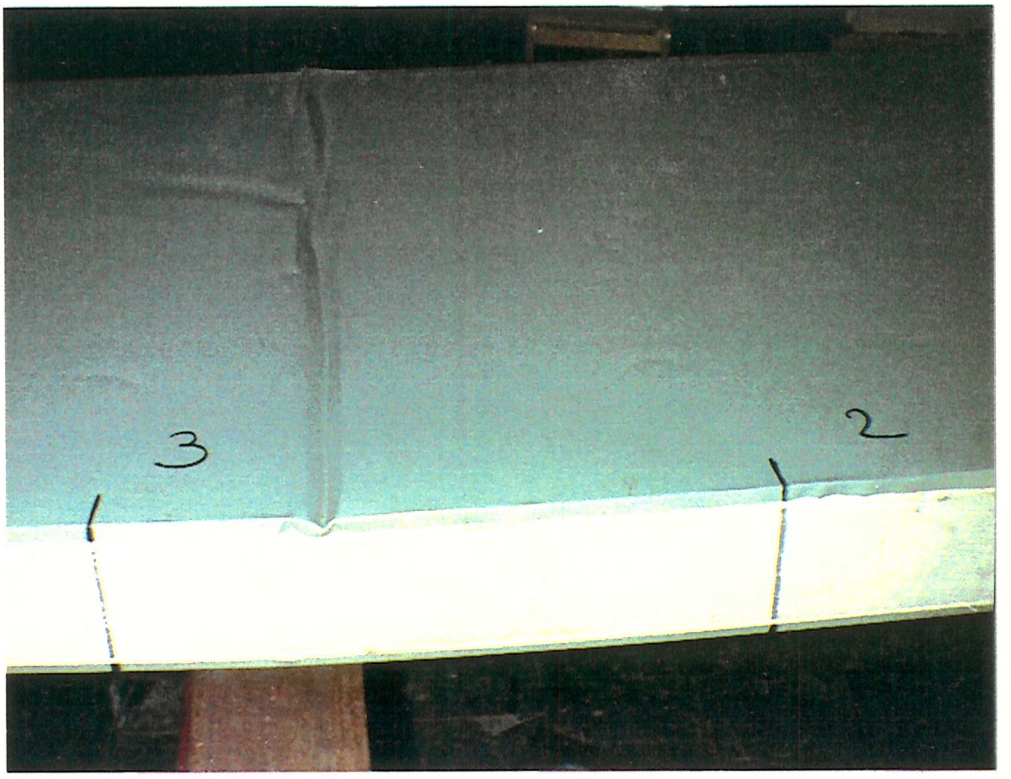

Fig 5.6 Typical wrinkling of the upper steel face.

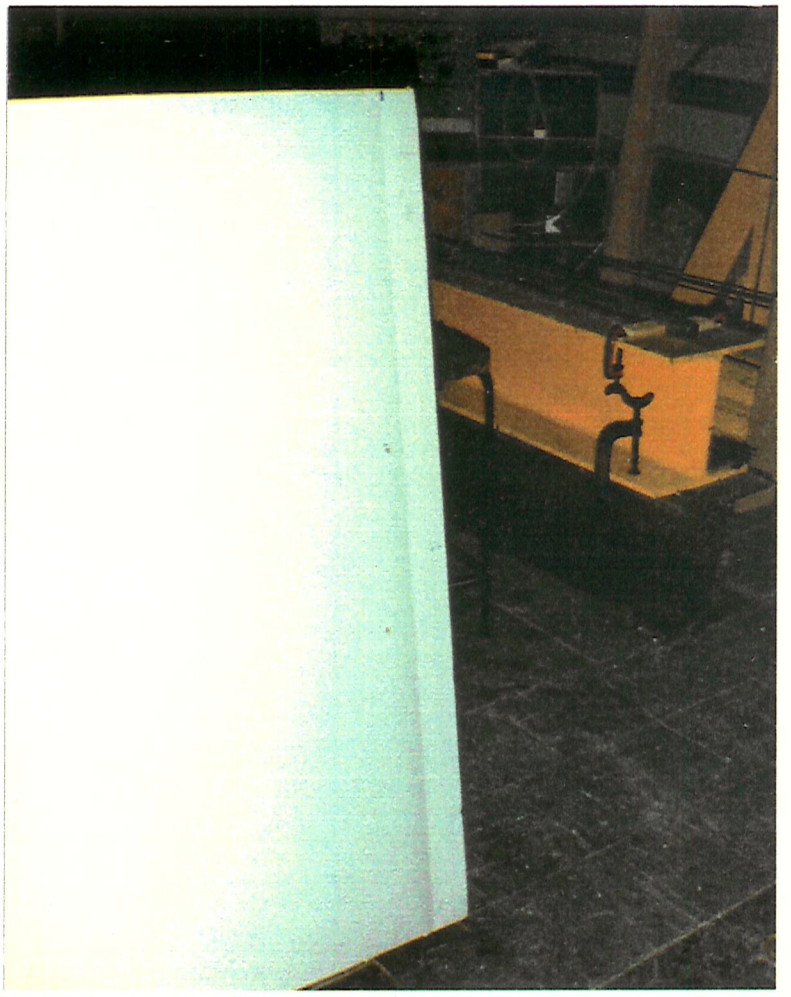

Fig 5.7 Typical crushing of the lower steel face at the supports

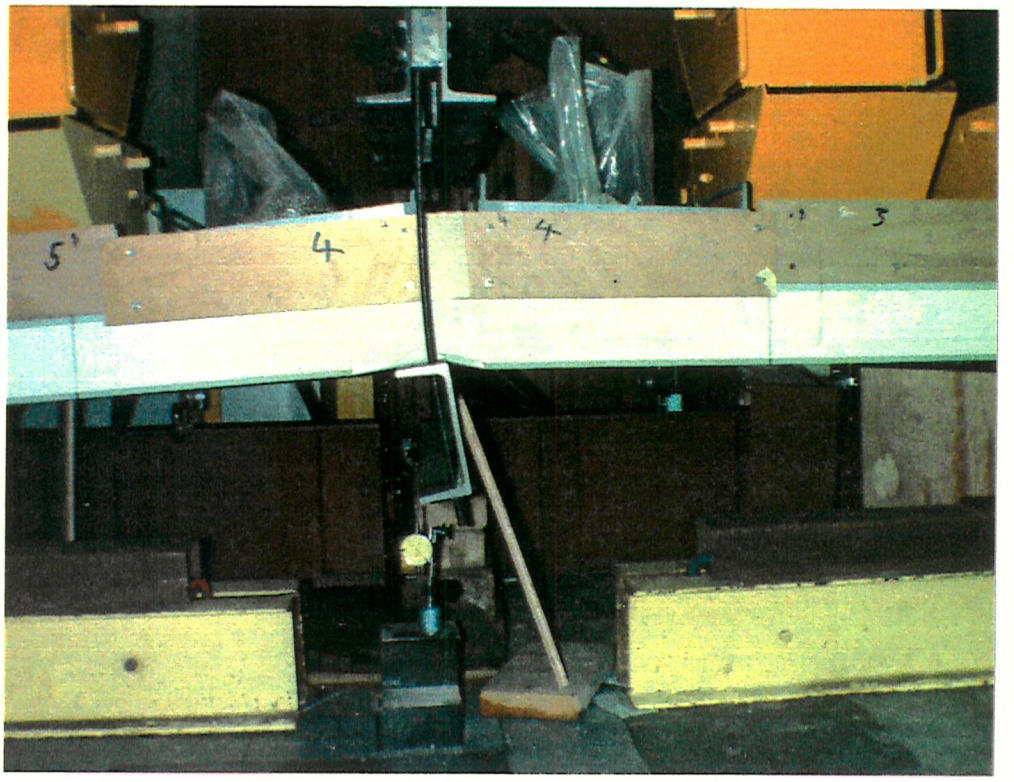

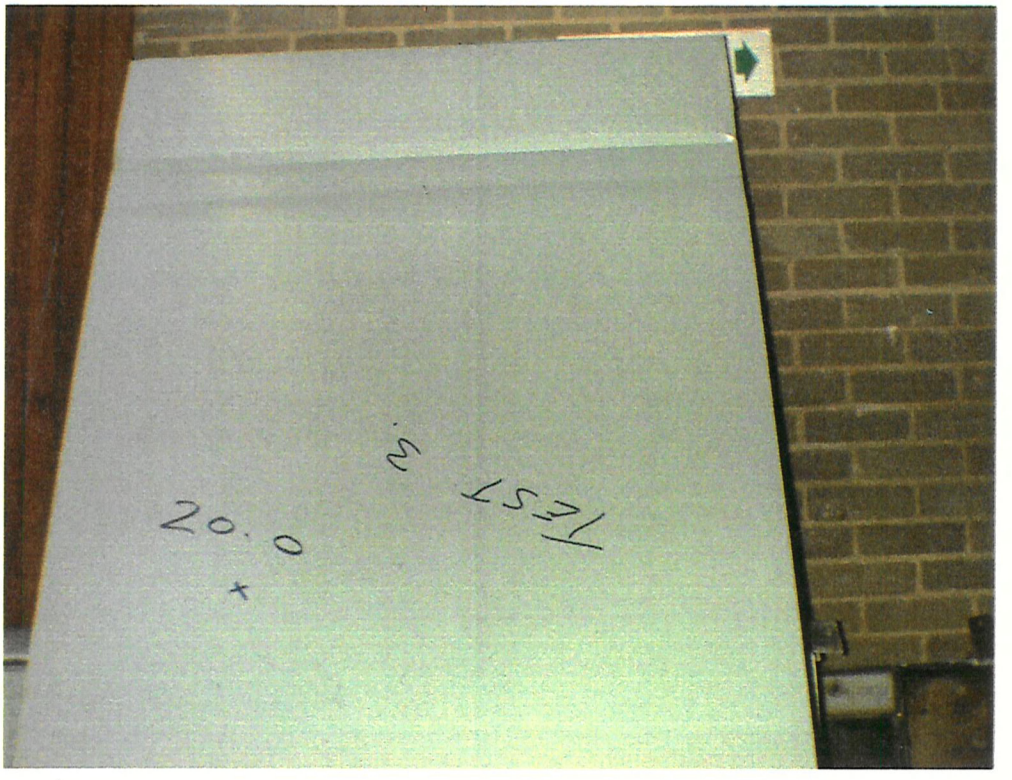

Fig 5.8 Typical crushing of the lower steel face at the internal support.

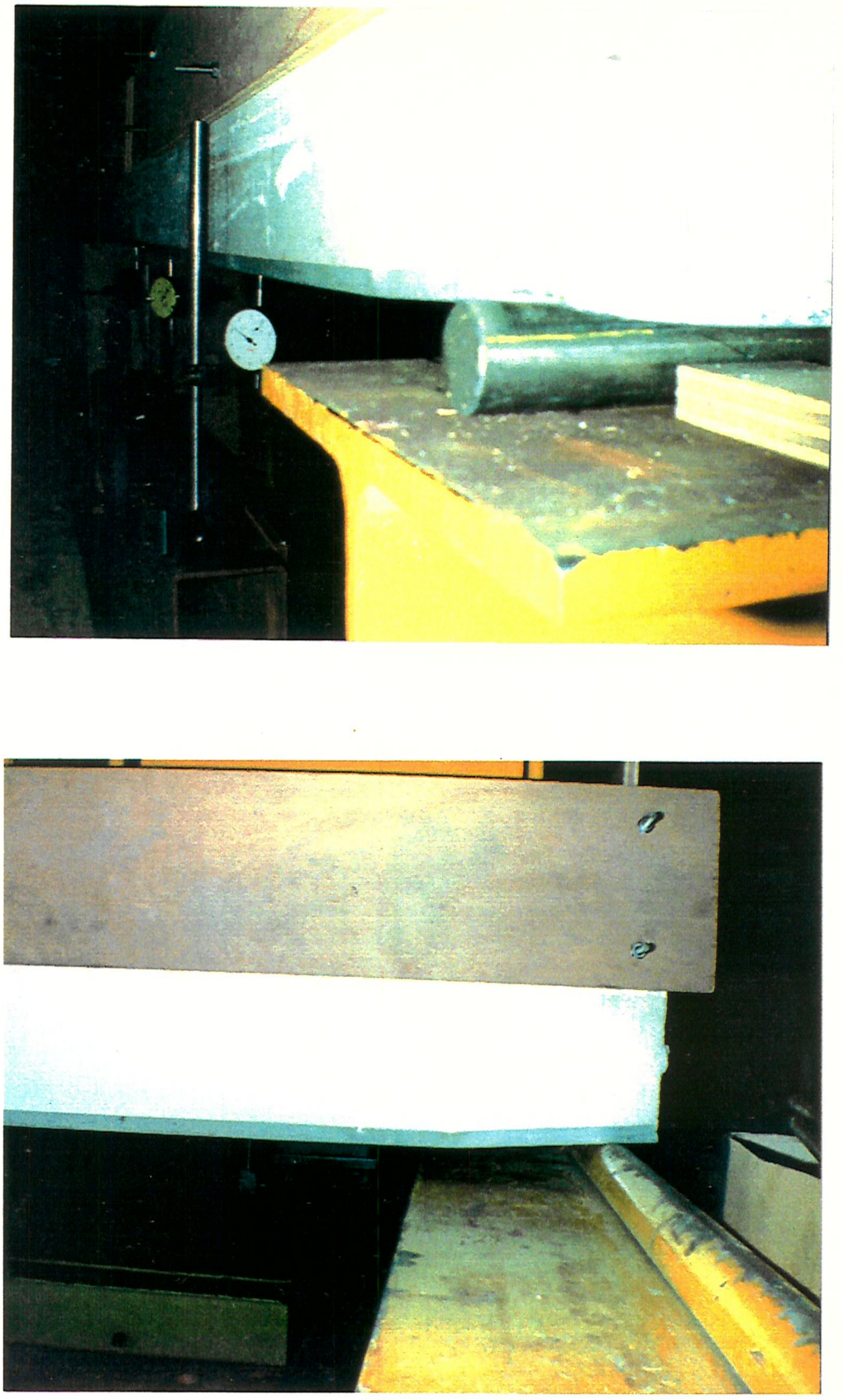

Fig 5.9 Typical support deflection.

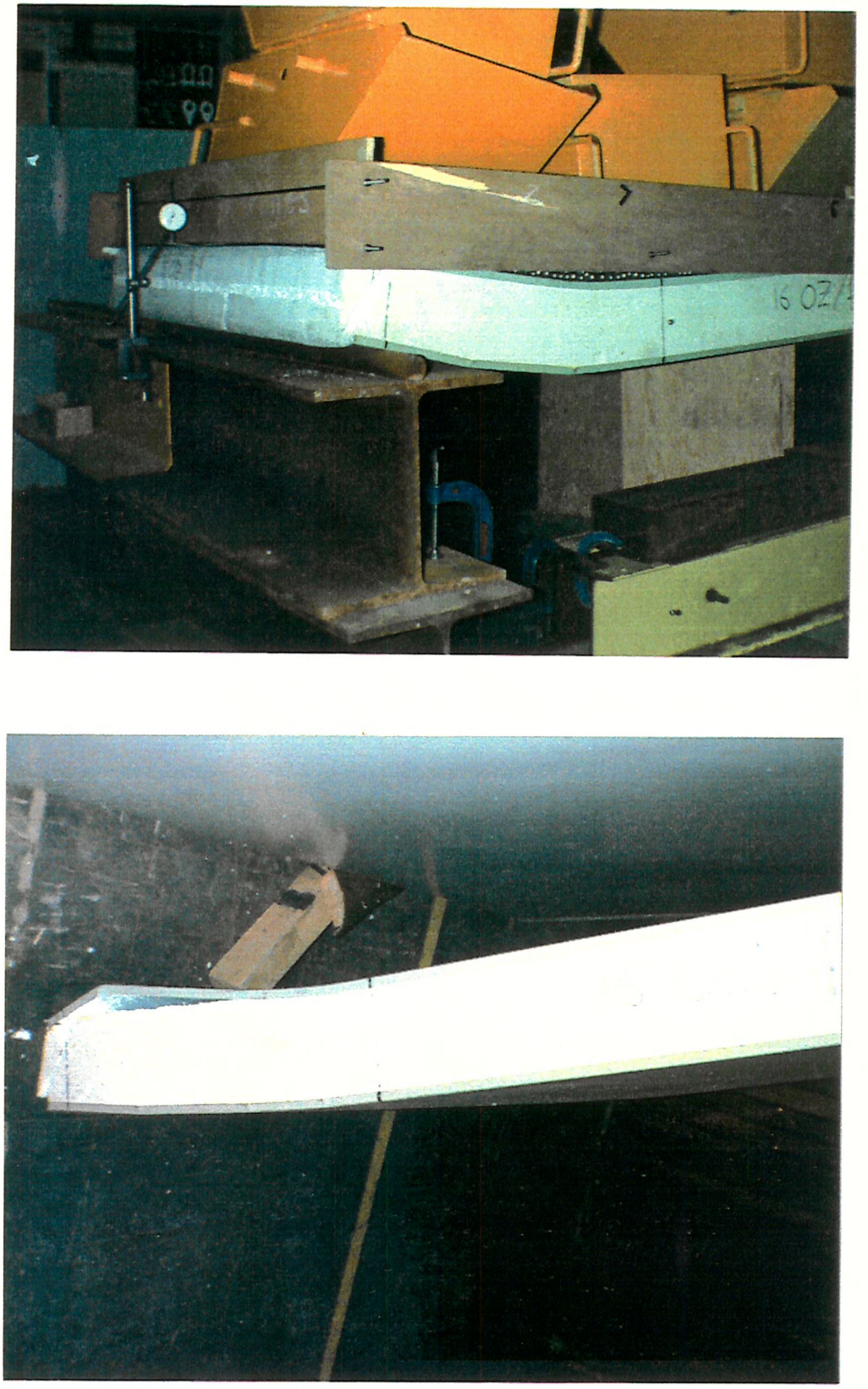

Fig 5.10 Core shear failure at the fixed support end of the third panel.

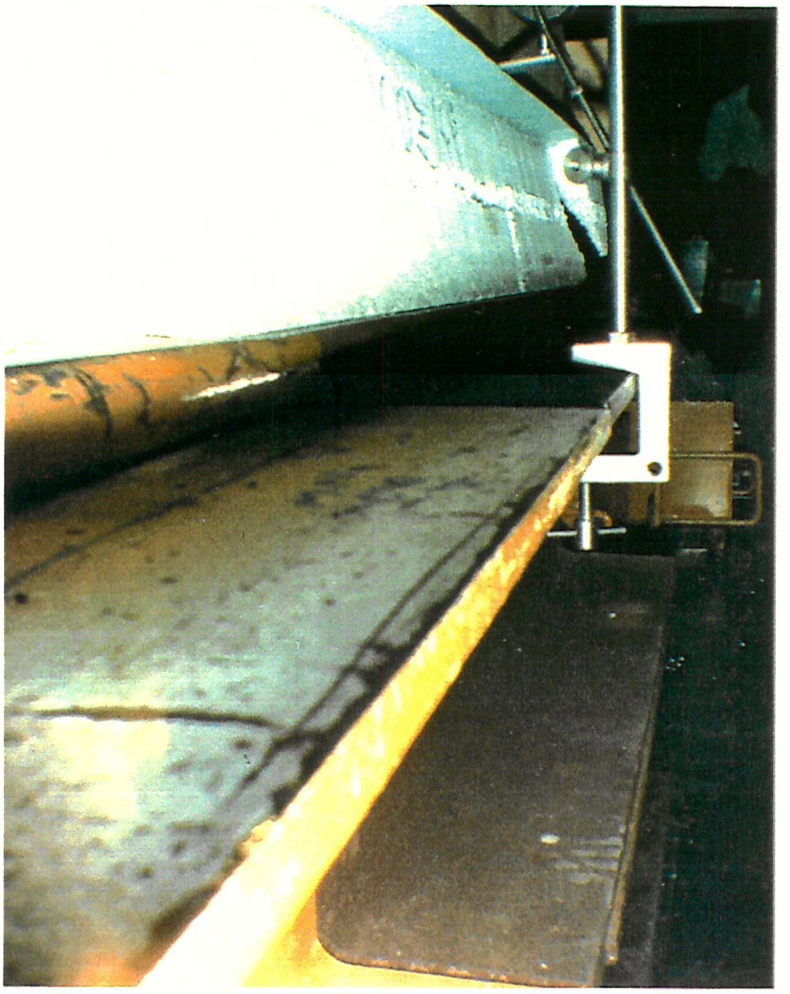

Fig 5.11 Interfacial delamination of the steel/polystyrene at the fixed support end of the third panel.

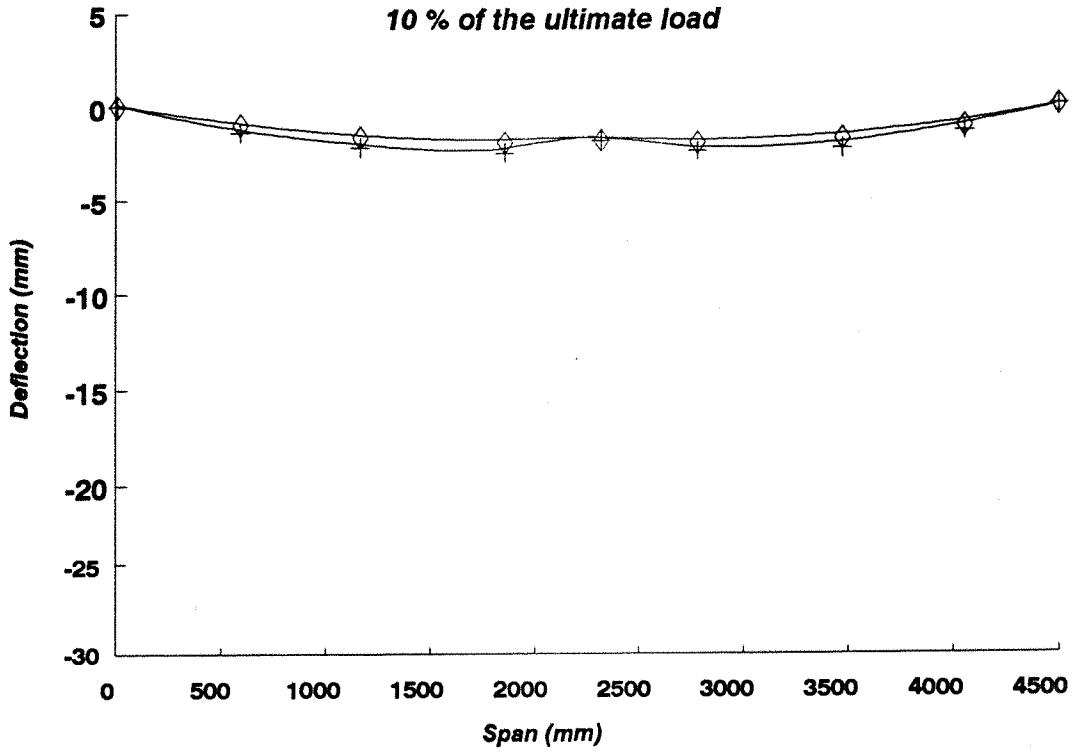

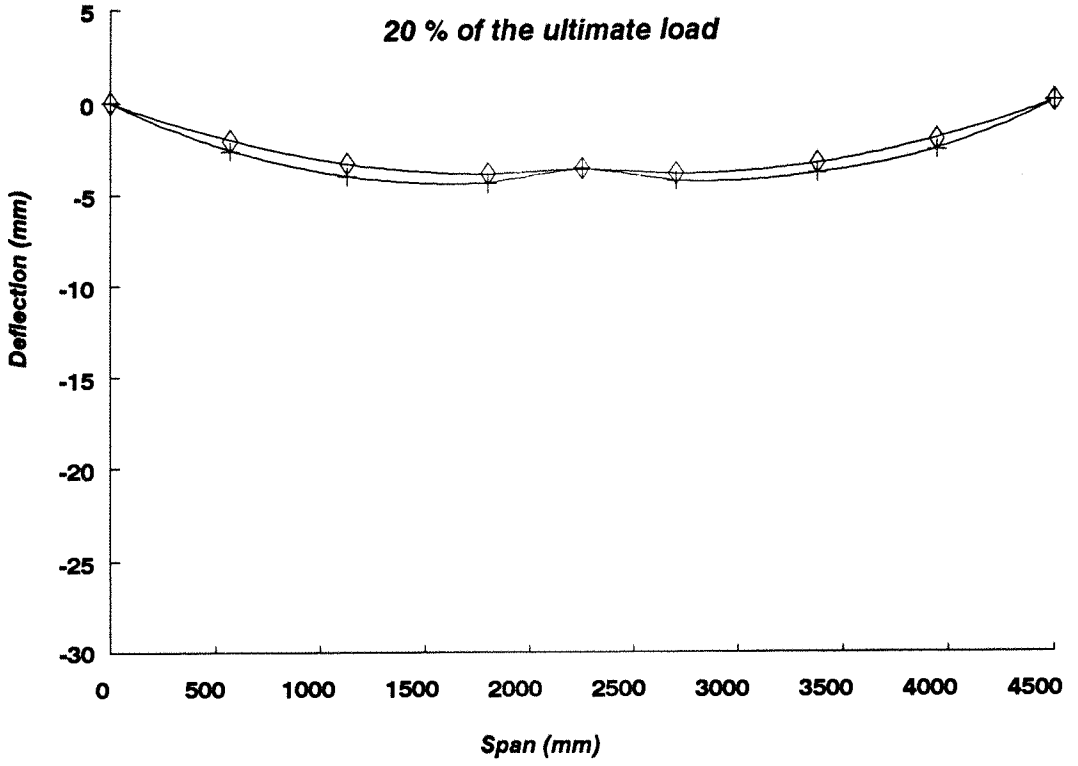

Fig 5.12 Variation of the deflection along the span of the first panel.

◇ Computational results

\+ Experimental results

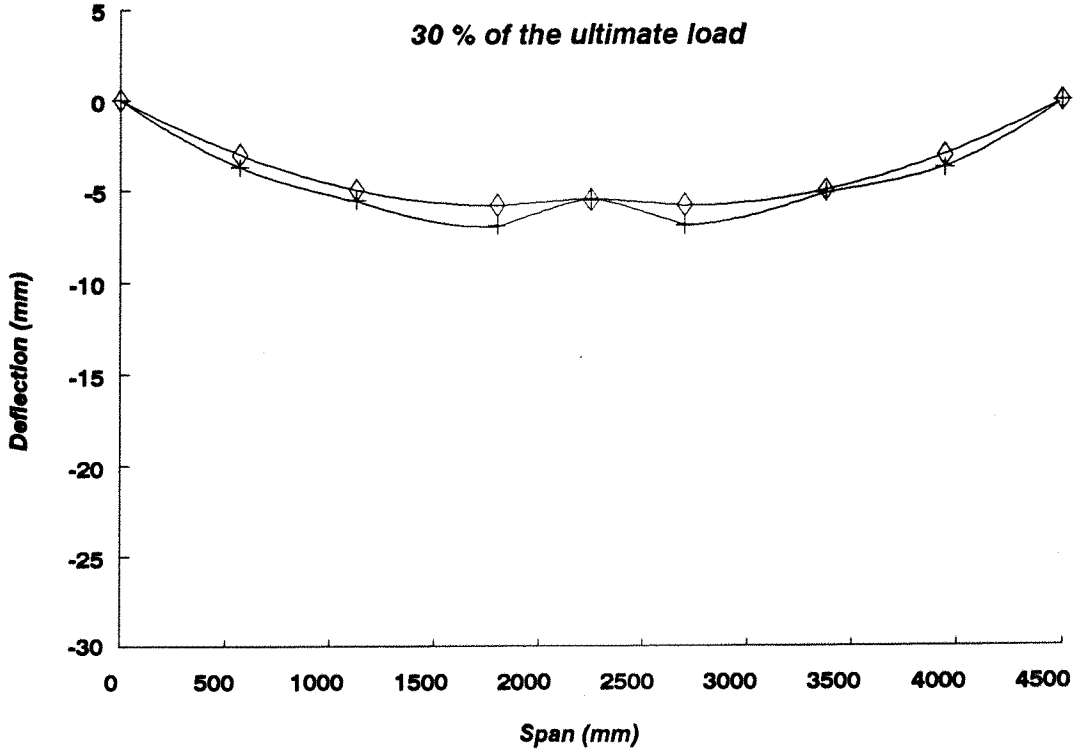

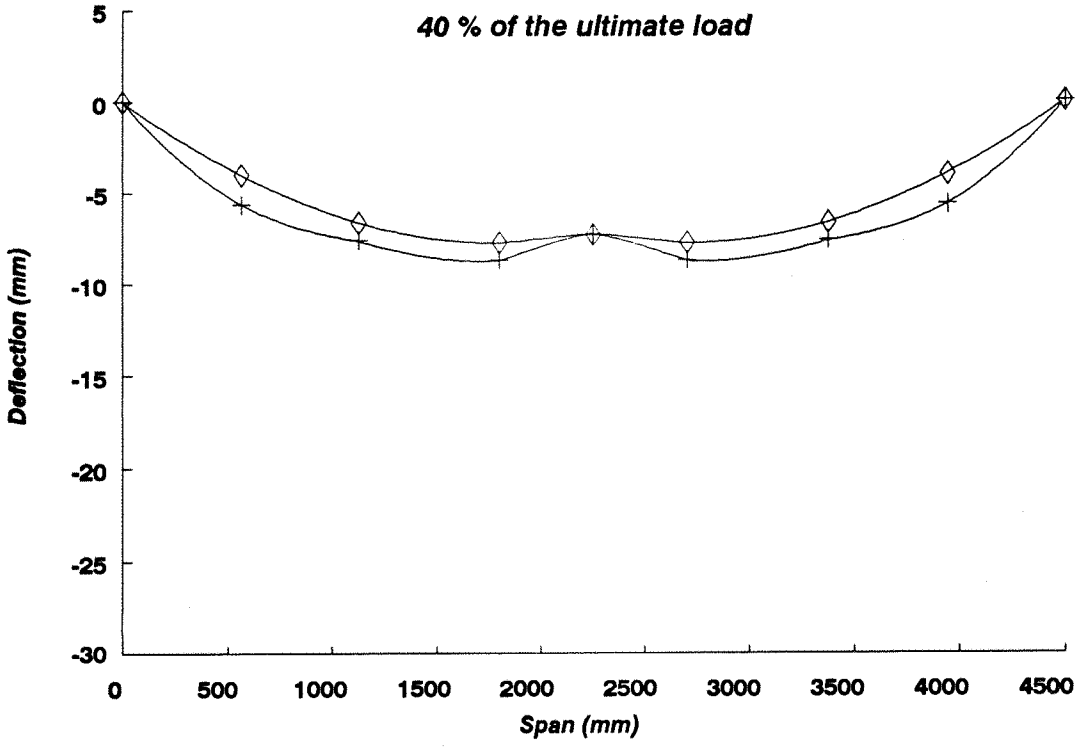

Fig 5.13 Variation of deflection along the span of the first panel.

◇ **Computational results**

\+ **Experimental results**

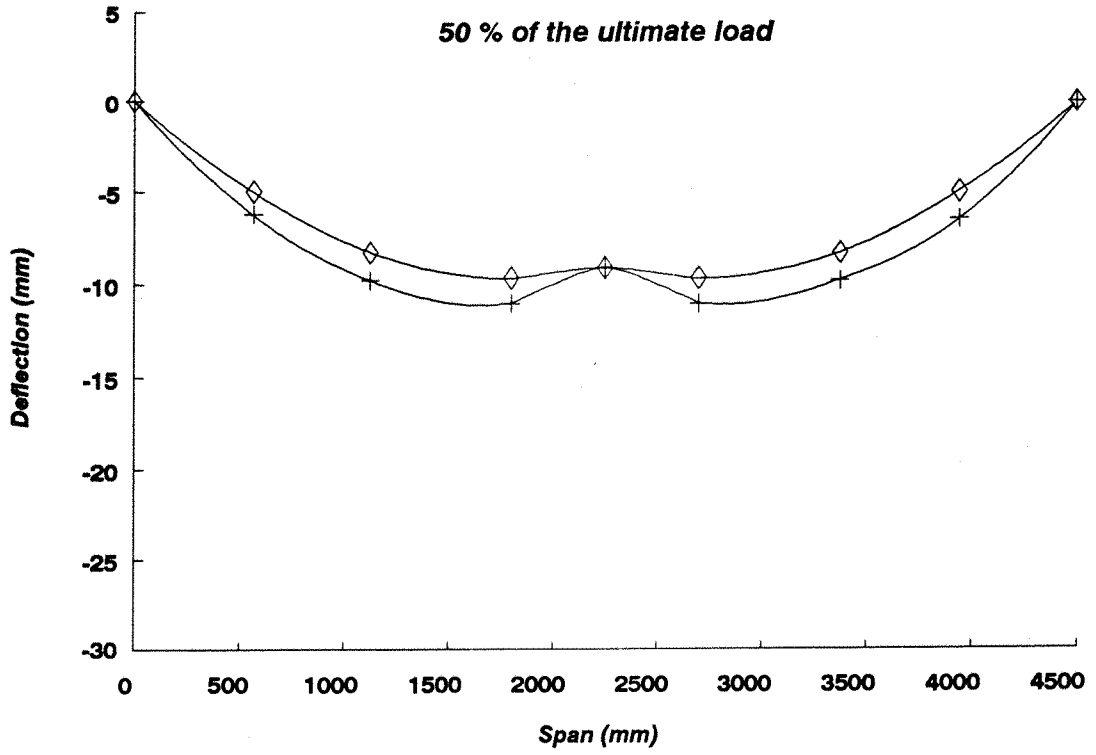

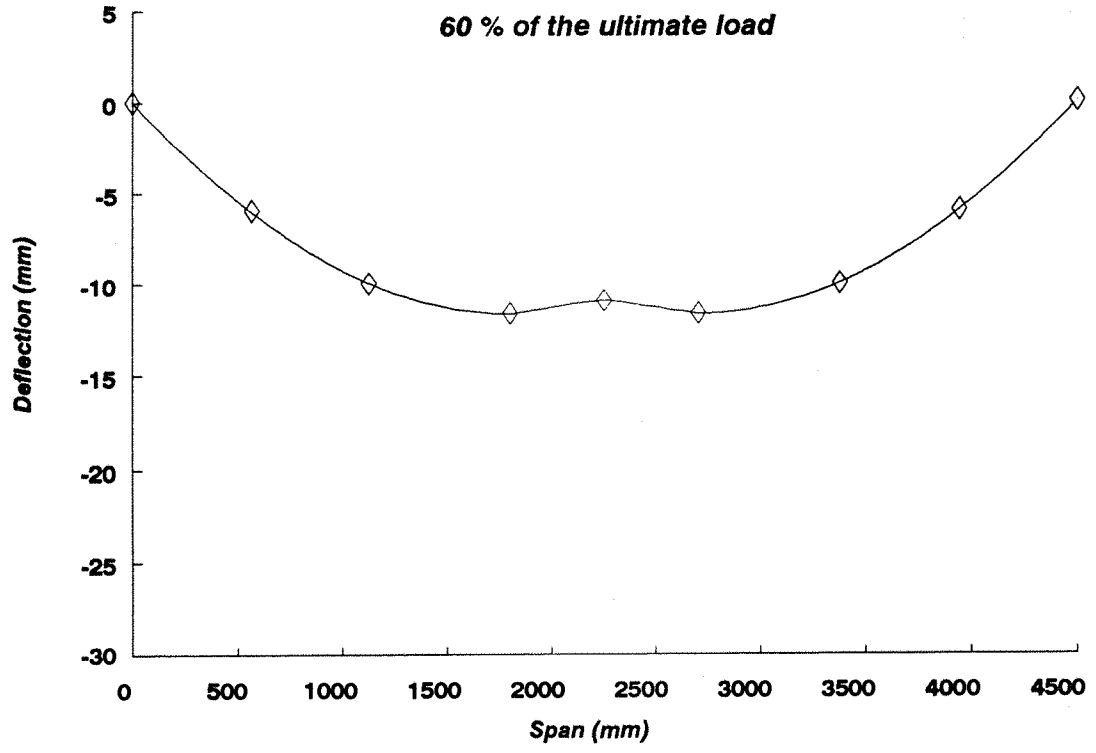

Fig 5.14 Variation of deflection along the span of the first panel.

◇ Computational results

\+ Experimental results

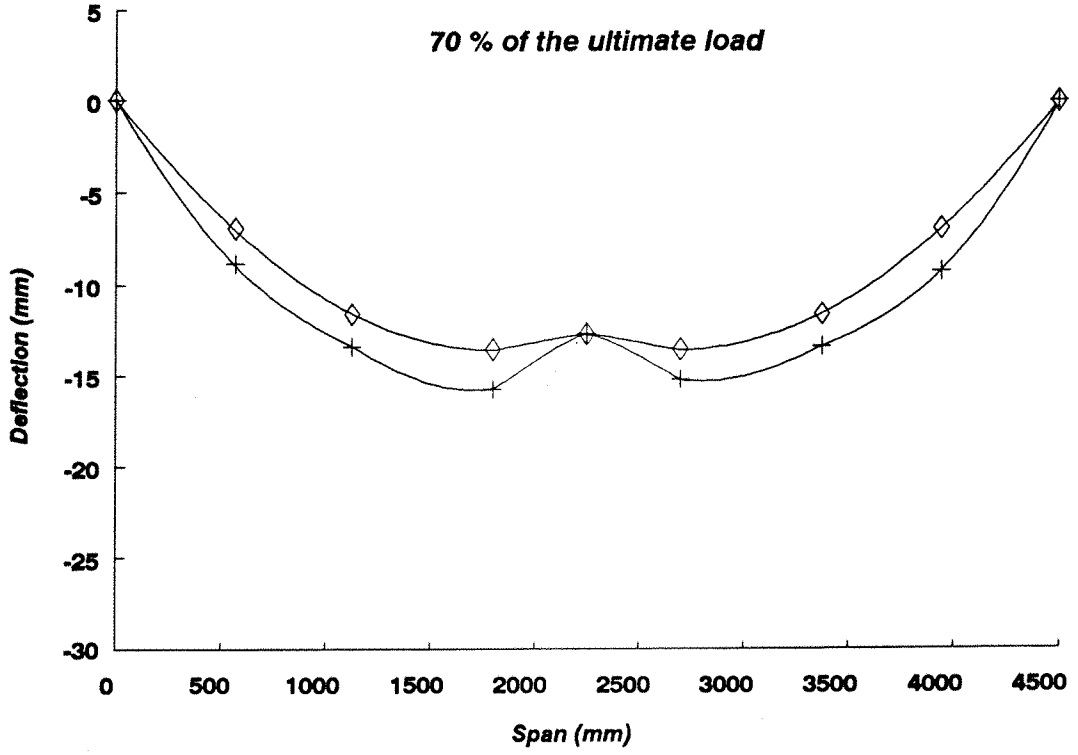

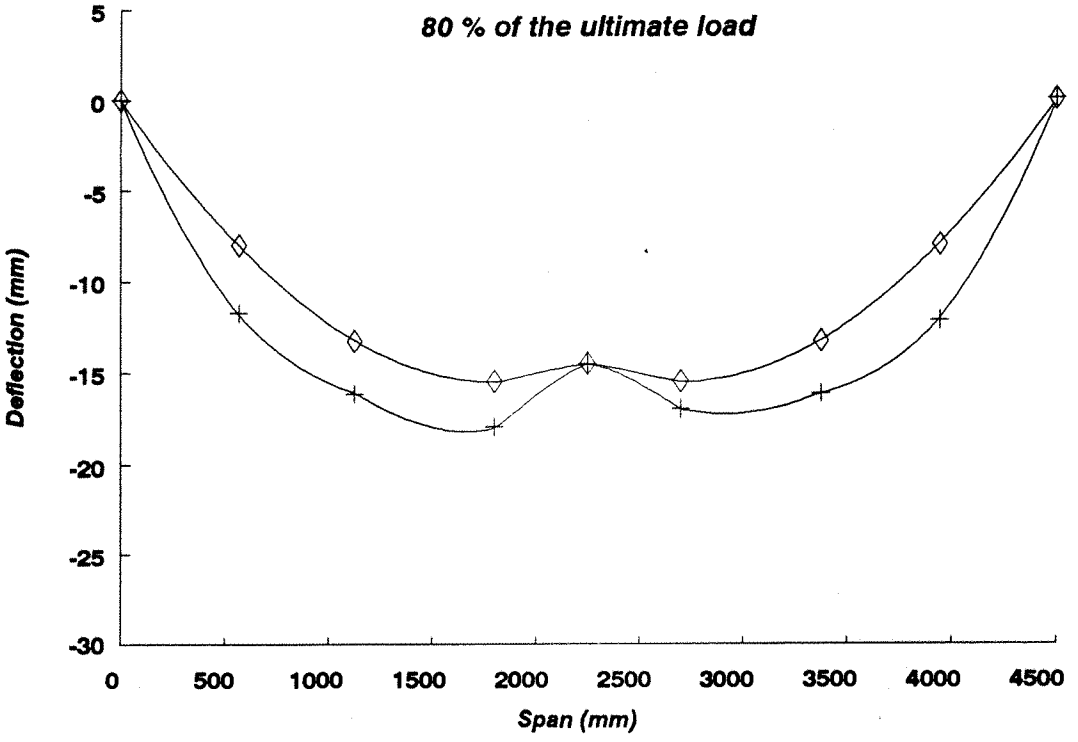

Fig 5.15 Variation of deflection along the span of the first panel.

◇ Computational results

\+ Experimental results

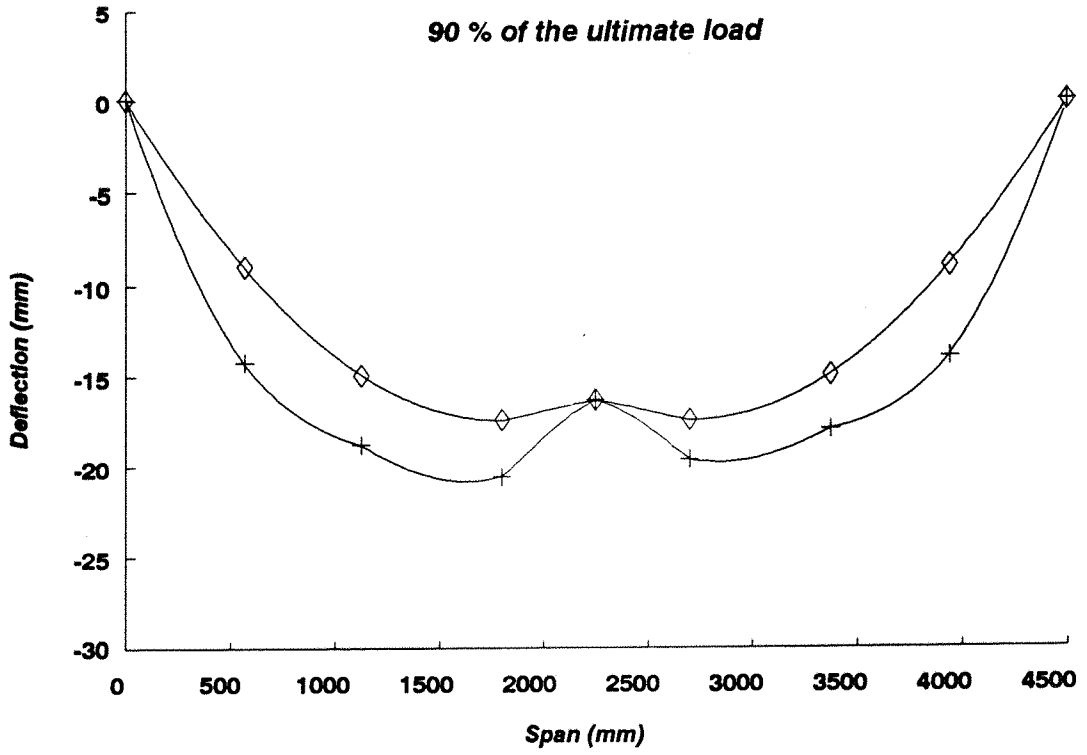

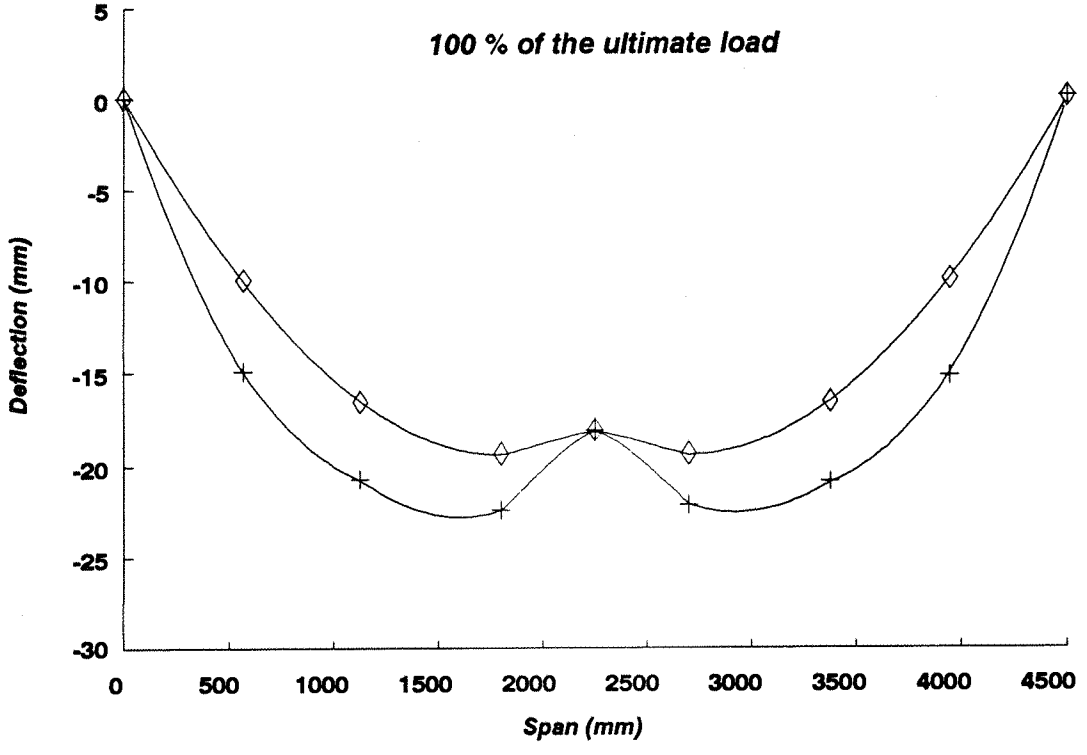

Fig 5.16 Variation of deflection along the span of the first panel.

◇ **Computational results**

Experimental results

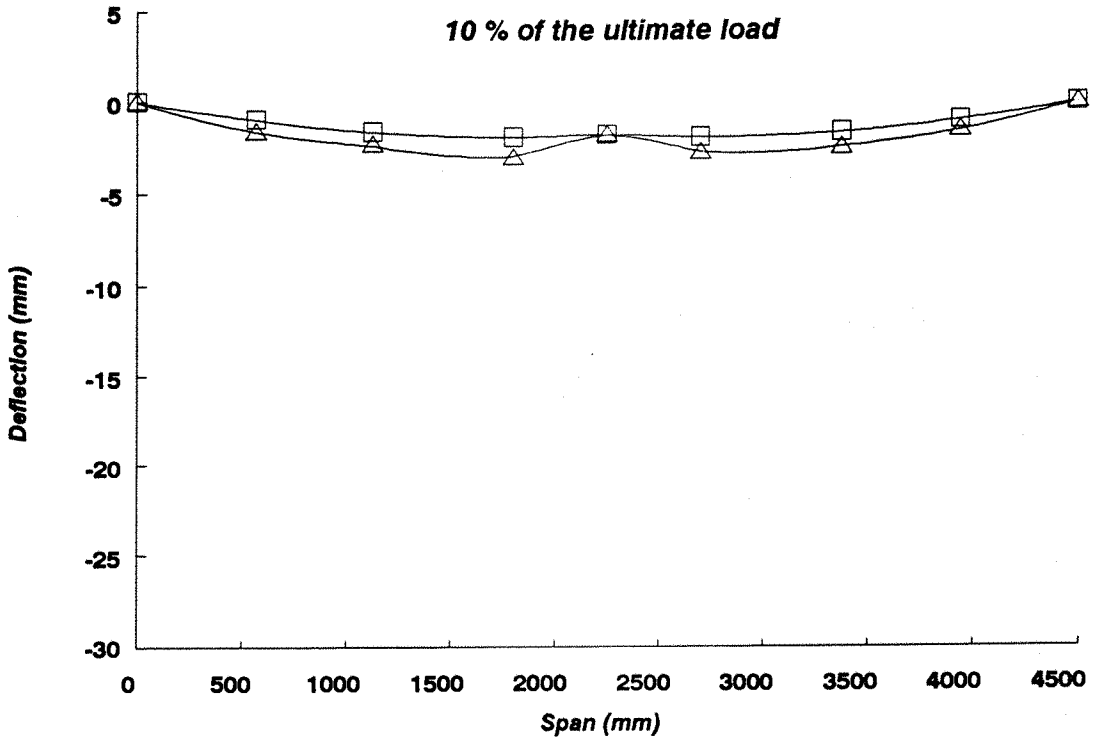

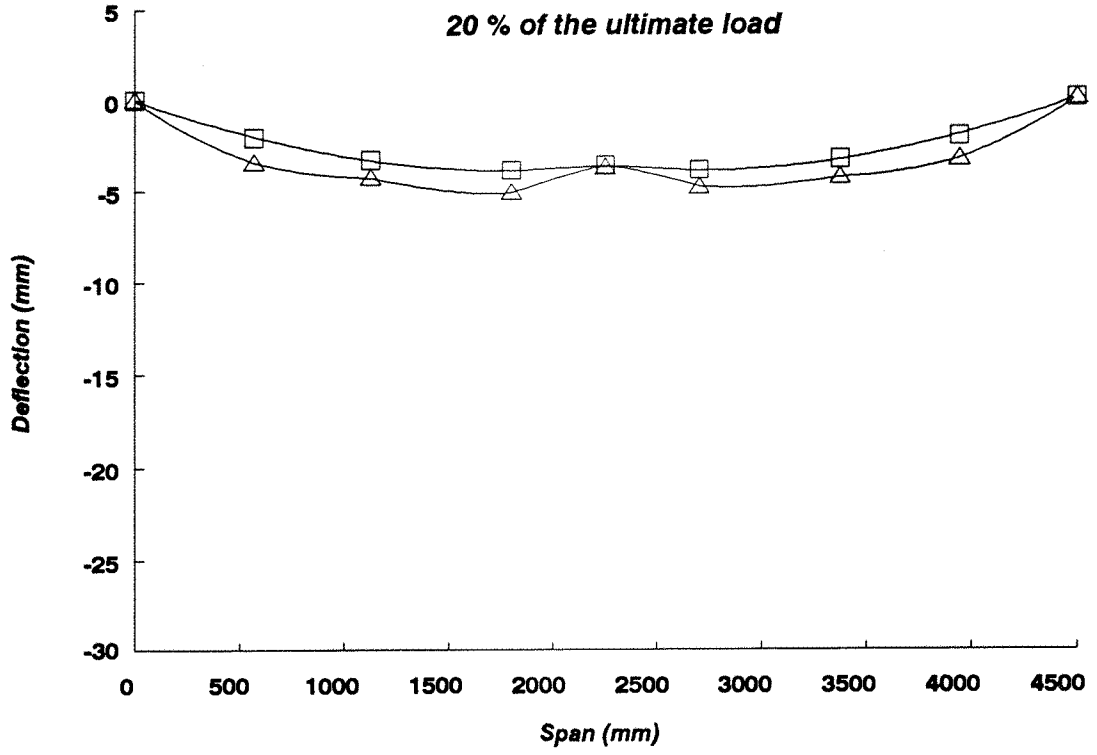

Fig 5.17 Variation of deflection along the span of the second panel.

□ Computational results

△ Experimental results

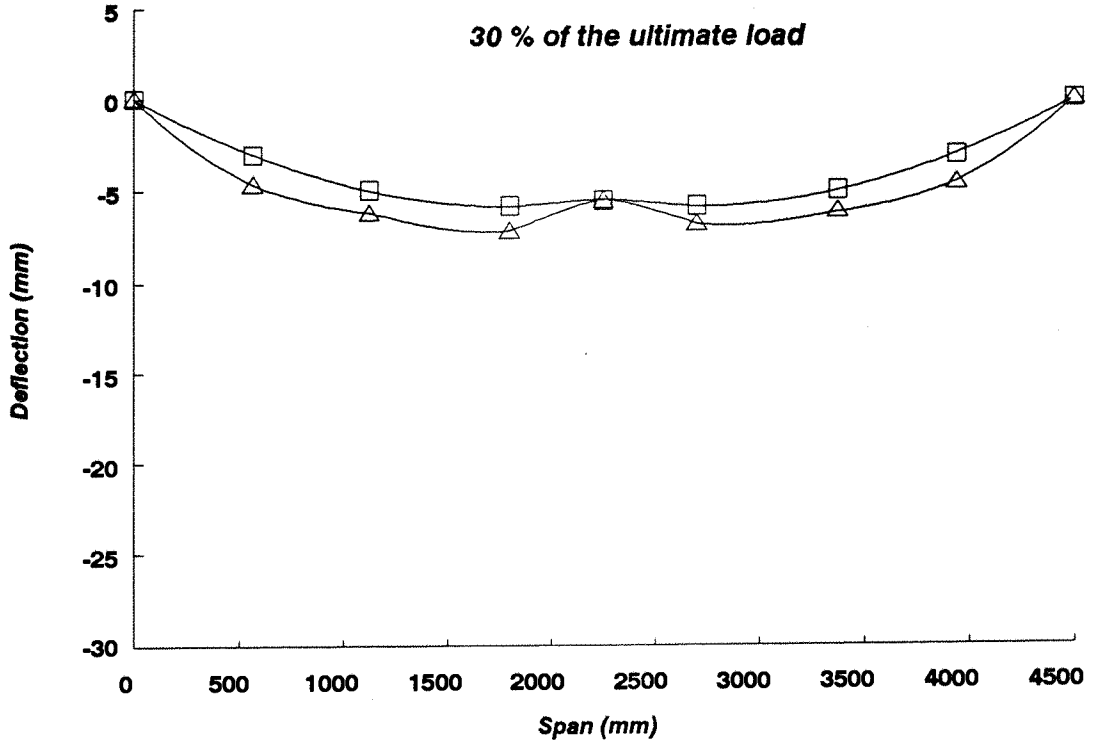

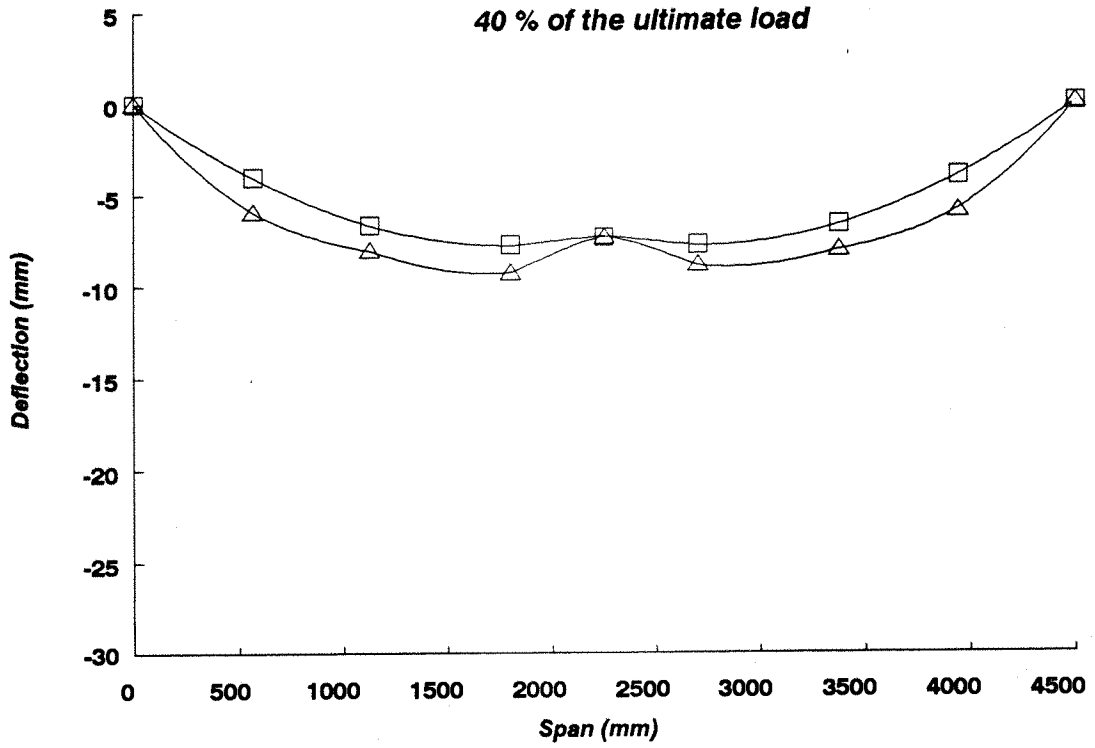

Fig 5.18 Variation of deflection along the span of the second panel.

□ Computational results

△ Experimental results

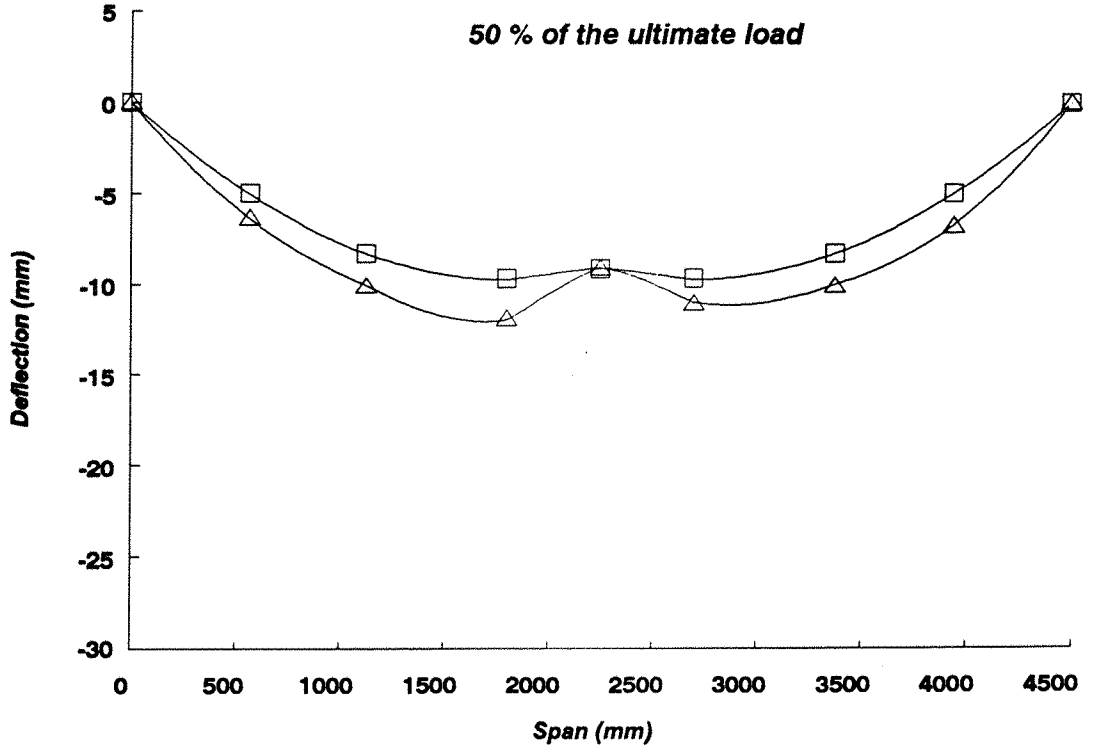

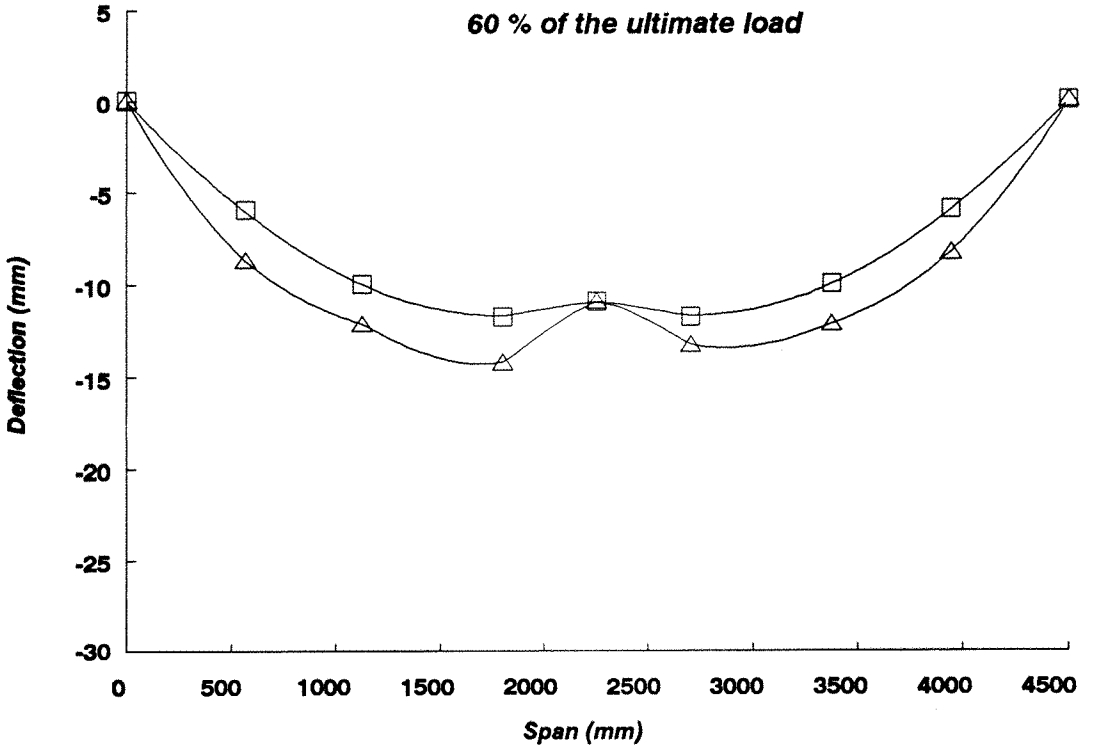

Fig 5.19 Variation of deflection along the span of the second panel.

□ Computational results

△ Experimental results

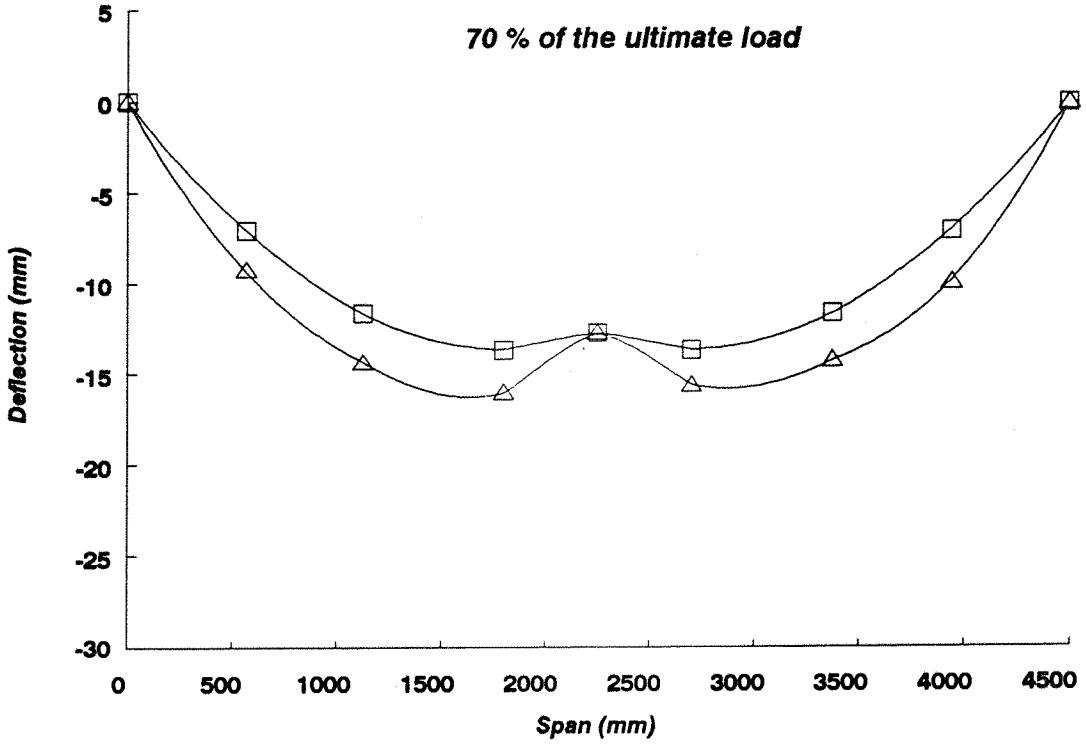

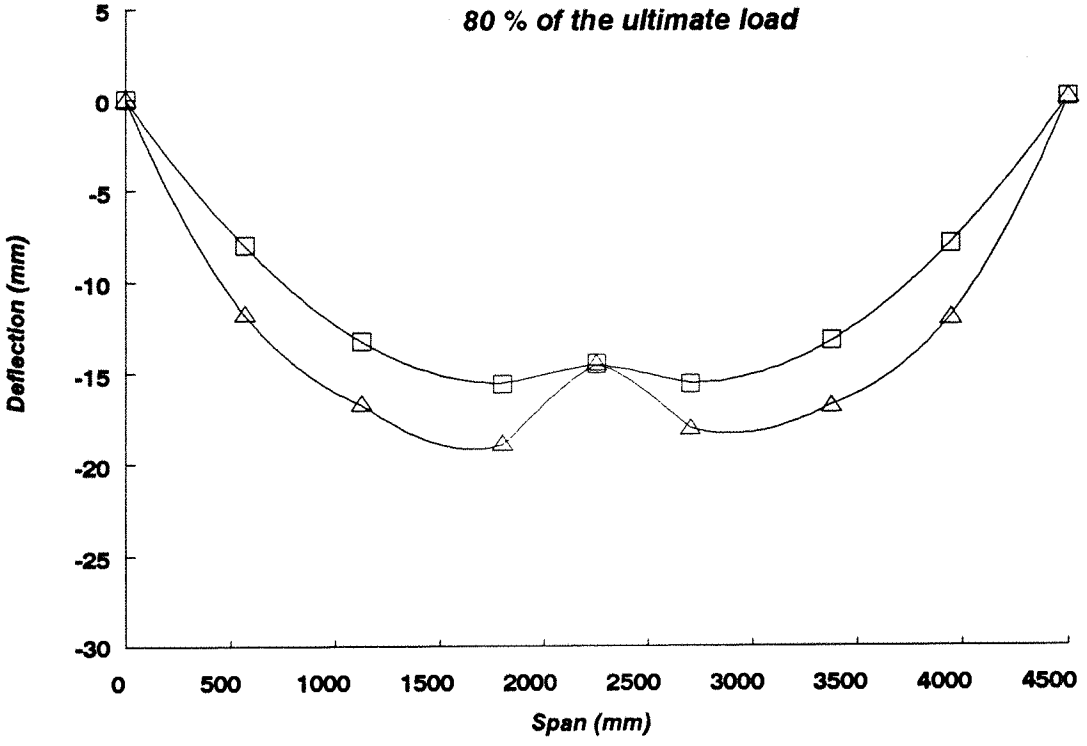

Fig 5.20 Variation of deflection along the span of the second panel.

□ **Computational results**

△ **Experimental results**

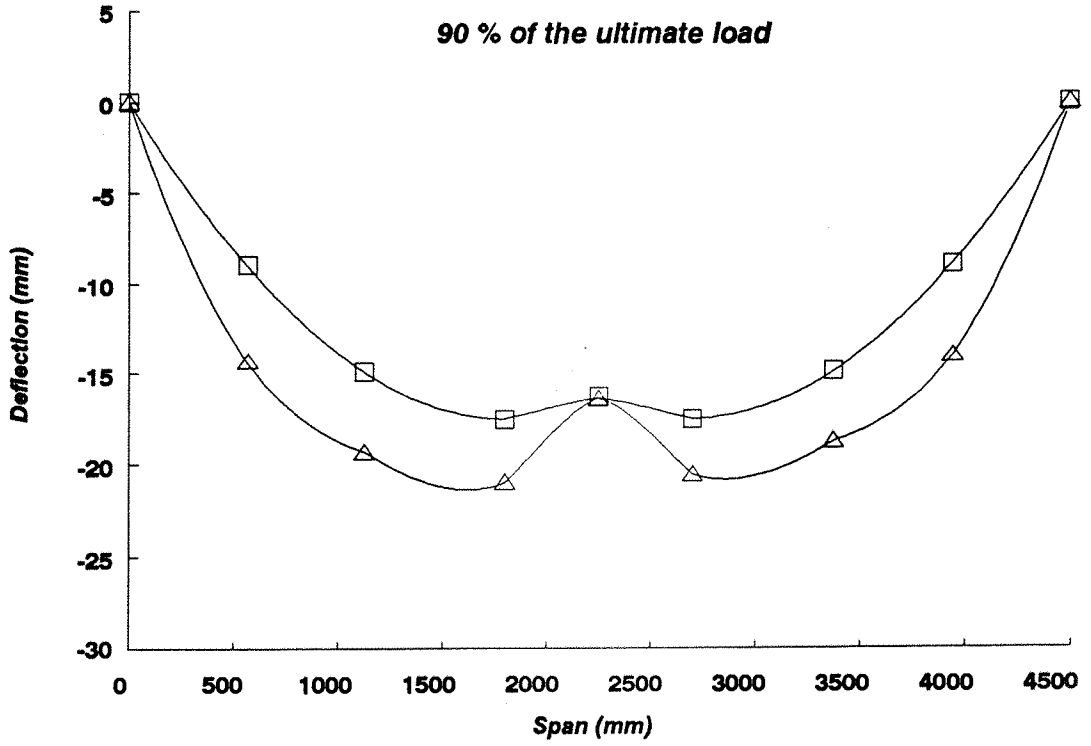

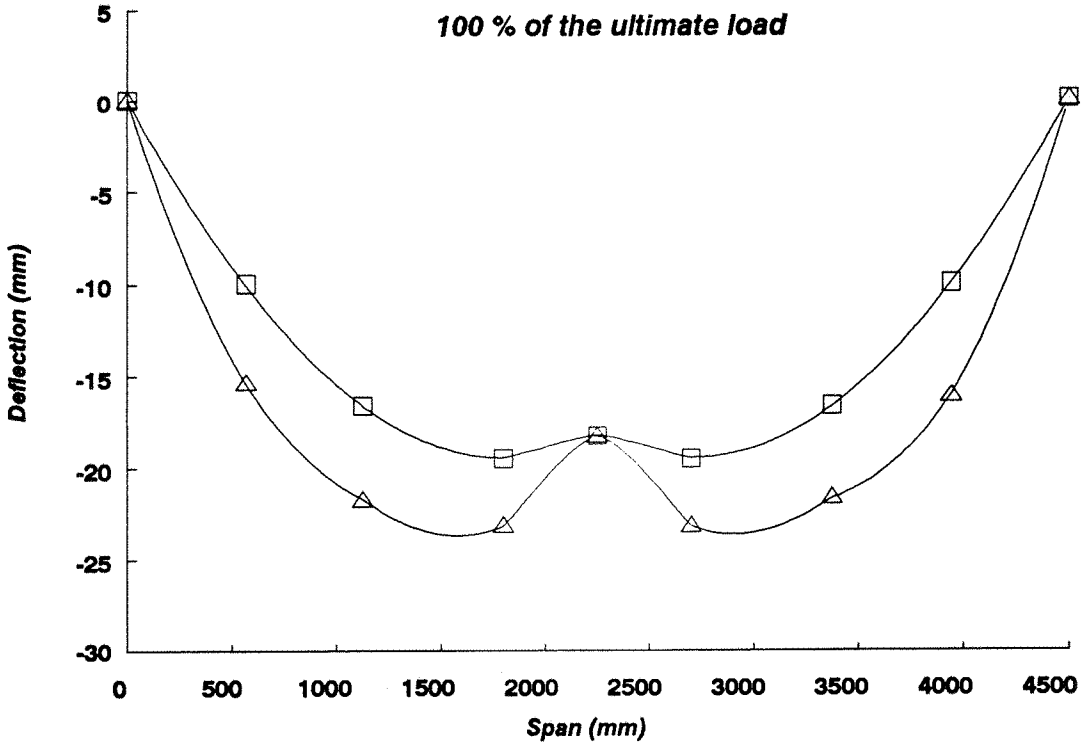

Fig 5.21 Variation of deflection along the span of the second panel.

□ Computational results

△ Experimental results

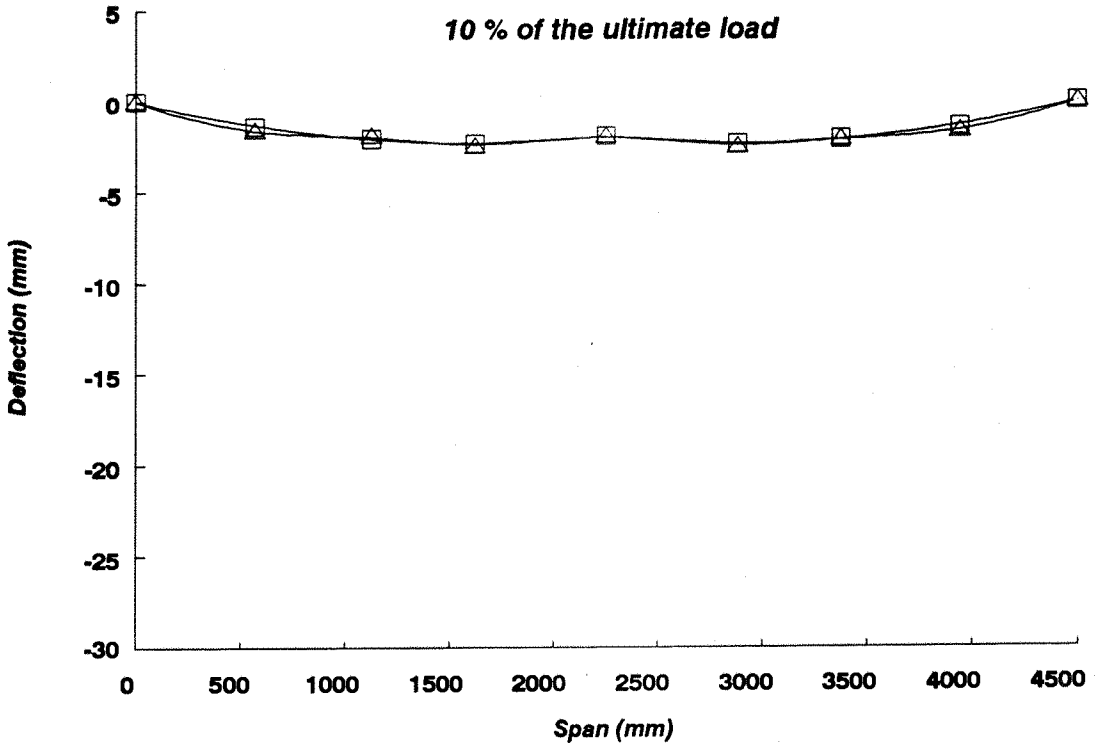

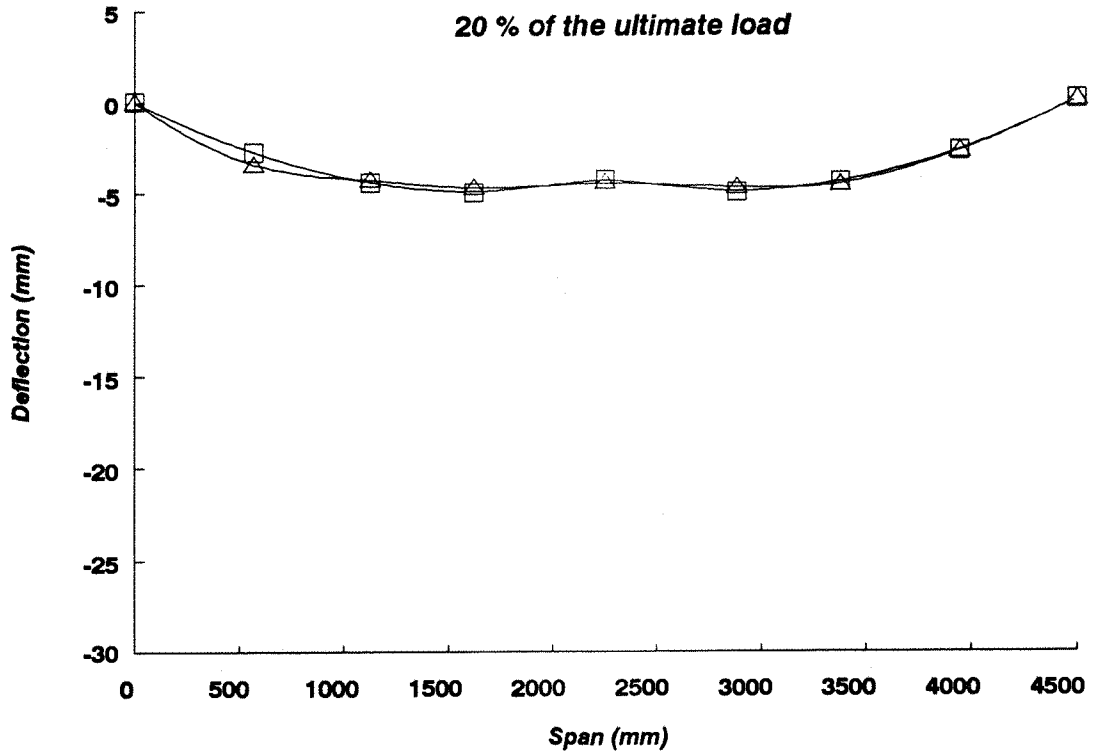

Fig 5.22 Variation of deflection along the span of the third panel.

□ **Computational results**

△ **Experimental results**

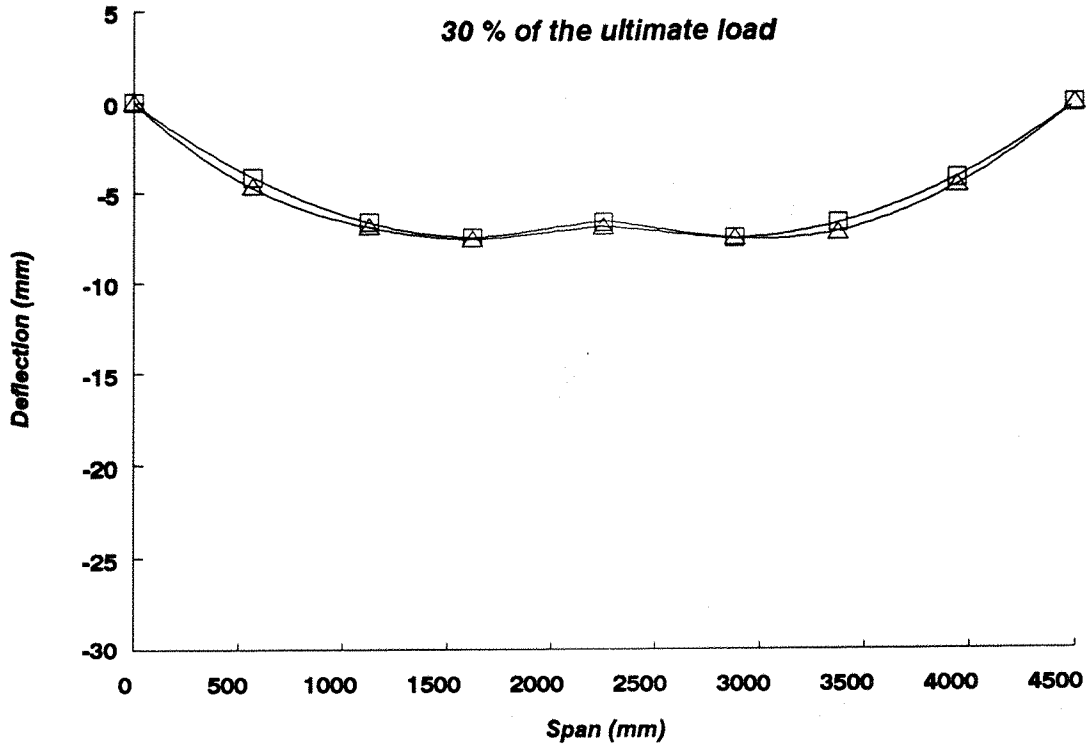

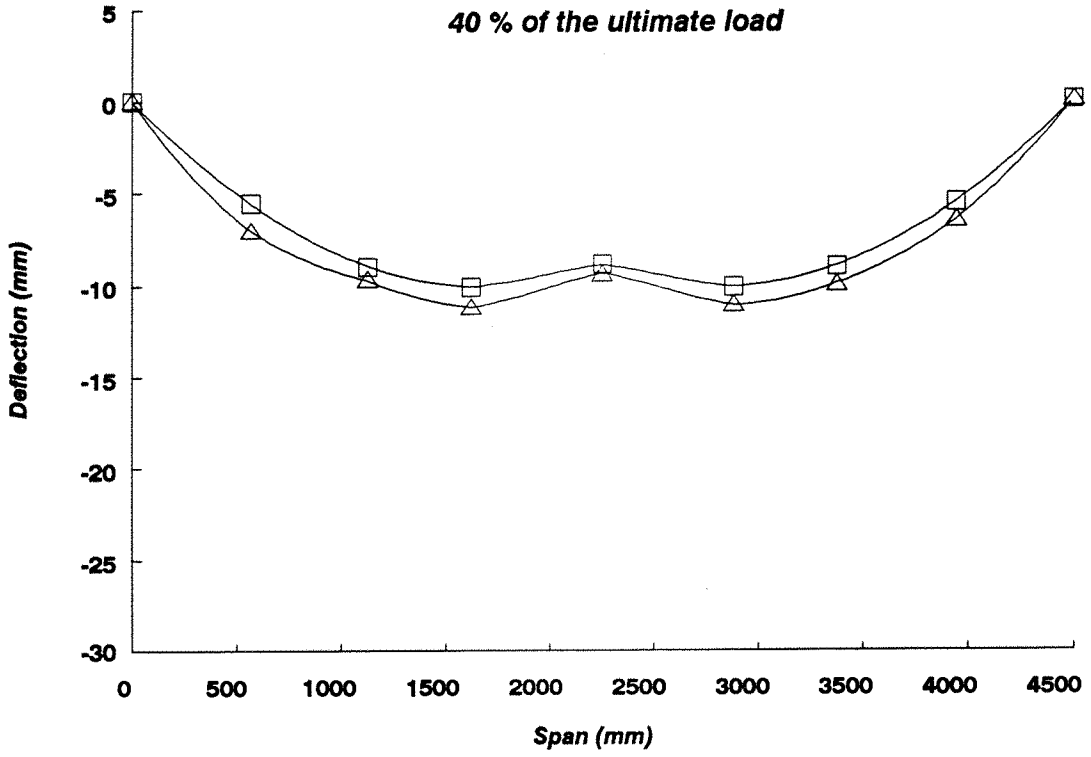

Fig 5.23 Variation of deflection along the span of the third panel.

□ Computational results

△ Experimental results

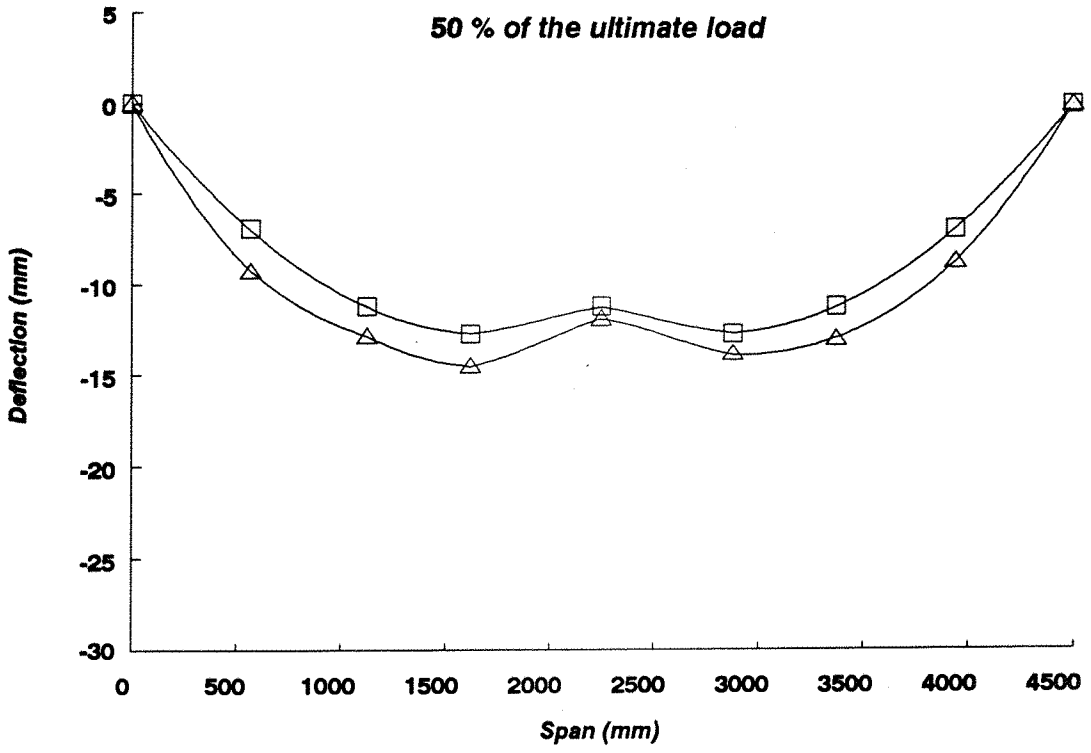

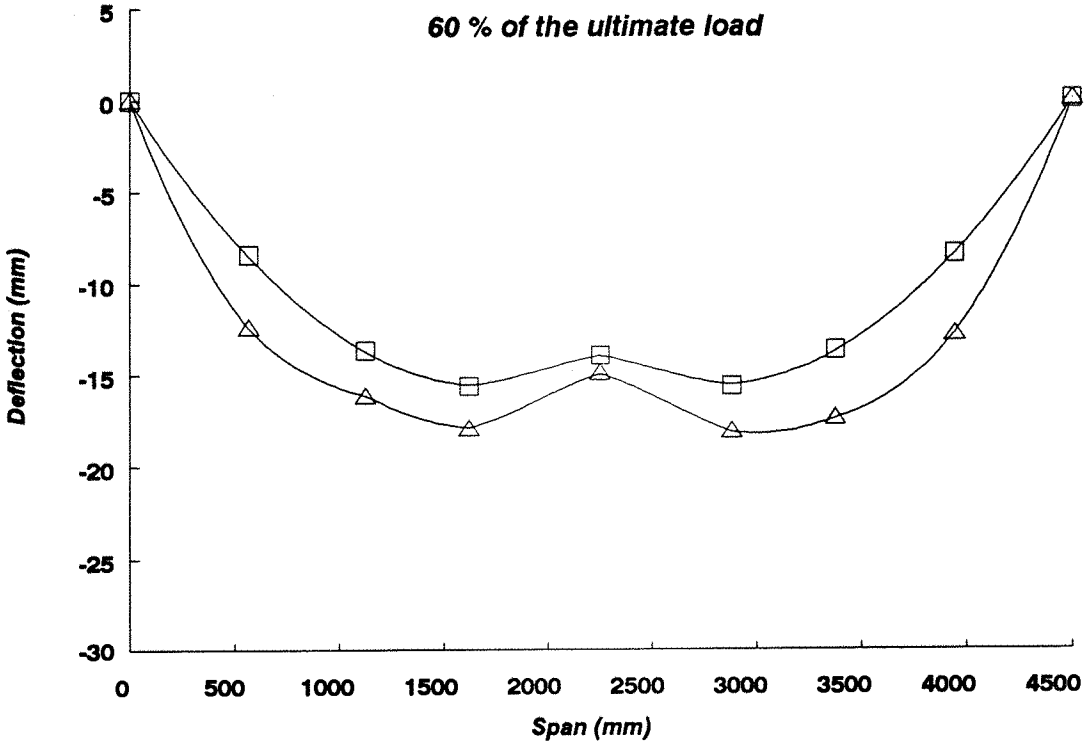

Fig 5.24 Variation of deflection along the span of the third panel.

□ Computational results

△ Experimental results

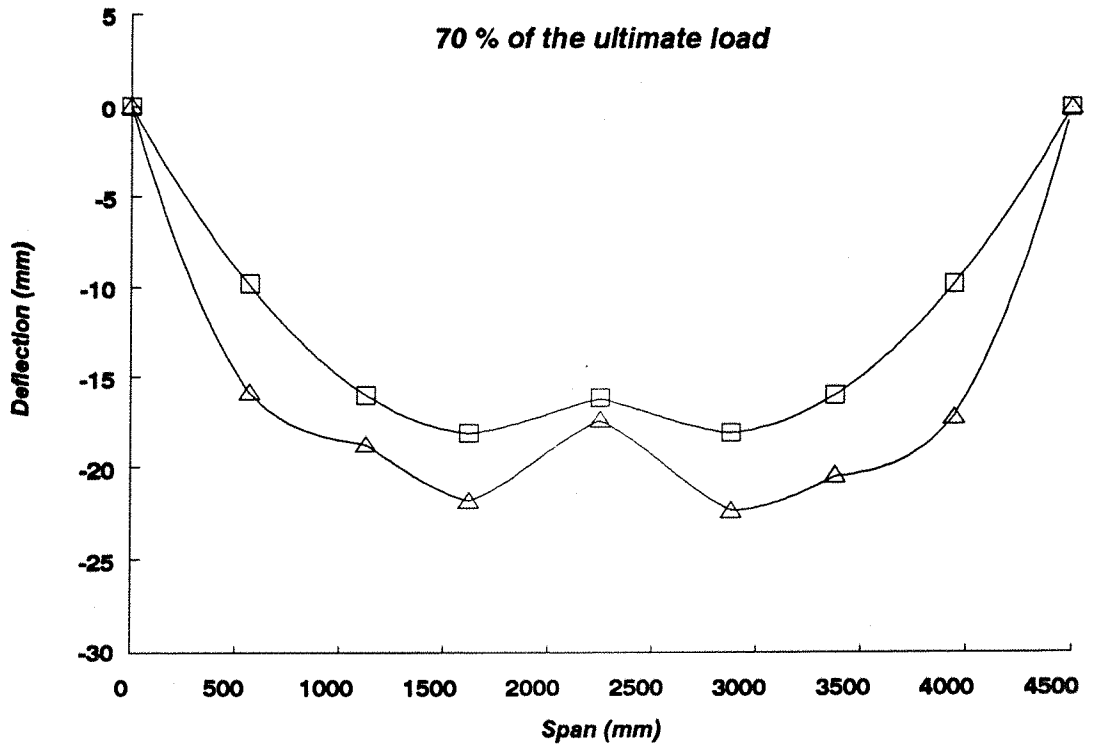

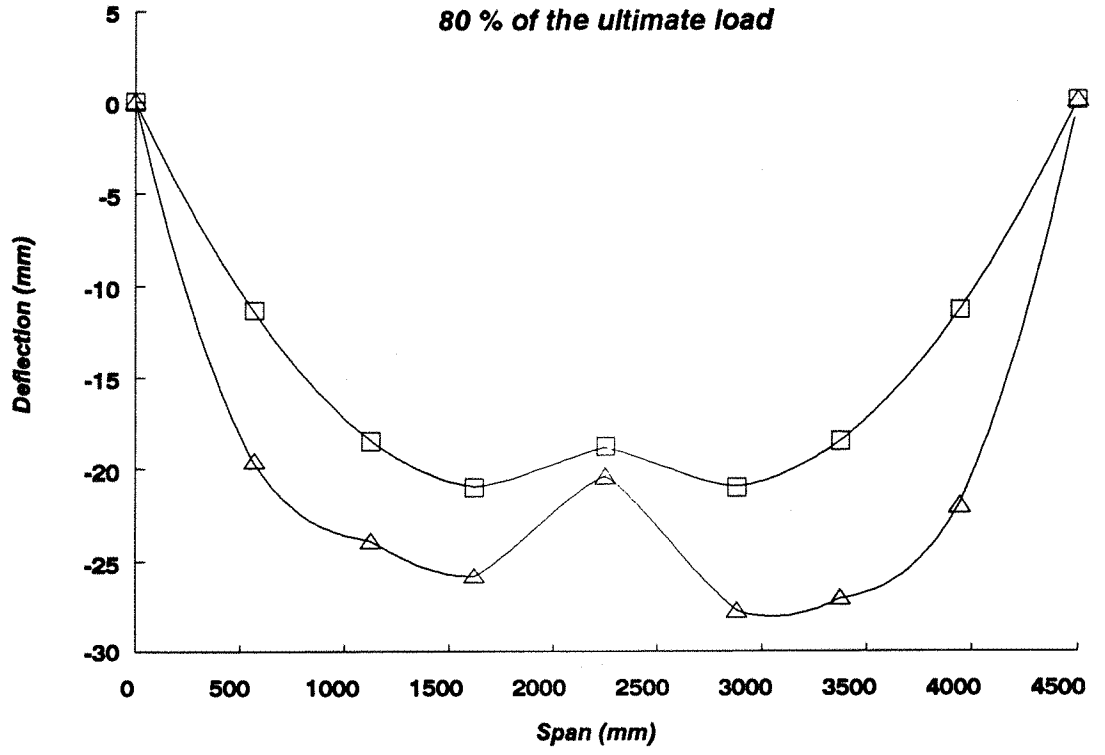

Fig 5.25 Variation of deflection along the span of the third panel.

□ **Computational results**

△ **Experimental results**

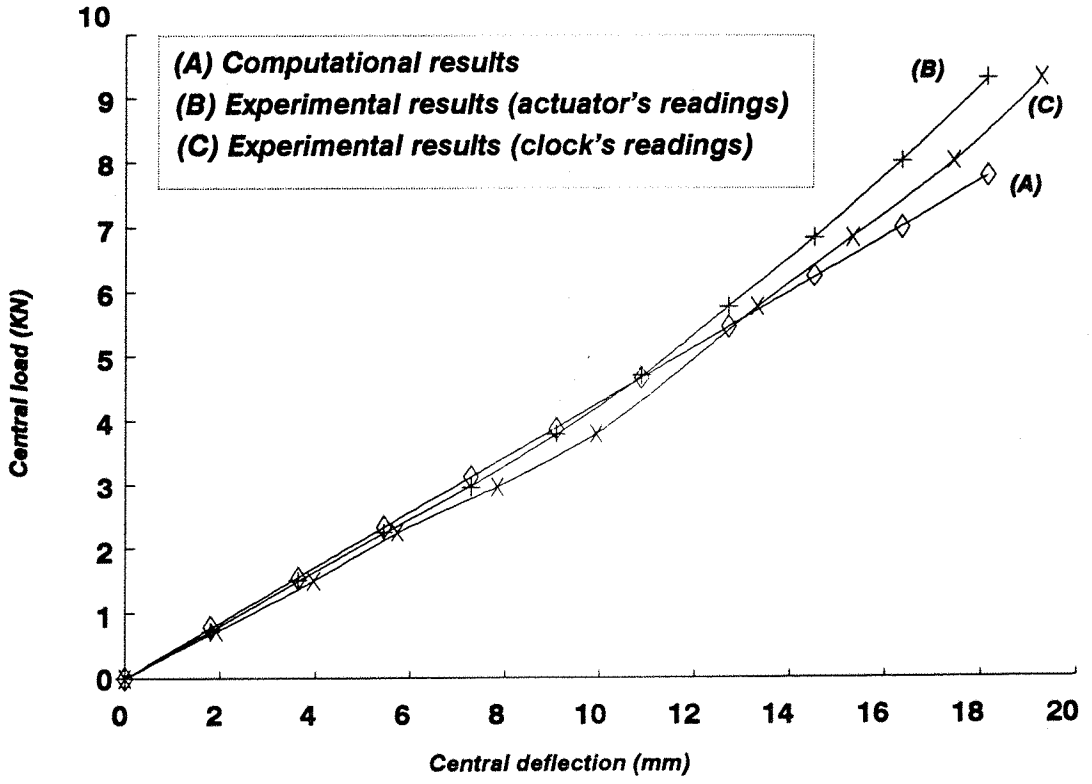

Central deflection (mm)	Central load (KN)
0.000	0.000
1.816	0.778
3.632	1.557
5.448	2.335
7.264	3.114
9.078	3.892
10.892	4.671
12.705	5.450
14.527	6.228
16.343	7.006
18.159	7.785

(A)

Central deflection (mm)	Central load (KN)
0.000	0.000
1.800	0.720
3.630	1.490
5.450	2.240
7.260	2.970
9.080	3.790
10.900	4.700
12.710	5.770
14.530	6.850
16.340	8.020
18.160	9.310

(B)

Central deflection (mm)	Central load (KN)
0.000	0.000
1.925	0.720
3.942	1.490
5.720	2.240
7.850	2.970
9.910	3.790
N.A	4.700
13.332	5.770
15.315	6.850
17.450	8.020
19.295	9.310

(C)

Fig 5.26 Central load / deflection diagram of the first panel (20 oz / ft3)

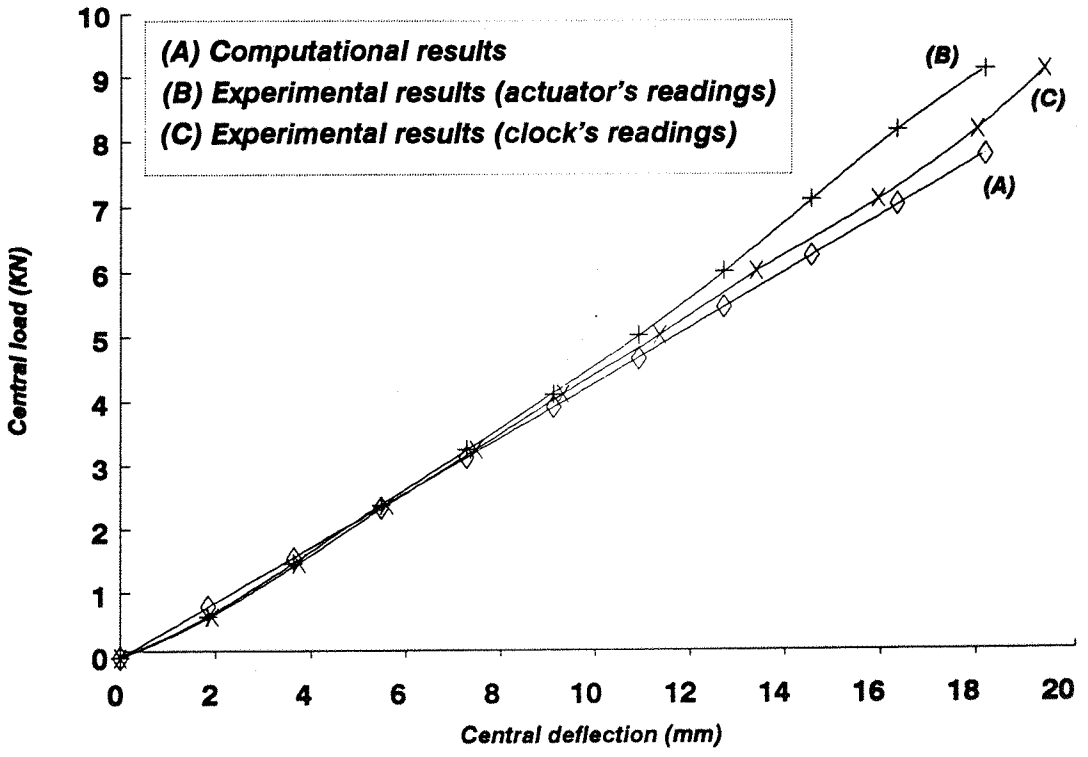

Central deflection (mm)	Central load (KN)
0.000	0.000
1.830	0.780
3.640	1.560
5.460	2.340
7.270	3.120
9.100	3.900
10.920	4.680
12.730	5.460
14.550	6.240
16.370	7.020
18.190	7.800

(A)

Central deflection (mm)	Central load (KN)
0.000	0.000
1.830	0.637
3.650	1.477
5.460	2.377
7.290	3.237
9.100	4.127
10.930	5.017
12.740	6.007
14.560	7.097
16.380	8.187
18.200	9.137

(B)

Central deflection (mm)	Central load (KN)
0.000	0.000
1.905	0.637
3.765	1.477
5.600	2.377
7.460	3.237
9.335	4.127
11.345	5.017
13.405	6.007
15.940	7.097
18.035	8.187
19.455	9.137

(C)

Fig 5.27 Central load / deflection diagram of the second panel (18 oz / ft3)

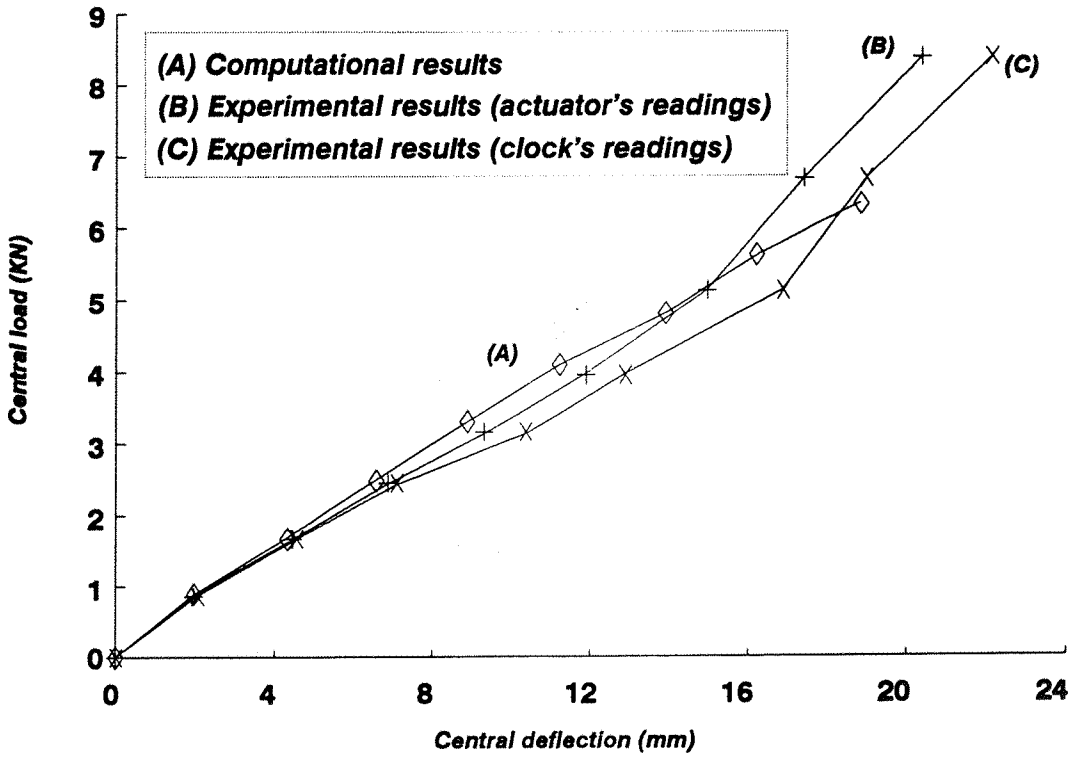

Central defection (mm)	Central load (KN)
0.000	0.000
1.968	0.888
4.307	1.686
6.557	2.505
8.866	3.309
11.235	4.100
13.936	4.809
16.237	5.616
18.850	6.346

(A)

Central defection (mm)	Central load (KN)
0.000	0.000
1.970	0.870
4.470	1.670
6.850	2.440
9.320	3.150
11.880	3.960
14.970	5.130
17.420	6.700
20.390	8.380

(B)

Central defection (mm)	Central load (KN)
0.000	0.000
2.055	0.870
4.550	1.670
7.115	2.440
10.380	3.150
12.890	3.960
16.885	5.130
19.000	6.700
22.160	8.380

(C)

Fig 5.28 Central load / deflection diagram of the third panel (16 oz / ft3)

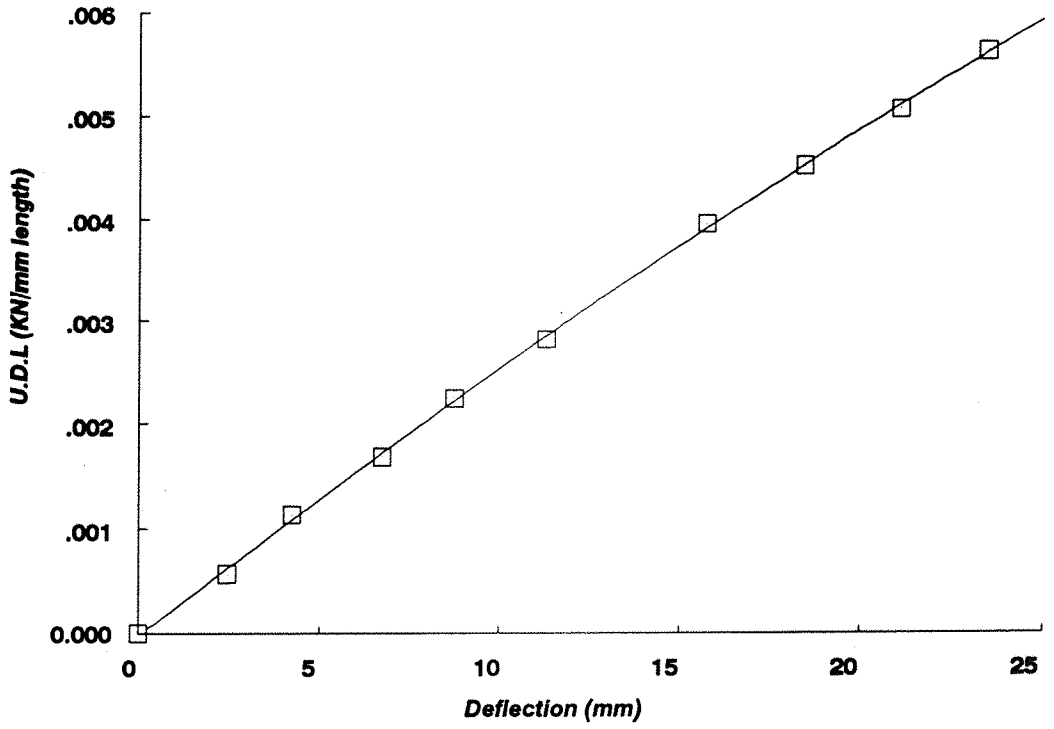

Fig 5.29 Load / deflection graph at 1536 mm from the roller support of the first panel (20 oz / ft3).

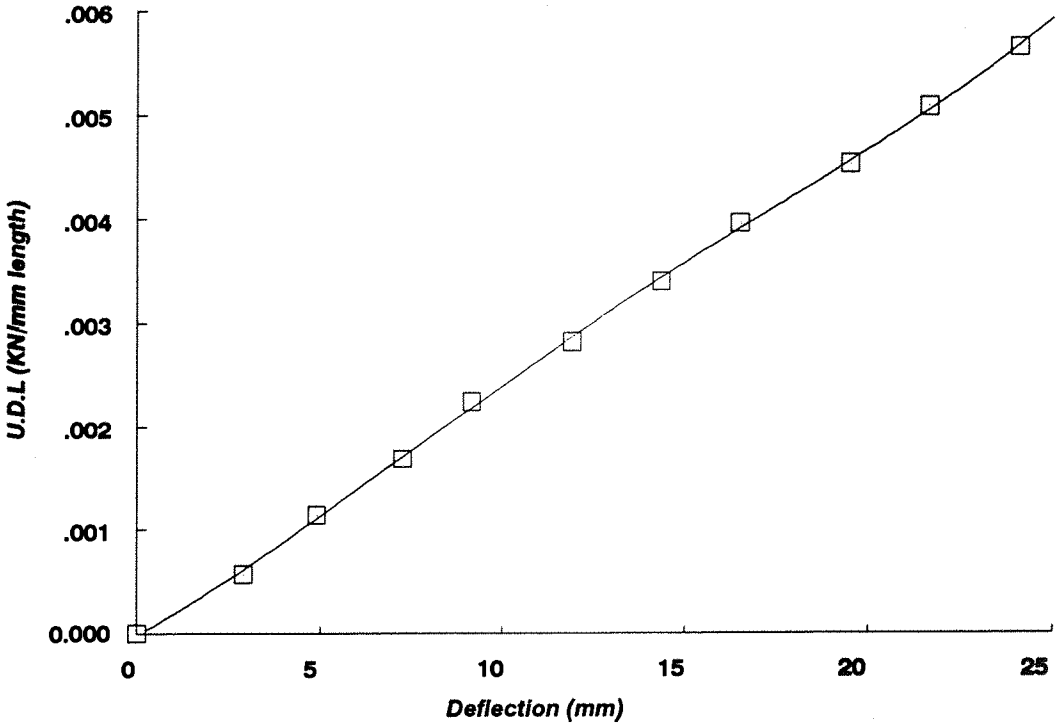

Fig 5.30 Load / deflection graph at 1572 mm from the roller support of the second panel (18 oz / ft3).

CHAPTER SIX

CONCLUSION AND PLAN FOR FUTURE WORK

6.1 Introduction

Sandwich panels design requirements can either be general (mechanical, physical, productional and economical) or special (security, function, insulation and durability). Meeting all the requirements at one time requires compromise. In general, the desirable properties should be combined with the performable possibilities of fabrication. In the building industry, the cost to effectivity relationship should be considered as the first priority. This is due to the intense competition in the types of construction elements.

In the design of sandwich panels, failure modes should be considered carefully. Wrinkling of the metal faces, shear failure of the core and shear bond failure and crushing at the supports are the most common failure modes.

Single span sandwich panels can be designed on the basis of calculated stresses and deflections. For panels which are continuous over two or more spans, the design becomes more complicated as it can be limited by wrinkling and shear deflection at the internal supports. In addition, thermal gradient may cause significant stresses and deflections which cannot be ignored in the design.

This research investigated the type of sandwich panels which are suitable for semi - structural building application with an insulating function. These are panels made from thin, flat sheets of steel for the faces and a polystyrene foam core. Such panels used in cold stores are subjected to

large temperature differences between the outer and inner steel faces.

6.2 Summary of the present work

6.2.1 Theoretical work

The performance of two - span sandwich panels was the subject of the present study. Such panels used as cladding units were subjected to simulated wind load and thermal gradient. Due to the lack of any general design theory regarding these panels, this research presented a new design approach adopted in the analysis of two span panels under wind and temperature loads.

The design theory adopted in this research was based on using the method of consistent deformation. This method assumes that for a two - span sandwich panel under uniformly distributed load (case I), the deflection of the panel can be considered as the sum of deflections from two design cases: The first is the case of a single span panel subjected to the uniformly distributed load (case II). The second is the case of a single span panel subjected to an upward central point load equivalent to the internal support reaction of the two span panel (case III).

Wind and temperature loads were assessed before the analysis. Wind load was easily calculated and simulated as a uniformly distributed load over the panel. Thermal gradient however proved to be quite difficult to simulate in practice for a large scale test. Therefore, two analyses were made regarding the thermal gradient:

- The first analysis was based on the assumption that the deflections due to thermal gradient may be reproduced by the application of a "simulated temperature load". This is due to the fact that it is impractical to maintain a large constant thermal

gradient over a long period of time.

In addition, this analysis considered that for multi - span panel, the tendency of the panel to bend under thermal gradient is prevented by the internal supports. The introduction of intermediate supports causes the full length panel, which is deflecting under thermal gradient, to carry the reaction point loads at the same time. These point reactions cause significant stresses. As a result, large support reactions occur. Consequently, bending moment and shear forces at the internal support increase. Therefore, failure might occur due to thermal effects alone.

This first analysis was based on the assumption that the core of the panels is relatively stiff and would therefore introduce face stresses due to thermal gradient. Hence, the "simulated temperature load" used in this analysis was calculated from stresses assumed to be induced in the faces as a result of thermal gradient. This analysis was adopted in the development of experiments carried out on the designed panels.

- The second analysis was based on the assumption that for single span panels with thin, flat faces, no stresses are developed in the faces or the core due to thermal gradient. Therefore, the calculation were made for panels under a thermal gradient between outer and inner steel faces. The deflection along the span of the panel was independent of the core material density. It only depended on the thickness of the sandwich and the coefficient of thermal expansion of the steel faces. Unfortunately, experimental work was not carried out for this analysis due to the difficulties and impracticalities of such an experiment.

For each of the two above analyses, deflection equations of the fourth order were derived for design cases of the method of consistent deformation (case I, II and III).

The internal support was simulated by a sheeting rail. The deflection of this sheeting rail, which was a function of the reaction it provided to the panels, varied according to the position of the panels along the sheeting rail (end, inside and middle panels). The design was based on the deflection of the middle panel only.

Deflection at the internal support was expected because the middle support was not considered rigid compared with the two end supports. In practice, one of the end supports is fixed to the ground and the other is fixed to the roof beam. Therefore, no movement is allowed at either of the supports.

The limiting deflection of span/240 was considered as a design criterion in the analysis. The internal support reactions corresponding to this limiting deflection were assessed and the deflection along the span of the panels was evaluated for all design cases and for the two thermal gradient analyses. The computer program based on the derived equations evaluated the deflection and the internal support reactions for the specific data of the panels under consideration. The results of this program were the basis of the tests carried out on the panels.

6.2.2 Experimental work

Three different core density panels were investigated in this work (16 oz/ft^3, 18 oz/ft^3 and 20 oz/ft^3). It was necessary to assess some of the material properties of the three panels before testing them under wind and temperature loads. The three panels were 150 mm thick. Adopting standard material tests proved to be impractical. Because of the relatively thick panels, the recommended material test specimens dimensions were too big to be cut from the available specimens and would have been too big to handle in the laboratory or to fit under any testing machine. Therefore, modified standard tests had to be considered for both tensile and shear tests.

To assess the tensile strength and modulus of the three different core density panels, square specimens of a side length equal to twice the sandwich thickness were tested. The dominant failure mode was a bond failure between the core and steel faces.

Shear tests were carried out on three test pieces corresponding to each of the three panels. A trial test was first adopted on a small specimen in a shear box.

The second shear test (double shear test) took into consideration the dimensions of the specimen in proportion to its thickness. The setting up of this test was not based on any standard test. Two specimens were tested from each panel. The dominant failure mode was mainly bond failure between steel faces and the polystyrene core. A slight misalignment of the actuator, which applied the load, caused the failure to start always in one of the two test pieces. A core shear failure was recorded in one specimen only.

Based on the analytical design adopted in this research and the results of the computer program, experiments were carried out on three different core density, two - span panels. Each of the panels was subjected to a uniformly distributed dead load representing wind and temperature loads.

The internal support was simulated by a sheeting rail held in place by a hydraulic actuator which applied a load equivalent to the internal support reaction. The uniformly distributed load was simulated by evenly applied ball bearings over the span of 4500 mm. The load was applied in increment of 10 % of the predicted ultimate load at a time. The deflections along the span were measured on the underside of the panels by means of dial gauges.

The simulated loads were applied on the first and second panels and the deflection was recorded along the span. The bottom steel face of these two panels showed some distortion

which caused crushing of the core. This resulted in some top surface deflection at the end supports which was not predicted before testing. For the third panel, the central support load applied by the actuator was increased by the average deflection at the end supports measured by means of a dial gauge positioned at each support. As a result of this increased central reaction, the computational results had to be adjusted in order to make a more realistic comparison between experimental and analytical results.

6.3 Conclusions from the results of this research

The results of the first shear test proved to be unsatisfactory, the core shear modulus was evaluated as equal to 0.69 N/mm^2 compared with its design value of 2.25 for the first panel. The test piece dimensions were not in proportion with the sandwich thickness as recommended by standard tests. In addition, the test piece kept tilting to one side in the shear box. This movement prevented the efficient application of the force along the length of the specimen. Moreover, the travel of the shear box was small with regard to the core thickness. Therefore, the applied force acted only on the bond between the steel faces and the metal plates glued to the specimen. Hence the need to develop the second shear test.

The core shear moduli evaluated from the second shear test results (2.797, 2.682 and 2.129 N/mm^2 for the first, second and third panels respectively) were found to conform more closely to their design values given by the manufacturer (3.99, 3.95 and 2.25 N/mm^2). From the obtained results it can be concluded that the second shear test may be considered satisfactory for adoption to test panels with a relatively thick core.

The shear and bond test results showed that the material properties of sandwich panels depend on the density of the core material. As the density increases, the shear and

tensile strengths and moduli increase too.

Testing the three different core density panels under dead load showed that the first two panels of core density 20 oz/ft^3 and 18 oz/ft^3 respectively failed by wrinkling of the upper steel faces. The third panel of core density 16 oz/ft^3 failed by core shear failure followed by interfacial delamination of the steel / polystyrene core at the fixed support end. A core discontinuity due to poor gluing caused partial delamination of the steel / polystyrene core at the roller support end when this third panel failed.

The wrinkling of the upper steel faces in the first two panels occurred at a distance 1536 mm and 1572 mm from the roller support. Wrinkling load was evaluated as equal to 2.8242 E-03 KN/mm length and 3.955 E-03 KN/mm length for the first and second panel respectively. The theoretical wrinkling loads were estimated as equal to 2.647 E-03 KN/mm length for the first panel and 3.826 E-03 KN/mm length for the second panel. These results showed that the first and second panels performed as predicted and the failure occurred at a load nearly equal to the theoretical predicted load.

Failure often takes place at a stress significantly lower than that given by the theoretical wrinkling stress. In the theoretical calculations, it was assumed that the properties of the core material remain linear up to the point where bifurcation of equilibrium takes place, whereas in practice, these ideal assumptions were not satisfied. Hence the failure occurred at a stress lower than the calculated theoretical wrinkling stress. Experimentally failure occurred at stresses of 0.0608 and 0.0619 KN/mm^2 for the first and second panels respectively. The theoretical stresses however were calculated as equal to 0.07842 and 0.07816 KN/mm^2.

At the central support, crushing of the lower steel faces of the three panels was recorded. This was due to the lower

steel faces being under excessive compression from the internal support reaction. From the results plotted on load / deflection curves, It can be concluded that crushing of the steel faces at the internal support occurred at points where the curves began to depart from a straight line. Crushing of the lower faces started at a load of 4.70 KN, 5.017 KN and 5.13 KN for first, second and third panels respectively.

The maximum core shear stresses at the end supports obtained from the experiment (0.04506 N/mm^2 and 0.04555 N/mm^2 for the first and second panels respectively), were in close agreement with their estimated theoretical values (0.04934 N/mm^2 and 0.04928 N/mm^2) and the values assessed from the shear test (0.0606 N/mm^2 and 0.0525 N/mm^2 for the first and second panels respectively). This was not the case for the third panel. Increasing the central deflection of the third panel by the average of the supports deflection lead to a reduced central support reaction up to the fifth loading increment (3.96 KN compared with an estimated 4.1 KN). Consequently, the shear force at the support increased, increasing the likelihood of the resulting core shear failure.

Deflections at the end supports were not considered in the analytical design. However, the experimental results showed some upward deflections. These deflections were due to a metal face distortion and core crushing across the width of the three panels at the points of end supports.

Comparing the theoretical results of the first and second analyses with the experimental results shows that:

- Core shear stresses at the central support evaluated from the second analysis (0.00931, 0.00935 and 0.00973 N/mm^2 for the first, second and third panels respectively) are not considered crucial when compared with the theoretical results of the first analysis (0.0217, 0.0218 and 0.0176 N/mm^2) and with the

experimental results (0.026, 0.0256 and 0.0234 N/mm^2 respectively). Therefore, core shear is not critical at the central support for the first or the second analyses.

- The ratio of maximum compressive stresses in the steel faces at the two critical positions of central support and mid-span, evaluated theoretically (0.805, 0.804 and 0.794 for the first, second and third panels respectively) and experimentally (0.666, 0.686 and 0.496) for the first analysis, do not agree with those estimated from the second analysis (1.426, 1.494 and 2.070). The stresses at the central support were estimated to be smaller than those at mid-span from the first analysis and the experimental results. For the second analysis, calculations show that stresses at the central support are expected to be higher than the mid-span stresses. Therefore, the first analysis predicts failure to occur at the mid-span position whereas the second analysis expects it to occur at the central support position.

The agreement between the first analysis results and the experimental results proves that the simulation of temperature effects as a uniformly distributed load can be considered satisfactory providing the assumptions made in this research are satisfied.

6.4 Applications

The material properties of sandwich panels tested in this research proved to be dependent on the density of the core. However, the complexity of the core material and the additives used (such as fire retardants) could modify the cell structure and the physical properties of the sandwich unit. It is to be noted that the density of the core material is not constant over the cross - sectional area of the sandwich panels.

Furthermore, the properties of the core material are not necessarily the same in all directions due to their dependency on the machinery used in the foaming process and the operating conditions.

Moreover, the mechanical properties of the rigid foam cores are temperature and humidity dependent. The results of the tests adopted in this work were obtained at an ambient temperature and humidity. It is not definite that the same results can be obtained under different conditions of temperature and humidity.

Therefore, the results obtained in this research of the sandwich material properties can be adopted in future designs only providing that the same testing conditions are satisfied.

The introduction of internal support for wall panels proved to have reduced the central deflection of a single span panel by a noticeable amount without causing any premature shear or bond failure. This is considered true for the first analysis adopted. It is not clear whether or not the panels behave in the same way if tested according to the second analysis.

The first analysis overestimates the stresses at mid-span and hence will be conservative for mid-span and end support conditions. This analysis leads to an underestimate of the central support stresses. These stresses can easily be checked separately by an analysis of the panel under three point load bending.

The position of the internal support may vary in practice. However, the analysis may be considered the same as for equal span panels. The internal support reactions may be calculated as equal to the reactions which satisfy the limiting deflection at the section under consideration.

The boundary conditions of sandwich panels with thin flat

faces varies according to the end support conditions. At a simply supported edge x = 0, the deflection is considered zero and the overall bending moment associated with face stresses is also zero. At the clamped edge x = 0, the deflection is zero and the line which joins the faces does not rotate in the zx-plane. The slope $\frac{dy}{dx}$ is not zero. These boundary conditions are sufficient to determine the transverse deflection. In either cases, the extra boundary condition $\gamma_{yz} = 0$ or $M_{xy} = 0$ is required if the stresses in the panel are to be evaluated. The first condition $\gamma_{yz} = 0$ is equivalent to the insertion of an edge stiffener which is rigid in the yz-plane but free to twist. The second condition $M_{xy} = 0$ implies that there is no shear stress at the edges of the faces.

6.5 Plan and recommendations for future work

The first analytical design of two-span sandwich panels adopted in this research, and the experimental work proved to be in reasonable agreement. Providing the assumptions made in this research are satisfied, both computational and experimental analyses can be considered in the design of multi - span sandwich panels of similar materials and subjected to similar loading combinations.

For the material tests, it is suggested that the same tests covered in this work are adopted but under different conditions of temperature and humidity. The material properties should be checked and compared with their values obtained in this research. These proposed tests will demonstrate the variation of the material properties with temperature and other testing conditions.

The second analytical design outlined in the present work ought to be considered experimentally. Both analytical and experimental results of this analysis should be compared with those of the first analysis.

It is recommended that similar sandwich panels are tested under a uniformly distributed dead load representing the wind load, a constant thermal gradient between outer and inner steel faces and an upward central point load representing the internal support reaction. This experiment is expected to be very costly and difficult. Costly, because it needs very special equipment i.e the heating chamber, thermometers, strain gauges and thermistors. Difficult, because maintaining a constant thermal gradient between the two faces of a relatively large scale sandwich panel is not a simple task.

Until such an experiment is carried out, the theoretical predictions of the first analysis and the experimental results obtained in this research can be considered applicable only providing the assumptions made in this work are satisfied.

REFERENCES

-1- **FAIRBAIRN, W** ; "An account of the construction of the Britannia and Conway tubular bridges", John Weale et al, London, 1849.

-2- **ALLEN, H.G** ; "The analysis and design of structural sandwich panels", Commenwealth and International library, Pergamon press, 1969.

-3- **PLANTEMA, F.J** ; "Sandwich construction", John Wiley & sons, 1966.

-4- **EUROPEAN COMMITTEE FOR CONSTRUCTIONAL STEELWORK ECCS**; "European recommendations for good practice in steel cladding and roofing", ECCS - TC7, 1983.

-5- **DAVIES, J.M** ; **ALLEN, H.G** et al ; "Design of structural sandwich panels", paper presented at a short course in the department of Civil Engineering , University of Salford, September 1985.

-6- **L.R.INSULATIONS LIMITED** ; "Larin panels system", typical constructional details.

-7- **ICI** ; "Fabrication of sandwich panels using rigid polyurethane foam applied by the press injection process", ICI Document, No. PU 1004.

-8- **DAVIES, J.M** ; "Design criteria for structural sandwich panels", The structural Engineer, volume 65A, No. 12, December 1987.

-9- "Technical guidance - sheet cladding - non-loadbearing asbestos cement, steel and aluminium", 2nd edition,

Method of Building MOB 01.705, Property Services Agency, January 1979.

-10- **BS 5950** ; "The structural use of steelwork in building", Part 5, Code of practice for the esign of cold formed sections, London, British Standards Institution, 1987.

-11- **ASTM Annual book of ASTM standards** ; "Structural Sandwich Construction", Part 16, Easton, Md, U.S.A, July 1971, p.p: 1 - 35.

-12- **ISO, International Standard Organisation** ; "Cellular rubbers and plastics - Determination of apparent density", ISO R 845, 1977.

-13- **ISO, International Standard Organisation** ; "Cellular plastics - Determination of tensile properties of rigid materials", ISO 1926, 1979.

-14- **ISO** ; "Rigid cellular plastics - Determination of shear strength", ISO 1922, 1972.

-15- **ISO** ; "Rigid cellular plastics - Bending test", ISO 1209, 1976.

-16- **ISO** ; "Cellular plastics - Compression test of rigid materials", ISO R 844, 1978.

-17- **GERMAN STANDARD (DEUTSCHE NORM)** ; "Determination of density", DIN 53420.

-18- **DIN** ; "Testing of sandwiches - Tensile test, bond test", DIN 53290.

-19- **DIN** ; "Testing of rigid cellular plastics - Tensile test", DIN 53430, September 1975.

-20- **DIN** ; "Testing of rigid cellular pastics - Compression

test", DIN 53421, June 1984.

-21- **DIN** ; "Testing of sandwiches - Shear test", DIN 53294, February 1982.

-22- **DIN** ; ""Determination of shear strength of rigid cellular materials sandwiched between metal plates", DIN 53427, November 1986.

-23- **BS 5350, PART C6** ; "Adhesives - Determination of bond strength in direct tension in sandwich panels", British Standards Institution, 1981.

-24- **BASU, A.K** ; "Zur herstellung und zum werkstoffverhalten von sandwichtragwerken des werkstoffverbund systems-stahlfeinblech-polyurethan-hartschaum" (The manufacture and behaviour of sandwich panels made of the material combination of steel sheets and polyurethane foam), Dr.Ing.Dissertation, Technischen Hochschule Darmstadt, D17, 1976 (In German).

-25- **DIN** ; ""Determination of bending strength and modulus for core material only", DIN 53423.

-26- **DIN** ; "Testing of sandwiches - Tensile test perpendicular to the faces", DIN 53292, February 1982.

-27- **DIN** ; "Testing of sandwiches - Bending test", DIN 53293, February 1982.

-28- **KUENZI, E.W** ; "Structural sandwich design criteria", National Academy of Sciences, National Research Council, Publication 798, 1960, p.p: 9 -18.

-29- **CHONG, K.P , WANG,K.A , GRIFFITHS,G.R** ; "Analysis of continuous panels in building systems", Building and Enviroment, volume 14, 1979, p.p.125 - 130.

-30- **GHALI, A ,NEVILLE, A.M** ;"Structural analysis", a

unified classical and matrix approach, Intext Educational Publishers, Scranton, P.a, 1972.

-31- **COATES,R.C , COUTIE,M.G , KONG,F.K** ; "Structural analysis", London, Nelson, 1972.

-32- **CP 3** ; British standards, " Wind loads", chapter V, part 2, 1972.

-33- **RAZ Sarwar alam** ; "Analytical methods in structural engineering", New Delhi, Wiley Eastern, 1974.

-34- **CHONG, K.P, HARTSOCK, J.A** ; "Flexural wrinkling of foam filled sandwich panels", Journal of the Engineering Mechanics Division, American Society of Civil Engineers (ASCE), February 1974, p.p.95 - 110.

-35- **CHONG, K.P, HARTSOCK, J.A** ; "Flexural wrinkling mode of elastic buckling in sandwich panels", Proceedings ASCE, special conference on composite materials, Pittsburgh, 1972.

-36- **CHONG, K.P, ENGEN, K.O, HARTSOCK, J.A** ; "Thermal stress in determinate and indeterminate sandwich panels with formed facings", Presented at a special conference ASCE first engineering mechanics division, Waterloo, Canada, 1967.

-37- **CHONG, K.P, ENGEN, K.O, HARTSOCK, J.A** ; "Thermal stresses and deflection of sandwich panels", Journal of structural division, ASCE, January 1977, p.p.35 - 49.

-38- **HARTSOCK, J.A, CHONG, K.P** ; "Analysis of sandwich panels with formed faces", Journal of the structural division, April 1976, p.p.803 - 819.

-39- **GRIFFITHS,G.R** ; "Testing of continuous sandwich panels", Senior paper directed by K.P.CHONG, Department of Civil Engineering , University of Wyoming, 1976.

-40- **KINNEY, J.S** ; "Indeterminate structural analysis", Addison-Wesley, Reading, MA 1957.

-41- **HARTSOCK, J.A** ; "Design of foam filled structures", Technomic Publishing co, Stamford, Conn, 1969.

-42- **DAVIES, J.M, TEXIER, F** ; "Thermal stresses in structural sandwich panels", Composite steel structures, advances,design and construction, Proceeding of international conference on steel and aluminium structures, Elsevier Applied Science, Cardiff, July 1987.

-43- **MAI, Y.W** ; "Performance evaluation of sandwich panels subjected to bending, compression and thermal bowing", Mate'riaux et constructions, volume 13, No. 75, 1980, p.p.159 - 168.

-44- **CIB** ; "Recommendations for the structural design of lightweight sandwich panels", CIB report, Publication 59, 1978.

-45- "Acceptance criteria for sandwich panels", Internaional conference of building officials, Whittier, California, April 1977.

-46- **KUENZI, E.W** ; "Flexure of structural sandwich construction, U.S Forest Products Laboratory, report No. 1829, 1951.

-47- **MARCH, H.W** ; "Effects of shear deformation in the core of a flat rectangular sandwich panel", U.S Forest Products Laboratory, report No. 1583, 1948.

-48- **ALLEN, H.G** ; "Sandwich panels with thick or flexural stiff faces", sheet steel in building, Proceeding, meeting on Iron and Steel Institute, RIBA, March 1972.

APPENDIX I

FINAL FORM OF EQUATIONS USED IN THE COMPUTATIONAL AND NUMERICAL ANALYSIS.

From the general form equations derived in Chapter three (section 3.4.2.1),the deflections of the sheeting rail y_1, y_2 , y_3 , y_4 and y_5 at points a, b, c, d and e respectively are calculated for each of the following loading cases:

- A.1 - Case of middle panel 3 loaded with a uniformly distributed load of intensity W_3 :

With reference to section (3.4.2.1) in Chapter three, the deflection of the sheeting rail satisfies the following equation:

$$EI_s y = \left[\frac{-W_3 b x^3}{12} + \frac{W_3 b (3l^2 - b^2) x}{48} \right]_0^{2400}$$

$$+ \left[\frac{-W_3 b x^3}{12} + \frac{W_3 (x - a)^4}{24} + \frac{W_3 b (3l^2 - b^2) x}{48} \right]_{2400}^{3600}$$

$$+ \left[\frac{-W_3 b (l - x)^3}{12} + \frac{W_3 b (3l^2 - b^2) (l - x)}{48} \right]_{3600}^{6000}$$

Where:

$$W_3 = \frac{F_3}{1200} \quad , \quad E = 210 \ N/mm^2$$

$$a = 2400 \ mm \quad , \ b = 1200 \ mm \quad , \ l = 6000 \ mm$$

I_s is the moment of inertia of the sheeting rail.

The following computer program calculates the deflection at any section along the span of the sheeting rail.

```
      REAL EI,B,L,A,W3,X,Y3,A1,B1,C,D,F
      PRINT *,'EI?'
      READ *,EI
      PRINT *,'SPAN OF THE SHEETING RAIL (L)?'
      READ *, L
      PRINT *,'LOADED SPAN (B)?'
      READ *,B
      PRINT *,'DISTANCE FROM LEFT SUPPORT TO LOAD (A)?'
      READ *,A
      PRINT *,'DISTANCE FROM LOAD TO RIGHT SUPPORT (A)?'
      READ *,A
      DO 20 I=1,3
      READ (1,*)W3
      WRITE(2,11)
11    FORMAT(9X,'X',9X,'Y3')
      DO 10 X=0.0,L,100.0
      A1=((-W3*B)*(X**3))/(12.0*EI)
      B1=((W3*B*(3*(L**2)-(B**2))*X))/(48.0*EI)
      C=(W3*((X-A)**4))/(24.0*EI)
      D=((-W3*B)*(L-X)**3)/(12.0*EI)
      F=((W3*B)*((3*(L**2)-(B**2))*(L-X)))/(48.0*EI)
      IF(X.LE.A)THEN
      Y3=A1+B1
      ELSE IF(X.GE.A.AND.X.LE.A+B)THEN
      Y3=A1+B1+C
      ELSE
      Y3=D+F
      END IF
      WRITE(2,2)X,Y3
 2    FORMAT(4X,F9.4,4X,F9.4)
10    CONTINUE
20    CONTINUE
      STOP
      END
```

- A.2a - Case of panel 1 loaded with a uniformly distributed load of intensity W_1:

With reference to section (3.4.2.1) Chapter three, the deflection of the sheeting rail follows the equation below:

$$EI_s y = \frac{W_1 x}{24l}\left[2a(2l - a)x^2 + x^3 l + a^2(2l - a)^2\right]_0^{1200}$$

$$+ \frac{W_1 a^2}{24l}\left[(l - x)(4xl - 2x^2 - a^2)\right]_{1200}^{6000}$$

Where:

$$W_1 = \frac{F_1}{1200} \quad , \quad a = 1200\ mm \quad , \quad l = 6000\ mm$$

The computer program shown below calculates the deflection at any section on the sheeting rail for the loading case under consideration:

```
      REAL EI,A,L,W1,X,Y1,A1,B1
      PRINT *,'EI?'
      READ *,EI
      PRINT *,'SPAN OF THE SHEETING RAIL?'
      READ *,L
      PRINT *,'LOADED SPAN (A)'
      READ *,A
      DO 20 I=1,3
      READ (1,*)W1
      WRITE(2,11)
11    FORMAT(9X,'X',9X,'Y1')
      DO 10 X=0.0,L,100.0
      A1=((W1*X)/(24.0*EI*L))
      B1=(((-2*A)*(2*L-A)*(X**2))+((X**3)*L)+
         ((A**2)*((2*L-A)**2)))
      IF (X.LE.A)THEN
      Y1=A1*B1
```

```
      ELSE
      Y1=(((W1*(A**2))*(L-X))*((4*X*L)-(2*(X**2)))-(A**2))
         /(24.0*EI*L)
      END IF
      WRITE(2,2) X,Y1
 2    FORMAT(4X,F9.4,4X,F9.4)
10    CONTINUE
20    CONTINUE
      STOP
      END
```

- A.2b - Case of panel 5 loaded with a uniformly distributed load of intensity $W_5 = W_1$

Referring to section (3.4.2.1) Chapter three, the deflection of the sheeting rail under this case of loading satisfies the following equation:

$$EI_s y = \frac{W_1) a^2 x}{24l} \left[4(l - x)l - 2(l - x)^2 - a^2\right]_0^{4800}$$

$$+ \frac{W_1(l - x)}{24l} \left[-2a(2l - a)(l - x)^2 + (l - x)^2 + a^2(2l - a)^2\right]_{4800}^{6000}$$

and the following program calculates the deflection at any section along the span of the sheeting rail:

```
      REAL EI,A,B,L,W,X,Y1,C,M,K,B1,F
      PRINT *,'EI?'
      READ *,EI
      PRINT *,'LOADED SPAN (A)?'
      READ *,A
      PRINT *,'SPAN OF THE SHEETING RAIL (L)?'
      READ *,L
      WRITE(2,11)
11    FORMAT(9X,'X',9X,'Y5')
```

```
      DO 20 I=1,3
      READ (1,*)W5
      B=L-A
      DO 10 X=0.0,L,100.0
      C=((W5*(A**2)*X))/(24.0*EI*L)
      M=((4*(L-X)*L)-(2*((L-X)**2))-(A**2))
      K=((W5*(L-X))/(24.0*EI*L))
      B1=((-2*A)*((2*L)-A)*((L-X)**2))+(((L-X)**3)*L)
      F=((A**2)*((2*L)-A)**2)
      IF(X.LE.B)THEN
      Y5=C*M
      ELSE
      Y5=K*(B1+F)
      END IF
      WRITE(2,2) X,Y5
 2    FORMAT(4X,F9.4,4X,F9.4)
10    CONTINUE
20    CONTINUE
      STOP
      END
```

- A.3a - Case of panel 2 loaded with a uniformly distributed load of intensity W_2 :

Based on the calculation in section (4.3.2.1) Chapter three, the deflection of the sheeting rail under this loading case satisfies the following equation:

$$EI_s y = \left[\frac{-W_2 bn}{6l}x^3 + \frac{W_2 bn}{24l}[4m(n+l) - b^2]x\right]_0^{1200}$$

$$+ \left[\frac{-W_2 bn}{6l}x^3 + \frac{W_2 (x-a)^4}{24} + \frac{W_2 bn}{24l}[4m(n+l) - b^2]x\right]_{1200}^{2400}$$

$$+ \left[\frac{-W_2 bn}{6l}x^3 + \frac{W_2 (x-a)^4}{24} - \frac{W_2 (x-a-b)^4}{24}\right]$$

$$+\left[\frac{W_2 bn}{24l}\left[4m\ (n+l)\ -\ b^2\right]\ x\right]_{2400}^{6000}$$

Where:

$$W_2 = \frac{F_2}{1200}$$

$a = 1200\ mm$, $b = 1200\ mm$, $c = 3600\ mm$

$n = 1800\ mm$, $m = 4200\ mm$

Below is a computer program to calculated the deflection at any point along the span of the sheeting rail for the case of loading under consideration:

```
      REAL EI,A,B,C,L,N,M1,W2,X,Y2,M,K,H,F
      PRINT *,'EI?'
      READ *,EI
      PRINT *,'SPAN OF THE SHEETING RAIL (L)?'
      READ *,L
      PRINT *,'LOADED SPAN (B)?'
      READ *,B
      PRINT *,'DISTANCE FROM LEFT SUPPORT TO LOAD (A)?'
      READ *,A
      PRINT *,'DISTANCE FROM LOAD TO RIGHT SUPPORT (C)?'
      READ *,C
      WRITE(2,11)
11    FORMAT(9X,'X',9X,'Y2')
      DO 20 I=1,3
      READ (1,*)W2
      DO 10 X=0.0,L,100.0
      N=C+(B/2)
      M=A+(B/2)
      M1=((-W2*B*N)*(X**3))/(6.0*EI*L)
```

```
      K=(W2*((X-A)**4))/(24.0*EI)
      H=(-W2*((X-A-B)**4))/(24.0*EI)
      F=((W2*B*N)*(((4*M)*(N+L))-(B**2))*X)/(24.0*EI*L)
      IF (X.LE.A)THEN
      Y2=M1+F
      ELSE IF(X.GE.A.AND.X.LE.A+B) THEN
      Y2=M1+K+F
      ELSE
      Y2=M1+K+F+H
      END IF
      WRITE(2,2) X,Y2
 2    FORMAT(4X,F9.4,4X,F9.4)
10    CONTINUE
20    CONTINUE
      STOP
      END
```

- A.3b - Case of panel 4 loaded with a uniformly distributed load of intensity $W_4 = W_2$:

$$EI_s y = \left[\frac{-W_2 bn}{6l}(l-x)^3 + \frac{W_2(l-x-a)^4}{24} - \frac{W_2(l-x-a-b)^4}{24}\right]$$

$$+ \left[\frac{W_2 bn}{24l}[4m(n+l) - b^2](l-x)\right]_0^{3600}$$

$$+ \left[\frac{-W_2 bn}{6l}(l-x)^3 + \frac{W_2(l-x-a)^4}{24}\right]$$

$$+ \left[\frac{W_2 bn}{24l}[4m(n+l) - b^2](l-x)\right]_{3600}^{4800}$$

$$+ \left[\frac{-W_2 bn}{6l}(l-x)^3 + \frac{W_2 bn}{24l}[4m(n+l) - b^2](l-x)\right]_{4800}^{6000}$$

The following computer program is used to calculate the deflection of the sheeting rail at any point along the span for this loading case.

```
      REAL EI,A,B,C,M,N,L,W4,X,Y2,M1,H,F,K
      PRINT *,'EI?'
      READ *,EI
      PRINT*,'SPAN OF THE SHEETING RAIL (L)?'
      READ *,L
      PRINT *,'LOADED SPAN (B)?'
      READ *,B
      PRINT *,'DISTANCE FROM LEFT SUPPORT TO LOAD (C)?'
      READ *,C
      PRINT *,'DISTANCE FROM LOAD TO RIGHT SUPPORT (A)?'
      READ *,A
      WRITE(2,11)
11    FORMAT(9X,'X',9X,'Y4')
      M=A+(B/2)
      N=C+(B/2)
      DO 20 I=1,3
      READ (1,*)W4
      DO 10 X=0.0,L,100.0
      K=((-W4*B*N)*((L-X)**3))/(6.0*EI*L)
      M1=(W4*((L-X-A)**4))/(24.0*EI)
      H=(-W4*((L-X-A-B)**4))/(24.0*EI)
      F=((W4*B*N)*(((4*M)*(N+L))-(B**2))*(L-X))/(24.0*EI*L)
      IF (X.GE.B+C)THEN
      Y4=K+F
      ELSE IF(X.LE.B+C.AND.X.GE.C)THEN
      Y4=K+M1+F
      ELSE
      Y4=K+M1+F+H
      END IF
      WRITE(2,2) X,Y4
 2    FORMAT (4X,F9.4,4X,F9.4)
10    CONTINUE
20    CONTINUE
      STOP
      END
```

The deflection of the sheeting rail corresponding to each of the loading cases detailed above is plotted against the position along the span (Fig A.1). This Figure A.1 also shows the deflection along the span when the sheeting rail is subjected to all the loading cases at the same time.

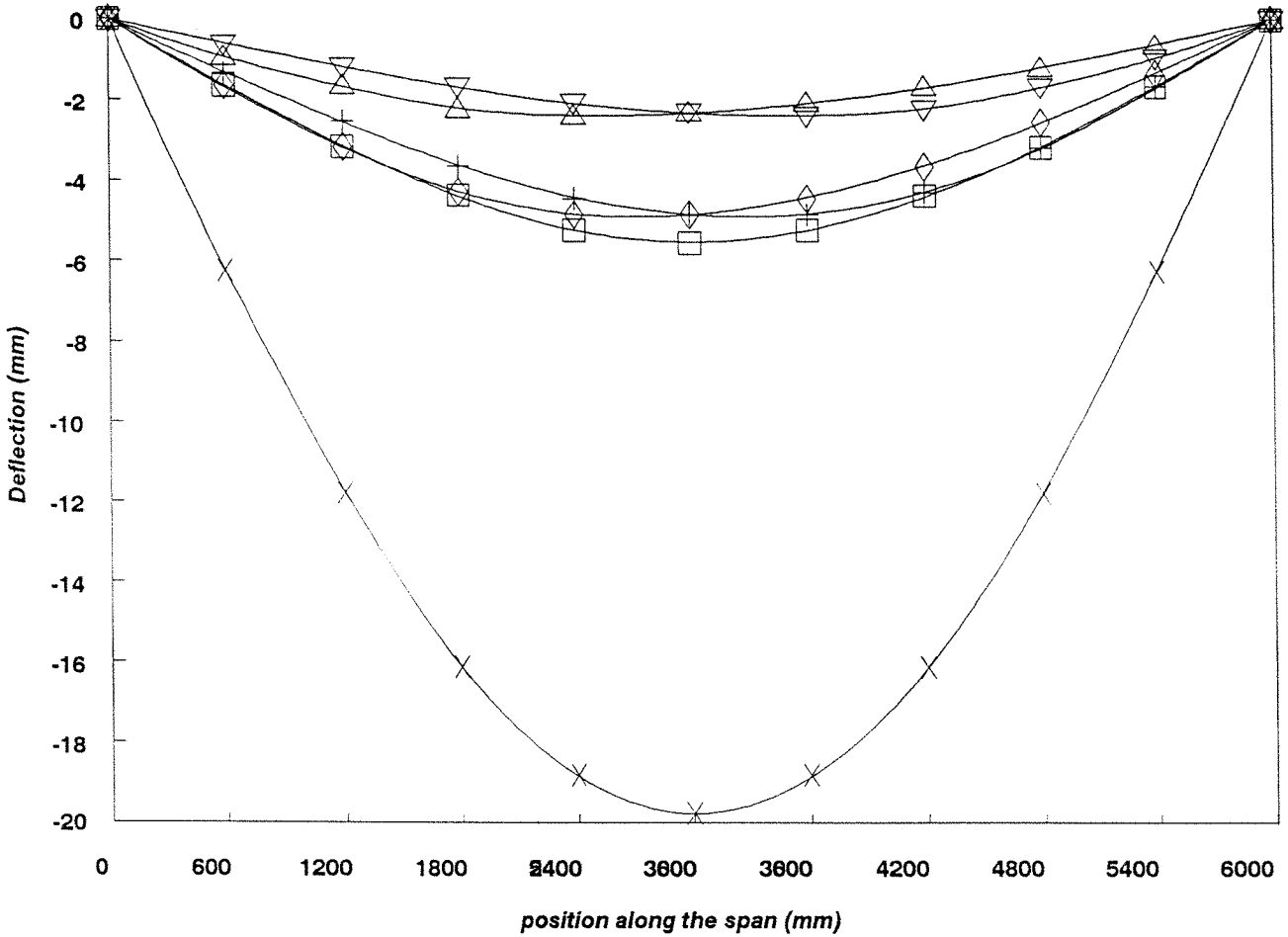

Fig A.1 Deflection of the sheeting rail under various loading cases.

□ *Load case A.1* △ *Load case A.2a* ▽ *Load case A.2b*

◇ *Load case A.3a* + *Load case A.3b* X *Sum of all cases*

APPENDIX II

MAIN COMPUTER PROGRAM

```
C  ***********************************************************
C  THIS PROGRAM CALCULATES THE INTERNAL SUPPORT REACTIONS
   EQUIVALENT TO THE LOAD ON THE SHEETING RAIL
C  ***********************************************************

   REAL AZ(3,3),BZ(3),CZ(3)
   REAL EI,E,IS,AG,L,L1,W,F1,F2,F3
   REAL D1,D2,D3,DELTAX,DELTA1,DELTA2
   REAL DELTA3,X1,X2,X,A,B,C,D,M,N,M3,N3,P,R,S,T,Q,V,K,U
   REAL Y,Y1,YA,YS,YF1,DELTA,DELTF1,YB1,YS1,M1,N1,R5,B1
   REAL F(10),WW(10),Z(10)
   REAL K1,K2,K3

C  ***********************************************************
C  EI IS THE FLEXURAL RIGIDITY OF THE SANDWICH
C  E IS THE MODULUS OF ELASTICITY OF THE STEEL FACES
C  IS IS THE MOMENT OF INERTIA OF THE SHEETING RAIL (MM4)
C  L IS THE SPAN OF THE SANDWICH PANEL (MM)
C  L1 IS THE SPAN OF THE SHEETING RAIL (MM)
C  W IS THE WIND AND TEMPERATURE LOAD (KN/MM')
C  B IS THE LOADED SPAN ON THE SHEETING RAIL = PANEL WIDTH
   (MM)
C  ***********************************************************

   DATA E,IS,L,L1,W/210,33900000,4500,6000,5.648E-03/
   DATA EI,B,A,C,D,M,N/1.48E+09,1200,2400,3600,1200,
   1800,4200/
   DATA X,X1,X2/3000.0,600.0,1800.0/
   PRINT *,'SHEAR STIFFNESS OF THE CORE (AG)?'
   READ *,AG
```

```
C  ********************************************************
C  X1 IS THE DISTANCE FROM LEFT SUPPORT A TO MID SPAN OF
   PANEL 1
C  X2 IS THE DISTANCE FROM LEFT SUPPORT A TO MID SPAN OF
   PANEL 2
C  X IS THE DISTANCE FROM LEFT SUPPORT A TO MID SPAN OF
   MIDDLE PANEL 3
C  ********************************************************

   M=(B/2)+D
   N=(B/2)+C
   FAC1=8*(L1**3)
   FAC2=B**3
   FAC3=-4*(B**2)*L1
   M3=(FAC1+FAC2+FAC3)/(384*E*IS)
   N3=((3*B*L1*L1)-(2*B*B*B))/(48*E*IS)
   P1=(-N*(L1**2))/(24*E*IS)
   P2=(((0.5*L1-D)**4)-((0.5*L1-D-B)**4))/(12*B*E*IS)
   P3=((4*M*(N+L1)-(B**2))*N)/(24*E*IS)
   P=P1+P2+P3
   R1=(-X1**3)/(12*E*IS)
   R2=(((3*L1*L1)-(B**2))*X1)/(48*E*IS)
   R=R1+R2
   S1=(-2*B*(2*L1-B)*(X1**3))+((X1**4)*L1)+((B**2)*((2*L1-B)
      **2))*X1
   S2=((B*X1*(L1-X1))/(6*E*IS))-((B*X1*((L1-X1)**2))/
      (12*L1*E*IS))
   S3=(-(B**3)*X1)/(24*L1*E*IS)
   S=(S1/(24*L1*B*E*IS))+S2+S3
   T1=((X1**3)+((L1-X1)**3))*(-N/(6*L1*E*IS))
   T2=(((L1-X1-D)**4)-((L1-X1-D-B)**4))/(24*B*E*IS)
   T4=((L1-X1)*(N*(4*M*(N+L1)-(B**2))))/(24*L1*E*IS)
   T3=(X1*(N*(4*M*(N+L1)-(B**2))))/(24*E*L1*IS)
   PRINT *,T1
   PRINT *,T2
   PRINT *,T3
   PRINT *,T4
   T=T1+T2+T3+T4
   PRINT *,T
```

```
      Q1=-(X2**3)/(12*E*IS)
      Q2=(X2*(L1**2))/(16*E*IS)
      Q3=-((B**2)*X2)/(48*E*IS)
      Q=Q1+Q2+Q3
      Q=(X2*((-4*(X2**2))+3*(L1**2)-B**2))/(48*E*IS)
      V1=(D*X2*L1)/(4*E*IS)
      V2=-((X2**2)*D)/(4*E*IS)
      V3=-((B**2)*D)/(24*E*IS)
      V=V1+V2+V3
      K1=(((X2**3)+(L1-X2)**3)*(-N))/(6*L1*E*IS)
      K2=(((X2-D)**4)+((L1-X2-D)**4)-((L1-X2-D-B)**4))/
     *   (24*B*E*IS)
      K3=((4*M*(N+L1)-(B**2))*N)/(24*E*IS)
      K=K1+K2+K3
      U=((L**3)/(48*EI))+(L/(4*AG))

C     ************************************************************
C     D1 IS THE CENTRAL DEFLECTION OF THE SANDWICH DUE TO F1
      (PANEL 1 OR 4)
C     ************************************************************

      D1=U*F1

C     ************************************************************
C     D2 IS THE CENTRAL DEFLECTION OF THE SANDWICH DUE TO F2
      (PANEL 2 OR 5)
C     ************************************************************

      D2=U*F2

C     ************************************************************
C     D3 IS THE CENTRAL DEFLECTION OF THE SANDWICH DUE TO F3
      (MIDDLE PANEL)
C     ************************************************************

      D3=U*F3

C     ************************************************************
C     DELTAX =DELTA(L/2) IS THE CENTRAL DEFLECTION OF THE
```

```
      SANDWICH DUE TO W
C     ************************************************************

      DELTAX=(5*W*(L**4)/(384*EI))+(W*(L**2)/(8*AG))

C     ************************************************************
C     DELTA1 IS THE DEFLECTION OF SHEETING RAIL AT MID SPAN OF
      END PANEL 1,5
C     DELTA2 IS THE DEFLECTION OF SHEETING RAIL AT MID SPAN OF
      PANELS 2 OR 4
C     DELTA3 IS THE DEFLECTION OF SHEETING RAIL AT MID SPAN OF
      MIDDLE PANEL
C     ************************************************************

      AZ(1,1)=(S+U)
      AZ(1,2)=T
      AZ(1,3)=R
      AZ(2,1)=V
      AZ(2,2)=(K+U)
      AZ(2,3)=Q
      AZ(3,1)=N3
      AZ(3,2)=P
      AZ(3,3)=(M3+U)
      DO 70 I=1,3
      DO 70 J=1,3
70    WRITE(65,*) AZ(I,J)
      BZ(1)=DELTAX
      WRITE(66,*) DELTAX
      BZ(2)=DELTAX
      BZ(3)=DELTAX
      CALL SOLVE(AZ,BZ,CZ)
      DO 60 I=1,3
60    WRITE(67,*) CZ(I)
      F3=CZ(3)

C************************************************************
C     THIS PROGRAM COMPUTES THE DEFLECTION OF SANDWICH PANELS
      SUBJECTED TO A UNIFORMLY DISTRIBUTED LOAD AND / OR A
      CENTRAL POINT LOAD.
```

```
C  SHEAR , BENDING AND COMBINED SHEAR AND BENDING
   DEFLECTIONS ALONG THE SPAN OF THE PANEL ARE OBTAINED
   UNDER LOAD.
C ******************************************************

   WRITE(2,11)
11 FORMAT(9X,'X',9X,'DELTA')
   WRITE(3,12)
12 FORMAT(9X,'X',9X,'YS')
   WRITE(4,13)
13 FORMAT(9X,'X',9X,'Y')
   WRITE(7,14)
14 FORMAT(9X,'X',9X,'DELTF1')
   WRITE(8,15)
15 FORMAT(9X,'X',9X,'YF1')
   WRITE(9,16)
16 FORMAT(9X,'X',9X,'Y1')
   WRITE(10,17)
17 FORMAT(9X,'X',9X,'D1')
   WRITE(11,18)
18 FORMAT(9X,'X',9X,'YS1')
   WRITE(12,19)
19 FORMAT(9X,'X',9X,'YB1')
   DO 20 I=1,10
   Z(I)=FLOAT(I)/10
   F(I)=F3*Z(I)
   WW(I)=W*Z(I)
   DO 10 X=0.0,4500.0,45.0

C  ******************************************************
C  Y = BENDING DEFLECTION DUE TO W (WIND AND TEMPERATURE
   LOAD)
C  ******************************************************

   YA=((-WW(I)*L*(X**3))/(12.0*EI))+((WW(I)*(X**4))/
      (24.0*EI))
   Y=-(YA+((WW(I)*(L**3)*X)/(24.0*EI)))
   M1=-(-F(I)*((X-0.5*L)**3))/(6.0*EI)
   B1=-(((F(I)*(X**3))/(12.0*EI))-((F(I)*(L**2)*X)/
```

```
     (16.0*EI)))
      R5=-(F(I)*X)/(2.0*AG)

C     ********************************************************
C     YS = SHEAR DEFLECTION DUE TO W (WIND AND TEMPERATURE
      LOAD)
C     ********************************************************

      YS=-((WW(I)*L*X)-(WW(I)*(X**2)))/(2.0*AG)
      N1=+(F(I)*(X-0.5*L))/AG

C     ********************************************************
C     DELTA = TOTAL DEFLECTION DUE TO W (WIND AND TEMPERATURE
      LOAD)
C     ********************************************************

      DELTA=(Y+YS)
      IF (X.LE.2250.0)THEN

C     ********************************************************
C     Y1 = BENDING DEFLECTION DUE TO F (INTERNAL SUPPORT
      REACTION)
C     ********************************************************

      Y1=B1

C     ********************************************************
C     YF1 = SHEAR DEFLECTION DUE TO F (INTERNAL SUPPORT
      REACTION)
C     ********************************************************

      YF1=-R5

C     ********************************************************
C     DELTAF1 = TOTAL DEFLECTION DUE TO F (INTERNAL SUPPORT
      REACTION)
C     ********************************************************

      DELTF1=(B1+YF1)
```

```
C   ************************************************************
C   YB1 = BENDING DEFLECTION DUE TO (W + F)
C   ************************************************************

    YB1=(Y+B1)

C   ************************************************************
C   YS1 = SHEAR DEFLECTION DUE TO (W + F)
C   ************************************************************

    YS1=(YS+YF1)

C   ************************************************************
C   DELTF1 = TOTAL DEFLECTION DUE TO (W + F)
C   ************************************************************

    D1=((Y+B1)+(YS1))
    ELSE
    Y1=(B1+M1)
    YF1=-(R5+N1)
    DELTF1=((B1+M1)+YF1)
    YB1=(Y+(B1+M1))
    YS1=(YS+YF1)
    D1=(Y+(B1+M1))+(YS1)
    END IF
    WRITE(2,2)X,DELTA
2   FORMAT(4X,F9.4,4X,F9.4)
    WRITE(3,3)X,YS
3   FORMAT(4X,F9.4,4X,F9.4)
    WRITE(4,4)X,Y
4   FORMAT(4X,F9.4,4X,F9.4)
    WRITE(7,5)X,DELTF1
5   FORMAT(4X,F9.4,4X,F9.4)
    WRITE(8,6)X,YF1
6   FORMAT(4X,F9.4,4X,F9.4)
    WRITE(9,7)X,Y1
7   FORMAT(4X,F9.4,4X,F9.4)
    WRITE(10,8)X,D1
8   FORMAT(4X,F9.4,4X,F9.4)
```

```
      WRITE(11,9)X,YS1
9     FORMAT(4X,F9.4,4X,F9.4)
      WRITE(12,21)X,YB1
21    FORMAT(4X,F9.4,4X,F9.4)
10    CONTINUE
20    CONTINUE
      STOP
      END

C ********************************************************
C  SUBROUTINE TO SOLVE SIMULTANEOUS EQUATIONS
C ********************************************************

      SUBROUTINE SOLVE(AA,BB,CC)
      REAL AA(3,3),BB(3),CC(3),AAA(10,10),WK1(20),WK2(20)
      IFAIL=1
      CALL F04ATF(AA,3,BB,3,CC,AAA,3,WK1,WK2,IFAIL)
      RETURN
      END
```